STRUCTURAL, FUNCTIONAL, AND EVOLUTIONARY IMPLICATIONS OF A HISTIDINE MOIEITY IN CARDIAC TROPONIN I

by

Nathan Palpant

A dissertation submitted in partial fulfillment
of the requirements for the degree of
Doctor of Philosophy
(Molecular and Integrative Physiology)
in The University of Michigan
2009

Doctoral Committee:

Professor Joseph M. Metzger, Co-Chair
Professor Margaret V. Westfall, Co-Chair
Professor David Pinsky
Professor Blake J. Roessler
Professor Jessica Schwartz

© Nathan J. Palpant

All rights reserved

2009

To Darien

To the soul and the lips
Of the woman I love,
I dedicate
Every word, every
Whisper, all the earth,
All the fire in my song

(PN)

Acknowledgements

I would like to express a sincere word of gratitude to my mentor, Joe Metzger. His diligent guidance during these formative years of scientific professional development is sincerely appreciated. In addition to his guidance, I have enjoyed and appreciated my colleagues in the lab who have provided a great work environment. In particular I would like to thank Dr. DeWayne Townsend for training me in the *in vivo* Millar surgery which has been central to my experimental work. I would also like to thank all the members of my committee for the insight during the course of these studies to help me expand my experimental knowledge and enhance my scientific development.

I would also like to thank Fred Karsch and Ormond MacDougald for their guidance as graduate chairs during my tenure in the graduate program. Other faculty members that have been important include Dan Michele, Sharlene Day, and Mark Russell. I have also appreciate the work of the administrative staff, especially Michelle Boggs, for their generous assistance.

Lastly, I would like to thank my family for their support during my graduate work. First, my father, Sam, has been continually invested in my work and provided critical insights into the clinical implications of my work. As for my mom, Judy, her prayers are sustaining. Lastly, my wife, Darien, and our children, Elias and Clara, have been a source of daily support during these years.

Table of Contents

Dedication ii

Acknowledgements iii

List of Figures v

List of Tables viii

Abstract ix

Chapter

I. Introduction 1

II. Human revertant phenotypes support an evolutionary model of coordinated substitutions in cardiac troponin for enhanced mammalian lusitropic performance 67

III. Single histidine substituted cardiac troponin I confers protection from age-related systolic and diastolic dysfunction 150

IV. Single histidine button in cardiac troponin I sustains heart performance in response to severe hypercapnic respiratory acidosis in vivo 179

V. pH responsive titratable inotropic performance of histidine-modified cardiac troponin I attributed to imidazole ionization 214

VI. Conclusion 241

VII. Future Directions 256

Bibliography 284

List of Figures

Figure

1-1 Orientation to the troponin complex 9

2-1 Structure and function analysis of cardiac troponin I 70

2-2 Phylogenetic analysis of TnI functional domains 81

2-3 Theoretical isoelectric point (pI) analysis and sequence analysis of the troponin I switch arm 85

2-4 Molecular modeling and structural analysis 91

2-5 Molecular simulation modeling of interface separation caused by alanine substituted sTnI 95

2-6 Proposed model for molecular evolution of cardiac troponin during chordate evolution 100

2-7 Taxanomic tree showing the relationship of chordate species identified in this study 126

2-8 Identification of primary mRNA sequences of TnI isoforms from numerous species 127

2-9 Identification of primary amino acid sequences of TnI isoforms from numerous species 133

2-10 Alignment of cardiac troponin T protein sequences expressed in numerous chordate species 137

2-11 Alignment of cardiac troponin C protein sequences expressed in numerous chordate species 139

2-12 Alignment of troponin I protein sequences expressed in numerous chordate species 141

2-13 Justification for use of the fast skeletal troponin crystal structure 143

2-14 Structure and function analysis of troponin C 144

2-15 Crystal structure analysis of electrostic interactions between TnI and TnC 147

2-16 Alignment of cardiac myosing binding protein C (MBP-C) and phospholamband (PLN) sequences expressed in numerous chordate species 149

3-1 Age-dependent gene expression changes in cTnIA164H Tg mice 153

3-2 Age-dependent changes in baseline cardiac function by echocardiography and Millar catheterization 159

3-3 *In vivo* hemodynamic differences between aged Ntg and Tg mice during an acute hypoxic challenge 165

3-4 *In vivo* hemodynamic function and survival of aged mice during an acute hypoxic challenge 167

3-5 Analysis of calcium homeostasis in young mice 168

3-6 Changes in protein expression and phosphorylation in Ntg and Tg mice 170

4-1 Cardiac function assessed by echocardiography at baseline and during acidosis 188

4-2 Radio-telemetry based blood pressure recordings in vivo 196

4-3 Raw data traces of real-time conductance micromanometry during hypercapnic acidosis 198

4-4 Summary of real-time in vivo hemodynamic data 201

4-5 Hemodynamic analysis of inotropic function during esmolol and acidosis 202

4-6 Survival data during respiratory hypercapnic acidosis 205

4-7 Mean data showing cardiac function by echocardiography at baseline and during hypercapnia 212

4-8 Continuous *in vivo* radio-telemetry ECG measurements during a prolonged hypercapnic acidosis challenge 213

5-1 Adenoviral gene transfer of TnI into adult rat cardiac myocytes 227

5-2 Sarcomere length shortening and tension pCa measurements under physiologic and acidic conditions 230

5-3 Structural analysis of cTn molecular simulations 232

5-4 Interatomic distance measurements during cTn simulations 233

6-1 Funcational implications of different switch arm motifs in TnI 243

6-2 Model for structural and functional implications of cardiac troponin isoforms during chordate evolution 254

7-1 Evidence of global *in vivo* transduction of cardiac tissue after intravenous injection with rAAV-LacZ 259

7-2 Analysis of mRNA and protein expression of hearts transduced with AAV cTnI A164H 262

7-3 Testable hypotheses for residues important in cTn function 279

List of Tables

Table

2-1 Species abbreviations 73

2-2 Sources for protein and nucleotide sequences 114

2-3 Identification of novel troponin genes 120

2-4 Predicted pK titration calculations for ionizable groups in sTnI, cTnI and cTnC 122

2-5 Evolutionary pressure on the mammalian cTnI switch peptide 125

3-1 Baseline Cardiac Function of Aged Mice 161

3-2 Heart and Body Weight Analysis 163

4-1 Changes in Cardiac Function during Acidosis 189

4-2 Arterial Blood Gas Analysis 192

5-1 Sarcomere dynamics at baseline and acidosis 239

5-2 Myofilament calcium sensitivity and coorperativity analysis at baseline and acidosis 240

Abstract

Regulation of cardiac output is mediated by intrinsic and extrinsic factors that modulate the rhythmic transitions between contraction (systole) and relaxation (diastole). At the level of cardiac myofilaments, the troponin complex (troponin I (TnI), troponin C (TnC), and troponin T (TnT)) is the allosteric regulatory unit that controls the transition between active and inactive actomyosin cross-bridges. This is accomplished by the C-terminal switch arm of TnI toggling between actin during diastole and cTnC during systole in a calcium-dependent manner.

These studies elucidate new knowledge regarding the structural, functional, and evolutionary implications of a histidine residue in the switch arm of troponin I. Molecular modeling of TnI isoforms and large scale bioinformatics analysis of chordate phylogenies were used to study the evolution of the cardiac troponin complex. At the molecular level, a single histidine to alanine substitution in the cTnI switch arm was the most effective mechanism for decreasing the binding free energy at the regulatory interface of TnI and TnC. Evidence suggests that this single amino acid substitution increases the intrinsic relaxation potential of the cTn complex enhancing diastolic performance to meet mammalian lusitropic demands.

A histidine button in TnI is known to provide a therapeutic basis for pH responsive titratable inotropy in response to various cardiac stresses. As such, the physiological implications of a histidine button in mammalian cardiac TnI (cTnI A164H) were studied. Whole organ *in vivo* cardiac hemodynamic analysis shows that cTnI A164H Tg mice protect cardiac function from age-induced cardiomyopathy. Furthermore, cTnI A164H Tg hearts sustain cardiac performance during severe hypercapnic acidosis compared to complete pump failure with 100% mortality observed in control mice.

In situ and *in silico* site-directed protein mutagenesis, *in vitro* cellular biophysics, and atomic resolution molecular dynamics simulations were used to analyze the therapeutic basis for a histidine button in cTnI. Evidence suggests that differential ionization of histidine mediates the titratable inotropy observed in myofilaments containing cTnI A164H. Under physiologic conditions, histidine remains deprotonated and behaves functionally and structurally like WT cTnI. However, acidosis induces a protonation of histidine's imidizole group causing enhanced intermolecular electrostatic and hydrophobic side chain contacts at the interface between cTnI and cTnC in the calcium saturated state. These data indicate that differential histidine ionization is required for cTnI A164H to act as a molecular rheostat capable of therapeutically modulating sarcomere performance in response to changes in the cytosolic milieu.

Chapter I

Introduction

At its most fundamental level, the maintenance of cardiac output is required for proper communication between organ systems. This pertains to the earliest bilaterian organisms which have a single heart tube that lacks valves or chambers and does not drive unidirectional flow as well as the mammalian heart that is four chambered, has valves, and drives blood in a directed fashion to all tissues of the body[1]. During repetative cycles of contraction and relaxation, the maintainance of the heart occurs at the molecular level where a carefully orchestrated process of protein synthesis and degradation maintains the capacity for efficient performance over the lifetime of an organism[2, 3].

Variance in organ structure (chambers, valves etc) and function (heart rate, ejection fraction) are dependent on organismal demands. Phylogenic studies show a remarkable range of possibilities that meet the physiological requirements of different organisms. For example, fish regulate cardiac output primarily through modifications in stroke volume as opposed to changes heart rate[4, 5]. The flounder heart has the highest reported stroke volume of a teleost measured at 2.3 mL per gram of body weight[6]. On the other hand, endothermic chordates regulate cardiac output by modulation of heart rate and, to some

extent, modifications in stroke volume[5]. The fastest heart rate ever recorded in any vertebrate was found in a mammal, the Etruscan shrew, with a measured rate in excess of 1500 bpm[7]. At the level of energetics, all of the ATP stores of the human heart are replaced every 10 seconds[8].

During evolution, organisms have also developed important mechanisms of regulating heart function in response to environmental changes[9-13]. These interactions between systems of the body are designed to maintain cardiac output. Given the critical importance of cardiac output for maintenance of normal physiological health, it is no surprise that disruptions to this system (e.g. myocardial infarction) significantly compromise the survival capacity of an organism. In the human population, heart disease has come to be the leading cause of morbidity and mortality worldwide[14]. To address this public health concern, biomedical research into the fundamental functions of the heart as well as novel therapeutic approaches for treatment of heart disease are critical. This dissertation provides new insights into the role of the myofilament protein troponin I (TnI) in sarcomere function. Studies described here also outline a novel approach to modifying TnI in order to therapeutically modulate sarcomere function in response to numerous cardiac pathologies.

Structure of the Sarcomere

The following is a discussion of the current state of knowledge regarding proteins that compose the sarcomere. The major protein complexes that regulate cardiac

contraction and relaxation include the thick filament and the thin filament. Together these multi-protein based filaments are organized to form the striated pattern of cardiac and skeletal muscle. There are numerous structural proteins required for proper functioning of the myofilaments (e.g. Z disk proteins) and the myocyte as a whole (e.g. dystrophin) that will not be discussed. For the purposes of this dissertation, a major focus is placed on the members of the troponin complex as opposed to other proteins that regulate functions of the sarcomere or calcium cycling of the myocyte.

The contractile unit of muscle is the sarcomere. Repeating units of sarcomeres in series are termed myofibrils. Within the sarcomere are parallel units of thick and thin filaments. The proteins of the thick filament are numerous, but the molecular motor protein of the sarcomere is myosin. The proteins of the thin filament that regulate myosin motor activity include actin, tropomyosin (Tm), and the troponin complex (Tn). Under the control of intracellular calcium fluxes the thin and thick filaments slide past each other resulting in sarcomere shortening at the molecular level and contraction of muscle at the whole organ level. The sliding-filament theory of muscle contraction was originally proposed over fifty years ago[15].

The Thick Filament of the Sarcomere

Since this discussion will focus mostly on the thin filament proteins with only the following cursory analysis of the thick filament, I refer readers to a

number of excellent reviews on or including in-depth analysis of the thick filament[2, 16-22]. The thick filament is primarily composed of the bipolar polymer myosin heavy chain (MHC) with its various associated proteins (e.g. C, H, X, M, and titin). Myosin, a 200 kDa protein, has four light chains. These light chains include two essential and two regulatory subunits of about 20 kDa each. The parallel two chain coiled-coil structure of myosin forms the backbone of the thick filament while the N-terminal globular head, subfragment 1 (S1), protrudes at regular intervals. The S1 domain of myosin is essential for the binding of the thick filament to actin on the thin filament during muscle contraction[23]. This globular domain is also the site of ATP hydrolysis, the reaction required for force generating movements between myosin and actin[17]. Different isoforms of myosin hydrolyze ATP at different rates. The fast motor protein, α-MHC, hydrolizes ATP 3-7 time faster than the slow motor protein, β-MHC[24-26]. However, maximal force generation is not different between these isoforms[27]. Overall, myosin is a protein centrally involved in the actions of sarcomeric contraction and relaxation.

The ATPase activity of myosin has been reviewed in great deal elsewhere[18, 28]. To emphasize the principles and necessity of this process, the following is only a brief synopsis of the critical aspects of myosin ATPase activities as they occur during muscle contraction and relaxation. The S1 subfragmant of myosin is the functional domain required for binding and processing of ATP and its isomers as well as the cyclical binding and release of actin. In the fully relaxed state when actin and myosin are not in contact, the myosin cross-bridges are in an energized state having hydrolyzed ATP into ADP

and inorganic phosphate (P_i). Thus there is a great deal of potential energy contained within this S1 fragment in the relaxed state of the myofilaments. Upon calcium activation, this energized myosin develops an initial weakly bound association with actin (A-M-ADP-P^i). This weak connection then isomerizes into a strong actomyosin interaction (AM-ADP-P_i). AM-ADP-P_i is then further isomerized in the force generating power stroke that releases the high free energy through release of ADP and P_i. During the power stroke, actin and myosin are tightly bound. Release from this rigor conformation is enabled by the allosteric effects caused by rapid binding of ATP to form actomyosin-ATP (AM-ATP). Importantly, at this stage ATP functions exclusively as an allosteric modulator of actin-myosin interactions and not as an energy source. Upon myosin dissociation from actin to form myosin-ATP (M-ATP), myosin S1 subsequently hydrolyzes ATP into ADP and P_i (M-ADP-P_i) resulting in the cocked highly energized pre-power stroke position. As long as calcium is present for activation of the myofilaments, crossbridge cycling will continue. Relaxation occurs when calcium is removed from the thin filament regulatory protein troponin C and actin binding sites are no longer accessible to myosin. These descriptions of thin myofilament changes during contraction and relaxation are grossly over simplified and greater detail will be provided in subsequent sections to elaborate on specific molecular mechanisms of myofilament contraction and relaxation.

The Thin Filament of the Sarcomere: actin and tropomyosin

The thin filament is comprised of a complex of proteins formed into an allosteric regulatory complex that governs calcium-mediated contraction of the sarcomere[29]. The backbone of the thin filament is composed of polymerized globular actin molecules (G-actin) complexed into an actin parallel pseudodouble helical filament (F-actin)[30-32]. F-actin is composed of two intertwined right-handed helical arrays with each repeat spanning approximately 700 Å and a pitch of approximately 13 monomers per turn[33]. Structural analysis of actin crystals has shown that it has four subdomains that surround a binding pocket for a divalent ion and nucleotide[30, 31]. The atomic model of F-actin derived from X-ray diffraction patterns of oriented actin filament gels shows that the larger subdomains 3 and 4 are axially located and have direct contacts with subdomains 3 and 4 of the second actin strand[32]. The smaller subdomains 1 and 2, located at the periphery and exposed to the solvent, contain the amino and carboxy terminals of actin and are the site for myosin binding.

Located at specific regions and intervals along actin are a number of regulatory proteins. Tropomyosin (Tm) is an elongated protein containing hepta-peptide repeats having the greatest number of contacts with actin along the length of the thin filament[34, 35]. Tm is a largely α-helical coiled-coil dimer about 400 Å long that lies within the groove of the actin filament with each Tm molecule spanning over seven actin monomers[36]. A high resolution crystal structure has shown that the N-terminus of Tm contains a high concentration of alanine residues thought to be critical for the bending of the molecule and the formation

of the coiled coil[37]. Tm molecules interact in a head to tail manner through a single disulfide bridge forming a continuous strand along the entire length of the actin filament[36, 38]. Electrostatic interactions between actin and Tm[32] allow it to shift positions in an azimuthal motion within the actin groove depending on the phase of the contraction cycle[17, 18]. The position of Tm is regulated by a heterotrimeric protein complex called troponin (Tn). Tm is the primary means of potentiating the regulatory actions of Tn to the rest of the sarcomere. However, the structural basis for this regulation of Tm by Tn remains obscure. The stoichiometry of Tm and Tn is 1:1 along the length of the thin filament. Together Tm and Tn regulate about 13 actin monomers and their interaction with myosin[39-42]. Based on X-ray structural studies, it was originally hypothesized that Tm was the molecule primarily responsible for regulating actomyosin ATPase activity, the steric blocking model of muscle regulation[43-45]. More recent evidence, however, suggests that Tm facilitates the transmission of structural changes from one actin monomer to its neighbor along the thin filament during the transitions between diastole and systole[46, 47]. Essentially, Tm acts to amplify on actin the effects of upstream conformational changes caused by troponin, although the specific mechanism of this structural transmission is still unclear. Patchel and colleagues suggest that this transmission of structural changes on actin by Tm enable all actin molecules within a functional unit (1 Tm: 7 actin) to interact (bound or unbound) with myosin in concert depending on the phase of the cardiac cycle. Functionally upstream from these events is the troponin complex, whose

subunits are centrally involved in the regulation of contractile functions of the sarcomere.

The Thin Filament of the Sarcomere: troponin

Setsuro Ebashi was the first to describe the troponin complex over fifty years ago[48] (Figure 1-1). Troponin is a heterotrimeric protein complex comprised of three subunits. These include the Tm binding subunit, troponin T (TnT), the calcium binding subunit, troponin C (TnC), and the actomyosin ATPase inhibitory subunit, troponin I (TnI)[49, 50]. The coordinated actions of the troponin complex are specifically designed to regulate the actions of all other members of the sarcomere in the transition between systole and diastole. Specifically, the mechanism of control by troponin involves a tight regulation of an otherwise highly favorable interaction between actin and myosin in the transition between activated and inactivated cross-bridges. Thus, the troponin complex plays a central role in regulating a system that is, by necessity, highly sensitive to stimulus. Reports of the calcium saturated crystal structures for fast skeletal troponin[51] and cardiac troponin[52] have been instrumental in helping interpret a great deal of functional data on the troponin regulatory complex.

To begin, TnT is considered the structural “glue” that holds all the proteins of the thin filament proteins together due to its interactions with TnC, TnI, Tm and actin[18]. The various isoforms of TnT in different muscle types as well as during various stages of development have been found to play critical roles in regulating

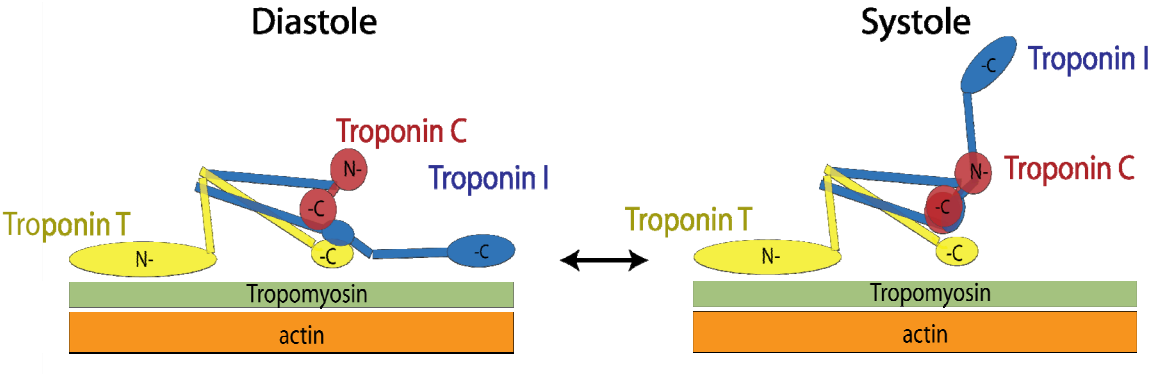

Figure 1-1. Orientation to the troponin complex. The troponin complex is situated on the thin filament and associates in a regulatory fashion with tropomyosin and actin. Schematic diagram showing structural alterations during the diastolic (left) and systolic (right) phases of the cardiac cycle.

calcium sensitivity, activation of actomyosin ATPase activity, and possibly regulate aspects of cooperativity within the thin filament during contraction[53-56]. Mild chymotryptic digestion has shown that TnT is composed of two domains, the extended N-terminal T1 domain (residues 1-158) and the globular C-terminal T2 domain (residues 159-259). The N-terminal T1 domain interacts with the C-terminal region of Tm[57] while the T2 domain interacts with the C-terminal head of TnC and the N-terminus of TnI[58]. Importantly, TnT plays an essential regulatory role in thin filament function by connecting the activities of TnC and TnI relative to the positioning of Tm in the actin groove[59, 60]. Despite our understanding of the important role TnT plays in the thin filament, a great deal of ambiguity remains in regard to the interactions between TnT, Tm, and actin[29]. Of utmost importance to its function, however, is the observation that TnT both increases the inhibition of actomyosin ATPase activity in the absence of calcium *and* augments the contractile response in the presence of calcium[55, 56].

Troponin C (TnC) is a small (18 kDa) protein that is expressed in two isoforms, skeletal TnC (sTnC) and cardiac TnC (cTnC). Although the sequence of sTnC and cTnC are about 70% homologous, the major difference between these isoforms is their calcium binding characteristics[61]. The fundamental role of TnC is to bind calcium, the second messenger that transmits electrical stimulation to sarcomeric contraction. This critical function has been illustrated previously in skeletal muscle depleted of TnC by washing with EDTA[62]. These studies showed that the sarcomere remained permanently relaxed regardless of

the calcium concentration. The calcium responsiveness of the fiber was restored after reconstitution with TnC.

Based on X-ray diffraction and nuclear magnetic resonance spectroscopy (NMR), the TnC structure has been found to be composed of two globular heads connected by a helical linker[63-65]. Based on current studies, it appears the linker domain (helix D and E) allows the two heads of TnC to function independently of each other[64, 66] while keeping the N and C terminal domains within optimal proximity to their target sites on TnI[67, 68]. The contractile function of the sarcomere is dependent on calcium binding to the N-terminal lobe of TnC[69-71]. Together with helix 3 of TnI (residues 150-159), this region of TnC is known as the “regulatory head’ of the troponin complex.

The ability for TnC to bind calcium is based on its structural composition which contains essential EF-hand calcium binding motifs characterized by α-helix loop helix structures[63]. TnC has eight α-helices comprising four calcium binding sites plus one extra helix at the N-terminus (N-helix). The N-terminal regulatory domain of TnC contains binding sites I and II[72]. In cardiac muscle only one of these sites is functional (site II) whereas both sites are functional in the skeletal isoform of TnC[65, 71, 73]. This difference is due to primary amino acid sequence differences between the isoforms at key residues with cTnC having an insertion (V^{28}) and several significant substitutions in the pentagonal bipyramidal coordinating site relative to sTnC (Leu^{29}, Ala^{31} in cTnC compared to Asp^{30} and Asp^{32} in sTnC)[61]. The functional N-terminal EF hand motif of TnC (site II) has a binding affinity for calcium calculated at a K_{Ca} of about $2x10^5$ per mol[71]. Studies

have shown that the acid side chains in the EF hand of site II are highly conserved and involved in coordinating the binding of calcium to cTnC[74]. Site-directed mutagenesis and experiments using fluorescence stopped flow analysis of calcium exchange have shown that calcium binds and releases cTnC site II within the physiologic range[75, 76]. This binding affinity is of critical importance because it allows calcium to bind and release from TnC in direct correlation with calcium cycling in the myocytes on a beat-to-beat basis. As with other calcium binding proteins, the calcium-TnC interaction results in a wide range of structural and energetic changes including exposure of a critical hydrophobic patch[77-79]. Specific details of conformational changes in TnC during calcium binding (systole) will be discussed later. However, in the apo state, when the intracellular calcium concentration is low, the calcium binding sites on NTnC form short β-strands[80] and, importantly, the hydrophobic residues involved in activation of the regulatory arm of TnI remain inaccessible[77]. This closed state is specifically characterized by a close association between the B-C helix and the central helix (D/E) where helices B and D are roughly parallel to each other.

The D-E linker of TnC is a critical region because of its largely electrostatic interactions with TnI during the transitions between systole and diastole. Studies by Kobayashi et al have performed mutagenesis experiments and assessed actomyosin ATPase activity to show that acidic residues within this region of TnC are required for actomyosin activity. Specifically, they found that alanine mutagenesis of E85 and D86 retained complete inhibition of actomyosin ATPase activity in the presence and absence of calcium[81]. Whether this was due to

disruption of calcium binding to TnC was not clarified. Additional mutagenesis studies with the inhibitory region of TnI have shown the importance of the interaction between TnI IR and the TnC D-E linker (to be discussed) for the regulatory functions of Tn.

The C-terminal domain of TnC has two corresponding EF hand motifs (sites III and IV), however, the function of these sites are thought to be mostly structural, providing an important role in anchoring TnC to the thin filament[82]. More specifically, these sites have a much higher affinity for calcium (K_{Ca} $2x10^7$ per mol) and for magnesium (K_{Mg} $5x10^3$ per mol)[71] and, in accordance with this, kinetic analysis has shown that these sites are constitutively bound with a metal ion under normal physiological conditions[62, 83].

Fluorescence has been used as a methodology to study TnC function in regard to calcium binding and dissociation kinetics by linking TnC to IAANS, an environment sensitive fluorophore which covalently alkylates protein sulfhydryl groups via its iodoacetamide functionality[84]. It has been shown[85] that the IAANS fluorescence of labeled WT cTnC increases by about 60% with Ca^{++} binding to site II. This provides an effective means of measuring changes in calcium binding to cTnC by means of changes in fluorescence. Furthermore, studies in which either Cys35 or Cys84 was substituted with serine demonstrate that the IAANS label at Cys84 alone is responsible for this fluorescence change in isolated cTnC[86, 87].

Toponin I (TnI) is the Tn subunit responsible for inhibition of actomyosin ATPase activity[88]. In all vertebrate chordates, there are three genes that encode

three different TnI isoforms, the slow skeletal (ssTnI), fast skeletal (fsTnI), and cardiac (cTnI). In the heart, the slow skeletal isoform is expressed during embryonic development and transitions to the adult cardiac isoform around the time of birth[2, 89]. In humans this isoform transition occurs during the first year of life[90]. Details of these biochemical and functional differences in these isoforms will be discussed later. As proposed by Farah and colleagues[33] and confirmed more recently in structural studies[52], TnI is situated in the Tn complex such that it interacts in an anti-parallel orientation with TnC with the N-terminal domain of TnI engaging with the C-terminal domain of TnC. The fundamental function of TnI is to transmit calcium binding on TnC to other units of the thin filament. Essentially, TnI acts as a calcium dependent molecular switch of the thin filament making it a critical protein involved in this interdependent allosteric regulatory complex[9, 91-93]. Despite extensive biochemical studies on TnI, much remains unknown about certain structural characteristics of this protein and, functionally, how it interacts with other members of the thin filament.

Seminal work in recent years has provided important structural information about troponin I[52, 94-98]. The first domain of TnI is the N-terminal cardiac-specific extension (cNTnI, residues 1-43). Syska and colleagues showed that this region of TnI binds to TnC[99]. It has subsequently been shown, using recombinant TnI molecules, that this interaction is independent of calcium[55, 100]. One of the critical characteristics of the N-terminus of cTnI is the presence of PKA-dependent serine phosphorylation sites (S23/24). Fundamentally, the phosphorylation status of cTnI (occurring in response to adrenergic signaling in the myocyte) has

significant structural and functional effects on the N-terminal lobe of TnC that effect the calcium sensitivity of the myofilament[93, 101-104]. Cross linking studies have shown that cTnI (residues 1-29) interacts with the N-terminus of TnC[105, 106] and phosphorylation of cTnI effects this interaction[102]. However, the binding of calcium to the N-terminus of TnC is not affected by changes in the interaction between TnC and cTnI mediated by phosphorylation events[102]. Furthermore, both cTnI (residues 1-29) and residues from the switch arm of TnI (residues 147-163) can simultaneously bind TnC in the presence of calcium. The current model by which cTnI modulates calcium sensitivity in response to adrenergic signaling is by depressing the affinity of the switch arm of TnI for the calcium saturated hydrophobic patch of TnC[102, 107]. Let it be known, however, that there are disagreements about this which have been outlined in previous studies and reviews indicating the need for further investigation on this matter[108, 109].

Beyond the N-terminal extension of cTnI, the first α helix of TnI (H1, residues 43-79) binds the C-terminal domain of TnC through multiple polar and van der Waals interactions. The C-terminal region of H1 (residues 66-79), a flexible linker (residues 80-89) and the second α helix of TnI (residues 90-135) wrap around the H2 helix of TnT (residues 226-271) and interact by multiple hydrogen bonds and hydrophobic interactions, thus forming a hydrophobic core. A critical component of this domain is the coiled-coil formed by the H2 helix of TnI and H2 helix of TnT that form inter-chain contacts. These interactions are well conserved across species reinforcing the important functional and structural characteristics of this region[52]. TnC also converges with the TnI and TnT in this

domain making it a tripartite interaction (termed the IT arm). Crystal structure and solution experiments have suggested that the conformational state of the ion bound C-terminus of TnC opens the hydrophobic patch of TnC such that it binds the N-terminal amphiphilic α-helix of TnI as well as the H2 helix of TnT thus anchoring TnC to the rest of the troponin complex[52, 95]. The IT arm is thought to remain unchanged as a unit regardless of the concentration of intracellular calcium or the physiological state of the myofilaments (contracted or relaxed)[52]. Although the IT arm is thought to be a rigid structure, recent studies by Sun and colleagues have found that the domain does toggle during the phases of the cardiac cycle based on its sensitivity to myosin head binding[66]. This study also showed that, when contraction is blocked, the position of the IT arm is only mildly effected by the binding of calcium and significant conformational changes of the N-terminal lobe of TnC. Together these findings indicate that the IT arm is involved in cross-bridge dependent activation and not the calcium-mediated response of the myofilaments. Lastly, there is no evidence to date that the IT domain interacts with any other thin filament proteins such as tropomyosin or actin[52] suggesting that this region is crucial only for transfer of energy within the Tn molecule between phases of the cardiac cycle. Lastly, in terms of the inhibitory role of TnI, early biochemical studies using recombinant fragments showed that the N-terminal region of TnI up to residue 102 were not necessary for the complete inhibition of actomyosin ATPase activity[55].

Beyond the IT domain is a basic inhibitory region (IR) (residues 137-148). The IR region through to the C-terminus of TnI (residues 137-210) is considered

the regulatory domain (TnI_{reg}) due to its central role in the allosteric functions of the TnI. The IR region is the first actin binding domain but is poorly defined in the crystal structure suggesting significant flexibility[52, 110-113]. These observations have been confirmed by cross-linking and Förster resonance energy transfer (FRET) experiments showing the IR region to exist in a flexible β-hairpin during diastole[114]. Interestingly, a truncated TnI molecule containing only the minimal IR region (residues 138-147) was found to recapitulate the actin inhibitory and Tm accentuating functions of the full TnI molecule illustrating the importance of this region in TnI function[47]. Proton NMR spectroscopy and cross-linking studies have suggested that the IR region of TnI binds the N-terminus of actin at sites also implicated in myosin S1 subfragment binding during cross-bridge activation[115]. More recent structural studies using peptide fragments have gone further to show that a significant conformational change occurs in actin upon the binding of the IR region of TnI during diastole that fully impedes the binding of myosin to actin[46, 47]. Additionally, the three-dimensional reconstructions from electron micrographs fitted with the atomic model of actin show that Tn binds the N-terminus of actin during relaxation of the myofilaments[116]. As mentioned previously, these structural changes on the actin surface are propagated along from monomer to monomer within a functional actin unit (as defined by the distribution of 1 Tm along 7 actin monomers) by Tm. Thus, during diastole, the specific interactions between Tn, Tm, and actin coordinately prevent actomyosin activity with the IR region of TnI playing a central role in the blocked state of the myofilament. A recent study by Kobayashi et al using alanine scanning across the IR domain has

shown that residues L145-R149 are required for activation of the myofilaments[117]. In other words, when these residues are substituted for alanine, TnI continues to inhibit actomyosin ATPase activity even in the presence of calcium. This raises an important question regarding the role of these IR residues play in 1) actin binding for inhibition of cross bridge cycling and 2) binding of TnI IR to the D/E linker of TnC. These data would suggest that the IR domain (145-149) is more involved in the electrostatic interactions with TnC as opposed to actin.

The IR region of TnI is followed by a switch domain (or, mobile domain) that begins with the amphiphilic helix H3 (residues 150-159) and continues through helix 4 (residues 164-188) and the C-terminal domain (residues 192-210). The flexibility of TnI, a hallmark of this protein, is exemplified in this mobile domain, aptly named because even in the absence of calcium this region remains highly mobile[118]. Rarick and colleagues have shown that two independent actin binding sites exist on TnI between residues 151-210[119, 120]. This TnI domain is positioned on azimuthally related actin monomers similar to other actin binding proteins such as caldesmon in smooth muscle thin filaments (which lack Tn)[121, 122]. During diastole, the primary function of this region is to provide a second actin and Tm binding site for TnI. Consistent with this, a recent study showed that a truncated cTnI molecule (containing residues 1-193) had increased actin-activated S1 ATPase activity[123]. By docking the switch arm of TnI into the cryo-electron micrograph map of the thin filament, Murakami and colleagues were able to visualize the atomic structure of this region to the level of

single amino acids[124]. Together with previous studies, they show that actin and TnI interact weakly in this region despite the formation of numerous salt bridges. This weak contact likely explains the observation that no conformational changes in the surface structure of actin occur in the interaction between TnI and actin in this domain. In contrast to the role of the IR region in actively inhibiting myosin-actin interactions by alterations of the actin surface structure as discussed above, the binding sites between actin and the regulatory arm of TnI are distinct from the attachment sites of the myosin head. In fact, three-dimensional EM reconstructions of actin filaments decorated with myosin light chain showed that the interactions between these molecules occurred at the C-terminus of actin, exactly where the mobile domain of TnI was found to interact[124, 125]. Additionally, previous studies have shown that when peptides associated with the second actin binding domain of TnI are mixed with actin or actin-Tm, myosin does not dissociate from the actin binding sites[47]. As such, several hypotheses have been proposed regarding the function of this domain. It is thought that this region does not act to specifically inhibit actomyosin ATPase activity but, rather, limits the possible configurations of the C-terminus of TnI during diastole. Thus, the C-terminal actin binding sites on TnI make the relaxed state more robust: a “fail-safe molecular latch”[124]. Another hypothesis proposed by Kobayashi and colleagues is that this second actin binding site on TnI increases the local concentration of the TnI molecule for actin. This would facilitate the critical interaction between actin and the first actin binding domain of TnI in the inhibitory region (IR)[126, 127]. The interaction between Tm and the C-terminus of TnI is also a

key component of this thin filament regulation. Recent studies using electron micrograph image reconstruction on filaments saturated with a construct representing the C-terminal domain of TnI indicate that TnI competes with Tm for binding sites on actin thus shifting Tm into the blocking position[122].

Overall, it has been proposed that the Tn complex as a whole plays a critical role in stabilizing a more rigid conformation of the thin filament during the blocked state which is released during calcium activation of the myofilaments[122]. Specifically, it is thought that TnI, acting as a molecular tie, straddles the two long pitch strands of actin thus increasing the rigidity of this complex[122, 128, 129]. Bringing the thin filament proteins together, it seems that both steric and allosteric effects of multiple myofilament proteins (e.g. cTnI-actin and TnT-actin-Tm) converge to inhibit the actomyosin binding sites on actin during diastole.

Whole Organ and Cellular Transitions between Systole and Diastole

Given the above detailed analysis of myofilament proteins that compose the sarcomere, the following discussion outlines the specific processes that are involved in the transition of these proteins during the systolic and diastolic phases of the cardiac cycle. These subcellular events, including calcium cycling and myofilament responses to calcium, will provide context for descriptions of whole organ cardiac function. Although the correlation between cellular and whole organ functionality is very complicated, the correlate of LV pressure is sarcomere tension, and that of LV volume is sarcomere length. The relationship

between LV pressure (tension) and volume (length) is the basis of Starling's law of the heart. Consistent with this, classic experiments on the Frank-Starling response by Gordon and colleagues [130] illustrated that the sarcomere length-tension relationship was based on characteristics of thin and thick filament overlap. Specifically, it was observed that optimum myocyte force generation was reached when sarcomere lengths reached a specific point that maximized thin and thick filament interactions. In addition to the thin and thick filaments, numerous other proteins (e.g. titin) are centrally involved in regulating the Starling response by modulating the distensibility and tension dynamics of the myocyte and whole heart[4].

Several methodologies have been put to use in the studies composing this dissertation to experimentally investigate the process of cardiac whole organ as well as myocyte contraction and relaxation in the context of health and disease. To study whole organ cardiovascular performance *in vivo,* mice were instrumented with a 1.4 F Millar conductance micromanometry catheter. To understand the fundamental kinetics of calcium cycling and myocyte function, adult rat myocytes were isolated, exposed to adenovirus for gene transfer, and cultured for study using various *in vitro* cellular analytical techniques. The specific details of *in vivo* and *in vitro* study of cardiac physiology are well established by the Metzger laboratory as outlined extensively by studies outlined in this dissertation as well as previous reports (for example[24, 131-133]).

To provide sufficient background for the forthcoming studies, the following discussions will outline the critical actions of calcium cycling followed by an

integration of concepts involving whole organ hemodynamics as well as the molecular biophysics of myocyte function during contraction and relaxation.

Calcium Cycling

Cardiac excitation-contraction coupling is the mechanism by which the heart undergoes cyclic contraction and relaxation during each beat. Calcium mediates the transmission of extracellular depolarization to intracellular myofilament activation[134]. A number of excellent reviews have been written on calcium handling in the myocytes[134-137] as only a brief overview is discussed here. Upon stimulation by an action potential, membrane depolarization causes an influx of calcium through the L-type calcium channel (LTCC). This local concentration of calcium causes an opening of the ryanodine receptor (RyR) in a mechanism termed calcium induced calcium release. The RyR is the pore through which all of the calcium stores of the sarcoplasmic reticulum (SR) are released into the myoplasmic space. This alters the cytoplasmic calcium concentration from sub-micromolar during diastole to micromolar during systole. The primary target of this calcium is the thin filament protein Troponin C (TnC) which enables activation of the sarcomere. The events leading to this point occur during the systolic phase of the cardiac cycle.

As calcium stores are reduced in the SR, the RyR is inactivated leading to the subsequent resequestration events during the diastolic phase of the cardiac cycle. Several mechanisms are involved in the removal of calcium from the

myoplasm. The most significant mode of calcium resequestration is through the Sarco(endo)plasmic reticulum calcium ATPase pump, SERCA2a. Closely associated with SERCA2a, phospholamban is a negative regulator of SERCA ATPase activity and is itself functionally responsive to β-adrenergic signaling. Another mechanism of calcium removal from the myoplasm is the sarcolemmal sodium-calcium exchanger, NCX. The relative contributions of SERCA2a and NCX in calcium removal are species dependent. The periodic calcium oscillations, mediated by these various regulatory proteins, are called calcium transients and fundamentally determine the systolic and diastolic phases of the cardiac cycle. Among various mammalian species, machanisms of calcium regulation via various channels is widely varying.

Overview of Cardiac Contraction and Relaxation

At the onset of systole, myocardial stimulation is initiated at the sinoatrial node of the heart and directed through the atrioventricular node and to the rest of the myocardium through the Purkinje fibers. From the hemodynamic standpoint, this myocardial stimulation begins the stage of isovolumic contraction where the LV contracts against the closed aortic valve (afterload). At the level of the myofilaments, sarcomere tension increases but length does not change during this phase of the cardiac cycle. It has been proposed by Wolff and colleagues that K_{tr} (the rate constant reflecting the cross-bridge cycling kinetics) may limit the rate and extent of ventricular pressure development during isovolumic

contraction[138]. This is based on the observation that calcium transients are significantly shorter in duration than the tension development. When pressure in the LV exceeds that in the aortic root (usually around 120 mmHg) the valve opens, pressure plateaus, myofilaments contract, and LV volume decreases by ejection through the aorta. The transition from systole to diastole occurs somewhere around the point preceding aortic valve closure when pressure in the aortic root exceeds pressure generated by the ventricle. Hemodynamically, this point is characterized at the point of end systolic pressure and end systolic volume. The onset of relaxation requires the re-sequestration of calcium into the SR, however, the specific mechanisms of relaxation at the myofilament level remain very unclear. Although calcium removal is unequivocally required for relaxation, myofilament characteristics have been found to be rate limiting. Strong evidence of this has been shown by studies revealing the myosin isoforms significantly affect the rate of relaxation[139]. Furthermore, studies have demonstrated that enhanced relaxation is more closely correlated with cross-bridge cycling kinetics than calcium dissociation from TnC[140, 141]. Similar to systole, relaxation begins with a period of isovolumic pressure decay as pressure in the LV exceeds that of the mitral valve. When atrial pressure rises above ventricular pressure (very close to 0 mmHg), LV volume rapidly increases in the filling phase of the cardiac cycle. From the myofilament standpoint, sarcomere length increases with a mild increase in tension until end diastolic volume and pressure are reached and the cardiac cycle begins again at the onset of systole.

The hemodynamic relationship between pressure and volume (or myofilament length and tension) as outlined by Starling's law of the heart, can be analyzed *in vivo* by altering venous return. Briefly, Starling's law states that within the physiologic range there is an inexorable correlation between pressure (tension) and volume (length) and the performance of the heart involves a constant synchronous adjustment of these parameters during any given heart beat depending in response to changes in preload. Experimental analysis of this relationship is accomplished by occlusion of the inferior vena cava which feeds venous blood back to the heart via the right atrium. Reducing preload directly impacts the function of the LV as illustrated by a sudden collapse of the PV loops during this manipulation. A line drawn through the end systolic pressure and volume during collapse of the PV loops provides insight into the load-independent function of the heart (the end systolic pressure volume relationship). Specifically, hearts that are performing well and have a broad dynamic range of activation of the myofilaments will have a steeper slope. In contrast, hearts that are injured or performing poorly will have a shallower slope indicating a blunted range of myofilament performance.

Although other models exist, the widely prescribed view of muscle regulation is grounded in a three state description of the molecular mechanism of myofilament function first proposed by Hill and colleagues in 1980 and elaborated upon since[142-145]. As the name suggests, this model delineates three different states of the myofilaments during the cardiac cycle. These states include the blocked state (B) reflecting full steric block of actomyosin ATPase

activity; a closed state (C), reflecting the formation of weakly bound cross-bridges; and an open state (M) reflecting strongly bound actin-myosin cross-bridges associated with sarcomeric contraction.

In the B state (diastole), when cytoplasmic calcium concentrations are sub-micromolar, the regulatory site on Tn is closed and Tm is positioned at the outer domain of actin sterically blocking actomyosin crossbridge formation. In the C state, when calcium is released from the SR, conformational changes in Tn cause Tm to move closer to the inner domain of actin allowing for weak, non-force generating but stereo-specific interactions to occur between myosin and actin. Using electron microscopy and 3-D reconstruction of the thin filament, Lehman et al have shown that TnI actively regulates azimuthal movements of Tm in the transitions between the B and C states[146, 147]. Kinetics of myosin S1 binding indicate that the B and C states are not entirely distinct events. Rather, findings show that during relaxation of the myofilaments (diastole), about 50% of the cross-bridges are in the B state and 50% in the C state[148]. The transition from the C state to the M state is thought to rest entirely on the kinetics inherent in cross-bridges and is dependent on the load of the muscle[22, 149]. The M state is characterized by strong force generating cross-bridges forming between actin and myosin with subsequent sarcomeric contraction. Importantly, cooperativity within and among neighboring regulatory units has been found to be a central characteristic of myofilament function[17, 18, 145]. This propagated activation of the sarcomere seems to be of particular importance in cardiac muscle. Specifically, evidence has shown that small changes in strongly bound cross-bridges

markedly increase the calcium sensitivity of force and cross-bridge kinetics in the myocardium[150, 151]. Lastly, experimental studies suggests that active, force-generating cross-bridges of the M state extend beyond the loss of bound calcium, a finding that has significant implications on the duration of cardiac ejection and the timing of myocardial relaxation[22, 152]. Even so, calcium dissociation from TnC is ultimately required for relaxation of the myofilaments in anticipation of a second contractile stimulus[76, 153]. The myofilament proteins (with a major focus on the thin filament) involved in this process as well as the specific structural features of the sarcomere during the phases of relaxation and contraction are outlined in further detail as follows.

Myofilament Structural Changes During Systole

As discussed in detail above, the systolic phase of the cardiac cycle is initiated upon depolarization of the myocyte and the subsequent flux of calcium ions out of the sarcoplasmic reticulum into the cytosol. The direct target of this calcium for activation of the myofilaments is the the N-terminal domain of TnC. As originally proposed by Herzberg and colleagues[63, 153], calcium binding fundamentally changes the structure of TnC from the apo “closed” conformation, its thermodynamic nadir, to the calcium saturated “open” conformation. Interestingly, the “open” configuration of cTnC is markedly different from that of sTnC and appears to contribute to the wide range of isoform specific differences between skeletal muscle and cardiac muscle that result in fundamentally different

myofibrillar dynamics[17, 18]. The following discussion focuses on the current understanding of cTnC during systole. Various studies have established that calcium binding to site II at the N-terminus of cTnC is solely responsible for initiating processes involved in sarcomeric contraction[71, 85]. However, the calcium sensitivity of the regulatory domain of cTnC is highly dependent on other myofilament proteins. For example, a very recent study using a reconstituted thin filament containing an IAANS labeled cTnC and a truncated cTnI has shown that the C-terminal domain of TnI (193-210) is a negative regulator of calcium binding to TnC under normal physiologic conditions[123]. Furthermore, solution studies have shown that binding of cTnC to cTnI and cTnT increases the calcium binding affinity of cTnC by at least an order of magnitude primarily due to a slowing of the calcium dissociation rate[85, 154, 155]. Studies have also shown that the cooperative binding of calcium to TnC only occurs when the Tn complex is fully incorporated into the thin filament[126, 156]. This further suggests that feedback mechanisms between Tn, actin, and Tm are of critical importance proper calcium activation of the myofilaments. Binding of calcium to the regulatory domain of cTnC results in a wide range of structural and energetic changes[78, 79]. These changes include a decrease in the flexibility of the backbone of cTnC and a more rigid loop in the defunct calcium binding site (site I)[157]. The binding of calcium to site II, however, is considered a priming of cTnC for binding of the regulatory arm of cTnI because this event does not provide enough activation energy to fully open the hydrophobic pocket of cTnC[64].

With the change in the structure and biochemistry of the calcium-bound N-terminal region of TnC, the switch arm of TnI develops an affinity for cTnC measured as an increase of two orders of magnitude[158]. Förster resonance energy transfer (FRET) experiments have shown that the movements of the regulatory arm of TnI during systole and diastole are essential for the transmission of the calcium signal to the rest of the myofilament proteins[159, 160]. This increased affinity causes a translocation of the entire regulatory arm of TnI and binds with cTnC by multiple van der Waals contacts[52, 161]. With this important role, TnI has come to be known as the molecular switch of the myofilament[9]. According to the 'drag and release' model for myofilament regulation of contraction[29], calcium induces a movement of the switch domain of TnI toward the N-terminal lobe of TnC, dragging along the downstream actin binding domain and ultimately releasing the inhibition on actin. The 'drag and release' model suggests that TnC and actin compete for the binding of the regulatory arm of TnI. This model has also recently been supported by Xing et al using FRET analysis of fluorescence quenching between labeled residues on the C-terminus of actin (C374) relative to Cys-modifed residues on the C-terminus of cTnI[162]. Fundamentally, this translocation and the subsequent interaction between TnI (residues 150-166) and cTnC during systole is a requisite step in developing enough energy to complete the opening of the hydrophobic patch (e.g. Met[45, 60, 80, 81]) on cTnC[163, 164]. Interestingly, Bell and colleagues recently reported that the calcium-dependent structural transitions of TnC also precede force development[165]. This supports the hypothesis that these initial events during

systole involving calcium and TnC are not the rate limiting steps of contraction. Studies have also shown that the rate of thin filament activation by calcium is independent from and thus does not impact cross-bridge cycling kinetics[166]. Specifically, studies where calcium-induced conformational changes were measured in conjuction with force development have shown that calcium binding kinetics to be much faster than cross-bridge cycling[167]. Other studies have countered this assertion. Specifically, Regnier et al have shown using photolysis of caged calcium that the rate of calcium induced sarcomere contraction (K_{Ca}) was significantly slower than the rate of force re-development (K_{tr})[168]. These data suggest that there is some relationship between calcium activation of thin filament regulation and thick filament force development.

Based on the crystal structure of the calcium saturated troponin complex, helix 4 and the C-terminus of TnI during systole are found to form a protruded and extended α-helix with no direct interactions with the rest of the molecule[52]. Indeed, Takeda et al found that this region of TnI (residues 164-210) did not crystallize well due to a high degree of flexibility. Interestingly, despite the continuing struggle to acquire structural information about the C-terminus of cTnI, Xing and colleagues have shown by FRET analysis that the C-terminus is very stable [162]. Specifically, they analyzed the distribution of inter-site distances between the C-terminus of actin (C374) and sites on the C-terminus of cTnI (188C and 210C) as a surrogate indicator of conformational flexibility. They found that regardless of calcium activation and myosin S1-ADP binding, the conformational flexibility of the C-terminal domain of cTnI was more stable than

regions more N-terminal (131C, 151C, 160C, and 167C). Of further importance, this study also showed that the inter-site distance between C374 on actin relative to the most C-terminal labeled residues on cTnI (188C and 210C) did not translocate as far as residues in the middle of the switch domain (e.g. 167C) in the transition from diastole to systole (e.g. relative to C374 on actin, cTnI C210 shifts 10.2 Å compared to 19.9 Å for 167C). It is difficult to interpret these findings given that numerous studies have shown that the C-terminal region of TnI is highly unstable[9, 52]. In fact, recently Hoffman and colleagues used measures of intrinsic disorder to show that the C-terminus is disordered in all TnI isoforms[169].

The toggling of the switch arm during systole and diastole is thought to be critical in altering the conformational state of the inhibitory region (IR) of TnI, the domain centrally involved in regulating actomyosin ATPase activity[33, 55]. With the translocation of TnI_{reg} this IR region transitions from a β-hairpin to an extended α-helical structure[52, 170]. Correlatively, the IR region has been shown to bind to actin during diastole and to TnC during systole. However, the specific site of interaction between TnI IR and cTnC during systole is unclear at this point. Various studies have shown TnI IR binding to the N-terminus[171, 172], the C-terminus[173], or the linker region between the domains[114]. Differences in experimental methodologies and/or peptide fragments used likely account for these observations. Although direct interactions have been difficult to identify, recent functional studies have found the D/E linker of TnC to be necessary for activation of the myofilaments. Specifically, several groups have found that mutation of various acidic amino acids in this region to neutral residues

completely blocked the ability for calcium to activate the myofilaments[81, 174, 175]. This indicates that these specific resides play a key role in the intermolecular dynamics of the troponin complex required for actomyosin ATPase activity.

With the switch arm of cTnI bound to the calcium saturated N-terminal hydrophobic patch of cTnC and the translocation of the IR domain into its α-helical position away from Tm and actin, Tm is released from its blocked position leading to an azimuthal motion around the actin filament thus uncovering the essential myosin binding sites required for actomyosin ATPase activity and sarcomeric contraction[23, 43, 176]. Because weak ionic interactions between myosin and actin occur independent of calcium, the actomyosin cross-bridges are poised for activation just prior to systole with the products of ATP hydrolysis remaining in the myosin head. Upon calcium activation of the myofilaments, force generation by the sarcomere is mediated by a strong hydrophobic interaction between myosin and actin and a subsequent isomerization of the myosin head by release of a phosphate[177]. The specific biophysics of cross-bridge cycling are complex and have been discussed in detail elsewhere and are beyond the scope of this discussion[16, 18, 19, 145, 178, 179]. It has been proposed that the rate limiting step of sarcomeric contraction could be the transition from weak to strongly bound cross-bridges as proposed by Moss and Stehle[19, 180] or the process of phosphate release from the myosin head as proposed by Hinken[22, 181]. Illustrating the cooperative nature of thin filament activation, this azimuthal motion of cTm is thought to extend beyond a single stoichiometric unit of the thin filament and thus, may weaken the actin-cTnI interactions on neighboring units[156, 182].

Recent studies have also shown that myosin binding to actin has a major reciprocal effect on calcium sensitivity of the thin filament and cooperativity of the sarcomere[22]. Evidence suggests that the binding of myosin to actin further displaces Tm from its blocking position which would then displace actin bound TnI[122]. By facilitating the dissociation of TnI from actin, myosin indirectly causes a transient increase in calcium sensitivity (approximately six fold)[156, 165]. However, the specific mechanism for this is unknown. Davis et al. and others have suggested that the myosin-actin interaction may cause structural changes in actin thus moving cTm and, subsequently, increasing the cTnC-cTnI binding probability[122, 156]. The importance of myosin binding has been further confirmed recently in studies showing that full activation of the thin filament requires calcium and rigor myosin S1[183]. More recent studies have also elucidated some very interesting dynamics between myosin and actin during myofilament activation. Several studies have shown that the structural states of the seven actin monomers in a regulatory unit are not identical[145, 184, 185]. These studies suggest that myosin preferentially binds halfway between the Tm-Tm overlap region close to where Tn sits on the thin filament. A functional explanation for these observations in the context of myofilament cooperativity was not elucidated. Based on the intramolecular kinetics of calcium activation in the sarcomere described here, contractility of the filaments is literally transmitted in a highly cooperative manner providing the molecular basis of the cell and whole organ systolic actions of the heart.

In looking at the kinetics of force activation, it has been observed that k_{ACT} (the force development following maximal calcium activation) as well as the k_{TR} (rate constant reflecting the cross-bridge cycling kinetics) are not limited by the activation of the thin filament by calcium[186, 187]. Furthermore, substitution of native Tn with cardiac Tn or a Tn chimera containing ssTnI in rabbit psoas myofibrils markedly effects Ca^{++} sensitivity and cooperativity of force generation but does not affect force activation kinetics[186]. Together these findings provide strong evidence for the role of isometric cross-bridge turnover rates as limiting determinants of myofilament activation.

Myofilament Structural Changes During Diastole

Diastole begins when myoplasmic [Ca^{++}] begins to decrease which initiates the dissociation of cross-bridges and the onset of force decay. Three different stages of diastole can be attributed to the process of sarcomeric relaxation including calcium decay (primarily mediated by re-sequestration into the SR via SERCA2a or extrusion through the sarcolemmal membrane via NCX), the kinetics of myofilament inactivation, and cross-bridge kinetics(reviewed in[11, 188]). The interdependence of these processes and the inherent coordinated activities of the myofilaments has made it difficult to specifically elucidate the relative contributions of the component parts. Although the processes of contraction have been fairly well characterized, the events occurring during relaxation are less well understood. In all myofibril types studied to date,

relaxation has been observed to be biphasic with an initial, slow, linear phase followed by a fast, mono-exponential relaxation phase when isometric sarcomere conditions collapse[186,187].

Although calcium is required for relaxation of the myofilaments, the resequestration of calcium is not correlated functionally with relaxation of the sarcomere. Studies using various methodologies have shown that the fall in thin-filament bound calcium precedes the fall in force in an isometric twitch of heart muscle[188-190]. Specifically, in studies using the stopped flow apparatus to measure changes in calcium dissociation from Cys^{84} IAANS labeled TnC or Trp fluorescence changes in TnC^{F27W} found that the off rate of calcium from the regulatory domain of TnC were at least an order of magnitude faster than the mechanical relaxation of the myofilaments[191-193]. Essentially, force relaxation lags behind diminution of the calcium transient.

These findings indicate that the rate limiting step of sarcomeric relaxation is myofilament inter and intra-protein structural transitions. To address this issue in the context of thin filament proteins, a very recent study by Xing et al used FRET calcium titration and FRET stopped-flow measurements to examine structural changes that occur between thin filament proteins induced by calcium dissociation[194]. Their results suggest a two phase transition at the interface between TnC, TnI, and actin. The first transition shows fast kinetics (132-147 s^{-1}) correlated with the closing of the N-terminal lobe of TnC and interaction between the C-terminal regulatory region of TnI and actin. The second transition shows slow kinetics (56-69 s^{-1}) and is correlated with movement of the TnI inhibitory

region (IR) from TnC to actin. It was proposed that the flexibility of the mobile domain of cTnI (165-210) contributes to the fast kinetics of the first phase by binding to actin which then facilitates the dissociation of the regulatory arm of TnI from the hydrophobic patch of TnC. These data would suggest that the marked delay in cross bridge inhibition after calcium dissociation is due, at least in part, to the delayed kinetics of the TnI IR release from TnC and binding to actin observed in the second phase of thin filament deactivation.

Janssen et al have previously shown using phase plane analysis of calcium versus force at physiologic temperatures that cross-bridge cycling kinetics are rate limiting for cardiac relaxation[195]. Specifically, as opposed to other myofilament proteins (e.g. TnC or TnI), the critical role of activated actomyosin ATPase in regulating the cooperative nature of the myofilaments makes the dispersion of cross-bridges a major rate limiting step in myofilament relaxation[188, 189, 196, 197]. This is supported by the recent study by Xing et al showing that binding of S1 to thin filament proteins markedly reduced the kinetics of the first and second phases of thin filament inactivation[194]. Maughan has argued that myosin release from actin at the end of the power stroke is likely the rate limiting step[16]. Consistent with this, many have argued that the rate limiting step of sarcomeric contraction and relaxation shifts depending on the load[16, 149, 198]. Specifically, kinetic studies have shown that the greater the force developed during a single beat (in direct correlation with the number of strongly activated cross-bridges), the longer the cooperative ensemble of myofilament proteins can maintain force and the longer the delay in relaxation[149]. In support of this

paradigm, some forms of heart failure are characterized by slowing of the calcium transient such that calcium removal becomes the rate limiting step[199]. SERCA2a dysfunction and reduced protein level have been implicated in these findings[137, 200]. In these cases the proportion of cross-bridges attached would remain in equilibrium with the proportion of regulatory sites still bound with calcium thus causing calcium decay and myofilament relaxation to mirror each other.

In addition to the actin-myosin interactions as rate limiting for relaxation, the molecular kinetics of myosin function also markedly affect the process of myofilament relaxation. Similar to studies on MHC isoform dependence of myofilament activation[21, 24], it has also been found that cardiac muscle expressing α-MHC relax several times faster than those expressing β-MHC[139, 150].

At the whole organ level in vivo or the working heart ex vivo, it is repeatedly observed that the rate of pressure decay during diastole (- d*P*/d*t*) is not markedly different than the positive rate of pressure development (+ d*P*/d*t*) during systole. In contrast, at the isolated myocyte level, calcium decay is observed to occur much slower than calcium release from the SR. As model predictions suggest[123], if whole organ functional kinetics of contraction and relaxation were to follow calcium cycling, then isovolumic relaxation (- d*P*/d*t*) should occur much slower than the rate of positive pressure development (+ d*P*/d*t*). It has been suggested that the observed rapidity of isovolumic relaxation at the whole organ level favors the argument for unique sarcomere dynamics in

hastening the rates of cross-bridge detachment during relaxation independent of calcium kinetics[123].

Protein Kinase Modulation of Cardiac Systolic and Diastolic Performance

Beyond the intrinsic biophysics of myofilament function during systole and diastole, there is another level of regulation at the level of the myocytes that modulates calcium handling and myofilament function in response to various stress signals. Unlike skeletal muscle, which is able to alter speed and force by recruiting different muscle fibers, the heart requires a coordinated interaction of the molecular machinery in the myocytes to alter whole organ cardiac function in response to external cues. Covalent modifications of specific intracellular protein targets by kinases are at the core of this regulation in the heart. There are multiple pathways known to modulate myocyte function, the most well studied of which include phosphorylation of protein kinase A (PKA) and protein kinase C (PKC).

β-adrenergic signaling acting through PKA is a primary means by which the heart modulates cardiac inotropic and lusitropic function to meet whole animal physiological demands during stress. On the basis of numbers, the β_1-adrenergic receptor predominates in cardiac muscle[201]. The ligands responsible for mediating these responses are catecholamines, epinephrine and norepinephrine. At the whole organ level, adrenergic stimulation results in increases in contractile parameters (e.g. the rate of LV pressure development

(+d*P*/d*t*) and ejection fraction) heart rate, stroke volume, cardiac output, and relaxation parameters (e.g. -d*P*/d*t* and tau)[132]. At the cellular level, treatment with a β-adrenergic agonist such as isoproterenol has similar effects in hastening calcium cycling as well as augmenting myofilament activation and relaxation[202]. This response illustrates the presence of a cardiac reserve available to meet hemodynamic demands placed on the heart. In light of this, pharmacologic suppression of adrenergic drive (experimentally or therapeutically) has significant implications on the hemodynamic readout of cardiovascular performance[203]. Specifically, in experimental settings described here, there is a decrease in contractile parameters and heart rate, dilation of the ventricle, and prolongation of relaxation parameters. These global responses are mediated by the following events that are regulated at the subcellular level.

The major response of the heart to adrenergic stimulation is activation of the G(s)-adenylyl cyclase-3',5'-adenosine monophosphate (cAMP)-protein kinase A (PKA) signaling cascade. The downstream targets of this signaling result in the phosphorylation of numerous proteins including the sarcolemmal L-type calcium channel which increases calcium influx into the cell, phospholamban which releases its inhibition of SERCA2a and thus increases the rate of calcium reuptake during diastole, troponin I which decreases myofilament calcium sensitivity, and the ryanodine receptor which enhances calcium release from the SR. Although a brief overview will be given below, adrenergic signaling has been reviewed in detail elsewhere[204, 205]. Drugs used to manipulate this response both clinically and experimentally (as outlined in this dissertation), include β-

adrenergic suppression by esmolol or β-adrenergic stimulation using dobutamine. Esmolol specifically blocks β_1 adrenergic receptors thus inhibiting the targeting of endogenous catecholamines. Dobutamine, in contrast, directly stimulates β_1 adrenergic receptors resulting in a sympathomimetic effect.

Troponin I is one of the critical targets of PKA phosphorylation. Ser23/24 at the N-terminus of TnI have been found to markedly regulate myofilament function based on alterations in their phosphorylation status[206]. Although differences have been shown (likely attributable to types or stages of heart failure)[207], studies indicate that there is a reduction in phosphorylation at these sites in the failing heart[208-210]. In response to adrenergic stimulation, phosphorylation of Ser23/24 of TnI results in a weakening of the interaction between the N-terminal domain of cTnI and the N-terminus of TnC[108, 211]. This destabilizes the calcium bound state of TnC and results in a desensitization of the myofilaments to activating calcium as well as an increase in cross-bridge cycling kinetics[123]. Studies of Tg mice with cardiac expression of slow skeletal TnI, which lacks the N-terminal 32 amino acids present in cTnI, have shown that this substitution blunts the PKA-mediated response of the heart[212]. Due to the critical importance of this cTnC-cTnI interaction in contributing to hastened lusitropy during β-adrenergic stimulation, ssTnI Tg mice have significant diastolic dysfunction[213]. This dysfunction is evident at baseline because adrenergic drive is naturally very high in the resting mouse. Tg mice expressing ssTnI were also shown to have a blunted inotropic response which[212], together with other

studies[140, 205, 214], points to the critical role of cTnI phosphorylation in regulating cardiac performance.

In an alternative approach, cardiac specific expression of cTnI with a Ser23/24Asp modification, which mimics constitutive phosphorylation, were shown to have enhanced LV inotropy and lusitropy[215]. Yasuda et al have also recently supported these findings using these cTnI S23/24D Tg mice as well as gene transfer strategies to show a central role for the N-terminal domain of cTnI in regulating cardiac lusitropic performance[202].

There is also evidence to suggest that S23/24 phosphorylation on TnI by PKA results in a positive inotropic effect. Studies have shown that PKA phosphorylation increases the cross-bridge cycling rate and shortening velocity[140, 213, 214, 216]. Several studies have tried to address the role of TnI. Layland and colleagues studied the adrenergic responsiveness of Tg mice expressing ssTnI, which lacks the N-terminal PKA phosphorylation sites. They found that inotropic indices were markedly attenuated in Tg mice compared to Ntg mice during adrenergic stimulation[212]. Other studies using Tg mice with pseudophosphorylated cTnI PKA sites exhibited markedly enhanced systolic performance at baseline[215]. Although these data are very preliminary, it suggests that covalent modifications of TnI enhance both lusitropic and inotropic myofilament performance.

In addition to PKA modulation of myocyte function, protein kinase C (PKC) has also been coupled with regulation of heart performance[9, 217-219]. In contrast to a fairly well understood mechanism involving adrenergic regulation through PKA,

PKC signaling is not well understood[205]. Part of the complexity arises from the numerous PKC isoforms that have been reported all of which may have overlapping and/or specific effects[9, 205]. PKC is activated in response to G-protein coupled receptor agonists such as angiotensin II, endothelin-1, and the α-adrenergic agonist phenylephrine. Numerous intracellular targets are phosphorylated by PKC including the L-type calcium channel, cTnI, cTnT, and MLC2[220-223]. Under pathophysiological conditions such as heart failure, PKC expression is increased[224]. The known targets of PKC phosphorylation on TnI include S23/24, S43/45, and T144[222, 225]. The effect of S23/24 phosphorylation has been discussed already in terms of PKA and shows similar effects on relaxation in the context of PKC phosphorylation[219, 221]. The effect of PKC-mediated phosphorylation at S43/45 and T144 are not well understood. However, studies have suggested that S43/45 phosphorylation results in a decrease in maximum calcium activated force and cross bridge cycling rate[226-228]. Covalent modification of T144 has been shown to decrease myofilament sliding velocity and may contribute to the relaxation effects observed with S23/24 phosphorylation[221, 226]. The current evidence suggests that PKC and PKA have somewhat opposing effects. Furthermore, the combined effects of PKA and PKC modulation reveal a significant level of fine-tuning required for proper myofilament function.

Responses and Adaptations to Acute and Chronic Cardiac Stress

In the United States, a CVD related death occurs once every thirty-five seconds. By 2020, the prevalence of CVD is expected to increase to three fourths of all deaths in the U.S. and become the leading cause of morbidity and mortality world-wide[14, 229]. Coronary artery disease is the greatest contributor to cardiomyopathies associated with CVD and is also the most common cause of heart failure[230]. Furthermore, heart failure is the most common discharge diagnosis in the U.S with greater than 1 million people suffering from this disease[231]. Despite considerable advances in medical technology and pharmacologic and mechanical therapeutics, the overall risk of mortality and sudden cardiac death related to coronary artery disease and heart failure remain high[232, 233].

Acute myocardial infarction, a pathology associated with coronary heart disease, is caused by clot formation within a ruptured atherosclerotic plaque, which obstructs blood flow to the region of the heart distal to the site of occlusion. This acutely compromises regional cardiac contractility and increases the risk for arrhythmias and heart failure. In severe cases, cardiac dysfunction results in chronic ischemic cardiomyopathy and congestive heart failure. Pathologies associated with other organ systems but which have a significant effect on cardiac performance include sepsis[234] or severe chronic pulmonary artery disease (COPD)[235]. Common to all of these conditions at the outset is the development of severe acidosis due to reduced plasma oxygen tension (hypoxic acidosis), as in cases such as myocardial ischemia[230, 236], or accumulated levels of plasma carbon dioxide (hypercarbia), as in cases of COPD. Despite the

etiological basis, it has been well established that acidosis has deleterious effects on the contractile function of the heart[237-242]. More specifically, the studies in this dissertation as well as others show that the myofilaments play a central role in the response to cardiac injury[242]. An understanding of the underlying dysfunction associated with this and other types of cardiomyopathy provides a substrate on which current research can investigate novel therapeutic modalities[131].

Effects of Acidosis on Myofilament Function

Cardiac contractile dysfunction can result from a wide range of pathophysiological conditions ranging from acute ischemic events to chronic heart failure. At the molecular level, some of the central deficiencies of the heart that give rise to poor cardiac performance are mishandling of calcium cycling or an inability of the myofilaments to properly respond to calcium signals. Murphy and others have reported that altered phosphorylation, proteolytic degradation, or oxidative damage may be specific mechanisms by which myofilament and calcium handling proteins may be modified causing a decrease in systolic and diastolic performance of the heart[242, 243]. In any case, there is an uncoupling of the normal coordination required between excitation and contraction necessary for proper heart function. In cases such as myocardial ischemia, this uncoupling occurs primarily as a result of acidification due to reduced blood supply to the highly energetic heart tissue[231]. Studies have shown that the myocardial pH drops from 7.0 during normal function to about 6.2 during acute ischemia[237].

Acute pump failure arises in these cases because the myofilaments have reduced responsiveness to normal or even heightened levels of activating calcium[237]. Although the events that give rise to cardiac pump dysfunction during disease are complex, it has long been argued that the myofilaments play a central role[238, 241, 242, 244-246]. Studies supporting this hypothesis have shown that oxidative or proteolytic modifications of myofilament proteins may contribute to the observed decline in cardiac function during ischemia or acidosis[243, 247, 248]. Furthermore, studies using acutely isolated adult rat myocytes have shown that the tension-pCa curve undergoes a marked rightward shift during acidosis[133]. Specifically, studies have shown that the pCa (-log[Ca^{2+}]) required for 50% activation of myofilaments in acutely isolated adult cardiac myocytes, which express the adult isoform of TnI (cTnI), drops by more than 1 pCa units during acidification of pH (from pH 7.0 to 6.2)[133]. Furthermore, acidosis decreases both maximal Ca^{2+}-activated tension and the Ca^{2+} sensitivity of tension as represented by a rightward shift of the calcium dependence of force development at low pH[236, 246, 249-252]. Decreases in myocyte maximal sarcomere length shortening amplitude and shortening velocity are also found to occur during acidosis[246, 253, 254]. These experiments illustrate that myofilament Ca2+ desensitization at low pH is a fundamental molecular deficiency responsible for myocyte and myocardial dysfunction associated with myocardial acidosis[242].

Clearly, there is a long history of experimental evidence showing that low pH effects myofilament function at the cellular level and pump performance at the whole organ level. But, beyond these gross observations what is the underlying

molecular deficiency that disrupts proper myofilament protein-protein interactions? Several key studies have provided significant insight into this question. Very early solution studies suggested that the calcium binding to cTnC could be the rate limiting step in maintaining myofilament functionality and, furthermore, that low pH directly effects this critical interaction[255, 256]. Further evidence for a Ca^{++}-TnC interaction issue arose from studies showing that higher proton concentrations (reduced pH) decreased the reactivity of Ca^{++} coordinating oxygens within the regulatory sites of TnC[257].

To further address this question, Parsons and colleagues[238] used a technique in which cTnC was labeled at cysteine 84 with IAANS. They showed that changes in fluorescence directly paralleled the changes in force in these TnC-depleted cardiac fibers indicating a tight correlation between calcium binding to cTnC and activation of the myofilaments. When these fibers were placed under acidic conditions (pH 6.5), the force-pCa and fluorescence-pCa curves underwent a marked rightward shift thus changing the pCa_{50} for both curves to higher [Ca^{++}]. From these studies, it can be concluded that acidosis decreases the Ca^{++} affinity for the regulatory sites on cTnC in a reconstituted cardiac muscle preparation. To look more specifically, the context within which TnC functions significantly influences the Ca^{++}-TnC interaction. Other variables to account for are: TnC isoforms and their different affinities for Ca^{++}, the influence of different TnI isoforms, as well as myosin cooperativity and its distant allosteric affects on calcium binding to TnC. Although numerous studies have addressed the pH

sensitivity of different TnC isoforms[245, 258, 259], the following discussion will focus on the allosteric effects of myosin and different TnI isoforms on TnC function.

Very early kinetic studies by Moss[260] and Ebus[261] showed that there is a pH dependence of cross bridge formation in slow-twitch, fast-twitch, and cardiac muscle. Consistent with prior discussions on the cooperative nature of the myofilaments, it is reasonable to hypothesize that decreased actin-myosin interactions at low pH would further exacerbate this reduction in calcium affinity for TnC. To specifically address the role of actin-myosin interactions on Ca^{++}-TnC interations, Parsons and colleagues treated their myofibers with 2,3-butanedione monoxime (BDM) which specifically inhibits steady state force development by stabilizing weakly attached working cross-bridges[262]. They found that treatment with BDM did not affect the force/fluorescence relationship of TnC at low pH. These data suggest that the primary deficiency of myofilament functionality in acidosis is a decreased affinity of Ca^{++} for TnC. As illustrated by these and other studies, the problem is multifaceted where low pH impacts various aspects of the contractile apparatus resulting in diminished sarcomeric contractile performance.

In addition to the role of myosin on regulating the affinity of calcium for TnC, other avenues of investigation have focused on the role of TnI on modulating this Ca^{++} - TnC interaction. Several important reports have studied various isoforms of TnI (ssTnI, fsTnI, and cTnI) in the context of different TnC isoforms (sTnC and cTnC). This discussion will focus on the effects of different TnI isoforms on cTnC. Studies by Wattanapermpool and Solaro assessed the role of ssTnI on the binding affinity of calcium to cTnC in column chromatography

purified preparations of thin filament proteins[263]. Similar to Parsons et al, calcium binding was assessed using an IAANS labeled cTnC. They found that both ssTnI and cTnI resulted in a rightward shift in the fluorescence-pCa curve at low pH. However, this shift was attenuated in the ssTnI-cTnC complex. Furthermore, although the fluorescence-pCa titration curve shifts when cTnC is placed in the context of TnI or TnI-TnT-Tm, the shift in pCa_{50} between pH 7.0 and 6.2 does not change. This indicates that although TnT and Tm influence the calcium binding affinity to TnC, these proteins do not confer a pH dependent affect on calcium sensitivity of cTnC. In contrast, the TnI isoform alone contributes this pH dependent effect. These conclusions were more recently confirmed by Liou et al using porcine cardiac muscle reconstituted with *N*-(1-pyrene)iodoacetamide (PIA) labeled TnC and either ssTnI or cTnI[264].

Additional studies have gone on to analyze specific regions of the TnI molecule in conferring the effect of pH on the calcium sensitivity of TnC. Initially, Guo and Solaro[265] used a truncated cTnI molecule missing 32 amino acids at the NH_2 terminus. They found that there was no difference in the pH effects on calcium sensitivity between myofilaments containing WT cTnI and the amino-truncated form of TnI. These data indicate that a region C-terminal to this domain is responsible for the pH dependent effect of TnI on the calcium sensitivity of TnC. This was corroborated by Westfall and colleagues using TnI chimeras[93, 266] (discussed later) and more recently by studies from Li and colleagues[267]. Similar to ssTnI, fsTnI confers protection of the calcium binding to cTnC at low pH. To address the domains of TnI involved in this effect they used the following TnI

chimeras: cardiac-N:Ip:fast skeletal C and fast skeletal N:Ip:cardiac C. They found that IAANS labeled TnC in complex with fsN:Ip:cC had the same calcium binding affinity as TnC_{IA}-cTnI. In contrast the cN:Ip:fsC construct in complex with TnC_{IA} attenuated the rightward shift in the ΔEC_{50} similar to that seen with TnC_{IA}-fsTnI. To further validate the importance of the C-terminal domain in conferring this pH-dependent effect, they measured Ca^{++}-force relations in skinned fiber bundles in which cTnI was replaced with the chimeras. The ΔEC_{50} values for the Ca^{++}-force titration curves directly reflected the ΔEC_{50} values for the Ca^{++}-fluorescence curves for TnC_{IA}. These data provide strong evidence for the C-terminal domain of TnI influencing the calcium binding properties of TnC at physiologic and low pH. However, further assays are required to define particular residues that may be involved in this interesting observation.

Cardiac Compensation to Stress and Injury

The primary response of the heart to significant injury such as myocardial infarction is structural compensation to maintain proper function. This process is regarded as myocardial remodeling. Every cardiomyopathy, regardless of its etiology (acquired or inherited), results in some kind of remodeling of the heart. The following is a brief discussion that focuses primarily on some general observations regarding post-infarct remodeling, although the process of acute and chronic myocardial remodeling can take various forms especially regarding

the transition into heart failure. Broader reviews on this topic have been published previously by Swynghedauw and others[12, 242].

In its most general sense, cardiac remodeling is seen as a process of rearranging normally existing structures to compensate for the emergence of injury or stress related dysfunction. Remodeling of the whole organ occurs because of adaptations developing at the level of the myocyte and the extracellular matrix, as well as in neurohormonal inputs which influence but are external to the heart. Initially, these changes help retain proper cardiac function by means of myocardial changes (to maintain Starling's law and whole organ economy), peripheral adaptations, and increased sympathetic drive. Over time, global changes associated with cardiac remodeling include, for example, myocyte hypertrophy, ventricular fibrosis (due to ischemia, inflammation, and hormone affects), and cell death. In the context of myocardial infarction, akinetic or dyskinetic regions of the heart result in volume-overload induced hypertrophy of the noninfarcted myocardium. In this context, systolic dysfunction emerges due to the loss of contractile force and diastolic dysfunction occurs as a result of reduced elasticity of the myocardium limiting its relaxation performance[11, 198]. Hemodynamically, these adaptations result in increased end diastolic pressure and delayed tau as well as reduced positive and negative pressure derivatives and increased end systolic volume. Over time, these acute changes that occur to maintain pump performance (such as hypertrophy) transition from a compensated heart to a de-compensated heart, seen as a transition into failure. This transition results from the cumulative effects of collagen deposition

throughout the heart as well as apoptosis causing dilation of the ventricle and the emergence of pathophysiological changes in the heart. This dysfunction at the level of the heart ultimately effects the function of other organ systems. One of the key implications of poor cardiac performance on peripheral organ systems is characterized by severe fluid retention (i.e. tachypnea, edema, and liver congestion).

It has been well documented that many of the structural changes of the myocyte in response to stress are the result of alterations in gene expression profiles[12, 268, 269]. The fetal gene program is so named because of the strong correlation with genes attributed to cardiac development. Alterations in gene expression associated with this stress response program include myosin heavy chain isozyme shifts[270], as well as up-regulation of ANF, and BNP[271, 272]. Alternatively, genes that are down-regulated include the SR calcium ATPase (SERCA2a)[273] and its regulatory protein phospholamban[273-276] as well as expression of the β-adrenergic receptor[277]. The loss of these proteins is a consistent finding across species and is implicated, at least in part, in the contractile dysfunction, impaired cardiac reserve, and propensity for arrhythmias during heart failure[242, 278-281]. Metabolically, the heart has been shown to transition from fatty acid oxidation to glycolysis in response to stress[282-284]. Lastly, it has been proposed that certain (unknown) genes that respond to stress signals of the heart regulate changes in myocyte morphometry during cardiac remodeling whether in terms of LV hypertrophy (building sarcomeres in parallel) or LV dilation (building sarcomeres in series)[285]. This latter process of myocyte

elongation occurs during cardiac development and thus it is consistent that such transitions occur during failure in concordance with fetal gene activation.

One of the significant causes of pathologic cardiac decompensation is chronic cardiac stimulation by catecholamines. In response to an initial stress, this response is important for maintaining cardiac performance. However, evidence has shown that the cardiac response to chronic sympathetic stimulation is reduction of β-adrenergic receptor density as well as uncoupling of the G_s-protein-adenylyl cyclase pathway[286]. More specifically, studies have shown that chronic β-adrenergic stimulation due to unmitigated stress switches the signaling cascade from the mediating effects of PKA to Ca^{++}/calmodulin-dependent protein kinase II (CaMKII) which leads to apoptosis and maladaptive remodeling[201, 204]. In vitro studies by Zhu and colleagues have shown that this process occurs by PKA-independent influx of intracellular calcium through the L-type calcium channel thus activating CaMKII in cardiac myocytes[287]. Both aging and disease such as congestive heart failure are clinical settings in which there is chronic sympathetic activity[10, 286, 288]. This data supports the current hypothesis that constitutive activation of β-adrenergic signaling in the aging or injured heart contributes to the transition from compensatory remodeling to decompensated cardiac remodeling in the etiology of heart failure.

Preliminary Arguments: Inotropic Therapy by Calcium Sensitization of the Myofilaments

Based on our understanding of the pathophysiology of heart failure, it has been suggested that novel therapies could be directed specifically toward improving the Ca^{2+} sensitivity of the myofilament[289]. The consequent improvement in contractility that results from an increase in Ca^{2+} sensitivity may appear to counter the logic of commonly prescribed therapeutics, which calls for the use of beta blockers to decrease contractility, allowing for reduced oxygen consumption and energy expenditure. Although there is proven value in the diverse effects of beta blockers, we have shown, conversely, that targeted alteration of myofilament calcium sensitivity to increase contractile performance is an effective mechanism for treatment of ischemic heart disease and heart failure[203, 242, 246, 290]. Others have supported this hypothesis, recognizing that augmentation of myofilament responsiveness to calcium would improve the force generating capacity of the sarcomere and thus redress global cardiac dysfunction[291]. Altering the functionality of troponin I, the calcium-mediated molecular switch of the myofilament, would be an effective means of specifically improving calcium sensitivity.

Studies have shown that force development in healthy myofilaments is only about 20-25% of maximum which indicates that inotropic agents targeted at augmenting sarcomeric contraction may be an efficacious therapeutic approach[292]. Current thoughts regarding the general failure of exisiting inotropic therapeutics are aimed at their propensity to increase activator calcium, worsen arrhythmias, activate maladaptive signaling pathways, and increase energy utilization in the failing heart[242, 293-295]. Preliminary evidence, however, has

emerged using a new class of inotropic drugs termed calcium sensitizers[291]. These drugs are aimed at influencing the manner in which intracellular calcium is transduced into muscle contraction. As opposed to targeting extracellular receptors (e.g. β-blockers) which have diverse targets, calcium sensitizers have been designed to modify myofilament function by interacting with proteins involved in regulating force production (e.g. motor proteins or troponin).

One of the myofilament targets for calcium sensitizers has been the interaction between the N-terminal hydrophobic patch of TnC and the switch peptide of TnI. One such drug is bepridil which binds to TnC and induces an open configuration of the N-lobe similar to that caused by calcium binding[296]. Li and colleagues hypothesized that bepridil acts as a calcium sensitizer by slowing down both the closure of the hydrophobic patch on TnC and the dissociation of the TnI switch peptide upon calcium release from site II of TnC[296]. Other calcium sensitizing drugs that target alternative sites within the sarcomere include the pyridazinone-dinitrile derivative levosimendan and the thiadiazinone EMD-53998[289, 291, 297-302]. Despite their utility as inotropic agents, these drugs also have off target effects including inhibiting cAMP phosphodiesterase activity or inhibition of ATP-sensitive potassium channels[291]. Even so, studies of these molecules support the hypothesis that calcium sensitization of the myofilaments may be a more advantageous strategy for ameliorating systolic dysfunction in heart failure.

Histidine Buttons as Molecular Biosensors

Regulation of molecular function through pH responsive histidine buttons are found throughout various physiological systems. At the level of individual molecules these moieties can function as a molecular switch by changing intermolecular or intramolecular contacts by differential ionization states that are pH-dependent. Through tertiary structural modifications, changes within a molecular micro domain can subsequently be transmitted to remote regions of the protein to transmit energy required to carry out important functions. The capacity for histidine to function in this way is a consequence of its unique imidazole side chain which ionizes within the physiologic range (pK≈6.0). The different ionization states of histidine are chemically different. Under normal pH (7.4) the imidazole group is largely not protonated making it hydrophobic and aromatic. Acidosis (pH 6.2) causes histidine to become protonated and thus acquire a hydrophilic and positively charged character. As a consequence of these two biochemical states, different ionization states of histidine enable it to alter its molecular interactions. Histidine buttons act as a molecular rheostat capable of altering protein function in response to environmental pH changes.

The important actions of the molecular switch behavior of histidine residues continue to emerge. To my knowledge, histidine buttons were first identified in hemoglobin nearly three decades ago[303-305]. In hemoglobin, a single histidine moiety (H146β) has been found to regulate the Bohr effect through the pH-dependent interaction with D94β[303, 304]. This event enables hemoglobin to

raise the fraction of oxygen carried that can be released in peripheral tissues. Further confirmation of the importance of this intermolecular contact has been shown by mutagenesis studies. Any substitution that replaces H146β or D94β dramatically reduces the alkaline Bohr effect[303].

The intermolecular and intramolecular contacts that mediate the switch function of histidine buttons markedly impact the propensity for histidine ionization. Studies by Perutz et al indicate that the interaction of H146β with D94β markedly increases the pKa of the imidizole side chain[303]. Furthermore, studies of sperm whale myoglobin have shown that most histidine buttons have a pK_a ranging from 6.73 to 5.43[303]. In contrast, only one histidine residue studied (H36) had a pK_a of 7.97 because of a key salt bridge interaction with an acidic residue (E60). These data provide important insights into how histidine buttons are modified through specific interactions in their protein micro domain.

In addition to hemoglobin and myoglobin, numerous other proteins have been found to contain histidine buttons that provide important functional characteristics to the molecule. HLA-DR contains pH-responsive molecular switches that control the stability of ligand complexes[306]. The key interaction within this molecule was found to occur between H33α and V136α[306]. The channel activation of G-protein coupled inward rectification potassium channels (GIRK) is dependent on several pH responsive histidine residues (H64, H228, and H352) in the M1-H5 linker[307]. Similarly, a histidine (H117) in the M1-H5 linker in the inward rectifier potassium channel HIR was found to modulate conductance through this channel[308].Zong and colleagues have shown that a

single histidine residue (H321) localized between the voltage sensing S4 helix and the cytoplasmic S4-S5 linker determines the pH sensitivity of the pacemaker channel HCN2[309]. Lastly, studies have shown that a pH responsive histidine (H98) near the pore selectivity filter regulates current in the tandem pore domain acid-sensitive potassium channel (TASK-3)[310].

Taken together, these studies show the critical importance of histidine moieties in regulating physiological functions within a wide range of proteins. By differential ionization of the imidazole side chain, histidine residues can interact with various amino acids to generate unique switch functions. As in the case of myoglobin described above, different types of interactions cause nuanced effects required for coordinated functions of a protein[303]. Another histidine button has been identified within an isoform of troponin I. The studies outlined in this dissertation are designed to address the basic physiology as well as therapeutic benefits of this residue on myofilament function.

Myofilament Biosensors: a histidine moiety in cardiac troponin I

In the heart of mammals and avian species two isoforms of TnI are expressed in a developmentally regulated manner[311]. The slow skeletal isoform (ssTnI) is expressed during embryonic development but, in the rodent, transitions to the adult cardiac isoform (cTnI) around the time of birth[312]. In other species the regulation of this isoform transition has been found to be different where, for example, in humans the transitions begins before birth and continues through the

first year[90, 313]. Although ssTnI and cTnI isoforms have 70% sequence homology[242], they are structurally and functionally unique. There are marked differences in baseline function as well as in several key responses to physiological stress. Specifically, these include the response to adrenergic stimulation as well as the effect of acidosis on TnI performance.

The functional differences between hearts expressing ssTnI or cTnI have been well characterized[133, 213, 252, 263, 266, 267, 314-318]. These functional differences are observed in terms of both inotropy and lusitropy. Studies looking at myofilament contractility have shown that ssTnI causes a dramatic increase in the inotropic capacity of the sarcomere compared to cTnI. The steady state isometric tension-Ca^{2+} relationship undergoes a marked leftward shift with ssTnI compared to cTnI[133, 252]. This indicates that sensitivity of the myofilaments to activating calcium is increased by ssTnI. Studies of intact myocytes have shown that sarcomere dynamics also reflect this increased inotropy as measured by a significant increase in the sarcomere length shortening amplitude with ssTnI compared to cTnI[252]. Furthermore, recent biochemical studies using cystine-53 labeled IAANS on TnC in the context of ssTn or cTn provided additional evidence supporting the conclusion that ssTnI has higher calcium sensitivity and lowers the TnC calcium dissociation rate compared to cTnI[156]. In conjunction with increased contractility, myocytes expressing ssTnI show significantly delayed relaxation. This has been shown in isolated myocytes and in the intact heart where various relaxation parameters indicate diastolic dysfunction with ssTnI compared to cTnI[213, 252].

In terms of adrenergic responsiveness, cTnI contains a 32 amino acid extension at its N-terminus that contains two key serine residues (23 and 24) required for phosphorylation by cyclic AMP (cAMP)-dependent protein kinase A (PKA) during β-adrenergic stimulation. Phosphorylation at these residues causes a decrease in myofilament calcium sensitivity that facilitates relaxation of the myofilaments[104, 202, 319]. This enhancement of relaxation occurs in tight conjunction with changes in calcium handling[320-323]. Specifically, phosphorylation of numerous calcium handling proteins, such as phospholamban, enable calcium cycling to occur at a faster rate. The coupling of calcium and myofilament dynamics are designed to meet contractile requirements of the mammalian heart during increases in chronotropic frequency in the heart rate[322].

Alignment of ssTnI and cTnI protein sequence shows that this critical extension containing the dual serine phosphorylation sites is absent in ssTnI. Although TnI functions in close relationship with TnT and TnC, studies have shown that the lack of this N-terminal extension of ssTnI in the context of cTnT and cTnC causes reduced responsiveness to β-adrenergic stimulation that is almost entirely attributed to the TnI isoform[316]. Functionally, the loss of PKA responsiveness on TnI causes E-C coupling to be inefficient because the myofilaments lack the capacity to relax in coordination with enhanced calcium cycling[202].

Another major difference between ssTnI and cTnI is their myofilament calcium sensitivity. Specifically, studies using adenoviral-mediated gene transfer into acutely isolated rat cardiac myocytes have shown a heightened calcium

sensitivity in response to acidosis in ssTnI transduced myocytes compared to those expressing cTnI[133]. Specifically, ssTnI expressing cardiac myocytes show an attenuated pCa shift during acidification of pH (from pH 7.0 to 6.2)[133]. These findings have been supported in studies using adult Tg mice expressing ssTnI instead of cTnI which had the capacity to protect cardiac pump function in response to severe acidosis and ischemia/reperfusion injury[297, 318]. Taken together, the findings of these biochemical and physiological studies clearly show a dominant effect of ssTnI as a pH dependent molecular rheostat capable of enhancing cardiac myofilament calcium sensitivity in response to acidic pH[324].

With this understanding, seminal work was carried out to identify the region(s) of ssTnI and cTnI responsible for the functional differences between these isoforms. Close analysis of the amino acids in the C-terminal domain of TnI showed a net positive charge difference of +3 in ssTnI compared to cTnI[33]. It was hypothesized that this difference could, at least in part, account for the difference in functional performance between these isoforms[242]. To investigate this further, chimeric TnI molecules were generated wherein the N-terminal region of one isoform was combined with the C-terminal domain of the opposite isoform[266, 314, 319]. These studies revealed that a significant portion of calcium sensitivity of ssTnI was localized to the C-terminal domain. Additional studies have also mapped out the TnI inhibitory region[99, 111-113] and actin binding domains of TnI[91, 119]. Specific amino acids in the C-terminal domain of TnI were suggested by Pearlstone et al based on biochemical assays analyzing the interaction between TnC and various TnI peptide fragments[325]. The residues suggested to be critical

for the functionality of the cTnI C-terminus included Q157, A164, and E166 (corresponding residues in ssTnI: R125, H132, and V134).

To study the effects of these residues on cTnI and fsTnI function, Dargis et al generated mutants of these TnI isoforms and assayed their effects based on actomyosin S1ATPase activity[249]. Their results show a cTnI Q155R/A162H/E164V markedly decreased the acid sensitivity of cardiac Tn. Further assays of single and double amino acid substitutions attributed this resilience to changes in pH to the A162H modification. In contrast, the Q155R/E164V double mutant behaved like WT cTnI. The reverse mutation in a reconstituted fast skeletal muscle troponin system (fsTnI H130A) had a reciprocal effect of increasing the sensitivity to acidosis. Similar to the role of histidine residues in the molecular switch function of other proteins[306, 326], these assays provided evidence for a dominant effect of a histidine button in TnI that modulates calcium sensitivity of troponin. However, ATPase activity may not be an accurate reflection of function in physiologically relevant systems such as intact myocytes or the whole heart where force development can be directly measured. More recent work described below, provides substantial evidence outlining the role of a histidine button in TnI based on *in vitro* and *in vivo* assays[246, 252].

Subsequent mechanical and functional studies showed that a histidine button engineered into the 164 codon of cTnI in place of alanine (cTnI A164H) confers the same biochemical resistance to acidosis in the adult heart[246, 249]. A seminal work by Day and colleagues used a transgenic mouse expressing cTnI

A164H in the heart and showed remarkable protection from various cardiac pathophysiological challenges[246]. In this study they showed that adult mice expressing cTnI A164H under control of the α-MHC promoter had stoichiometric replacement of about 80% of native cTnI in the heart. Using the Langendorff isolated heart preparation, cTnI A164H hearts perfused with acidic buffer performed markedly better than Ntg hearts. Additional Langendorff experiments showed that hearts expressing this histidine button had markedly improved systolic performance during ischemia and nearly full recovery of developed pressure during reperfusion. Of particular interest, these studies showed that Tg hearts were able to recover diastolic pressures at near baseline levels during reperfusion whereas Ntg hearts remained in a state of contracture. The basis of this protection of diastolic function, also observed in several other studies outlined in this dissertation, will require more data to fully understand. *In vivo* cardiac conductance micromanometry analysis was also performed on these hearts to assess hemodynamic function under various stress such as hypoxia and acute ischemia induced by ligation of the left anterior descending coronary artery (LAD). During hypoxia, hearts expressing this histidine-modified cardiac troponin I maintained cardiac performance and survived on average threefold longer than Ntg counterparts. Similar findings were shown with acute ischemia where cTnI A164H Tg mice had elevated ejection fraction and stroke work compared to Ntg mice. Additional experiments showed that cTnI A164H Tg mice had improved cardiac contractility and reduced post-infarct remodeling in a model of chronic heart failure induced by LAD ligation. Lastly, failing human

myocytes transduced with an adenoviral vector expressing cTnI A164H showed improved measures of contraction and relaxation as well as enhanced force-frequency response. Together, these seminal findings provided a strong basis to argue for the role of enhancing myocardial performance in the context of various cardiac pathologies by molecular manipulation of myofilament pH sensitivity through this histidine-substituted cTnI molecule.

In cardiac troponin I, this histidine substitution (A164H) is positioned in the regulatory domain between the amphiphilic switch region (helix 3) and the C-terminal actin binding domain (helix 4). Previous studies have shown that this region is critically involved in the interaction between TnI and TnC during systole through the electrostatic binding of the switch region of TnI with the calcium saturated N-terminal hydrophobic patch of TnC[52, 96-98, 327]. The potential implications of an ionized histidine in this position of TnI could either strengthen interactions with acidic residues on TnC or, alternatively, weaken interactions with basic residues on actin, as previously suggested[246, 249]. Although further studies are required to address the specific biophysical consequences of these potential interactions, the biochemical and physiological implications of this histidine modification have shown that cTnI A164H acts as a molecular rheostat maintaining systolic and diastolic pump function in models of severe acidosis[246, 249].

In more recent studies by Westfall et al., site directed mutagenesis was performed to engineer single amino acid substitutions of key residues in the C-

terminal domain of ssTnI (in isolation and in combination) to create a detailed functional map of the important domains involved in regulating the functionality of TnI under physiologic and acidic environments[252]. In support of findings by Dargis[249], a key finding from these studies showed that a single amino acid modification from a histidine to an alanine at position 132 of ssTnI fully converted the ssTnI to cTnI in measures of myofilament calcium sensitivity and sarcomere dynamics. This was manifest by a rightward shift of the tension-pCa curve, reduction in the sarcomere length shortening amplitude, and enhanced relaxation. Furthermore, the ssTnI H132A mutant eliminated the resilience of myofilament contractility at pH 6.2 based on an assay measuring isometric Ca^{2+} -activated tension development[250, 252]. The presence of other residue substitutions together with H132A (e.g. ssTnI QAE) did not have an additive effect on the single mutant suggesting that the H132A modification has a dominant effect.

In addition to the H132 residue, it was found that other single amino acid substitutions in residues in the H4 domain were involved in modulating TnI function under physiologic and acidic conditions (e.g. V134E and N141H). Assays with the ssTnI V134E mutant resulted in a shift of the pH-dependent calcium sensitivity of tension similar to cTnI and ssTnI H132A. In conjunction with this, the V134E mutant was found to decrease the sarcomere length shortening amplitude very similar to the cTnI control myocytes (physiologic pH). However, this mutant did not affect the relaxation parameters compared to ssTnI. Further c-terminal from the V134E mutation, the ssTnI N141H mutant was found to decrease the pCa_{50} of tension at physiologic pH. In terms of sarcomere

dynamics, the N141H mutant did not markedly impact sarcomere shortening but enhanced the relaxation capacity of ssTnI closer to cTnI (physiologic pH). Taken together, this study provided important insights into residue effects in the c-terminal region of ssTnI at the level of single myocytes function.

It is interesting to note that studies of single or multiple amino acid substitutions in the switch domain of TnI[246, 249, 252] do not always predict their affects within the context of different isoforms. This provides strong evidence for the importance of domain effects on residue function that together modulate troponin performance.

Recent publication of the crystal structures for the calcium saturated cardiac troponin [52]and fast skeletal troponin[51] complexes have helped explain some of the functional differences between these isoforms. Molecular modeling analysis of the regulatory domain of troponin showed a marked alteration in the position of TnI helix 4 between sTnI and cTnI relative to helix A and the hydrophobic patch of TnC (see chapter 5). The structural alignment of these crystal structures indicates that cTnI Q156 and ssTnI R125 on H3 have similar positioning in the two complexes. At the linker and into H4, cTnI A163, E165, and H172 in H4 translocate away from helix A and the hydrophobic patch of TnC. In contrast, H132, V134, and N141 of skeletal TnI curve directly across helix A of TnC and come into very close proximity to the key acidic residues (E14, E15, E19, and D25) that decorate the hydrophobic patch of TnC. In particular the skeletal Tn structure indicates that the distance between H132 and E19 is close enough to develop a salt bridge (3.05 Å). This suggests that an electrostatic

interaction between histidine (H132) of sTnI and glutamate (E19) of s/c TnC, two oppositely charged and hydrophilic residues, is a critical feature that influences structure and function of sTn compared to cTn.

The subsequent studies outlined in this dissertation provide new and important evidence elaborating our understanding of physiology of TnI function as well as the therapeutic role of a histidine button engineered into the adult cTnI isoform. The first study is the first phylogenetic meta-analysis of proteins comprising the cardiac troponin complex. This study provides evidence of coordinated modifications within troponin during chordate evolution of the mammalian cardiovascular system. The second chapter reveals a critical role for cTnI A164H in protecting cardiac function in a mouse model of age-induced cardiomyopathy[290]. The third study provides important insights into the role of cTnI A164H in protecting cardiac performance in a model of severe hypercapnic acidosis[203]. These chapters support a therapeutic role for cTnI A164H as a molecular biosensor of the myofilaments. The fourth study uses biochemical correlates of histidine to study the effects of different ionization states on troponin function.

Chapter II

Human revertant phenotypes support an evolutionary model of coordinated substitutions in cardiac troponin for enhanced mammalian lusitropic performance

Abstract

In cardiac muscle, the troponin complex serves as a molecular switch translating myocyte calcium fluxes into sarcomeric contraction and relaxation. Examined here is the molecular mechanism underlying changes in cardiac troponin (cTn) during chordate evolution of the mammalian cardiovascular system. Ancestral species including fish and amphibians have myofilaments with heightened calcium sensitivity. Human disease causing single nucleotide polymorphisms (SNPs) that cause pathologies recapitulating ancestral physiology, termed here as evolutionary revertant phenotypes, were used to understand the mechanism of evolutionary modifications in cTn required for proper functioning of the mammalian cardiovascular system. Nucleotide and peptide sequences of all members of the ternary troponin complex were aligned for pairwise comparison of cTn isoforms spanning chordate evolution. Large scale phylogenetic analysis, atomic resolution molecular dynamics simulations and modeling, and functional data support the hypothesis that a single histidine

to alanine substitution in the switch arm of TnI was a key evolutionary modification during evolution of the mammalian cTn complex. Molecular dynamics simulations and *in silico* alanine scanning of the cTn regulatory interaction indicate a reduction in the interface binding free energy (ΔΔG) and molecular untethering of cTnI switch arm during evolution of cTn into the mammalian lineage. In addition to the switch peptide of TnI, data indicate that single nucleotide substitutions in cTnC were coordinately modified during evolution of mammalian cTn. SNP studies of cTn show that patients with evolutionary revertant phenotypes have heart failure caused by heightened myofilament calcium sensitivity. In order to meet the requirements for refined mammalian lusitropic performance, it is proposed here that evolutionary pressures favored mutations that enhanced the relaxation properties of cardiac troponin by decreasing its sensitivity to activating calcium.

Introduction

Evolutionary pressures favor mutations that mitigate the susceptibility to disease, especially as it pertains to the reproductive fitness of an organism. Consequently, genetic diseases provide excellent reference points from which to understand the implications of certain changes as a retrospective view on evolutionary modifications. In other words, human disease causing evolutionary revertant phenotypes, defined as single nucleotide polymorphisms (SNPs) that cause pathologies recapitulating ancestral physiology, provide insight into the

influence of evolutionary pressures on specific residues or domains of a given protein to accommodate changing physiological requirements. This study assessed phylogenetic changes that occurred during evolution of the mammalian heart with a focus on troponin, the regulatory molecular switch complex of the myofilaments.

Discovered by Ebashi decades ago[328], troponin is a heterotrimeric protein complex comprised of three subunits. These include the Tm binding subunit, troponin T (TnT), the calcium binding subunit, troponin C (TnC), and the actomyosin ATPase inhibitory subunit, troponin I (TnI) (Figure 2- 1a). The coordinated actions of the troponin complex are specifically designed to regulate the functions of acto-myosin cross bridges in a calcium-dependent manner during the rhythmic transitions between systole and diastole[18].

During systole, myofilament activation is mediated through binding of the TnI switch arm to an exposed hydrophobic patch on the calcium-bound N-terminal domain of cTnC[69-71]. These actions enable coordination of the azimuthal positioning of Tm in the actin groove by TnT and subsequent sarcomeric contraction mediated by actin-myosin cross bridge cycling [18, 59, 60]. The intracellular biophysics of myofilament contraction are translated into ventricular inotropic performance at the whole organ level. During diastole, calcium is released from cTnC and sequestered into the SR allowing the regulatory arm of TnI to translocate into an inhibitory position on actin. This is sufficient to prevent actin-myosin cross bridge activation resulting in sarcomeric relaxation[159, 160]. Förster resonance energy transfer (FRET) experiments have

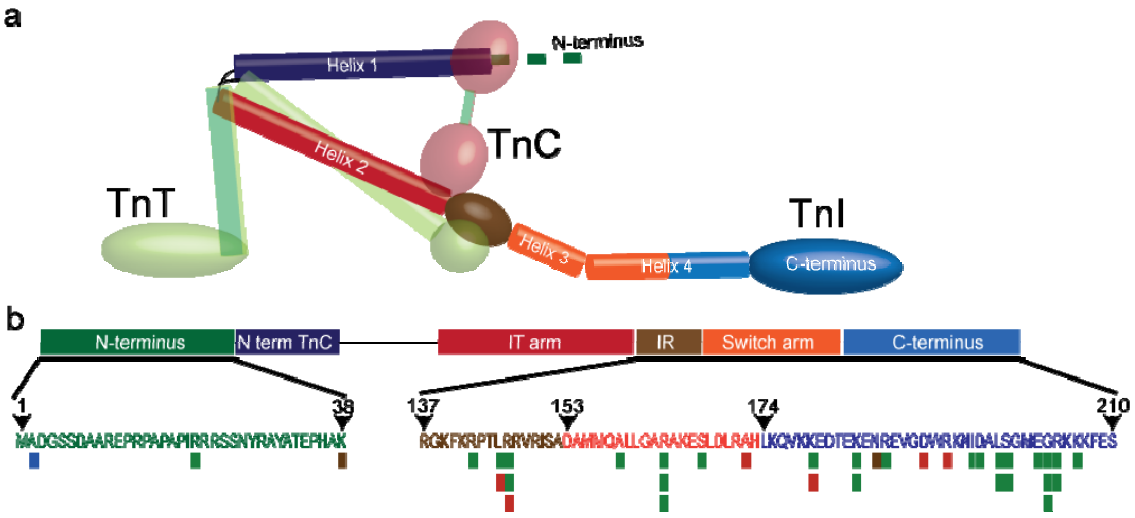

Figure 2-1. Structure and function analysis of cardiac troponin I. Schematic diagram of the heterotrimeric troponin complex including troponin I (TnI), troponin C (TnC), and troponin T (TnT). Coloring of structural components in TnI (e.g. helix 1- 4) in (a) are coordinated with functional domains including the N-terminus, the N-terminal TnC binding domain, the IT arm, the inhibitory region (IR), the switch arm, and the C-terminus as shown in (b). (b) Specific amino acid loci of the human cardiac troponin I gene sequence with known disease causing single nucleotide polymorphisms (SNPs); hypertrophic cardiomyopathy (green), dilated cardiomyopathy, recessive (blue), dilated cardiomyopathy, autosomal dominant (brown), and restrictive cardiomyopathy (red). Stacked bars at a single locus indicate multiple known mutations at that site. SNP data were acquired from the Harvard cardiogenomics website (genetics.med.harvard.edu) and recent reports[329].

shown that the movements of the regulatory arm of TnI during systole and diastole are essential for the transmission of the calcium signal to the rest of the myofilament proteins[159, 160]. Importantly, the inherent relaxation capacity of cTn is a major determinant of ventricular lusitropy during the filling phase of the cardiac cycle[162, 194, 330].

The specific amino acid composition of the cTn complex markedly affects its sensitivity to activating calcium which, ultimately, influences inotropic and lusitropic performance[155, 156, 252, 331-333]. Studies have shown that ancestral ectotherms such as fish and amphibians require heightened myofilament calcium sensitivity to maintain cardiac performance in the context of challenging environmental constraints such as cold temperatures and extended periods of hypoxia[4, 5, 334]. However, SNPs in cTn that cause increased myofilament sensitivity to activating calcium in mammals, termed here evolutionary revertant phenotypes, result in cardiomyopathy including arrhythmias, diastolic dysfunction, and increased susceptibility to sudden cardiac death[333, 335-337]. These clinical observations reveal an absolute requirement for enhanced ventricular relaxation in mammalian species. Using large scale bioinformatics and an array of molecular modeling techniques we propose that the intrinsic relaxation potential of cardiac troponin has been enhanced during chordate evolution to meet the lusitropic requirements of the mammalian cardiovascular system.

Methods

Amino acid and mRNA sequences and alignments Sequences were extracted by search of NCBI protein and nucleotide databases as well as the UniProt KB protein database. Defining the taxonomic relationship between species studied was accomplished by use of the NCBI taxonomy database (Figure 2-7). Table 2-1 outlines abbreviations used to reference specific species. Table 2-2 outlines all relevant details on the sequences acquired from NCBI or UniProt KB databases used in this phylogenetic analysis. To be consistent with prior studies, all amino acid numbering in this study refers to the adult rat isoform sequence (cTnI, cTnC, and cTnT) including the starting methionine unless otherwise stated. Protein and nucleotide sequences were aligned by Clustal W analysis as originally described by Thompson et al[338]. Multiple alignment parameters were as follows: gap penalty = 15; gap length penalty = 6.66; protein weight matrix: Gonnet Series. Pairwise analysis of percent identity between sequences was used to define the relationship between proteins or within proteins across designated species.

Genome scans for novel TnI genes New sequences for troponin I isoforms were acquired by whole genome scans of numerous species. Genome BLAST analysis for TnI isoforms were performed on *Anolis carolinensis* (lizard, USCS), *Taeniopygia guttata* (zebra finch, NCBI), *Cavia porcellus* (guinea pig, UCSC), and *Callithrix jacchus* (marmoset, UCSC). Query sequences from taxonomically

Table 2-1. Species abbreviations

Mammals	Human	H
	Sumatran orangutan	SO
	Chimpanzee	Ch
	Rhesus	Rh
	Marmoset	Ma
	Bovine	B
	Horse	Ho
	Goat	G
	Sheep	Sh
	Pig	P
	Dog	D
	Cat	C
	Guinea Pig	GP
	Rabbit	Rab
	Rat	R
	Mouse	M
	Opossum	O
	Platypus	Pl

Reptile	Lizard	L
Birds	Chicken	Ch
	Quail	Q
	Turkey	T
	Zebra Finch	ZF
Amphibians	Xenopus laevis	Xl
	Xenopus tropicalis	Xt
	Bullfrog	BF
	Marine Toad	MT
Fish	Salmon	S
	Zebrafish	Z
	Green pufferfish	GrP
	Dinosaur eel	DE
	Arctic lamprey	AL
Invertebrates	Ascidian 1	As1
	Ascidian 2	As2
	Amphoxius	A

related species were used for the genome scans. Predicted isoform for TnI sequences was accomplished by Clustal W analysis followed by sequence percent identity and phylogenetic tree analysis. The Kimura distance formula was used to calculate distance values, derived from the number of non-gap mismatches and corrected for silent substitutions. The values computed are the mean number of differences per site and fall between 0-1. Zero represents complete identity and 1 no identity. Scale of the phylogenetic tree indicates the number of nucleotide substitutions per 100 residues. Phylogenetic tree analysis was used to confirm identity of predicted TnI isoforms by sequence correlation with other TnI isoforms. Sequence ID and divergence values were calculated to define the relationship between novel TnI proteins and related TnI isoforms to assist in confirmation of postulated isoform designation. Divergence (i,j) is calculated as (100[Distance (i,j)] / Total Distance) where (i,j) is the sum of the branch lengths between two sequences and Total Distance is the sum of all branch lengths. All data regarding protein and mRNA sequences are outlined in Table 2-3, and Figures 2-8 (nucleotide) and 2-9 (protein).

Determination of evolutionary selective pressure Phylogenetic codon models were used to understand the selective pressure on both the full gene sequence of cardiac TnI and on the switch domain. Briefly, codon-based methods (recently reviewed by [339, 340]) make use of a continuous-time Markov process to model synonymous (dN) and non-synonymous substitutions (dS) along a phylogenetic

tree. Phylogenetic trees were estimated, using PHYML [341], independently for the full gene sequence and for the switch domain, since only a subset of full cTnI sequences were available for the mammalian taxa of interest. The switch domain is short (63 nucleotides), and thus some internal branches of the phylogeny had lengths of zero; we collapsed those branches into polytomies. It was assumed that synonymous and non-synonymous substitution rates at codon sites can be approximated using discrete distributions, the parameters of which are estimated by maximum likelihood. To rule out the potential confounding effect of recombination or gene conversion, the alignment was screened using GARD[342, 343]; no evidence for recombination was detected. To identify the distribution which best describes synonymous and non-synonymous rate variation across all sites a step-wise procedure was used starting at a single rate for all sites and progressively adding new rate classes, each time estimating the synonymous and non-synonymous rates of each class and evaluating model fit using the small sample correction to the Akaike's Information Criterion (AIC-c)[344]. The stepwise iteration was terminated once no further improvement in model fit was achieved. A Fixed Effects Likelihood (FEL) methods (implemented on www.datamonkey.org[345]) was used to estimate the synonymous to non-synonymous substitution rate at each site independently for the switch domain. Briefly, evidence for either positive (dN/dS > 1) or purifying selection (dN/dS < 1) was identified by comparing the fit of a model in which synonymous and non-synonymous rates are constrained to be equal, to that in which this constraint is

relaxed. Statistical significance was evaluated with a Likelihood Ratio Test ($P < 0.05$).

Molecular modeling and structural analysis All modeling was carried out using Maestro (Schrödinger, LLC, New York, NY; 2007). The solved X-ray crystallographic structures of human cardiac[52] (PDB: 1J1E) and skeletal[51] (PDB: 1YTZ) troponin in complex to Ca^{++} bound troponin C were taken from the Protein Data Bank. The missing hydrogen atoms were added to both X-ray structures followed by energy minimization using OPLS 2005 forcefield to optimize all hydrogen bonding networks. Structure comparison between the cardiac and skeletal troponin was carried out by superpositioning the two structurally conserved Ca^{++} bound TnC. From this superpositioning, truncated hybrid and homotypic crystal structures were analyzed including: cTnC/cTnI, cTnC/sTnI, cTnC, cTnI, and sTnI. The cTnC:TnI regulatory complex was isolated by exclusion of all other residues in the crystal structure except: sTnI R115 – L140, cTnI R148 – L173, and each TnI was complexed with cTnC M1 – K90. Mutagenesis of sTnI was accomplished by substitution of an alanine for histidine at position 132 (H132A).

Theoretical isoelectric point calculations Values for the theoretical isoelectric point (pI) were calculated using the algorithm from ExPASy's Compute pI/Mw program[346].

Theoretical pK_a calculations of Tn crystal structures The sTnI:cTnC and cTnI:cTnC structures were analyzed for determination of the theoretical residue ionization titration and electrostatic atomic energy binding interaction between all ionizable groups. Binding energy between two ionizable groups was calculated as atomic energy units and converted to kcal/mol by multiplying by the conversion factor 332. Analysis was accomplished as previously described and implemented on the Virginia tech H++ server[347-352]. Calculation was derived using the following inputs: salinity = 0.15; internal dielectric = 10; external dielectric = 80; structure protonation assuming pH = 7.2. Calculated by the Poisson Boltzmann method.

Molecular Dynamics Simulation Molecular Dynamics (MD) simulations were performed for sTnI:cTnC; cTnI:cTnC; and sTnIH132A:cTnC using NAMD [353] version 2.6 with CHARMM27 forcefield [354]. All the X-ray structures and derived mutants were prepared by CHARMM version c35b1. Each of the complex was solvated with explicit TIP3P water model [355] using a simulation solvent box with a 15 Å buffer region around the protein. Sodium counter ions were placed at 5 Å from the box boundary to neutralize the system. The solvated system was initialized with 5000 steps of conjugate gradient energy minimization with protein heavy atoms restrained at 50kcal/(mol•$Å^2$). The system was then gradually heated with the same restraint from 25K to 300K at 25 K increment at 10 ps interval for 100 ps followed by a 100 ps equilibration with gradual removal of the heavy atoms restraint at 10 ps interval under NVT condition. The final

unrestrained equilibration was carried out for 100 ps followed by 20 ns of production simulation at 1 atm and 300K NPT condition. All simulations were carried with periodic boundary condition using Particle Mesh Ewald (PME) [356] with SHAKE [357] method employed to constrain bond lengths involving hydrogen atoms. The time step in the simulations was 2 fs with coordinates saved at 1-ps time intervals, resulting in a total of 20,000 configurations for analysis.

Interatomic distance calculations All distances are measured in angstrom over the 40 ns simulations for each of the simulated trajectories. For the wild type and H132A simulation of the sTnI:cTnC complex, the alpha carbon distance was evaluated between sTnI H/A132 and cTnC E19.

Results and Discussion

The principle goal of this study was to assess how cardiac Tn proteins have been modified during evolution to accommodate the physiological requirements of the mammalian heart. To accomplish this, large scale phylogenetic analysis was performed by sequence alignment by clustal W analysis of 104 primary amino acid sequences of proteins including cTnT, cTnC, ssTnI, and cTnI from species throughout chordate evolution (Figures 2-7 through 2-12, Tables 2-1, 2-2). Summarizing the relevant taxonomy, table 2-1 lists species abbreviations used.

Disease causing polymorphisms in the C-terminus of cTnI recapitulate ancestral physiology

Consistent with previous reports[52, 252], the positional relationship between the functional domains and the secondary structural regions of TnI are outlined in Figure 2-1. Benign and disease causing single nucleotide polymorphisms (SNPs) have been identified along the full length of the human cTnI locus. Figure 2-1b outlines the location of known SNPs as well as their specific disease causing designations. Over 94% of known disease causing SNPs are located between the start of the IR domain and the end of the C-terminus, also referred to as the regulatory domain of TnI[52]. One of the physiological deficiencies observed in these cardiomyopathies is increased myofilament calcium sensitivity[333, 335, 337, 358]. The concentration of disease causing mutations within the regulatory region of TnI indicates that single amino acid alterations in this critical region of the molecule are not tolerated and have significant deleterious effects on TnI function that cause heart disease.

Studies have shown that environmental demands such as cold temperatures and hypoxic conditions require heightened myofilament calcium sensitivity to maintain sufficient cardiac performance in ancestral species such as fish and amphibians (for further discussion see Appendix A)[4, 5, 331, 334]. Taken together, these observations indicate that heightened myofilament sensitivity to activating calcium is a common feature of ancestral cardiovascular function and

some human cTn disease causing SNPs. We conclude therefore, that some human disease causing cTn SNPs cause evolutionary revertant phenotypes.

Phylogenetic analysis of slow skeletal and cardiac troponin I functional domains

Human evolutionary revertant phenotypes (e.g. SNPs in TnI) that cause pathologies recapitulating ancestral physiology can act as a retrospective view of evolutionary pressures providing insights into a mechanistic basis for observed modifications in cardiac Tn during evolution of the mammalian heart. Given the observed intolerance of SNPs in the C-terminus of TnI, we hypothesized that evolutionary pressures tightly regulated changes in these regions to modify the performance of Tn in accordance with the evolution of mammalian cardiovascular requirements. We subsequently analyzed the subdomains of TnI to understand the phylogenetic basis for sequence differences within these functional regions of the molecule between chordate species (Figure 2-2a-c).

Different isoforms of TnI are expressed in different species through chordate evolution. In amphibians the cardiac TnI isoform has been found to be the only TnI isoform encoded at the onset of heart formation in the larva and continuing in the adult heart of anuran species[359-361]. However, in avian and mammalian species the slow skeletal isoform is transiently expressed during heart development and is replaced in the adult heart by the cardiac TnI isoform[89, 311, 362]. Based on these different expression profiles, we hypothesized that comparative analysis of TnI isoforms expressed in the heart would provide a

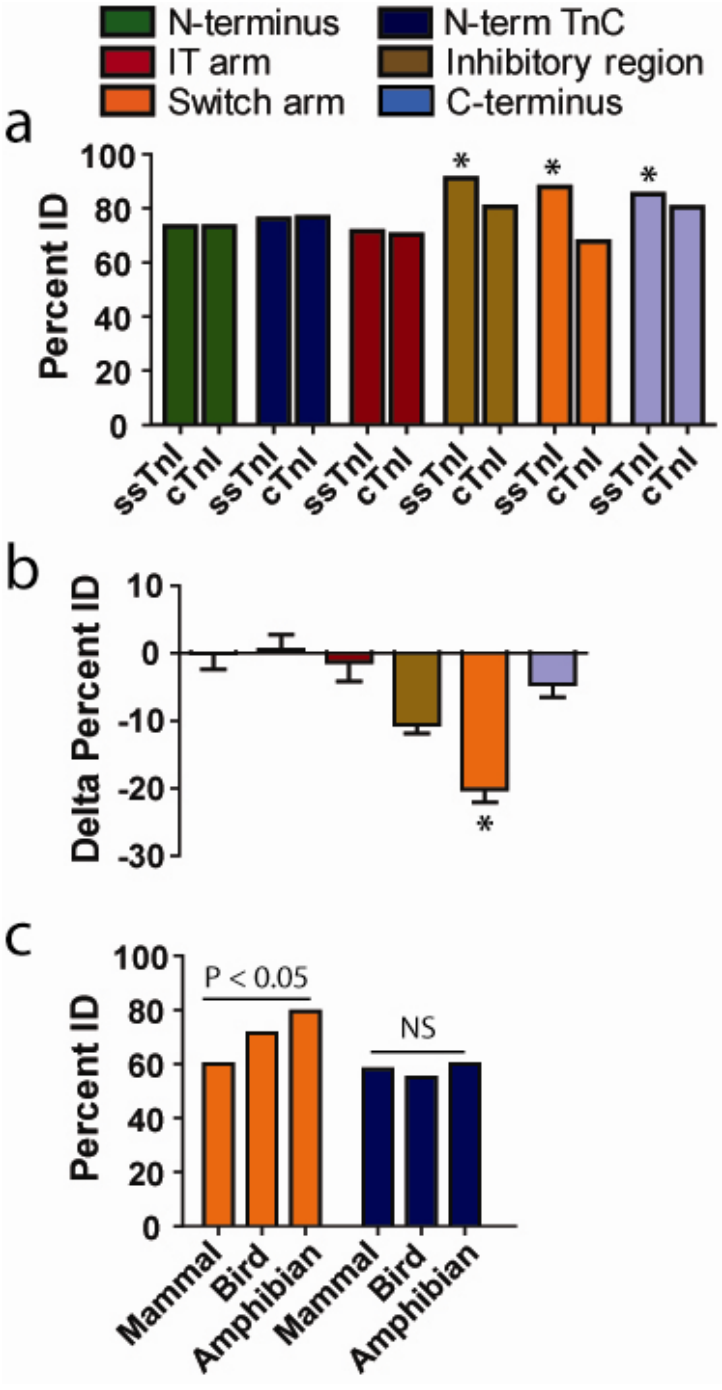

Figure 2-2. Phylogenetic analysis of TnI functional domains. (a) Direct pairwise comparison by Clustal W analysis of sequences within specific functional domains of slow skeletal and cardiac TnI only from species for whom both isoforms have been sequenced; these include H, P, Rab, R, M, Ch, Q, Xl, Xt, BF, and S. * $P < 0.05$ by students t-test comparing ssTnI to cTnI within a given functional subdomain. (c) The delta change in sequence percent identity between ssTnI and cTnI (as indicated in part a) within each given functional subdomain. * $P < 0.05$ by dunnet's test comparing significance of all other functional domains to the switch arm. (d) Comparison of sequence percent identity between ssTnI and cTnI for a given species and collated based on class including mammal (H, P, Rab, R, M), bird (Ch, Q), or amphibian (Xl, Xt, BF). Differences between mammal, bird, and amphibian TnI isoforms are shown for both the switch arm and N-terminal TnC binding domain. $P < 0.05$ based on 1 way ANOVA within each subdomain.

basis with which to interpret modifications in TnI during evolution of chordate cardiovascular systems.

To discern evolutionary pattern differences among the functional domains of TnI, discrete segments of the molecule were aligned and compared across all species. The functional domains of TnI analyzed included the N-terminus (1-44), N-terminal TnC binding domain (45-65), IT arm (91-136), inhibitory region (IR) (138-149), switch arm (152-172) and the C-terminus (153-210). To determine if protein sequences within these functional domains were different between ssTnI and cTnI across chordate organisms, sequence alignment analysis was performed on species where both isoforms are known (Figure 2-2a). This analysis showed that, in contrast to N-terminal domains, regions within TnI_{reg} all showed a significant diminution in sequence conservation within the cTnI isoform compared to ssTnI ($P < 0.05$). Furthermore, the cTnI switch arm had the greatest difference in sequence percent identity compared to the ssTnI switch arm (Δ percent ID = -20.1 ± 1.9%, $P < 0.05$ compared to all other domains) (Figure 2-2b).

To understand how this change in switch arm conservation correlates with specific phylogenic groupings, the ssTnI/cTnI sequence percent identity was analyzed in a pairwise fashion within each class (mammalian, avian, amphibian) (Figure 2-2c). This analysis showed that among amphibians the switch arm of ssTnI and cTnI isoforms are more similar than is the case for birds. The lowest degree of ssTnI:cTnI sequence conservation (greatest divergence) was observed in mammals. In contrast, other functional regions such as the N-terminal TnC

binding domain showed no difference in ssTnI:cTnI sequence conservation among the taxa studied (Figure 2-2c).

These phylogenetic data indicate that the switch arm was a site of rapid ssTnI:cTnI sequence divergence within the mammalian lineage. It is well established that the switch arm regulates the toggling of the entire regulatory arm of TnI between systole and diastole (residues 138-210)[18, 51, 52, 159, 160, 194]. A vast literature supports the conclusion that the properties of the TnI switch arm can markedly alter the mechanism by which troponin regulates the contractile properties of the myofilament[93, 133, 246, 251, 252, 266, 314, 363].

Analysis of the amino acid composition of the TnI switch arm

We next sought to determine the specific mechanism by which the mammalian switch peptide was modified. To begin, the theoretical isoelectric point (pI) was calculated for the switch arm fragment for each class (Figure 2-3a,i). These data show that the ssTnI switch arm pI did not change across all classes. In contrast, the pI for the cTnI switch arm decreased from amphibian (9.5 ± 0.5) and bird (8.75 ± 0.0) species to mammals (6.76 ± 0.0). These data also show no significant difference between the TnI isoform (ssTnI vs. cTnI) pI for amphibian and avian species. Comparatively, there is a significant reduction in the pI for mammalian ssTnI vs. cTnI (9.99 ± 0.0 vs. 6.76 ± 0.0, $P < 0.05$). These data are supported by crystal structure analysis of pI for the avian sTnI switch arm (pI = 11) and mammalian cTnI switch arm (pI = 8.6) (Table 2-3). Linear

Figure 2-3. Theoretical isoelectric point (pI) analysis and sequence analysis of the troponin I switch arm. (a) Analysis of theoretical pI alterations in the switch arm between ssTnI and cTnI for species where both sequences are available (H, P, Rab, R, M, Ch, Q, Xl, Xt, and BF). (a, i) Analysis of the average pI of the ssTnI and cTnI switch arm for amphibian, avian, and mammalian species. * $P < 0.05$ vs. all other groups by 1 way ANOVA. (a, ii) Linear regression analysis showing the relationship of the net difference in pI and sequence percent identity between ssTnI and cTnI within the switch arm. Precise overlap of values within classes reduced the number of visible points to 5 in comparison to the 10 calculations made (1 for each species). (b) Alignment of troponin I protein sequences expressed in numerous chordate species. Analysis was performed by the Clustal W method. Sequences are organized by isoform and within each isoform by species based on taxonomic classification. The key histidine to alanine amino acid modification is also shown (yellow). The platypus proline is highlighted as the potential evolutionary intermediate residue between histidine in pre-mammals and alanine in all other mammals. For alignment analysis of the full TnI molecule see Figure 2-12.

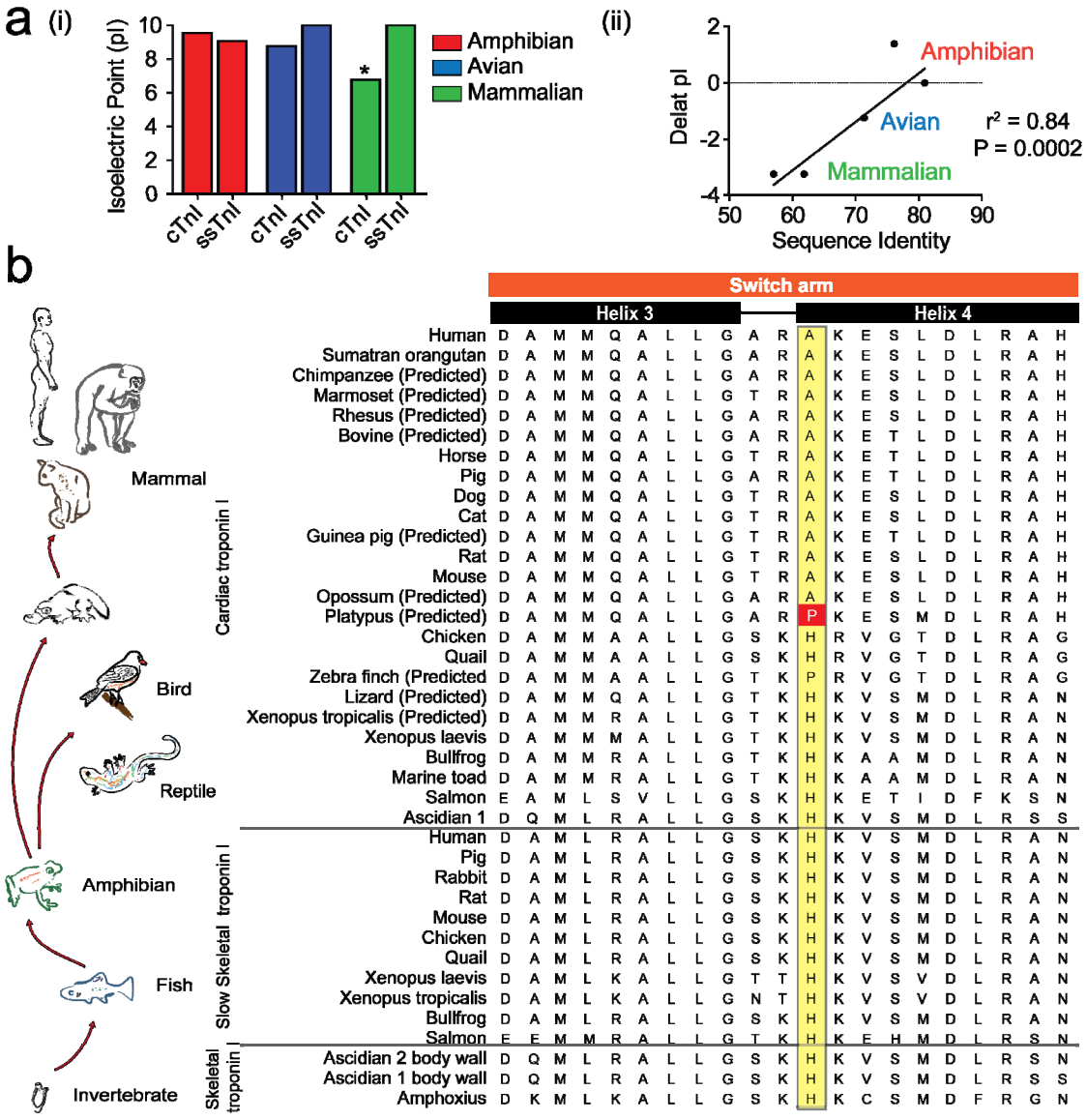
a
(i)
Isoelectric Point (pI)
10
8
6
4
2
0
cTnI
ssTnI
cTnI
ssTnI
cTnI
ssTnI
*
Amphibian
Avian
Mammalian
(ii)
Delat pI
2
0
-2
-4
50
60
70
80
90
Sequence Identity
Amphibian
Avian
Mammalian
r² = 0.84
P = 0.0002
b
Switch arm
Helix 3
Helix 4
Human D A M M Q A L L G A R A K E S L D L R A H
Sumatran orangutan D A M M Q A L L G A R A K E S L D L R A H
Chimpanzee (Predicted) D A M M Q A L L G A R A K E S L D L R A H
Marmoset (Predicted) D A M M Q A L L G T R A K E S L D L R A H
Rhesus (Predicted) D A M M Q A L L G A R A K E S L D L R A H
Bovine (Predicted) D A M M Q A L L G A R A K E T L D L R A H
Horse D A M M Q A L L G T R A K E T L D L R A H
Pig D A M M Q A L L G A R A K E T L D L R A H
Dog D A M M Q A L L G T R A K E S L D L R A H
Cat D A M M Q A L L G T R A K E S L D L R A H
Guinea pig (Predicted) D A M M Q A L L G T R A K E T L D L R A H
Rat D A M M Q A L L G T R A K E S L D L R A H
Mouse D A M M Q A L L G T R A K E S L D L R A H
Opossum (Predicted) D A M M Q A L L G A R A K E S L D L R A H
Platypus (Predicted) D A M M Q A L L G A R P K E S M D L R A H
Chicken D A M M A A L L G S K H R V G T D L R A G
Quail D A M M A A L L G S K H R V G T D L R A G
Zebra finch (Predicted D A M M A A L L G T K P R V G T D L R A G
Lizard (Predicted) D A M M Q A L L G T K H K V S M D L R A N
Xenopus tropicalis (Predicted) D A M M R A L L G T K H K V S M D L R A N
Xenopus laevis D A M M M A L L G T K H K V S M D L R A N
Bullfrog D A M M R A L L G T K H K A A M D L R A N
Marine toad D A M M R A L L G T K H K A A M D L R A N
Salmon E A M L S V L L G S K H K E T I D F K S N
Ascidian 1 D Q M L R A L L G S K H K V S M D L R S S
Human D A M L R A L L G S K H K V S M D L R A N
Pig D A M L R A L L G S K H K V S M D L R A N
Rabbit D A M L R A L L G S K H K V S M D L R A N
Rat D A M L R A L L G S K H K V S M D L R A N
Mouse D A M L R A L L G S K H K V S M D L R A N
Chicken D A M L R A L L G S K H K V S M D L R A N
Quail D A M L R A L L G S K H K V S M D L R A N
Xenopus laevis D A M L K A L L G T T H K V S V D L R A N
Xenopus tropicalis D A M L K A L L G N T H K V S V D L R A N
Bullfrog D A M L R A L L G S K H K V S M D L R A N
Salmon E E M M R A L L G T K H K E H M D L R S N
Ascidian 2 body wall D Q M L R A L L G S K H K V S M D L R S N
Ascidian 1 body wall D Q M L R A L L G S K H K V S M D L R S S
Amphoxius D K M L K A L L G S K H K C S M D F R G N
Mammal
Bird
Reptile
Amphibian
Fish
Invertebrate
Cardiac troponin I
Slow Skeletal troponin I
Skeletal troponin I

regression analysis was performed to determine if the change in sequence percent identity between the switch arm of ssTnI and cTnI for a given species was related to changes in the pI (Figure 2-3a, ii). This analysis showed that evolutionary pressure to modify the switch arm peptide sequence between ssTnI and cTnI are significantly related to alterations in the pI of the domain (r^2 = 0.84, P = 0.0002). Evidence that the ssTnI switch arm sequence composition and pI are not different across classes indicates that this isoform is not being modified during chordate evolution. Alternatively, modifications in ionizable residues in the cTnI switch arm are altered during evolutionary peptide adjustments of the mammalian cTn complex.

Sequence analysis of the troponin I switch arm

To further study the observed modification of the switch arm in cardiac TnI from amphibians to avian and mammalian species, predicted protein and mRNA cTnI sequences from numerous chordate species were collected. In addition, putative TnI sequences were recovered by BLAST analysis of genomes from *Anolis carolinensis* (Lizard), *Taeniopygia guttata* (Zebra Finch), *Cavia porcellus* (Guinea Pig), and *Callithrix jacchus* (Marmoset) (see Table 2-2 and Figures 2-8 and 2-9).

Changes in ionizable residues between ssTnI and cTnI in the switch arm were studied (Figure 2-3b). This analysis showed that a nonpolar hydrophobic moiety at position 164 in the switch arm of cTnI is 100% conserved in mammals

but was found to be a histidine in all other chordate species and TnI isoforms (with the exception of Zebra finch cTnI). Although alanine 164 was identified in all other mammals, a proline residue was surprisingly identified in the predicted platypus sequence. Taxonomically, platypus, the only egg laying mammal, is situated early in the mammalian lineage (Figure 2-7). This modification of an amino acid that is perfectly conserved through chordates prior to the bird/mammal divergence and subsequently altered (charged to uncharged or vice versa) only in mammals and thereafter perfectly conserved, was not observed at any other locus in the entire troponin complex (cTnI, ssTnI, cTnT, or cTnC). Analysis of selective pressure indicate that the mammalian cTnI switch arm is under significant purifying selection indicating that the current peptide composition has long been highly favorable for the proper regulatory functions of troponin in the mammalian heart (Table 2-5). Such a significant level of residue conservation suggests that the transition from a hydrophilic and polar amino acid to a hydrophobic and nonpolar moiety within the switch arm is likely a key modification in Tn during evolution of the mammalian heart. This is supported by a corpus of of literature showing the importance of this TnI histidine button on myofilament function[203, 242, 246, 252, 290].

Histidine has been found to be a critical moiety in regulating key physiological events in a number proteins including troponin I (ssTnI H132 or cTnI A164H)[203, 246, 252, 290], hemoglobin (H146β) [303, 326], HLA-DR molecules (H33α) [306], the pacemaker channel HCN2 (H321) [309] and numerous other proteins [364], [310], [307, 308]. The α-imidazole side chain of histidine is unique among

all of the amino acids in that it reversibly binds hydrogen ions within the physiologic range. Depending on the local protein environment, temperature, or solvent composition the pK_a of histidine can markedly shift. The non-protonated histidine is hydrophobic and aromatic in character whereas the protonated histidine is hydrophilic and positively charged. Of critical importance, in the context of the cTn regulatory complex, the imidazole side chain of histidine provides a substrate for different ionization states in response to changes in pH. Thus, at low pH, increased hydrophilicity of a protonated histidine (H132) at this position would help retain intermolecular electrostatic contacts between the TnI regulatory domain and the acidic residues decorating the hydrophobic patch of cTnC (e.g. E19). As such, the ionization states of histidine enable it to perform as a pH responsive molecular switch by differentially regulating the biophysics of inter and intramolecular interactions.

Crystal structure analysis of the calcium saturated troponin complex

The phylogenetic data indicate that the switch arm of amphibian cTnI is very similar to ssTnI from across all classes in terms of amino acid sequence and isoelectric point (Figure 2-3a, b). Studies have also shown that ancestral cTnI physiology seen in fish and amphibians is functionally recapitulated by ssTnI in the mammalian heart *in vivo* and *in vitro*[4, 133, 267, 317, 318, 332]. Importantly, what we know about mammalian ssTnI may therefore assist in our understanding of the structure/function relationship of pre-mammalian cTnI.

In recent years the crystal structures of the calcium saturated cardiac Tn complex[52] and fast skeletal Tn complex[51] have been reported. We assume that the regulatory domain of the putative ssTn complex mirrors that of the reported fsTn complex (for justification of this assumption and structural orientation see Figure 2-14). We propose that comparative molecular modeling of sTn and cTn through hybrid (sTnI[51] with cTnC[52]) and homotypic (cTnI with cTnC[52]) atomic resolution crystal structures provides insight into evolutionary modifications that occurred in cTn to accommodate the functional requirements of the mammalian heart.

We report the first structural alignment of the sTnI and cTnI crystal structures in complex with cTnC to accentuate the differences in the regulatory interaction between these protein complexes (Figure 2-4a). Comparison of the sTn and cTn crystal structure showed a marked alteration in the position of TnI helix 4 between sTnI and cTnI relative to helix A and the hydrophobic patch of TnC (Figure 2-4a). The structural alignment indicates that H3 has similar positioning in the two complexes. The structure of skeletal TnI indicates the unstructured helix 4 has His132 engaging helix A of TnC in very close proximity to a key acidic residue, Glu19, in the hydrophobic patch of TnC. This analysis showed that TnI H132 (protonated, pK_a = 8.25) and TnC E19 (pK_a = 2.51) are close enough to develop a salt bridge (Table 2-4, Figure 2-4a, inset). The binding energy of this interaction is 5.24 kcal/mol, the strongest interatomic bonding observed between any two ionizable groups analyzed in these crystal structures (Figure 2-4b). Decomposition data indicate that the ionization of these residues is

Figure 2-4. Molecular modeling and structural analysis. (a) Atomic level alignment of the crystal structures for sTnI and cTnI in complex with the cTnC focusing on regulatory interaction site between the switch arm of TnI and the N-terminal lobe of cTnC. cTnC (red), sTnI (blue), cTnI (yellow). Inset image highlights the critical interaction between sTnI H132 and cTnC E19. (b) Atomic level resolution of the interaction strength (kcal/mol) between ionizable groups in TnI and TnC are shown for the sTnI-cTnC structure (top) and cTnI-cTnC structure (bottom). Interactions are organized into intramolecular interactions within TnI (left) and cTnC (middle) and intermolecular interactions at the interface between TnI and cTnC (right). The strength of interaction cTnC E19 – sTnI H132 is indicated in red. Vertical bar = 1 kcal/mol. (c) Alanine scanning analysis of the change in binding free energy (ΔΔG) among all residues at the sTnI:cTnC regulatory interface. Important contributions to ΔΔG by cTnC E19 and sTnI H132 are shown in orange.

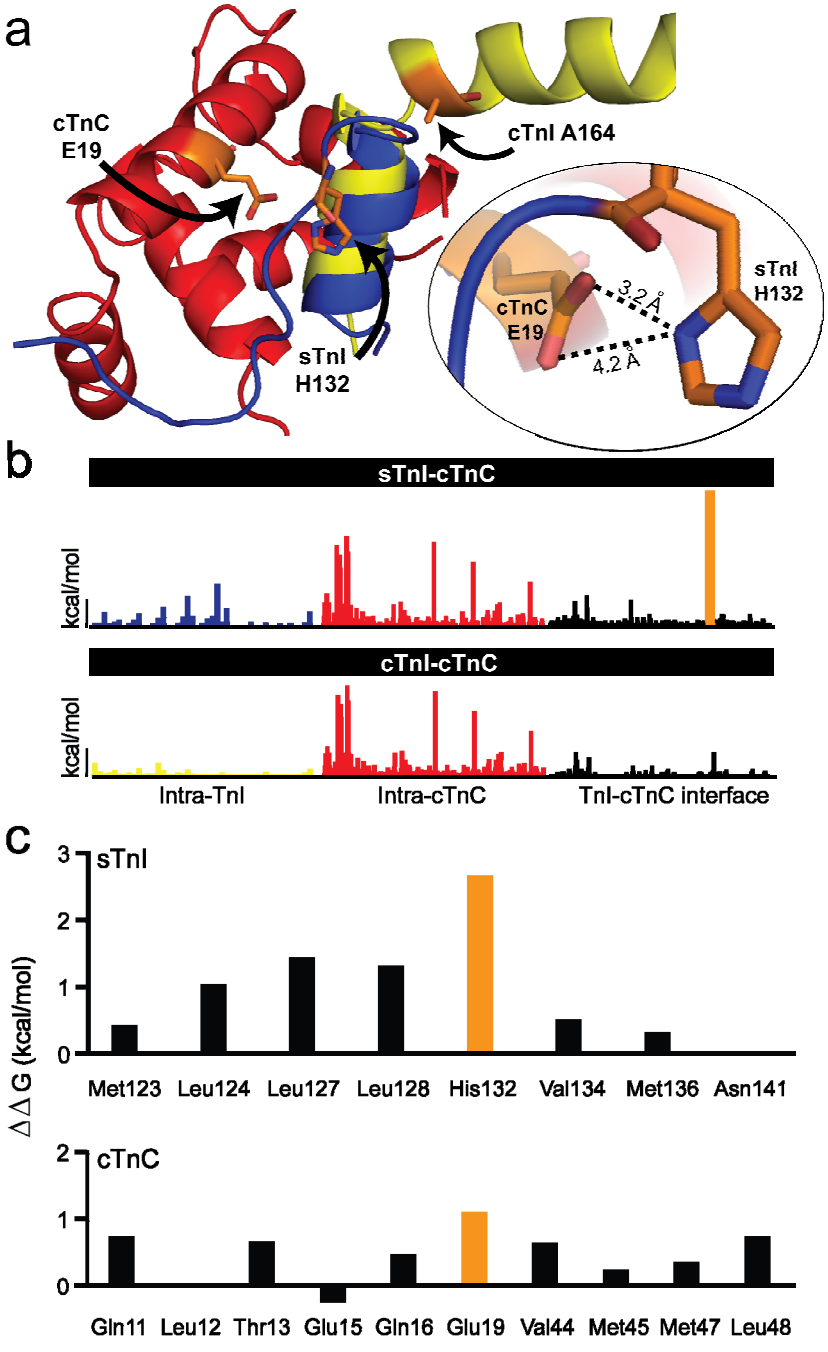
a
cTnC
E19
cTnI A164
sTnI
H132
cTnC
E19
3.2 Å
4.2 Å
sTnI
H132
b
sTnI-cTnC
kcal/mol
cTnI-cTnC
kcal/mol
Intra-TnI
Intra-cTnC
TnI-cTnC interface
c
sTnI
ΔΔG (kcal/mol)
3
2
1
0
Met123
Leu124
Leu127
Leu128
His132
Val134
Met136
Asn141
cTnC
2
1
0
Gln11
Leu12
Thr13
Glu15
Gln16
Glu19
Val44
Met45
Met47
Leu48

significantly influenced by the close electrostatic interaction between sTnI and cTnC at this locus (Figure 2-15a,b and Table 2-4). The characteristics of this key interaction between cTnC and sTnI (and thus its functional importance) are also observed in a unique histidine-aspartate interaction (H146β-D94β) in hemoglobin that forms a salt bridge and singularly contributes to about half of the maximal alkaline Bohr effect of human HbA[326].

In contrast to the sTn structure, at the H3-H4 linker and into the structured H4 of cTnI Ala164 translocates away from helix A and the hydrophobic patch of TnC (Figure 2-4a). Residue ionization titration analysis confirmed the hypothesis that cTnC and cTnI have limited electrostatic contact at this critical interaction site (Figure 2-4b, Table 2-4, Figure 2-15). Crystal structure analysis showed the strongest electrostatic contacts within the cTnI:cTnC complex to be over four times lower than E19-H132 of cTnC-sTnI.

To gain molecular insights into the marked differences between the sTnI-cTnC and cTnI-cTnC regulatory complexes, molecular dynamics simulation were carried out in nanosecond timescale to study the molecular motion of the two complexes in atomistic detail. These data show that the switch arm (H4 in particular) retains strong interface contacts between sTnI and cTnC but becomes highly mobile, molecularly untethered, in the cTnI-cTnC structure (Supplemental movies 1 (sTnI:cTnC) and 2 (cTnI:cTnC)).

This histidine to alanine substitution in TnI at the interface with TnC markedly effects the performance characteristics of the troponin complex. 2D NMR spectroscopy analysis of amide chemical shifts during calcium titration has

shown that the switch peptide dissociation constant for cardiac TnI is six times weaker than that of skeletal TnI[327]. Transgenic and gene transfer studies have shown that myofilaments containing ssTnI have sarcomere dynamics including hypercontractility, delayed relaxation, and increased propensity for arrhythmias compared to myofilaments containing cTnI[202, 252, 335]. Furthermore, consistent with the concept of a pH-responsive histidine button, TnI proteins with a histidine moiety in the switch arm (ssTnI H132 or cTnI A164H) perform as a molecular rheostat capable of maintaining inotropy in the context of severe acidosis or other pathologies[133, 203, 246, 249, 252, 290, 297, 317, 318]. Myofilaments containing cTnI with an alanine in the switch arm (A164), by contrast, are highly susceptible to acidosis induced contractile failure. Taken together, these structural and functional data indicate that significant alterations in the peptide composition and, consequently, tertiary protein structure of the cardiac Tn regulatory interaction markedly alter the functional properties of Tn.

We next sought to test the hypothesis that breaking of the His132-E19 interaction would markedly decrease the binding affinity between sTnI and cTnC. To test this, computational alanine scanning was performed to calculate the change in the binding free energy (ΔΔG) caused by alanine substitution of all residues involved in the intermolecular interface contacts of the sTnI-cTnC structure (Figure 2-4c). In cTnC alanine substitution of E19 was found to contribute most to the ΔΔG (ΔΔG E19A = 0.91kcal/mol). However, the greatest impact on the binding free energy among all residues engaged at the cTnC:sTnI interface was observed with the sTnI H132A substitution (ΔΔG H132 = 2.46

kcal/mol). These data support the conclusion that alanine substitution of sTnI H132 was the most effective mechanism of reducing the binding free energy at the interface of the calcium saturated sTnI-cTnC structure.

To further support this observation, interatomic distances were calculated between the alpha carbons of cTnC E19 and residue 132 of either WT sTnI or sTnI H132A across a 20 nanosecond atomic resolution molecular dynamics simulation (Figure 2-5a,b, Supplemental video 3 (sTnI H132A:cTnC)). These data show the WT sTnI:cTnC structure retains a highly stabile interface mediated by the high energy intermolecular interaction between His132:E19. In contrast, there was a marked increase in the distance between cTnC E19 and sTnI residue 132 in the alanine substituted structure indicating a significant time-dependent structural interface separation (Figure 2-5b). Functional data support these *in silico* observations. A recent study by Westfall et al has shown that ssTnI H132A significantly reduces the calcium sensitivity of the myofilaments (pCa_{50}) and enhances the relaxation performance of myocytes similar to the functional properties observed with myocytes expressing mammalian cTnI[252].

Given our initial assumption that sTnI recapitulates ancestral cTnI, the molecular modeling data indicate that there was evolutionary pressure to favor cTnI A164 in order to reduce the binding free energy ($\Delta\Delta G$) at the interface of cTnI and cTnC at the mammalian juncture. This was accomplished by eliminating the key high energy electrostatic interaction between TnI and cTnC (H132-E19) making H4 and the C-terminal domain of TnI molecularly untethered. Together with known functional data, the crux of the phylogenetic and molecular modeling

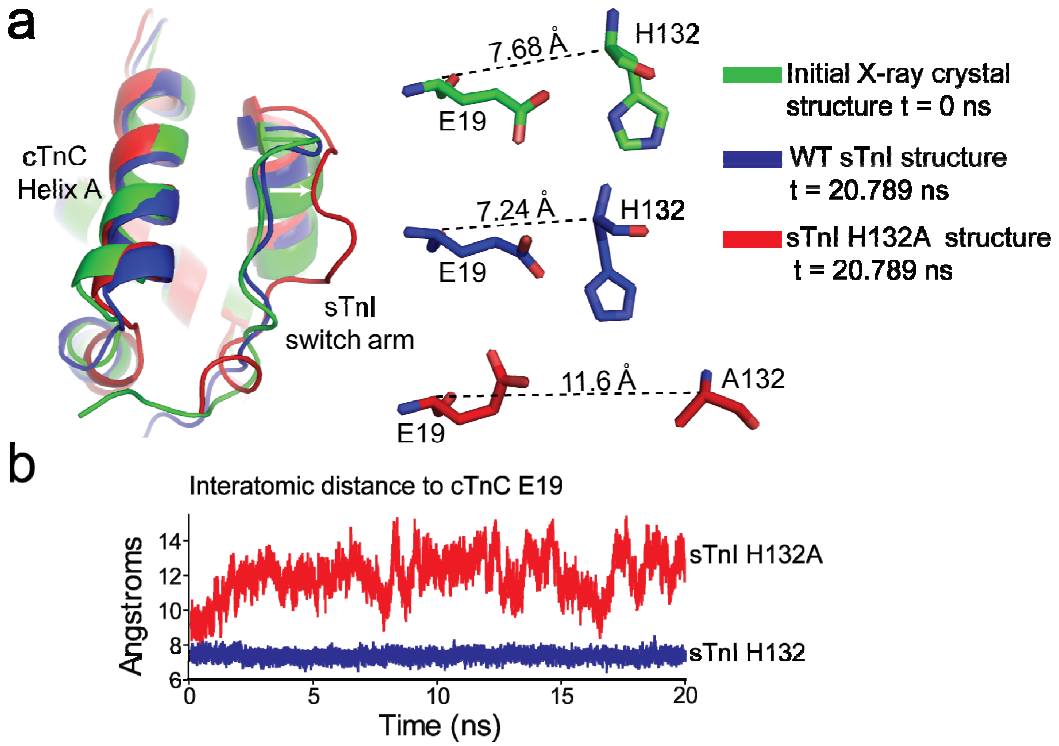

Figure 2-5. Molecular simulation modeling of interface separation caused by alanine substituted sTnI. (a) Structural alignment (left) of the initial X-ray crystal structure t = 0 ns; WT sTnI structure t = 20.789 ns; and sTnI H132A structure t = 20.789 ns showing interface separation only in the alanine substituted structure (arrow). Amino acid perspective showing separation of the alpha carbons of cTnC E19 from sTnI residue 132 (right). (b) Calculation of the interatomic distance between the alpha carbon of cTnC E19 and alpha carbon of residue 132 of WT sTnI (H132, blue) or sTnI H132A (red).

data indicates that the modification in the switch arm of cTnI between amphibians (histidine) and mammals (alanine) significantly enhanced the relaxation potential of cTn in the mammalian cardiovascular system. The proline residue observed in platypus cTnI accentuates this point. Proline is the archetypal helix breaker and is also nonpolar. Thus we believe that structurally and functionally, the platypus proline is an excellent intermediate to enhance relaxation in large part through disruption of the histidine-glutamate salt bridge predicted to occur in amphibian cTn.

Increased myofilament calcium sensitivity in pre-mammalian chordates

Previous reports have shown that residues at the N-terminus of cTnC are required for differentially modulating the calcium binding affinity of TnC between endotherms and ectotherms (Figure 2-13)[332]. It was suggested that, in ectotherms, four residues (GrP sequence: N2, I28, Q29, D30) were responsible for decreasing the energy barrier required for conformational changes in the N-terminus which increased calcium binding affinity at EF hand site II. In endotherms, these residues have been converted to D2, V28, L29, and G30 and markedly reduce myofilament calcium sensitivity by decreasing the calcium binding affinity of cTnC. In mammals, failure to modify these residues results in cardiomyopathy. Studies have shown that a single amino acid substitution L29Q in human cTnC causes a significant increase in myofilament calcium sensitivity that results in hypertrophic cardiomyopathy [365, 366]. Other evolutionary revertant

phenotypes associated with increased myofilament sensitivity to activating calcium have been found in SNPs within other regions of cTnC as well as cTnT[336, 358, 367-374].

Together with modifications in the cTnI switch arm, these data provide evidence that the ancestral cTn phenotype of heightened myofilament responsiveness to activating calcium was a physiological mechanism required for cardiovascular function of these species[4, 5, 334]. The physiological demands placed on these species including cold temperatures and extended periods of hypoxia support the need for myofilament function with pH responsiveness and heightened sensitivity to activating calcium. In addition to residues in cTnC, this study provides new knowledge suggesting that a histidine moiety in the switch arm of cTnI also contributes to the heightened myofilament calcium sensitivity and reveals the likely source for this residue as responsible for pH responsive inotropy observed in hearts of ancestral species.

Enhanced relaxation of cardiac troponin is required for mammalian heart function

A significant corpus of literature has emerged in recent years providing comparative analysis of cardiovascular function between chordate species [1, 4, 5, 13, 99, 334, 359-361, 375-383]. These studies elucidated important details about the differences in physiological requirements that necessitate unique mechanisms of cardiovascular support. The current study contributes to this knowledge base by providing the first evidence for molecular evolution of the cardiac troponin

complex. These data show that this cTn modification enhances the relaxation performance of the thin filament regulatory complex and may have evolved to accommodate cardiovascular demands of the adult mammalian heart (Figure 2-6).

The expression of TnI isoforms with inherently high calcium sensitivity in the developing hearts of all chordate species (fish/amphibian cTnI and mammalian/avian ssTnI) [311, 331, 361] indicates that heightened calcium sensitivity and pH responsiveness of the myofilaments are characteristics required for heart development in all chordate species (Figure 2-6). Several studies support this assertion. First, the fetal heart has high lactate levels and relies on glucose metabolism[384]. Second, there is evidence that the critical cardiac developmental transcription factor Nkx2.5 is regulated by hypoxia-inducible factor (HIF-1α)[385]. Third, immature sarcoplasmic reticulum and calcium cycling in the developing heart require heightened sensitization of the myofilaments to establish sufficient inotropy[386, 387].

However, in the adult heart, requirements for proper regulation of cardiac output are markedly different between chordate species. Numerous factors intrinsic and extrinsic to the heart affect the efficiency of heart rate and stroke volume to sustain cardiac output. Sufficient ventricular filling during diastole is a requisite precursor to systolic ejection. In human patients, incomplete LV filling even in the absence of systolic dysfunction is a key symptom of heart failure[388]. This makes diastolic performance a significant point of vulnerability in the maintenance of cardiac function.

Figure 2-6. Proposed model for molecular evolution of cardiac troponin during chordate evolution. Progressive modifications in organismal cardiovascular requirements resulted in marked changes in heart structure and functional regulation to meet evolving whole animal physiologic demands. Troponin isoforms expressed in species identified early in chordate evolution (e.g. fish (cTnI) and amphibians(cTnI)) together with developmental isoforms from all classes (fish (cTnI), amphibian (cTnI), avian (ssTnI), and mammalian (ssTnI)) have a high energy histidine-glutamate interaction in the regulatory intermolecular interface between cTnI and cTnC. This results in myofilaments with heightened calcium sensitivity and reduced pH sensitivity. During evolution of the mammalian adult cardiovascular system (developmental isoform transition to cTnI), the cardiac troponin I switch arm evolved to contain a proline moiety in place of the histidine (as seen with the platypus) that fundamentally altered the critical regulatory interaction between cTnI and cTnC. Together with all other mammals (which have A164), this resulted in myofilaments with reduced calcium sensitivity (enhanced relaxation) and increased pH sensitivity. Taken together, this study provides seminal insight into chordate cardiovascular evolution providing a model of enhanced relaxation efficiency in cTn required to meet mammalian lusitropic demands.

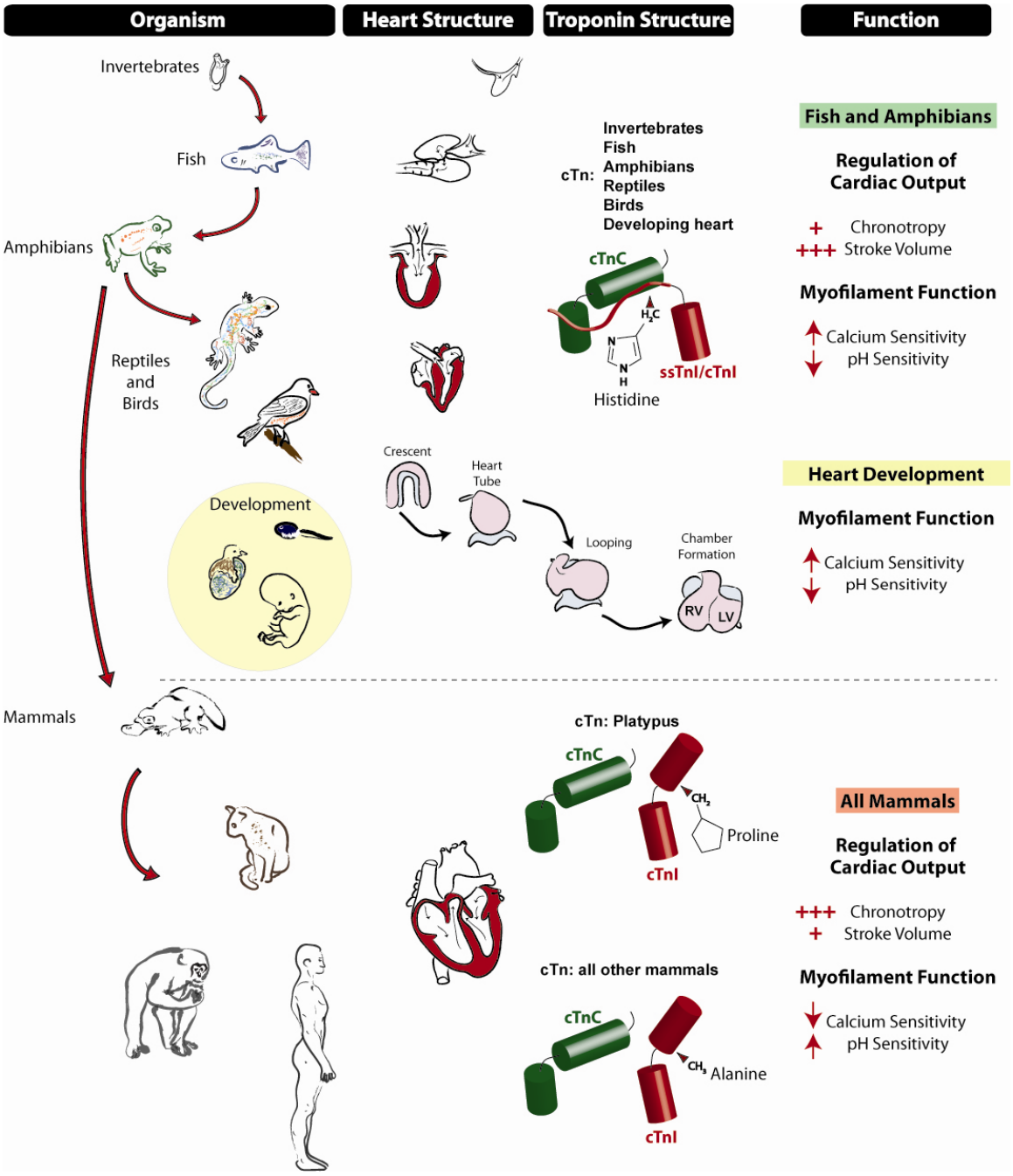
Organism
Heart Structure
Troponin Structure
Function
Invertebrates
Fish
Amphibians
Reptiles and Birds
Development
Mammals
cTn:
Invertebrates
Fish
Amphibians
Reptiles
Birds
Developing heart
cTnC
ssTnI/cTnI
Histidine
Crescent
Heart Tube
Looping
Chamber Formation
RV
LV
Fish and Amphibians
Regulation of Cardiac Output
+ Chronotropy
+++ Stroke Volume
Myofilament Function
Calcium Sensitivity
pH Sensitivity
Heart Development
Myofilament Function
Calcium Sensitivity
pH Sensitivity
cTn: Platypus
cTnC
cTnI
Proline
All Mammals
Regulation of Cardiac Output
+++ Chronotropy
+ Stroke Volume
Myofilament Function
Calcium Sensitivity
pH Sensitivity
cTn: all other mammals
cTnC
cTnI
Alanine

At the level of single myocytes, key regulators of myocardial relaxation include cytoplasmic calcium re-sequestration into the sarcoplasmic reticulum through SERCA2a and troponin I inhibition of actomyosin ATPase activity[46, 91, 103, 119, 120, 188]. Dysfunction in SR calcium uptake or cTnI inhibition of myofilament activation result in delayed sarcomeric relaxation[137, 200, 243, 274, 333]. Concerning cTnI function, inefficient lusitropy could either occur because of enhanced binding to cTnC during systole and/or incomplete inhibition of actomyosin crossbridge formation during diastole. In either case, the observed effect is an increase in myofilament calcium sensitivity[66, 123, 333, 389]. Cardiomyopathic SNPs identified in all members of the human heterotrimeric cardiac troponin complex have been found to cause an evolutionary revertant phenotype characterized by a marked increase in myofilament calcium sensitivity[333, 365, 366, 390-394]. Together, these studies show a strong correlation between evolutionary revertant phenotypes caused by cardiomyopathic SNPs in troponin and heart failure phenotypes including diastolic dysfunction, arrhythmias, and sudden cardiac death.

In the context of chordate evolution, our current understanding of fish and amphibian physiology support the need for heightened myofilament calcium sensitivity with pH-responsiveness[4, 5, 331, 334, 395]. Similar to cTnI, other proteins have shown analogous adaptions in these species. For example, hemoglobin in many fish has an exacerbated Bohr effect known as the Root effect, an extreme form of pH sensitive Hb O_2 binding[326, 396, 397]. On the part of regulating cardiac contractility at low pH, the N-terminal NIQD motif of cTnC and the switch arm

peptides of cTnI seen in fish and amphibians provide the required cardiovascular support to meet physiological demands of ectotherms (Figure 2-6). However, the observation that heart failure symptoms occur in patients with evolutionary revertant phenotypes including hypersensitive myofilaments indicates that enhanced relaxation properties at the level of the myofilaments were a necessary adaptation for the mammalian cardiovascular system.

Phylogenetic alignment data show the emergence of protein kinase (PKA and PKC) phosphorylation sites at the N-terminus of TnI (S23, 24) at the level of amphibians (Figure 2-12). One of the major purposes for protein kinase phosphorylation of these residues is to enhance relaxation of the myofilaments in coordination with changes in heart rate[9, 202, 205, 215]. Although covalent modifications of TnI emerged prior to mammals, this mechanism for augmenting lusitropy was evidently insufficient for mammalian cardiovascular function. As a consequence, this study supports the hypothesis that coordinated residue modifications in cTn enhanced the intrinsic relaxation potential of troponin independent of covalent modifications.

Structure and function data indicate that this occurred on cTnC by markedly decreasing the calcium binding affinity at EF hand site II[332]. On the part of TnI, this study provides important evidence that a histidine to alanine substitution in the switch arm disrupted a strong intermolecular electrostatic interaction between histidine of cTnI and glutamate of cTnC (Figure 2-6). *In silico* molecular dynamics alanine scanning simulations and functional data[252] support the importance of this modification in enhancing myofilament relaxation by

making cTnI molecularly untethered from cTnC reducing the intermolecular interface binding free energy. These data also indicate that loss of a therapeutically effective pH responsive histidine button in cTnI[203, 246, 290] was necessary to acquire proper relaxation[252]. This study provides the first evidence for the prominent role of troponin in the molecular evolution of mammalian diastolic performance. The model put forth by this study is that selective pressures during evolution of the mammalian cardiovascular system resulted in coordinated residue modifications in cardiac troponin enabling it to relax more efficiently to accommodate mammalian lusitropic requirements.

Acknowledgements

We thank the labs of the University of Minnesota Lillehei Heart Institue for questions oriented toward the phylogenetics of cardiac troponin which stimulated this study. We thank Nobubelo Ngandu, Dr. Cathal Seoighe, and Dr. Simon Frost for assistance with interpretation of selective pressures on the cTnI molecule. We also thank Dr. Antony Dean for advice on interpreting phylogenetic data. This study was supported by the National Institutes of Health (JM) and the American Heart Assocation (NP).

Appendix A

Phylogenetic analysis of slow/cardiac troponin C

Analysis of the cTnC sequence alignment (Figure 2-11) was also performed. Taken together with reported functional data[332, 366], this phylogenetic analysis revealed important differences between ectotherms (A, As1, AL, DE, GP, Z, and Xl) and endotherms (Q, Ch, M, R, Rab, P, B, and H) regarding the role of cTnC in cardiac function between these species. The functional domains of cTnC analyzed include EF hand I (15-47), EF hand II (55-82), EF hand III (94-125), and EF hand IV (134-161). Figure 2-11 shows the positional arrangement of the critical divalent cation binding sites, EF hand sites I-IV, relative to the secondary helix structures of the protein. Phylogenetic analysis of each EF hand site across all species showed that site II is the most highly conserved (Figure 2-13a). This is consistent with EF hand II being the only functional calcium binding site in cTnC and required for Tn function[65, 71, 73]. Studies have shown that the acid side chains in the EF hand of site II are highly conserved and involved in coordinating the binding of calcium to cTnC[74]. Comparison of the conservation of these EF hand sites within ectotherms and endotherms showed that all regions of the protein are significantly more highly conserved ($P < 0.05$) in endotherms than ectotherms (Figure 2-13b). This suggests that there is a concerted pressure

for stabilization of this protein in order to maintain evolutionary modifications within the protein that are critical for cardiovascular function in endotherms.

Functional differences within the cTnC isoform have been reported when comparing endothermic vs. ectothermic species[4, 332, 334]. Of particular interest, the acidic residues in the N-terminal hydrophobic patch of cTnC hypothesized to interact with the regulatory domain of TnI are 100% conserved across all species (Figure 2-13c). This indicates that functional alterations of cTnC during chordate evolution are not mediated through alterations in these acidic residues. However, previous reports have shown that residues at the N-terminus of cTnC are required for differentially modulating the calcium binding affinity of TnC between endotherms and ectotherms (Figure 2-13c)[332]. It was suggested that four residues (GrP sequence: N2, I28, Q29, D30) were responsible for this biophysical difference. This amino acid combination did not alter the open probability of the hydrophobic patch but decreased the energy barrier required for conformational changes in the N-terminus that affect calcium binding affinity at EF hand site II. When accounting for differences in temperature between the TnC calcium binding affinity of these ectothermic species compared to the binding affinity seen in endothermic TnC the calcium binding affinity was normalized. This indicates that these residue substitutions were required for proper maintenance of cardiac function during evolutionary adaptations in thermoregulation between these species.

The current analysis of an expanded number of sequences focusing on the cTnC isoform revealed, however, that N2 and I28 do not likely contribute significantly to this functional difference since these residues are not highly conserved within ectothermic species (e.g. instead of an asparagine, S and Xl have an aspartate similar to all endotherms). In contrast, Q29 and D30 are 100% conserved in all ectotherms and transition to L and G, respectively, in all endotherms with 100% conservation. This suggests that substitutions in the human s/cTnC L29Q and G30D would be sufficient to completely recapitulate the increased calcium binding affinity in the ectothermic cTnC molecule. In a recent report, Liang et al showed that the single amino acid substitution L29Q resembles the effects of the NIQD motif seen in ectotherms[365]. Furthermore, L29Q is a known TnC disease causing mutation and has been linked to a patient with familial hypertrophic cardiomyopathy[366]. Taken together, this analysis of cTnC protein indicates that the evolutionary pressures during the transition into the mammalian cardiovascular system fundamentally required a reduction in the calcium binding affinity of cTnC.

The functional implications of Tn modifications in cardiovascular function of ectothermic species

Fish and amphibian species are ectotherms and have many common features in terms of structural and functional regulation of cardiac output. Studies have shown that fish regulate cardiac output primarily through modifications in stroke volume as opposed to changes heart rate[4, 5]. The flounder heart has the highest reported stroke volume of a teleost measured at 2.3 mL per gram body weight[6]. Similarly, amphibians have the capacity to modulate cardiac output through changes in stroke volume but show increased regulation of heart rate compared to fish[4, 5]. An increase between 100-300% of resting stroke volume has been observed in exercising fish and amphibian species[398, 399]. Despite having resting sarcomere lengths similar to mammals, fish and amphibians are able to extend their sarcomeres beyond the optimal length of overlap and still develop force and thus function over a broader range of the Frank-Starling curve[334, 400, 401]. The near linear passive tension-extension properties of myocytes and the capacity to dramatically increase myofilament calcium sensitivity at longer sarcomere lengths are thought to mediate this phenotype[334, 402]. At the whole organ level, low passive tension of fish and amphibian hearts may facilitate decreased end systolic volume and increased end diastolic volume (ejection fraction near 100%[398]) enabling these species to regulate cardiac output by changes in stroke volume. Studies have shown that adrenergic-mediated alterations in chronotropy is less potent at lower temperatures making regulation of CO through modulation of HR less valuable in ectothermic species such as fish and amphibians[403]. Studies have also shown that heart rate is much lower in

ectotherms than endotherms making SV an optimal mechanism for regulating CO (Max ΔHR = 5bpm)[5, 404].

Together with other studies[332], this study provides an emerging picture of how the troponin complex plays an important role in cardiovascular performance of ectothermic species. As discussed previously, studies have shown that the calcium binding affinity of cTnC in ectothermic species is significantly higher than endothermic species. Prior evidence together with the current phylogenetic analysis of sequence percent identity suggests that two key amino acids responsible for this phenotype are Q29 and D30 (Figure 2-13). When accounting for physiological temperature differences, however, the calcium sensitivity of the myofilaments is not different between ectotherms and endotherms. Data from this study indicates that amphibian and fish cTnI also has properties that would enhance the calcium sensitivity of the myofilaments. Specifically, key amino acids in the switch domain have been attributed to a TnI phenotype with heightened contractile performance[252]. Furthermore, the histidine moiety has been shown to confer resistance to acidosis induced contractile failure[133, 246]. In species such as fish and amphibians this pH responsive regulation of inotropy is critical due to normal physiological conditions of hypoxia experienced by these species[405-408]. In fact, studies of perfused frog hearts have shown that amphibians can maintain normal cardiac function during severe hypoxia or ischemia[408]. We believe that a significant mediator of this response is the histidine button located in the switch domain of amphibian cTnI.

The current study also shows that the dual serine phosphorylation sites known to be critical for cardiac adrenergic responsiveness[9] are absent in fish but emerge with 100% conservation in amphibians through avian and mammalian species (Figure 2-12). This is consistent with the emergence of control of cardiac output through modulation of heart rate in these species. Furthermore, this indicates that the precise emergence of these PKA phosphorylation sites in species with very immature autonomic control of cardiovascular performance.

Taken together, regulation of cardiovascular function in fish and amphibians is primarily mediated through changes in stroke volume. As a consequence, the role of Tn in regulation of myofilament performance in these species is specifically designed to increase the calcium sensitivity of the myofilaments. This is accomplished through targeted amino acid modifications in the N-terminus of cTnC as well as the switch domain of cTnI. Furthermore, cTnI acts as a pH responsive molecular rheostat capable of modulating myofilament activation in response to changes in the intracellular milieu. Placed in the context of whole animal physiology, these intricate functions of the troponin complex are necessary for healthy cardiac performance in these species.

The functional implications of Tn modifications in cardiovascular function of avian species

Discussion of the impact of Tn in cardiovascular performance of avian species is difficult because of the limited number of cardiac studies is this phylogeny. As opposed to fish and amphibian species, avian and mammalian species show the emergence of the slow skeletal TnI isoform during early cardiac development with the transition to the cardiac isoform in the adult heart[89, 311, 362]. It is known that reptile and bird species regulate cardiac output through changes in heart rate[5]. In fact, some birds such as ducks and pigeons regulate cardiac output solely through changes in heart rate[4]. It is logical therefore that adrenergic responsiveness is a key mechanism at play in avian species. The presence of cTnI S23, 24 in avian species is important in modulating myofilament performance in response to chronotropic changes. In terms of the other major myofilament protein targeted by PKA, MBP-C, it is not known whether a threonine at site B can act as a surrogate phosphorylation site to initiate phosphorylation at sites A and C. Similar to mammalian species, avian species also have a cTnC molecule with reduced calcium binding affinity compared to amphibians and fish (L29, G30). In contrast to mammals, however, bird species have a switch domain very similar to amphibians in regard to the histidine button (with the exception of a proline observed in the zebra finch) and some of the other key residues of this domain. Overall, the functional importance of these characteristics of the troponin complex requires more knowledge of avian cardiovascular physiology.

Adrenergic regulation of myofilament function through cardiac TnI

Like bird species, mammals regulate cardiac output by modulation of heart rate and, to some extent, modifications in stroke volume[5]. Interestingly, the fastest heart rate ever recorded in any vertebrate was found in a mammal, the Etruscan shrew, with a measured rate in excess of 1500 bpm[7]. Due to a higher responsiveness to catecholamines in endothermic species[5, 403], mammals meet whole animal metabolic demands through adrenergic and cholinergic adjustments in chronotropy[9]. Covalent modifications at sites throughout cTnI are known to be regulated by protein kinases to fine tune myofilament performance in conjuction with chronotropic changes in heart rate[9, 202, 205]. This phylogenetic analysis provides new insights into how adrenergic control of myocytes function emerged during chordate evolution.

It has been shown that ssTnI diminishes the response to β-adrenergic stimulation[9, 202, 205, 213, 409] due to the absence of a key N-terminal extension found in cTnI. This region in cTnI contains dual serine residues (S23,24) first identified by Swiderek et al[410] which are known to be critical for the catecholaminergic response of the heart through cAMP-dependent protein kinase A (PKA) phosphorylation[9, 107, 127, 140, 202, 205]. Previous studies have shown that these phosphorylation sites are required for proper enhancement of relaxation during adrenergic stimulation[202, 215]. Although a great deal is unknown regarding the mechanism, it is generally accepted that PKA phosphorylation of S23, 24

facilitates faster relaxation rates by desensitizing the myofilaments to activating calcium[158, 411]. S23, 24 phosphorylation has also been shown to enhance inotropy at least in part by increasing the cross-bridge cycling rate[214, 215, 412]. Enhanced inotropy and lusitropy is a key mechanisms responsible for increasing cardiac output at higher heart rates during physiological stress[9, 205, 413]. The dual serine phosphorylation sites (S23, 24) at the N-terminus of cTnI appear at the level of the amphibian and are completely conserved through birds and mammals (Figure 2-12).

Sequence alignment of another PKA targeted myofilament protein, cardiac myosin binding protein C (MBP-C), shows that the critical phosphorylation site B (human sequence: S284) is a glycine in amphibians and is substituted for a serine residue only in mammals (Figure 2-16a). Phosphorylation site B has been found to be required for phosphorylation of sites A and C on MBP-C [414-416]. If the paradigm holds true for earlier vertebrates, this makes the amphibian MBP-C unresponsive to covalent modifications through PKA signaling. These observations suggest that adrenergic modulation of sarcomere function through PKA was initiated through targeted residues in TnI as opposed to MBP-C.

Calcium handling is also influenced by PKA signaling[321, 417]. Phospholamban (PLN) is the regulator of calcium sequestration through the sarco-endoplasmic reticulum calcium ATPase (SERCA2a). Dual phosphorylation of PLN (S16, T17) enables faster calcium cycling to enhance diastolic performance of the myocytes[321]. Studies have shown that S16 is sufficient for the

full adrenergic effect on calcium handling[323] and is required for phosphorylation of T17[418]. Whole genome scans were performed on *Xenopus tropicalis*, *Ornithorhynchus anatinus* (platypus), and *Monodelphis domestica* (opossum) to expand the number of sequences available for clustal W analysis of PLN (Figure 2-16b). Sequence alignment showed that the key S16 residue is present in all chordates from amphibian to avian and mammalian species. However, the T17 is only present in bird species and most mammals with the exception of the platypus (Figure 2-16b). Taken together, this alignment data suggests that adrenergic control of myocyte calcium handling and myofilament function emerged together in amphibians through PKA-mediated covalent modification of cTnI S23,24 and PLN S16.

Appendix B

Table 2-2. Sources for protein and nucleotide sequences

Name	Organism	Taxonomy	Accession number	Database
Human cardiac TnI	Homo sapiens	Mammalia	NP_000354	NCBI Protein
Human cardiac TnI	Homo sapiens	Mammalia	NM_000363	NCBI Nucleotide
Human slow skeletal TnI	Homo sapiens	Mammalia	NP_003272	NCBI Protein
Sumatran orangutan cardiac TnI	Pongo abelii	Mammalia	NP_001126240	NCBI Protein
Sumatran orangutan cardiac TnI	Pongo abelii	Mammalia	NM_001132768	NCBI Nucleotide
Chimpanzee cardiac TnI Predicted	Pan troglodytes	Mammalia	XP_001134934	NCBI Protein
Chimpanzee slow skeletal TnI Predicted	Pan troglodytes	Mammalia	XP_525019	NCBI Protein
Rhesus cardiac TnI Predicted	Macaca mulatta	Mammalia	XP_001086032	NCBI Protein
Rhesus slow skeletal TnI Predicted	Macaca mulatta	Mammalia	XP_001108591	NCBI Protein
Bovine cardiac TnI	Bos Taurus	Mammalia	CAH57016	NCBI Protein
Bovine cardiac TnI Predicted	Bos Taurus	Mammalia	XM_588363	NCBI Nucleotide
Horse cardiac TnI	Equus caballus	Mammalia	AAV68047	NCBI Protein
Horse cardiac TnI	Equus caballus	Mammalia	NM_001081904	NCBI Nucleotid

				e
Pig cardiac TnI	Sus scrofa	Mammalia	ABF84065	NCBI Protein
Pig cardiac TnI	Sus scrofa	Mammalia	NM_001098599	NCBI Nucleotide
Pig slow skeletal TnI	Sus scrofa	Mammalia	AAP37479	NCBI Protein
Goat cardiac TnI	Capra hircus	Mammalia	AAK56404	NCBI Protein
Goat slow skeletal TnI	Capra hircus	Mammalia	AAK56402	NCBI Protein
Dog cardiac TnI	Canis lupus familiaris	Mammalia	NP_001003041	NCBI Protein
Dog cardiac TnI	Canis lupus familiaris	Mammalia	NM_001003041	NCBI Nucleotide
Cat cardiac TnI	Felis catus	Mammalia	AAP23052	NCBI Protein
Cat cardiac TnI	Felis catus	Mammalia	NM_001009237	NCBI Nucleotide
Rabbit cardiac TnI	Oryctolagus cuniculus	Mammalia	P02646	NCBI Protein
Rabbit slow skeleteal Tni	Oryctolagus cuniculus	Mammalia	P02645	NCBI Protein
Rat cardiac TnI	Rattus norvegicus	Mammalia	NP_058840	NCBI Protein
Rat cardiac TnI	Rattus norvegicus	Mammalia	NM_017144	NCBI Nucleotide
Rat slow skeletal TnI	Rattus norvegicus	Mammalia	NP_058880	NCBI Protein
Rat slow skeletal TnI	Rattus norvegicus	Mammalia	NM_017184	NCBI Nucleotide
Mouse cardiac TnI	Mus musculus	Mammalia	NP_033432	NCBI Protein
Mouse cardiac TnI	Mus musculus	Mammalia	NM_009406	NCBI Nucleotide
Mouse slow skeletal TnI	Mus musculus	Mammalia	NP_001106173	NCBI Protein
Mouse fast	Mus musculus	Mammalia	NM_009405	NCBI

skeletal TnI				Nucleotide
Opossum cardiac TnI Predicted (69-262)	Monodelphis domestica	Mammalia	XP_001381826	NCBI Protein
Opossum cardiac TnI Predicted	Monodelphis domestica	Mammalia	XM_001381789	NCBI Nucleotide
Platypus cardiac TnI Predicted	Ornithorhynchus anatinus	Mammalia	XP_001508807	NCBI Protein
Platypus cardiac TnI Predicted	Ornithorhynchus anatinus	Mammalia	XM_001508757	NCBI Nucleotide
Chicken cardiac TnI	Gallus gallus	Aves	NP_998735	NCBI Protein
Chicken cardiac TnI	Gallus gallus	Aves	NM_213570	NCBI Nucleotide
Chicken slow skeletal TnI (aa 72-290)	Gallus gallus	Aves	XP_419242	NCBI Protein
Chicken fast skeletal TnI	Gallus gallus	Aves	NP_990748	NCBI Protein
Quail cardiac TnI	Coturnix coturnix	Aves	A41030	NCBI Protein
Quail cardiac TnI	Coturnix coturnix	Aves	QULTROPO1	NCBI Nucleotide
Quail slow skeletal TnI	Coturnix coturnix	Aves	AAC59937	NCBI Protein
Quail slow skeletal TnI	Coturnix coturnix	Aves	CCU37118	NCBI Nucleotide
Zebra Finch slow skeletal TnI Predicted	Taeniopygia guttata	Aves	XP_001368433	NCBI Protein
Salmon cardiac TnI	Salmo salar	Teleostei	ACM09452	NCBI Protein
Salmon cardiac TnI	Salmo salar	Teleostei	NM_001146587	NCBI Nucleotide

Salmon slow skeletal TnI	Salmo salar	Teleostei	ACM09762	NCBI Protein
Xenopus laevis cardiac TnI	Xenopus laevis	Amphibia	NP_001081378	NCBI Protein
Xenopus laevis cardiac TnI	Xenopus laevis	Amphibia	BC170405	NCBI Nucleotide
Xenopus laevis slow skeletal TnI	Xenopus laevis	Amphibia	NP_001079781	NCBI Protein
Xenopus laevis fast skeletal TnI	Xenopus laevis	Amphibia	NM_001086087	NCBI Nucleotide
Xenopus (silurana) tropicalis cardiac TnI	Xenopus (silurana) tropicalis	Amphibia	NP_001011410	NCBI Protein
Xenopus (silurana) tropicalis cardiac TnI	Xenopus (silurana) tropicalis	Amphibia	NM_001011410	NCBI Nucleotide
Xenopus (silurana) tropicalis slow skeletal TnI	Xenopus (silurana) tropicalis	Amphibia	NP_988959	NCBI Protein
Bullfrog cardiac TnI	Rana catesbeiana	Amphibia	AAO33937	NCBI Protein
Bullfrog cardiac TnI	Rana catesbeiana	Amphibia	AY166834	NCBI Nucleotide
Bullfrog slow skeletal TnI	Rana catesbeiana	Amphibia	AAO33938	NCBI Protein
Marine toad cardiac TnI	Bufo marinus	Amphibia	AAX69047	NCBI Protein
Marine toad cardiac TnI	Bufo marinus	Amphibia	AY773673	NCBI Nucleotide
Ascidian 1 cardiac TnI	Halocynthia roretzi	Tunicata	BAB83804	NCBI Protein
Ascidian 1 cardiac TnI	Halocynthia roretzi	Tunicata	AB077763	NCBI Nucleotid

				e
Ascidian 2 cardiac TnI	Ciona intestinalis	Tunicata	AAL27686	NCBI Protein
Ascidian 2 body wall TnI	Ciona intestinalis	Tunicata	AAC26988	NCBI Protein
Amphoxius TnI	Branchiostoma belcheri	Cephalochordata	BAA96549	NCBI Protein

Name	**Organism**	**Taxonomy**	**Locus**	**Database**
Human cTnC	Homo sapiens	Mammalia	NP_003271	NCBI Protein
Bovine cTnC	Bos taurus	Mammalia	NP_001029523	NCBI Protein
Pig cTnC	Sus scrofa	Mammalia	NP_001123715	NCBI Protein
Rabbit cTnC	Oryctolagus cuniculus	Mammalia	P02591	NCBI Protein
Rat cTnC	Rattus norvegicus	Mammalia	NP_001029277	NCBI Protein
Mouse cTnC	Mus musculus	Mammalia	NP_033419	NCBI Protein
Chicken cTnC	Gallus gallus	Aves	NP_990464	NCBI Protein
Chicken fast skeletal TnC	Gallus gallus	Aves	NP_990781	NCBI Protein
Quail cTnC	Coturnix japonica	Aves	P05936	NCBI Protein
Xenopus laevis TnC	Xenopus laevis	Amphibia	O12998	UniProtKB
Salmon cTnC	Salmo salar	Teleostei	B5X7T1	UniProtKB
Zebrafish cTnC	Danio rerio	Teleostei	AAO50211	NCBI Protein
Arctic Lamprey cTnC	Lethenteron japonicum	Hyperoartia	BAA23283	NCBI Protein
Dinasaur eel cTnC	Polypterus senegalus	Euteleostomi	AAO50212	NCBI Protein
Green Pufferfish cTnC	Tetraodon fluviatilis	Teleostei	AAO50213	NCBI Protein
Ascidian 1 TnC	Halocynthia roretzi	Tunicata	BAA13631	NCBI Protein

Amphoxius TnC	Branchiostoma lanceolatum	Cephalochordata	AAB30666	NCBI Protein

Name	Organism	Taxonomy	Locus	Database
Human cardiac TnT	Homo sapiens	Mammalia	NP_000355	NCBI Protein
Bovine cardiac TnT	Bos taurus	Mammalia	NP_777196	NCBI Protein
Sheep cardiac TnT	Ovis aries	Mammalia	P50751	NCBI Protein
Dog cardiac TnT	Canis lupus familiaris	Mammalia	NP_001003012	NCBI Protein
Cat cardiac TnT	Felis catus	Mammalia	NP_001009347	NCBI Protein
Rabbit cardiac TnT	Oryctolagus cuniculus	Mammalia	P09741	NCBI Protein
Rat cardiac TnT	Rattus norvegicus	Mammalia	NP_036808	NCBI Protein
Mouse cardiac TnT	Mus musculus	Mammalia	BAB19881	NCBI Protein
Chicken cardiac TnT	Gallus gallus	Aves	NP_990780	NCBI Protein
Turkey cardiac TnT	Meleagris gallopavo	Aves	AAG23714	NCBI Protein
Xenopus laevis cardiac TnT	Xenopus laevis	Amphibia	AAO33406	NCBI Protein
Salmon cardiac TnT	Salmo salar	Teleost	ACM09307	NCBI Protein
Zebrafish cardiac TnT	Danio rerio	Teleost	AAP33153	NCBI Protein
Ascidian 1 TnT	Halocynthia roretzi	Tunicata	BAA12720	NCBI Protein

Name	Organism	Taxonomy	Locus	Database
Human cardiac MBP-C	Homo sapiens	Mammalia	AAI36547	NCBI Protein
Dog cardiac MBP-C	Canis lupus familiaris	Mammalia	ABB72024	NCBI Protein
Rat cardiac MBP-C	Rattus norvegicus	Mammalia	NP_001099960	NCBI Protein
Mouse cardiac MBP-C	Mus musculus	Mammalia	CAQ51619	NCBI Protein

Chicken cardiac MBP-C	Gallus gallus	Aves	NP_990447	NCBI Protein
Xenopus laevis cardiac MBP-C	Xenopus laevis	Amphibia	NP_001082167	NCBI Protein
Xenopus tropicalis cardiac MBP-C	Xenpus tropicalis	Amphibia	NP_001106379	NCBI Protein

Name	**Organism**	**Taxonomy**	**Locus**	**Database**
Human cardiac PLN	Homo sapiens	Mammalia	P26678	NCBI Protein
Dog cardiac PLN	Canis lupus familiaris	Mammalia	P61012	NCBI Protein
Rat cardiac PLN	Rattus norvegicus	Mammalia	P61016	NCBI Protein
Mouse cardiac PLN	Mus musculus	Mammalia	P61014	NCBI Protein
Chicken cardiac PLN	Gallus gallus	Aves	P26677	NCBI Protein

Table 2-3. Identification of novel troponin genes

Name	**TnI isoform**	**Locus**	**Version**	**Seed Sequence**	**Database**		
Zebra Finch	Cardiac	CK302118	CK302118.1 GI:44811692	Quail cTnI	NCBI		
Name	**TnI isoform**	**Chromosome**	**Nucleotide start**	**Nucleotide end**	**Scaffold**	**Seed Sequence**	**Database**
Lizard	cardiac	76	3343233	3345327	76:3343233-3345327	Xenopus Laevis cTnI	UCSC
Lizard	Slow skeletal	16	2162166	2162324	16:2162166-2162324	Xenopus Laevis	UCSC

						ssTnI	
Lizard	Fast skeletal	230	1139968	1140123	230:1139968-1140123	Xenopus Laevis fsTnI	UCSC
Guinea Pig	Cardiac	70	264853	268756	70:264853-268756	Mouse cTnI	UCSC
Guinea Pig	Slow skeletal	12	21029211	21031388	12:21029211-21031388	Mouse ssTnI	UCSC
Guinea Pig	Fast skeletal	42	12650148	12650318	42:12650148-12650318	Mouse fsTnI	UCSC
Marmoset	Cardiac	unknown	4467	8995	Contig20809	Human cTnI	UCSC
Name	**PLN**	**Chromosome**	**Nucleotide start**	**Nucleotide end**	**Scaffold**	**Seed Sequence**	**Database**
Xenopus tropicalis		18	426911	427066	18:426911-427066	Chicken PLB	UCSC
Platypus		unknown	0	6948	Contig5074	Xenopus tropicalis PLB	UCSC
Opossum		2	387187570	387187725	387187570-387187725	Platypus PLB	UCSC

Details of novel troponin I (TnI) and phospholamban (PLN) genes identified in various species. Zebra Finch cTnI was extracted from NCBI GenBank by BLAST of expressed sequence tags (ESTs) in the Taeniopygia guttata genome. The locus identified was defined as SB02014B2A01.f1 normalized Keck-Tagu Library SB02 Taeniopygia guttata cDNA clone SB02014B2A01.f1 5, mRNA sequence. TnI isoforms identified for Lizard (*Anolis carolinensis*), Guinea Pig (*Cavia porcellus*), and Marmoset (*Callithrix jacchus*) were extracted by Blat analysis of the respected UCSC Genome from the bioinformatics genome site (http://genome.ucsc.edu/). Predicted PLN sequences were acquired by Blat analysis of genomes of the platypus (*Ornithorhynchus anatinus*), opossum (*Monodelphis domestica*), and Xenopus (*Xenopus tropicalis*).

Table 2-4. Predicted pK titration calculations for ionizable groups in sTnI, cTnI and cTnC

Structure	**cTnC**		**cTnC with sTnI**		**cTnC with cTnI**	
Isoelectric point	4.09		4.54		4.51	
Total charge at pH 6.5	-11		-7		-10	
Residue	**pKint**	**pKa**	**pKint**	**pKa**	**pKint**	**pKa**
ASP-2	3.971	3.534	3.987	3.425	3.95	3.439
ASP-3	4.202	3.921	4.205	3.907	4.2	3.919
TYR-5	10.218	12.499	10.269	12.456	10.177	12.399
LYS-6	9.971	11.908	9.98	11.91	9.979	11.877
GLU-10	4.581	4.332	4.588	4.335	4.576	4.325
GLU-14	4.844	2.851	4.831	2.807	4.829	2.836
GLU-15	4.268	4.311	4.467	4.225	4.215	4.251
LYS-17	10.199	12.999	10.226	13.248	10.171	13.037
GLU-19	4.656	4.768	7.365	2.512	4.591	5.197
LYS-21	9.657	13.188	9.681	13.282	9.641	13.214
ASP-25	5.388	2.888	5.413	2.839	5.354	2.808
Structure	**sTnI**		**cTnC with**			

			sTnI			
Isoelectric point	11		4.54			
Total charge at pH 6.5	3		-7			
Residue	**pKint**	**pKa**	**pKint**	**pKa**		
ARG-117	7.354	7.187	7.488	7.784		
ASP-121	3.987	2.015	4.058	1.646		
ARG-125	12.058	12.584	12.1	13.113		
LYS-131	9.971	9.746	9.896	10.36		
HIS-132	5.451	5.072	4.733	8.253		
LYS-133	9.769	9.755	9.726	10.188		
ASP-137	4.255	3.705	4.415	3.721		
Structure	**cTnI**		**cTnC with cTnI**			
Isoelectric point	8.6		4.51			
Total charge at pH 6.5	1		-10			
Residue	**pKint**	**pKa**	**pKint**	**pKa**		

ARG-149	7.362	7.237	7.172	7.653		
ASP-153	3.744	3.565	3.781	3.542		
ARG-163	11.861	12.073	11.862	12.275		
LYS-165	10.41	10.879	10.562	11.14		
GLU-166	4.721	4.426	4.8	4.417		
ASP-169	4.96	4.484	5.023	4.501		
ARG-171	12.051	12.224	12.051	12.289		
HIS-173	6.602	7.09	6.612	7.098		

Crystal structures were analyzed for each protein individually (sTnI, cTnI, and cTnC) or in complex (sTnI-cTnC and cTnI-cTnC). Values for the intrinsic pK (pK_{int}) and actual pK (pK_a) are shown for each ionizable residue in the N-terminal hydrophobic patch of TnC and H3/H4 of TnI. Intrinsic pK was calculated by analysis of each amino acid in the peptide backbone and in the absence of any other interacting amino acid R groups. Actual pK was calculated by including all interacting R groups influencing the pH titration curve of the given moiety. The isoelectric point and total charge at pH 7.2 are also shown for each structure analyzed. For consistency throughout the manuscript, amino acid numbering has been modified from the original structures and is shown as the human cTnI, sTnI, and cTnC.

Table 2-5: Evolutionary pressure on the mammalian cTnI switch peptide

Alignment		Number of classes	1st Rate class		2nd Rate class	
			dN/dS	P_1	dN/dS	P_2
cTnI arm	Switch	2	0.0	0.447	0.286	0.553

Analysis of evolutionary pressure on the mammalian switch arm was accomplished using methods described by Kosakovsky Pond & Frost[419]. This methodology based on mRNA sequences uses a continuous-time Markov process to model synonymous (dN) and non-synonymous substitutions (dS) along a phylogenetic tree. In this approach, the mammalian cardiac TnI switch arm analysis of synonymous and non-synonymous rate classes identified the presence of strong purifying selection. Approximately half the sites in the cTnI switch arm are characterized by strong purifying selection within the mammals. Similarly, fixed effects likelihood (FEL) analysis only identified sites experiencing purifying selection, and not positive selection, in the switch arm analysis (data not shown). These data show that the mammalian cTnI switch arm is under significant purifying selection indicating that the current peptide composition has long been highly favorable for the proper regulatory functions of troponin in the mammalian heart. Rate classes, inferred using an AIC stepwise model fit procedure (see methods), describe the distribution of non-synonymous to synonymous subsitution rates (dN/dS) across all sites of an alignment, where P_x is the proportion of sites belonging to class x. Messenger RNA sequences analyzed were derived from the following species: H, SO, Ch, Ma, Rh, B, Ho, P, D, C, GP, R, M, O, and Pl.

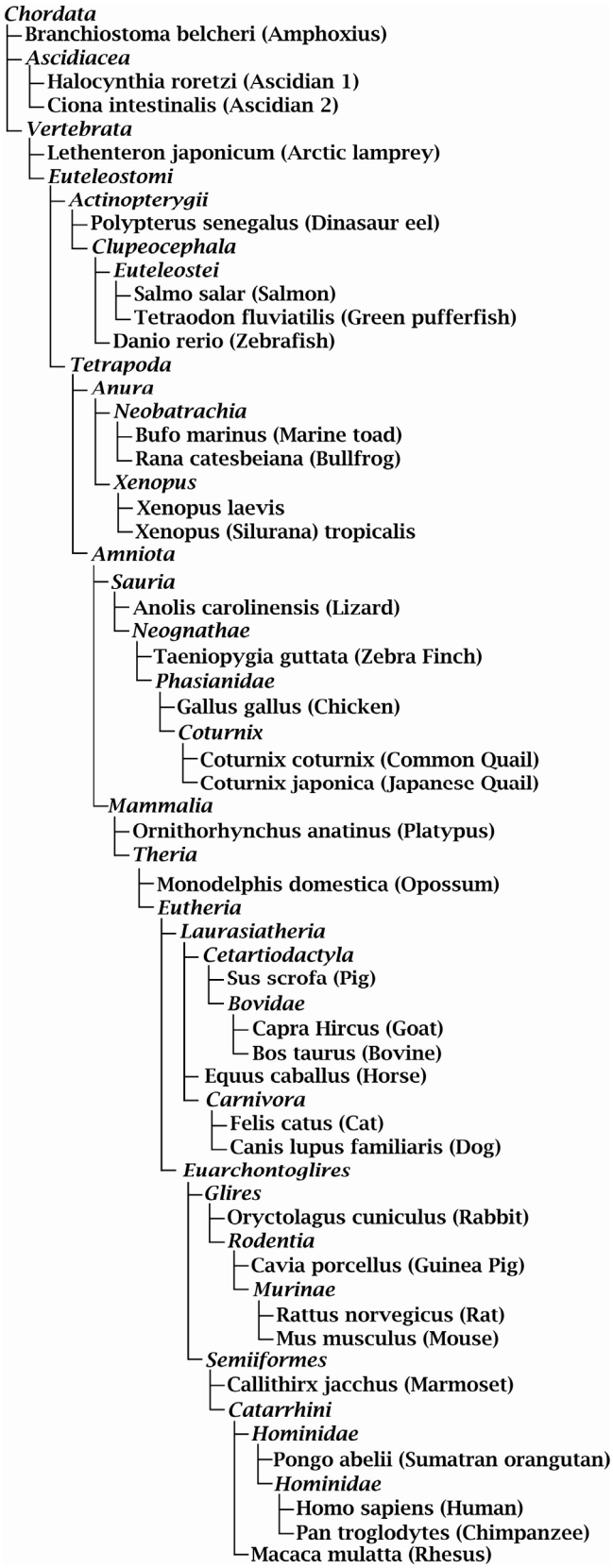
Chordata
Branchiostoma belcheri (Amphoxius)
Ascidiacea
Halocynthia roretzi (Ascidian 1)
Ciona intestinalis (Ascidian 2)
Vertebrata
Lethenteron japonicum (Arctic lamprey)
Euteleostomi
Actinopterygii
Polypterus senegalus (Dinasaur eel)
Clupeocephala
Euteleostei
Salmo salar (Salmon)
Tetraodon fluviatilis (Green pufferfish)
Danio rerio (Zebrafish)
Tetrapoda
Anura
Neobatrachia
Bufo marinus (Marine toad)
Rana catesbeiana (Bullfrog)
Xenopus
Xenopus laevis
Xenopus (Silurana) tropicalis
Amniota
Sauria
Anolis carolinensis (Lizard)
Neognathae
Taeniopygia guttata (Zebra Finch)
Phasianidae
Gallus gallus (Chicken)
Coturnix
Coturnix coturnix (Common Quail)
Coturnix japonica (Japanese Quail)
Mammalia
Ornithorhynchus anatinus (Platypus)
Theria
Monodelphis domestica (Opossum)
Eutheria
Laurasiatheria
Cetartiodactyla
Sus scrofa (Pig)
Bovidae
Capra Hircus (Goat)
Bos taurus (Bovine)
Equus caballus (Horse)
Carnivora
Felis catus (Cat)
Canis lupus familiaris (Dog)
Euarchontoglires
Glires
Oryctolagus cuniculus (Rabbit)
Rodentia
Cavia porcellus (Guinea Pig)
Murinae
Rattus norvegicus (Rat)
Mus musculus (Mouse)
Semiiformes
Callithirx jacchus (Marmoset)
Catarrhini
Hominidae
Pongo abelii (Sumatran orangutan)
Hominidae
Homo sapiens (Human)
Pan troglodytes (Chimpanzee)
Macaca mulatta (Rhesus)

Figure 2-7. Taxanomic tree showing the relationship of chordate species identified in this study. Tree was generated by use of the NCBI Taxonomy database.

Figure 2-8

Identification of primary mRNA sequences of TnI isoforms from numerous species. (a) Whole genome scans were performed to isolate putative TnI genes from various species including Marmoset, Guinea Pig, Zebra Finch, and Lizard. Sequences extracted from genome scans are given. (b) Phylogenetic tree analysis of all TnI proteins represented in the alignment. The Kimura distance formula is used to calculate distance values, derived from the number of non-gap mismatches and corrected for silent substitutions. The values computed are the mean number of differences per site and fall between 0-1. Zero represents complete identity and 1 no identity. Scale of the tree indicates the number of nucleotide substitutions per 100 residues. Phylogenetic tree analysis was used to confirm identity of predicted TnI isoforms by sequence correlation with other TnI isoforms. (c) Sequence ID and divergence values were calculated to define the relationship between novel TnI proteins and related TnI isoforms to assist in confirmation of postulated isoform designation. Divergence (i,j) is calculated as (100[Distance (i,j)] / Total Distance) where (i,j) is the sum of the branch lengths between two sequences and Total Distance is the sum of all branch lengths. Additional details on identified sequences is outlined in Table 2-5.

a

Lizard cardiac TnI

ATCaagGATCTGAACcagAAGATCtttGACCTAAGAGGCAAATTCAAACGCCCA
GCTCTTCGCCGTGTCCTCTCTCAGCGGATGCCATGATGcaaGCCCTACTCGG
CACCAAGCACAAGgtctccATGGATCTGCGGGCCAATCTCAAACAAGTCAAGG
AAGTGGGTGACTGGCGGAAGAACattGATGCTCTGAGTGGCATGGAGGGCC
GCAAGAAGAAGTTTGAGgccTCTcctGCAggaCAA

Lizard slow skeletal TnI

ATTaaaGACCTGaaattgAAAgtaCTGGACCTTCGAGGAAAGTTCAAGCGTCCTcc
cTTGAGGCGTGTCCGTgtcTCTGCAGATGCCATGctaAGGGCTCTGCTGGGTtct
AAGCACAAAgtttccATGGACTTGAGAGCCAACCTCAAAtctGTCAAG

Lizard fast skeletal TnI

GAAGATCTGagccagAAActgtttGACCTGAGGGGCAAGTTCAAGAGGCCTcctCT
GaagAGAGTCCGCatgTCAGCTGACGCTATGctgAGGGCTTTGTTGGGCtcaAA
ACACAAAgtctgcATGGATCTGAGAGCTAACCTGAAGCAAGTCAAG

Guinea Pig cardiac TnI

GCGGGGGAGCCAcgcCCCGCACCGGCCCCCGTGCGTCGTCGCTCCTCGGC
CAACTACCGCGCCTACGCCACGGAGCCGCACGCCAAGCTGcagACTCTTAT
GCTGCAGATCGCGAAGCAGGAGctgGAGCGCGAGGCGGAGGAGCGGCGCG
GAGAGAAGGGGCGCGTGCTGagtACACGGTGCCAGCCCCTGGAGCTGgctG
GCCTGGGCtccgggGAGCTGCAGGACTTATGCCGACAACTCCATaccCGGGTG
GACAAGGTGGACGAAGAGAGATACGACataGAGGCTAAAGTTACCAAGAATA
TCACAGAGATCGCAGATCTGaacCAGAAGATCtttGACCTCCGTGGCAAGTTTA
AGCGGCCCACGCTGCGGAGGGTGAGGATCTCTGCAGATGCCATGATGCAG
GCCCTGCTGGGAACCCGGGCCAAGGAGaccTTGGACCTGCGGGCCCACCT
CAAGCAAGTGAAGAAGGAAGACaccGAGAAGGAGAACCGGGAGGTTGGTGA
CTGGCGCAAGAACATCGATGCCCTGAGCGGCATGGAGGGCCGGAAGAAGA
AGTTCGAGGGC

Guinea Pig slow skeletal TnI

CAGGACCTATGCCGGgagCTGCACgccaagGTGgaggtgGTGGACGAGGAGCG
GTACGACATCGAGGCCAAAATTaagGATCTGaagctgAAGgtgttgGACCTCCGTG
GGAAGTTCAAGCGCCCAccaCTGCGCCGGGTCCGTgtcTCAGCTGATGCCAT
GctccgaGCCCTGCTGGGCtccaagcatAAGgtgtccatgGACTTGCGGGCCaacCTCA
AGtctGTGAAGAAGGAGGACACAGAGAAGGAGGTGGGCGACTGGAGGAAGA
ATgtggagGCTatgTCTGGCATGGAGGGTCGGAAGAAGatgTTC

Guinea Pig fast skeletal TnI

GACatgAACCAGAAGctgTTTGATCTGAGGGGCAAATTCAAGAGGCCCcctCTG
CGGCGGGTGCGCatgTCCGCCGATGCCATGctgaagGCGCTGCTGGGCtccaag
cacAAGgtgtgcatgGACCTGCGGGCTaacCTGAAGCAGGTCAAGAAGGAGGACA
CAGAGAAG

Marmoset cardiac TnI

GCTgggGAACCTCGCCCCGCACCAGCCCCGGTCAGACGCCGCTCCTCCAAC
TACCGCGCGTACGCCACGGAGCCGCACGCAAAAAGTCTAAGATCTCCGCC
TCGAGAAAACTGCACCCTGatgCTGCAGATTGCAAAGCAGGAACTGGAGCGA
GAGGCGGAGGAGCGGCGCGGAGAGAAGGGGCGCGCCCTGAGCACCCGC
TGCCAGCCGCTGGAGTTGGCCGGTCTGGGCTTCGCGGCTCCAGGACTTGT
GCCGACAGCTCCACACCCGTGTGGACAAGGTGGATGAAGAGAGATATGAC
ATAGAGGCAAAAGTTACCAAGAACATCGCAGATCTGACCCAGAAGATCTTTG
ACCTTCGCGGCAAGTTTAAGCGGCCCACCCTGCGGAGAGTGAGAATCTCTG
CGGATGCCATGATGCAGGCGCTGCTGGGGaccCGGGCTAAGGAGTCCCTG
GACCTGCGTGCCCACCTCAAGCAGGTGAAGAAGGAGGACACCGAGAAGgtg
aGAAatcCGGGAGGTGGGAGACTGGCGCAAAAACATTGATGCACTGAGTGG
AATGGAAGGCCGCAAGAAAAAGTTTGAG

b

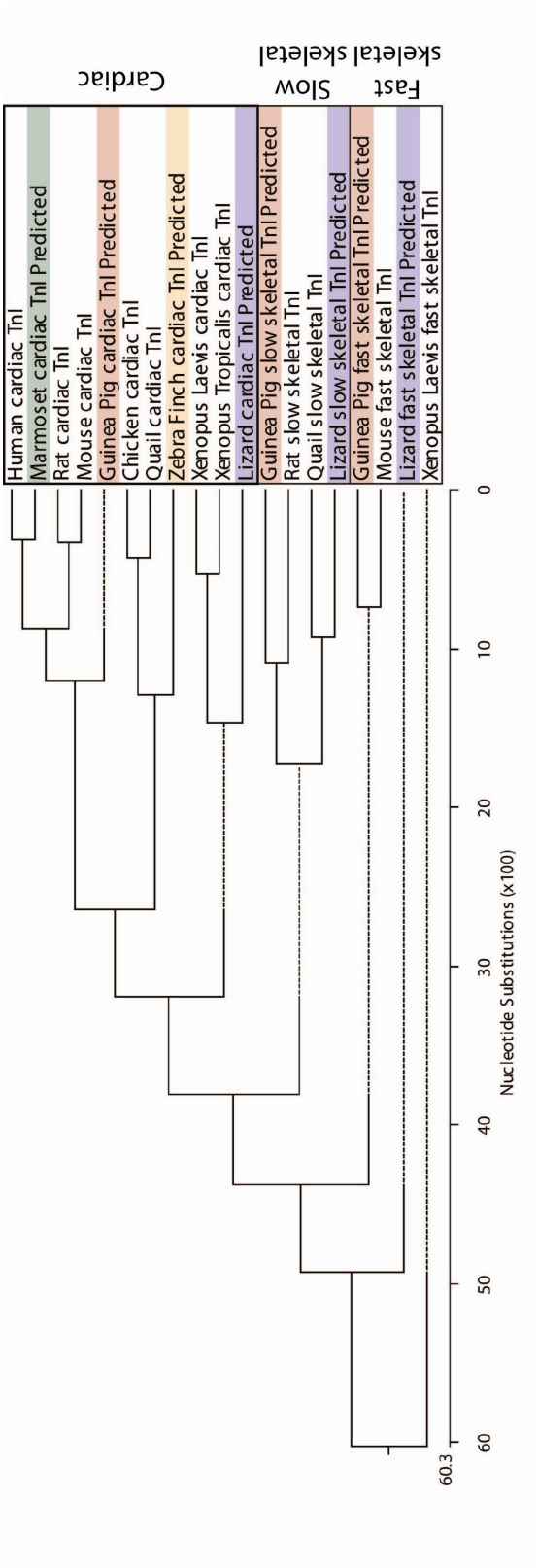
Cardiac
Fast
Slow
skeletal skeletal
Human cardiac TnI
Marmoset cardiac TnI Predicted
Rat cardiac TnI
Mouse cardiac TnI
Guinea Pig cardiac TnI Predicted
Chicken cardiac TnI
Quail cardiac TnI
Zebra Finch cardiac TnI Predicted
Xenopus Laevis cardiac TnI
Xenopus Tropicalis cardiac TnI
Lizard cardiac TnI Predicted
Guinea Pig slow skeletal TnI Predicted
Rat slow skeletal TnI
Quail slow skeletal TnI
Lizard slow skeletal TnI Predicted
Guinea Pig fast skeletal TnI Predicted
Mouse fast skeletal TnI
Lizard fast skeletal TnI Predicted
Xenopus Laevis fast skeletal TnI
60.3
60
50
40
30
20
10
0
Nucleotide Substitutions (x100)

c

Percent Identity

	1	2	3	4	5	6	7	8	9	10	11	12	13	14	15	16	17	18	19	
1		95.2	88.1	82.2	83.6	65.0	61.3	62.0	73.9	56.4	56.2	74.8	58.3	57.6	67.9	77.2	57.2	66.7	53.2	1
2	5.0		88.2	86.9	88.3	66.7	65.6	64.8	77.2	66.8	67.5	72.8	63.3	61.3	66.0	77.2	62.5	67.3	60.1	2
3	13.1	12.9		84.3	85.3	67.7	67.5	66.3	78.7	66.7	67.2	75.7	62.4	61.1	66.0	77.2	64.1	67.3	58.1	3
4	20.8	14.6	17.8		93.7	63.5	60.6	61.0	73.5	58.5	56.8	72.5	56.8	56.1	64.2	74.9	56.0	67.9	51.8	4
5	18.8	12.9	16.5	6.6		64.2	60.6	60.6	73.5	58.8	57.5	72.8	57.7	56.9	66.0	74.9	57.9	66.7	52.3	5
6	47.1	44.1	42.3	50.3	48.7		94.3	85.2	65.5	59.0	60.0	69.3	57.6	58.7	54.2	69.1	56.8	59.3	51.5	6
7	54.4	46.0	42.6	55.9	55.9	6.0		73.8	64.3	53.8	52.2	68.3	52.0	51.2	53.6	65.5	53.5	59.3	44.9	7
8	53.1	47.7	44.7	55.3	56.0	16.5	32.2		63.5	54.8	52.3	67.6	52.1	50.9	51.0	66.1	52.2	56.0	48.0	8
9	32.2	27.1	25.1	32.8	32.8	46.4	48.7	50.4		77.1	74.7	78.7	74.3	70.2	69.6	76.3	71.3	70.3	71.0	9
10	65.4	44.2	44.5	60.6	60.0	59.4	72.0	69.6	27.3		90.2	69.2	54.7	53.9	69.2	71.3	58.2	73.1	53.3	10
11	65.9	43.1	43.6	65.0	63.1	57.2	76.1	76.2	31.3	10.6		70.5	50.7	48.8	69.2	70.8	56.9	70.5	48.3	11
12	30.8	33.9	29.4	34.2	33.7	39.6	41.2	42.4	25.0	40.3	38.0		90.5	83.2	79.9	78.4	75.9	69.2	73.0	12
13	60.9	50.4	52.3	64.4	62.4	62.5	76.7	76.4	31.5	70.1	81.3	10.4		64.6	79.9	75.4	57.0	69.2	52.2	13
14	62.6	54.4	54.8	66.0	64.2	60.0	78.8	80.1	38.0	72.2	87.1	19.2	48.1		83.6	80.7	59.8	76.9	46.7	14
15	41.9	45.3	45.4	48.9	45.3	72.1	73.4	79.7	39.9	40.2	40.4	23.8	23.9	18.5		70.6	73.0	71.8	70.4	15
16	27.2	27.2	27.3	30.7	30.7	39.9	46.3	45.2	28.5	36.4	37.3	25.5	29.8	22.4	37.9		91.8	81.7	78.4	16
17	63.5	51.9	48.9	66.3	61.9	64.4	72.5	76.5	36.2	61.6	64.7	29.1	63.8	57.7	33.6	8.7		82.1	66.3	17
18	44.2	42.9	42.9	41.8	44.1	59.7	59.3	66.9	38.4	33.7	38.1	39.9	40.0	28.2	36.2	21.5	21.0		77.6	18
19	73.7	57.1	61.8	77.6	76.0	78.7	101.8	90.5	36.6	73.4	88.7	33.6	76.1	93.6	37.9	25.6	45.1	26.8		19
	1	2	3	4	5	6	7	8	9	10	11	12	13	14	15	16	17	18	19	

Divergence

1 Human cardiac TnI
2 Marmoset cardiac TnI Predicted
3 Guinea Pig cardiac TnI Predicted
4 Rat cardiac TnI
5 Mouse cardiac TnI
6 Chicken cardiac TnI
7 Quail cardiac TnI
8 Zebra Finch cardiac TnI Predicted
9 Lizard cardiac TnI Predicted
10 Xenopus Laevis cardiac TnI
11 Xenopus Tropicalis cardiac TnI
12 Guinea Pig slow skeletal TnI Predicted
13 Rat slow skeletal TnI
14 Quail slow skeletal TnI
15 Lizard slow skeletal TnI Predicted
16 Guinea Pig fast skeletal TnI Predicted
17 Mouse fast skeletal TnI
18 Lizard fast skeletal TnI Predicted
19 Xenopus Laevis fast skeletal TnI

Figure 2-9

Identification of primary amino acid sequences of TnI isoforms from numerous species. Protein sequences were generated by translation of mRNA sequences identified during genome analysis. (a) Clustal W alignment of novel predicted fragments of TnI proteins extracted from genome scans of species including Marmoset, Guinea Pig, Zebra Finch, and Lizard. These sequences are aligned with known sequences from other related species. (b) Phylogenetic tree analysis of all TnI proteins represented in the alignment. The Kimura distance formula is used to calculate distance values, derived from the number of non-gap mismatches and corrected for silent substitutions. The values computed are the mean number of differences per site and fall between 0-1. Zero represents complete identity and 1 no identity. Scale of the tree indicates the number of nucleotide substitutions per 100 residues. Phylogenetic tree analysis was used to confirm identity of predicted TnI isoforms by sequence correlation with other TnI isoforms. (c) Sequence ID and divergence values were calculated to define the relationship between novel TnI proteins and related TnI isoforms to assist in confirmation of postulated isoform designation. Divergence (i,j) is calculated as (100[Distance (i,j)] / Total Distance) where (i,j) is the sum of the branch lengths between two sequences and Total Distance is the sum of all branch lengths. Additional details on identified sequences is outlined in Table 2-3.

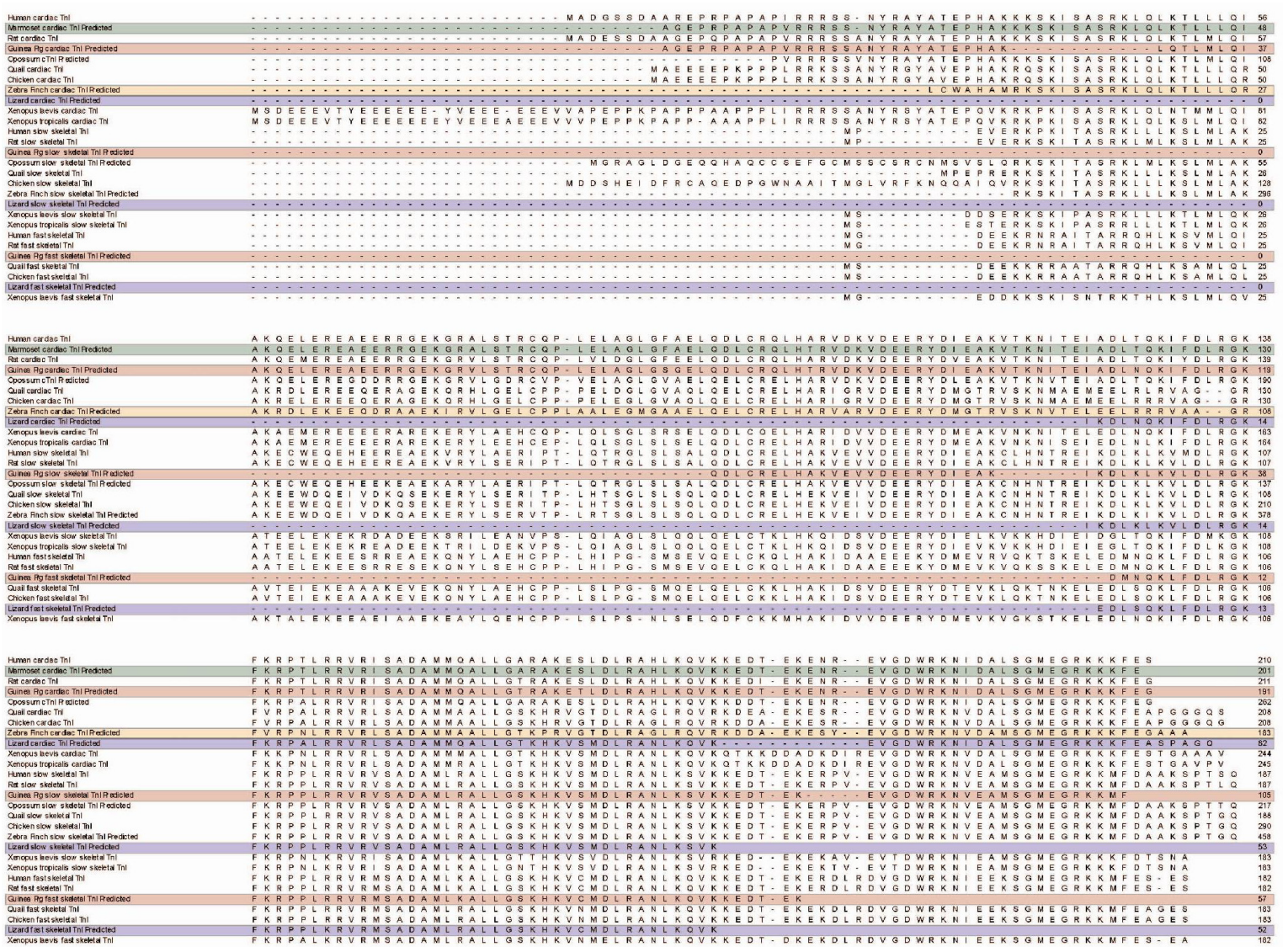
Human cardiac TnI
Marmoset cardiac TnI Predicted
Rat cardiac TnI
Guinea Pig cardiac TnI Predicted
Opossum cTnI Predicted
Quail cardiac TnI
Chicken cardiac TnI
Zebra Finch cardiac TnI Predicted
Lizard cardiac TnI Predicted
Xenopus laevis cardiac TnI
Xenopus tropicalis cardiac TnI
Human slow skeletal TnI
Rat slow skeletal TnI
Guinea Pig slow skeletal TnI Predicted
Opossum slow skeletal TnI Predicted
Quail slow skeletal TnI
Chicken slow skeletal TnI
Zebra Finch slow skeletal TnI Predicted
Lizard slow skeletal TnI Predicted
Xenopus laevis slow skeletal TnI
Xenopus tropicalis slow skeletal TnI
Human fast skeletal TnI
Rat fast skeletal TnI
Guinea Pig fast skeletal TnI Predicted
Quail fast skeletal TnI
Chicken fast skeletal TnI
Lizard fast skeletal TnI Predicted
Xenopus laevis fast skeletal TnI

b

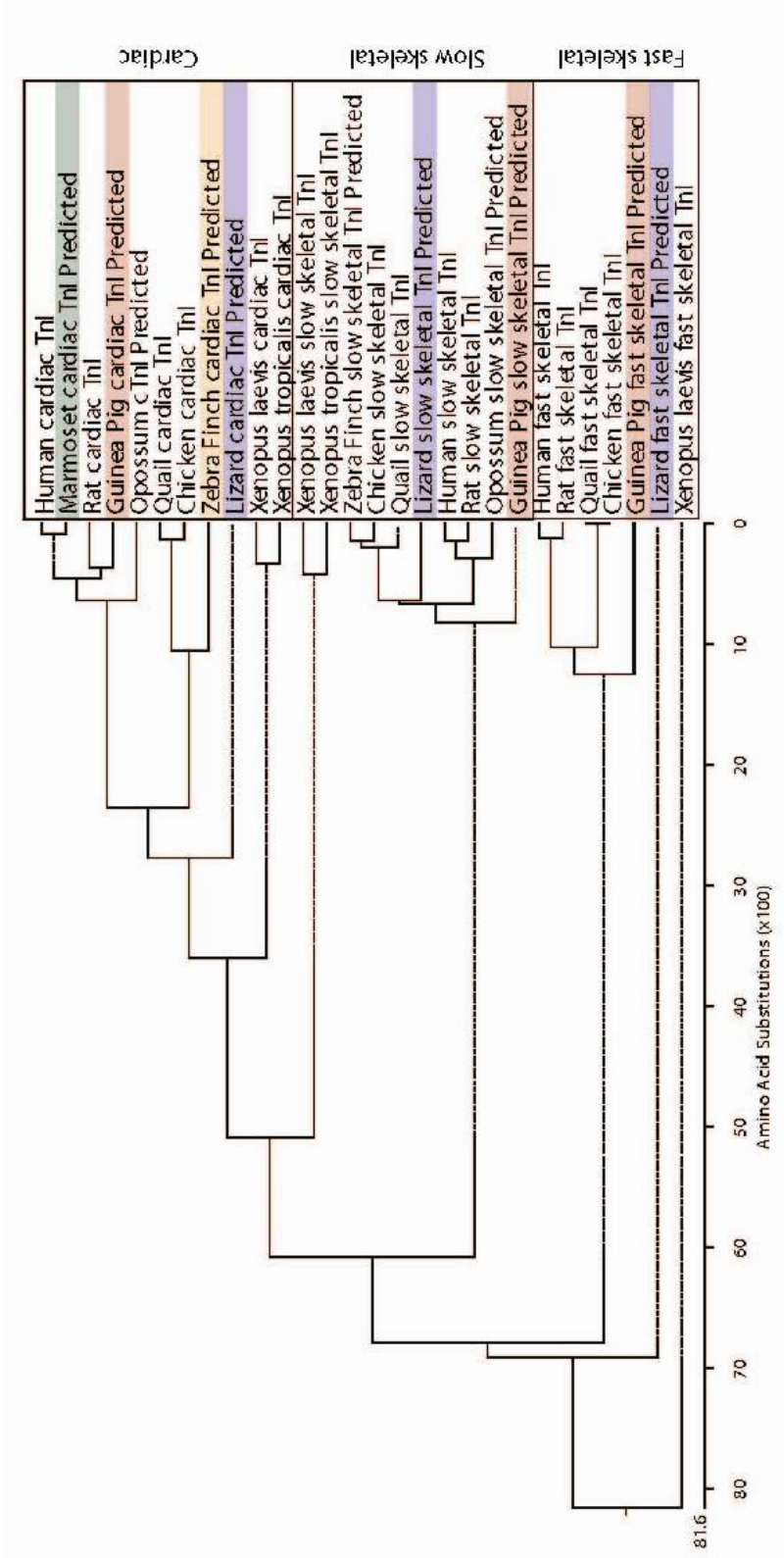
Cardiac
Slow skeletal
Fast skeletal
Human cardiac TnI
Marmoset cardiac TnI Predicted
Rat cardiac TnI
Guinea Pig cardiac TnI Predicted
Opossum cTnI Predicted
Quail cardiac TnI
Chicken cardiac TnI
Zebra Finch cardiac TnI Predicted
Lizard cardiac TnI Predicted
Xenopus laevis cardiac TnI
Xenopus tropicalis cardiac TnI
Xenopus laevis slow skeletal TnI
Xenopus tropicalis slow skeletal TnI
Zebra Finch slow skeletal TnI Predicted
Chicken slow skeletal TnI
Quail slow skeletal TnI
Lizard slow skeletal TnI Predicted
Human slow skeletal TnI
Rat slow skeletal TnI
Opossum slow skeletal TnI Predicted
Guinea Pig slow skeletal TnI Predicted
Human fast skeletal TnI
Rat fast skeletal TnI
Quail fast skeletal TnI
Chicken fast skeletal TnI
Guinea Pig fast skeletal TnI Predicted
Lizard fast skeletal TnI Predicted
Xenopus laevis fast skeletal TnI
81.6
0
10
20
30
40
50
60
70
80
Amino Acid Substitutions (x100)

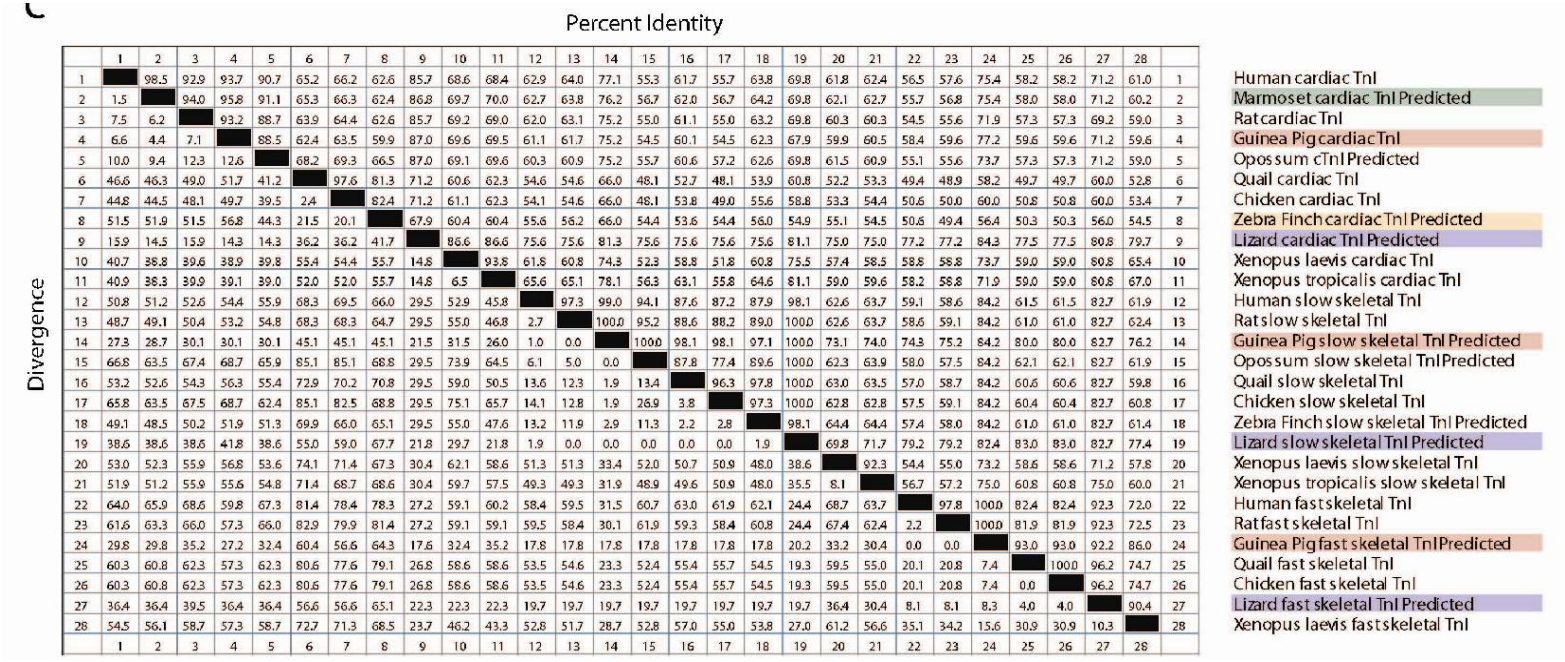
Percent Identity
Divergence
1 Human cardiac TnI
2 Marmoset cardiac TnI Predicted
3 Rat cardiac TnI
4 Guinea Pig cardiac TnI
5 Opossum cTnI Predicted
6 Quail cardiac TnI
7 Chicken cardiac TnI
8 Zebra Finch cardiac TnI Predicted
9 Lizard cardiac TnI Predicted
10 Xenopus laevis cardiac TnI
11 Xenopus tropicalis cardiac TnI
12 Human slow skeletal TnI
13 Rat slow skeletal TnI
14 Guinea Pig slow skeletal TnI Predicted
15 Opossum slow skeletal TnI Predicted
16 Quail slow skeletal TnI
17 Chicken slow skeletal TnI
18 Zebra Finch slow skeletal TnI Predicted
19 Lizard slow skeletal TnI Predicted
20 Xenopus laevis slow skeletal TnI
21 Xenopus tropicalis slow skeletal TnI
22 Human fast skeletal TnI
23 Rat fast skeletal TnI
24 Guinea Pig fast skeletal TnI Predicted
25 Quail fast skeletal TnI
26 Chicken fast skeletal TnI
27 Lizard fast skeletal TnI Predicted
28 Xenopus laevis fast skeletal TnI

Figure 2-10

Alignment of cardiac troponin T protein sequences expressed in numerous chordate species. Analysis was performed by the Clustal W method. Sequence alignment consensus strength is indicated graphically above each residue. Residues highlighted indicate amino acids that are modified from charged to uncharged exclusively in mammals.

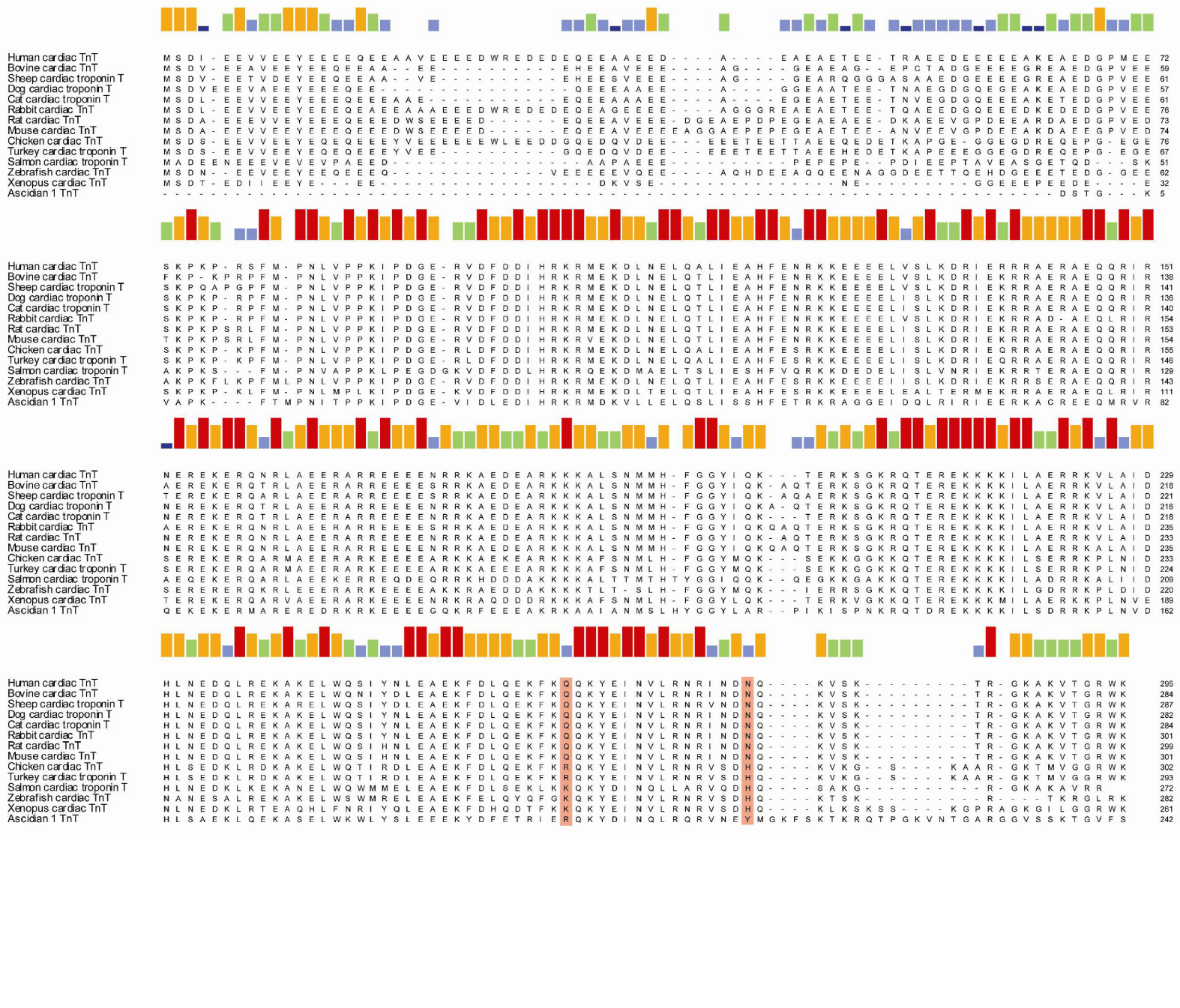
Human cardiac TnT
Bovine cardiac TnT
Sheep cardiac troponin T
Dog cardiac troponin T
Cat cardiac troponin T
Rabbit cardiac TnT
Rat cardiac TnT
Mouse cardiac TnT
Chicken cardiac TnT
Turkey cardiac troponin T
Salmon cardiac troponin T
Zebrafish cardiac TnT
Xenopus cardiac TnT
Ascidian 1 TnT

Figure 2-11

Alignment of cardiac troponin C protein sequences expressed in numerous chordate species. Analysis was performed by the Clustal W method. Sequences are organized species based on taxonomic classification. Sequence alignment consensus strength is indicated graphically above each residue. Structural delineations (Helix N and A-H) are indicated above residues involved in formation of those protein domains. The position of each EF hand motif is also indicated. Calcium coordinating sites for each EF hand are indicated (blue). Acidic residues around the rim of the hydrophobic patch are also indicated (orange).

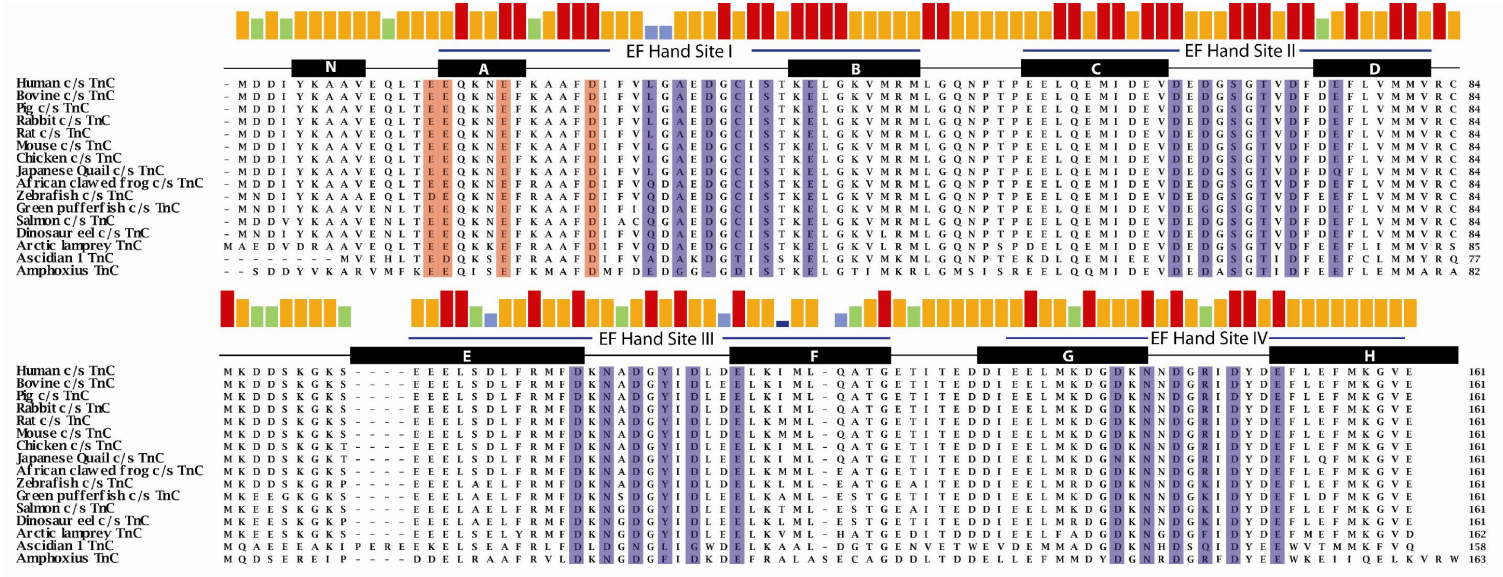
EF Hand Site I
EF Hand Site II
N
A
B
C
D
EF Hand Site III
EF Hand Site IV
E
F
G
H
Human c/s TnC
Bovine c/s TnC
Pig c/s TnC
Rabbit c/s TnC
Rat c/s TnC
Mouse c/s TnC
Chicken c/s TnC
Japanese Quail c/s TnC
African clawed frog c/s TnC
Zebrafish c/s TnC
Green pufferfish c/s TnC
Salmon c/s TnC
Dinosaur eel c/s TnC
Arctic lamprey TnC
Ascidian 1 TnC
Amphioxius TnC

Figure 2-12

Alignment of troponin I protein sequences expressed in numerous chordate species. Analysis was performed by the Clustal W method. Cardiac homologs and slow skeletal homologs are indicated where expression of both isoforms has been identified within a given species. Sequences are organized by isoform and within each isoform by species based on taxonomic classification. Sequence alignment consensus strength is indicated graphically above each residue. Structural delineations (Helix 1-4) are indicated above residues involved in formation of those protein domains. Phosphorylation targets (S23,24) are indicated (green). Key residues involved in the switch arm are indicated (orange).

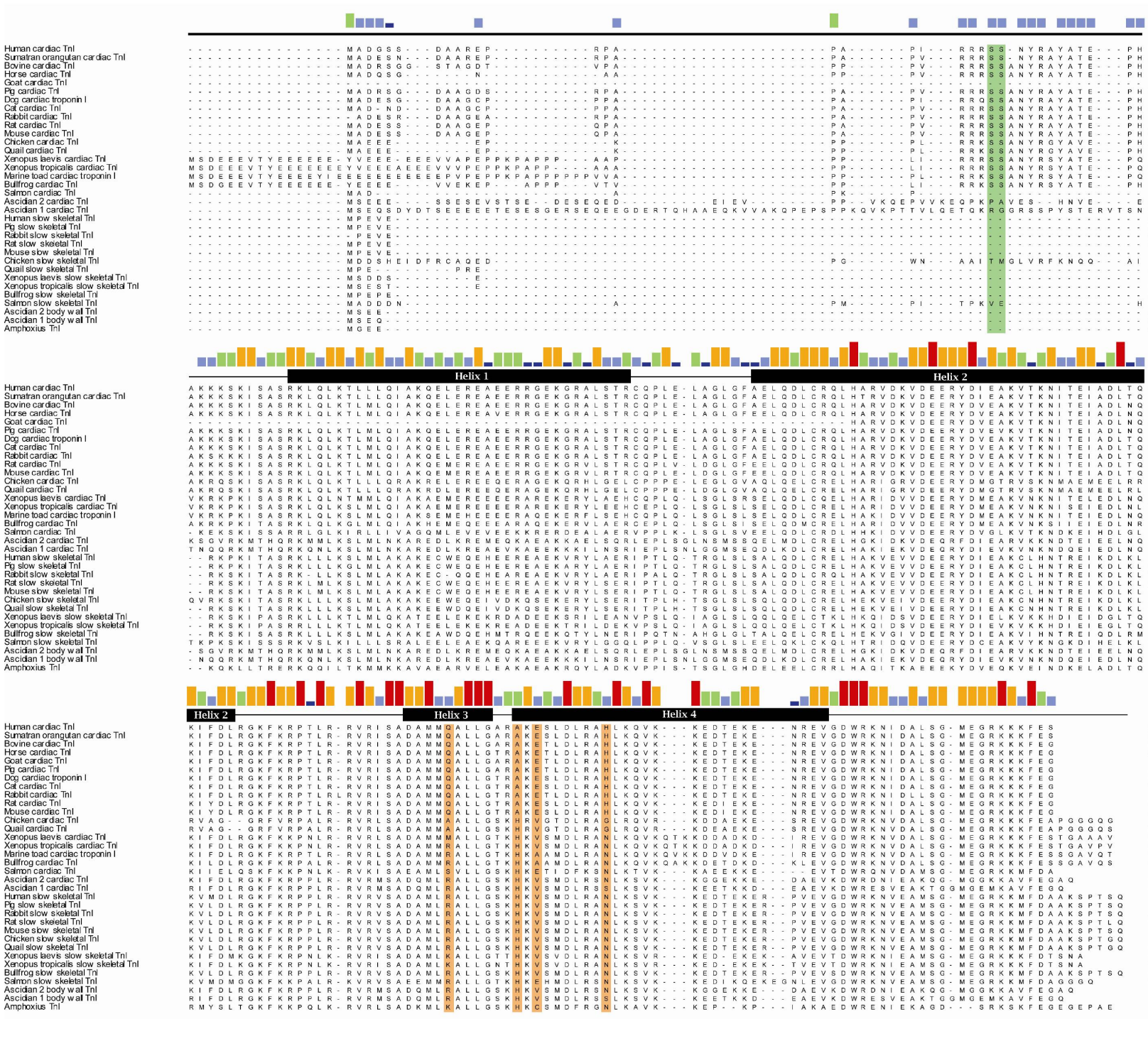
Helix 1
Helix 2
Helix 2
Helix 3
Helix 4

Figure 2-13

Justification for use of the fast skeletal troponin crystal structure. (a) Structural alignment of the fsTn and cTn crystal structures focusing on regulatory interaction site between the switch arm of TnI and the N-terminal hydrophobic patch of TnC. TnC (green), fsTnI (red), cTnI (orange). Critical residues of the switch arm are emphasized in each structure (sTnI: R, H, V, N; cTnI: Q, A, E, H). (b, c) Sequence alignment of the switch arm from chicken fast skeletal and slow skeletal TnI (b) as well as chicken fast skeletal and slow/cardiac TnC (c). Arrows indicate the key charged residues of the switch arm (a) and the acidic residues of the hydrophobic patch on TnC (c). We make the argument that the fast skeletal Tn crystal structure (fs TnI and fs TnC) is transposable with the slow skeletal Tn complex (ssTnI and cTnC) for the following reasons. Crystal structure alignment of the fast skeletal Tn (fs TnI and fs TnC) and cardiac Tn (cTnI and cTnC) show remarkable helix position similarity between TnC and TnI. At the amino acid level, there is a high degree of sequence similarity between fsTnI and ssTnI at the switch arm with only one amino acid different (as indicated in this figure). In terms of the cognate binding partner for TnI, it is well known that the amino acid sequence between fast and cTnC are markedly different, however, shown here are the perfectly conserved acidic residues that decorate the rim of the hydrophobic patch of TnC where the switch arm of TnI binds. Furthermore, the structural alignment of the cardiac and fast skeletal Tn complexes (Figure 7a) shows a perfect alignment of the N-terminus of TnC at the site where TnI binds suggesting that this structural interaction is highly conserved. In terms of function, very similar effects on sarcomere dynamics and myosin S1 ATPase activity are observed in fsTnI as seen with ssTnI[249, 267]. The skeletal and cardiac troponin complex have also shown similar structures in which the switch peptide is bound to the N-terminal hydrophobic patch of TnC between helices A and B[420]. In general, the structural agreement of cTnI, ssTnI, and fsTnI has been supported by numerous other reports[249, 252]. Consequently, we propose that structural data gleaned from the fsTn complex can be correlated with the ssTn complex. In the main text of the manuscript, sTnI refers to the skeletal TnI structure given that fast skeletal and slow skeletal undergo a similar folding arrangement within the calcium saturated state.

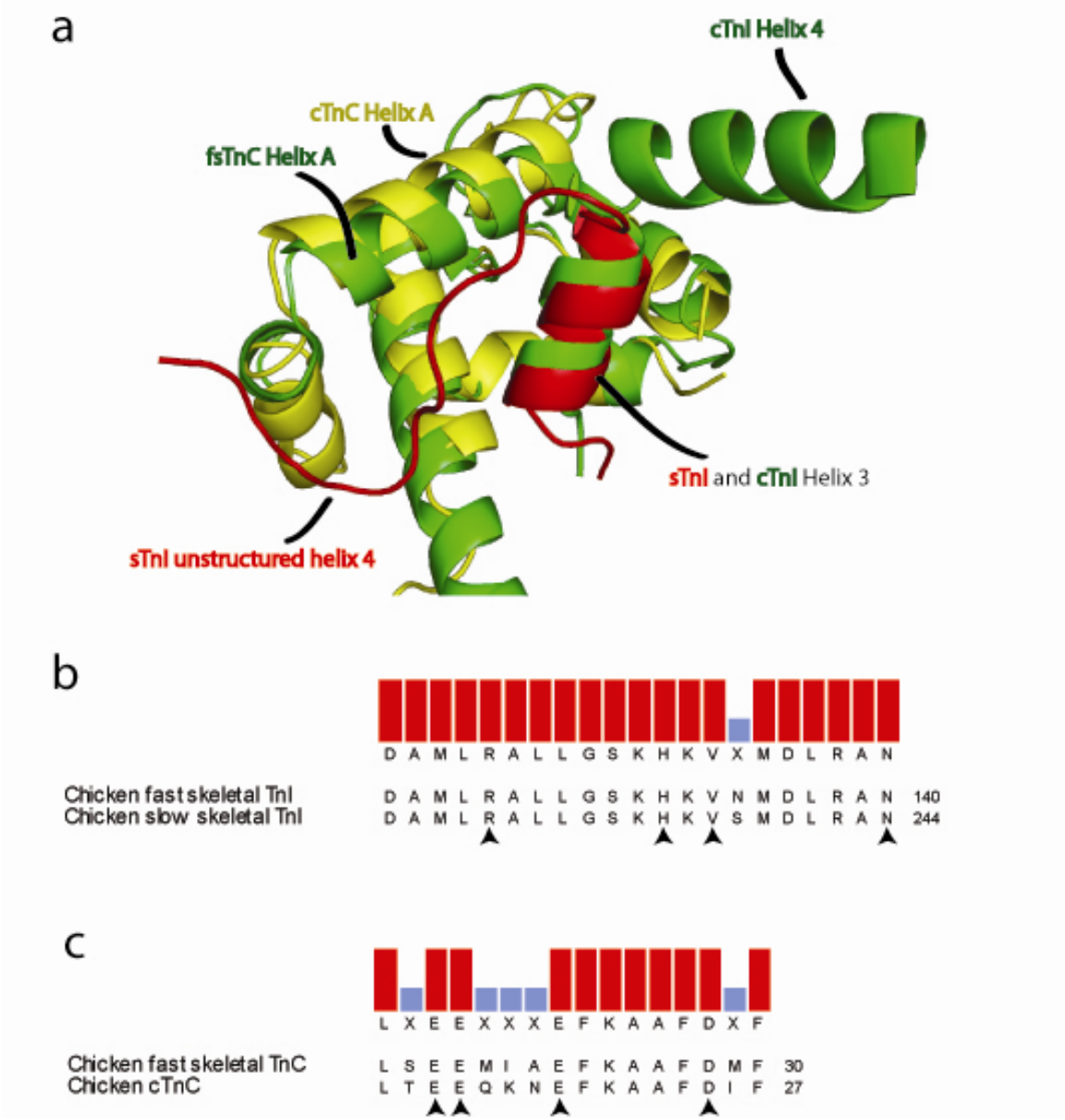
a
cTnI Helix 4
cTnC Helix A
fsTnC Helix A
sTnI and cTnI Helix 3
sTnI unstructured helix 4
b
D A M L R A L L G S K H K V X M D L R A N
Chicken fast skeletal TnI
Chicken slow skeletal TnI
D A M L R A L L G S K H K V N M D L R A N 140
D A M L R A L L G S K H K V S M D L R A N 244
c
L X E E X X X E F K A A F D X F
Chicken fast skeletal TnC
Chicken cTnC
L S E E M I A E F K A A F D M F 30
L T E E Q K N E F K A A F D I F 27

Figure 2-14

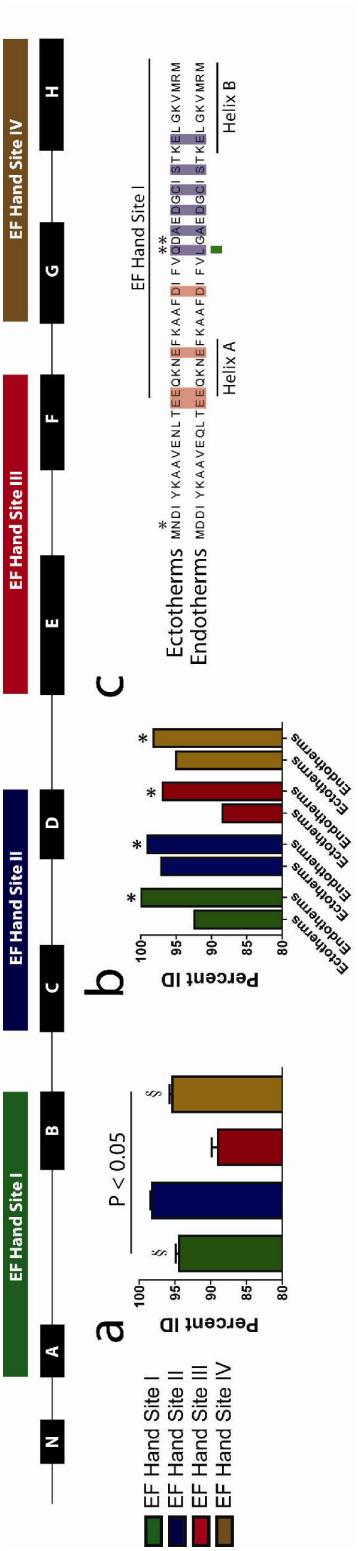
EF Hand Site I
EF Hand Site II
EF Hand Site III
EF Hand Site IV
N
A
B
C
D
E
F
G
H
a
Percent ID
P < 0.05
b
Percent ID
Ectotherms
Endotherms
c
EF Hand Site I
Ectotherms
Endotherms
Helix A
Helix B

Figure 2-14. Structure and function analysis of troponin C. Schematic diagram and analysis of subdomain sequence alignments in cardiac/slow troponin C. Functional domains including EF hand sites I-IV are indicated above their respective helical locations. Helix designations are shown over the full sequence of human cardiac troponin I. (a) Sequence ID comparison of all functional subdomains of cardiac/slow troponin C. Species include H, B, P, Rab, R, M, Ch, Q, Xl, Z, S, GP, DE, AL, As1, and A. (b) Direct pairwise comparison of sequences within specific functional domains from cardiac/slow TnC between ectotherms and endotherms. Ectotherm species: Xl, DE, GrP, Z, and S; endotherm species: H, B, P, Rab, R, M, Ch, and Q. * $P < 0.05$ by students t-test comparing ectotherms to endotherms within a given functional subdomain. (c) Consensus sequence after Clustal W alignment for ectotherm cTnC and endotherm cTnC. The position of Helix A and B as well as EF hand site I are indicated. Calcium coordinating sites for EF hand site I are indicated (blue). Acidic residues around the rim of the hydrophobic patch are also indicated (orange). * indicates residues shown to be responsible for the increased calcium binding affinity of ectotherm TnC^{332}. The only disease causing mutation (L29Q) identified in a human patient with hypertropic cardiomyopathy is indicated (green).

Figure 2-15

Crystal structure analysis of electrostic interactions between TnI and TnC. (a) The delta pK ($pK_a - pK_{int}$) for each ionizable residue was calculated for the cTnI-cTnC (blue) and sTnI-cTnC (green) crystal structures. The absolute pK shifts for His132 and Glu19 are shown in red. Vertical bar = 1 pK unit. (b) Decomposition of the residues that contribute to the pK shift for sTnI Histidine 132 and cTnC Glutamate 19. More than any other residue is the reciprocal effect of H132 and Glu19 on each others pK shift (red). Structural location for each residue in cTnC or sTnI is designated (top). Vertical bar = 1 pK units.

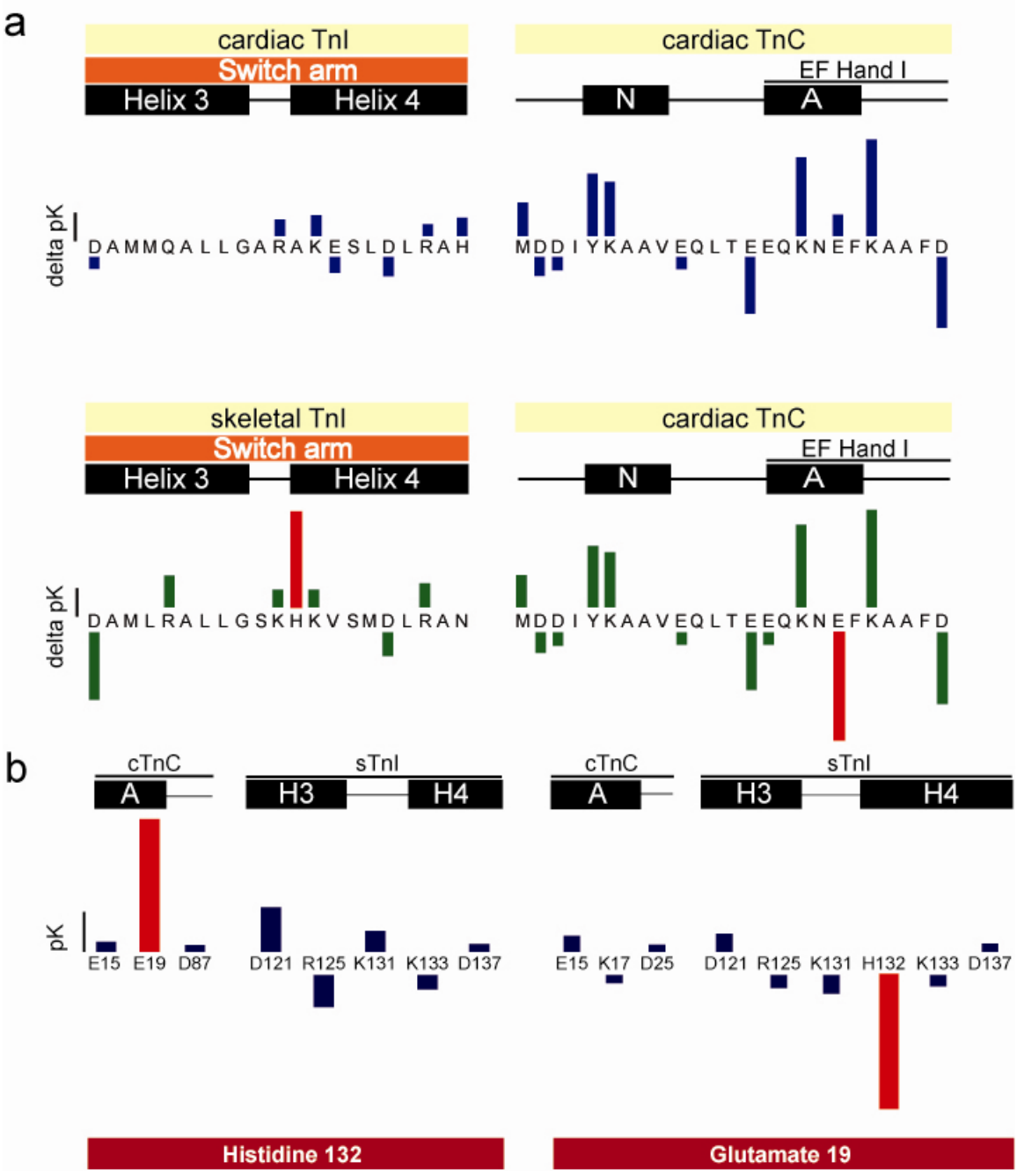
a
cardiac TnI
Switch arm
Helix 3
Helix 4
cardiac TnC
EF Hand I
N
A
delta pK
D A M M Q A L L G A R A K E S L D L R A H
M D D I Y K A A V E Q L T E E Q K N E F K A A F D
skeletal TnI
Switch arm
Helix 3
Helix 4
cardiac TnC
EF Hand I
N
A
delta pK
D A M L R A L L G S K H K V S M D L R A N
M D D I Y K A A V E Q L T E E Q K N E F K A A F D
b
cTnC
sTnI
A
H3
H4
cTnC
sTnI
A
H3
H4
pK
E15 E19 D87
D121 R125 K131 K133 D137
E15 K17 D25
D121 R125 K131 H132 K133 D137
Histidine 132
Glutamate 19

Figure 2-16

Alignment of cardiac myosing binding protein C (MBP-C) and phospholamband (PLN) sequences expressed in numerous chordate species. (a) Sequence alignment of MBP-C. Phosphorylation sites are highlighted and labeled A-D. It is known that site D is not actually phosphorylated perhaps by steric constraints from domain $C2^{415}$. Phosphorylation at site B is required for phosphorylation to occur at sites A and C^{415}. (b) Sequence alignment of PLN. Phosphorylation sites (S16, T17) are highlighted. All sequence information for MBP-C and PLN is provided in Table 3. Analysis was performed by the Clustal W method. Sequences are organized by species based on taxonomic classification. Sequence alignment consensus strength is indicated.

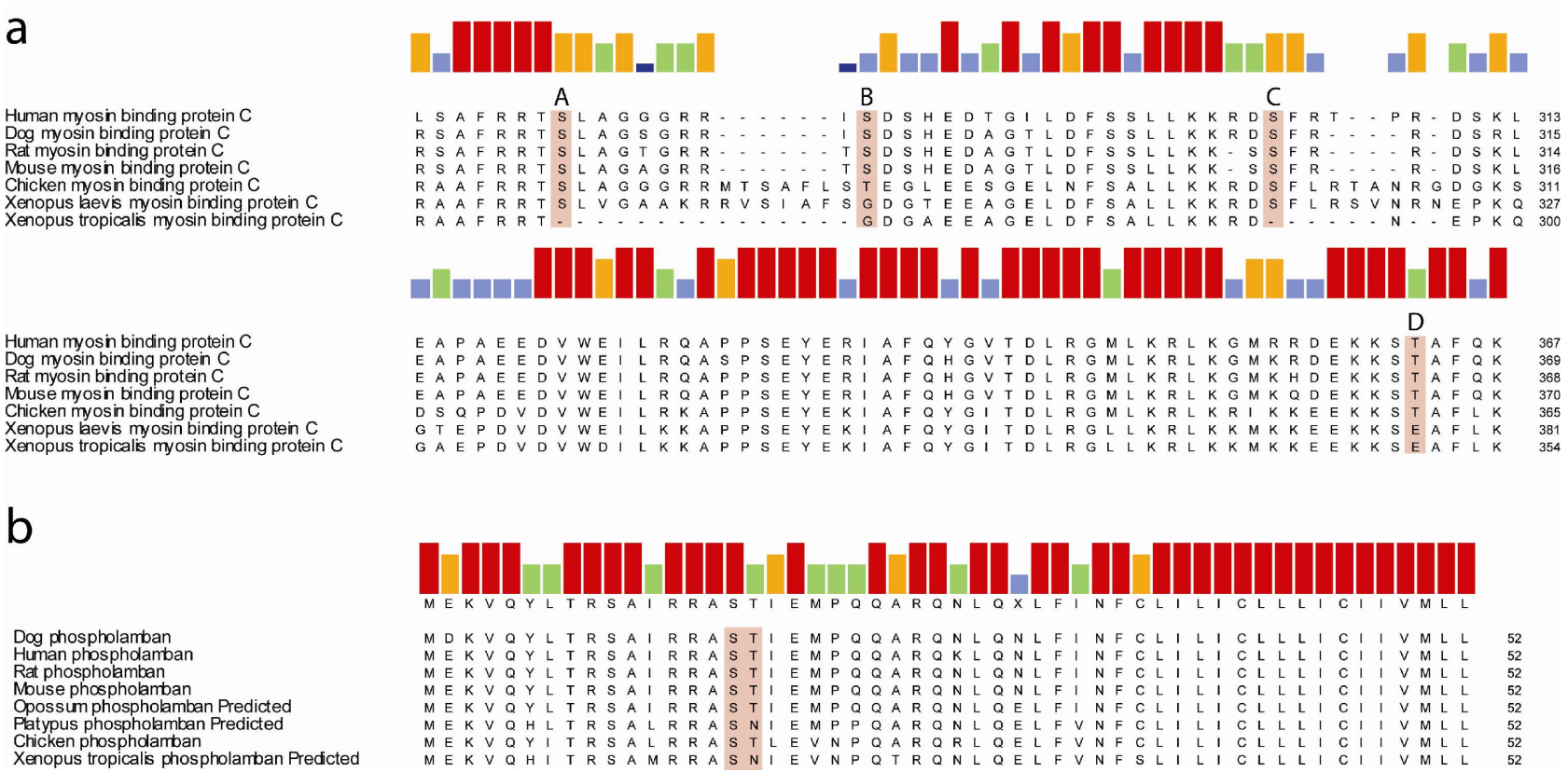
a
A
B
C
Human myosin binding protein C
Dog myosin binding protein C
Rat myosin binding protein C
Mouse myosin binding protein C
Chicken myosin binding protein C
Xenopus laevis myosin binding protein C
Xenopus tropicalis myosin binding protein C
D
b
Dog phospholamban
Human phospholamban
Rat phospholamban
Mouse phospholamban
Opossum phospholamban Predicted
Platypus phospholamban Predicted
Chicken phospholamban
Xenopus tropicalis phospholamban Predicted

Chapter III[1]

Single histidine substituted cardiac troponin I confers protection from age-related systolic and diastolic dysfunction

Abstract

Aims: Contractile dysfunction associated with myocardial ischemia is a significant cause of morbidity and mortality in the elderly. Strategies to protect the aged heart from ischemia-mediated pump failure are needed. We hypothesized that troponin I-mediated augmentation of myofilament calcium sensitivity would protect cardiac function in aged mice. **Methods**: To address this, we investigated transgenic (Tg) mice expressing a histidine-substituted form of adult cardiac troponin I (cTnI A164H), which increases myofilament calcium sensitivity in a pH-dependent manner. **Results**: Serial echocardiography revealed that Tg hearts showed significantly improved systolic function at four months, which was sustained for two years based on EF and Vcfc. Age-related diastolic dysfunction was also attenuated in Tg mice as assessed by Doppler measurements of the mitral valve inflow and lateral annulus DTI. During acute hypoxia, cardiac

[1] This chapter was adapted from: Palpant NJ, Day SM, Herron TJ, Metzger JM. *Single histidine substituted cardiac troponin I confers protection from age-related systolic and diastolic dysfunction*. Cardiovascular Research. 2008 Nov 1;80(2):209-18.

contractility significantly improved in aged Tg mice made evident by increased SV, ESp, and + dP/dt compared to Ntg mice. **Conclusion**: This is the first study to show that increasing myofilament function by means of a pH-responsive histidine button engineered into cTnI results in enhanced baseline heart function in Tg mice over their lifetime, and during acute hypoxia improves survival in aged mice by maintaining cardiac contractility.

Introduction

Cardiovascular disease (CVD) is the leading cause of morbidity and mortality worldwide, accounting for 16.7 million deaths globally each year[14, 232, 421]. Advancing age is a major risk factor for acquiring CVD[422-424]. Over one-third of all patients with CVD are sixty-five years of age or older. Despite significant advances in medical therapy and technology, ischemic heart disease in the elderly is associated with high mortality[232, 233]. Myocardial ischemia results from inadequate regional blood flow and leads to reduced contractility, often leading to heart failure.

Myocardial ischemia causes a drop in myocardial intracellular pH which desensitizes the myofilament to cytosolic Ca^{2+} fluxes, compromising myocyte contractility[238]. The pH-mediated changes in thin filament proteins, particularly the interaction between troponin C and troponin I, are primarily responsible for this reduction in myofilament calcium responsiveness and resulting decrement in contractile function[245]. Troponin I (TnI), the inhibitory subunit of the ternary

troponin complex, is the Ca^{2+} -sensitive molecular switch of the myofilament[33]. During diastole, the C-terminus of TnI interacts with actin which allows tropomyosin to sterically inhibit actomyosin ATPase activity. During systole, a conformation change in the troponin complex occurs wherein the C-terminal switch domain of TnI binds to the hydrophobic patch of the Ca^{2+} saturated N-terminal lobe of TnC[52]. This releases the inhibition on actomyosin ATPase resulting in cross-bridge cycling and subsequent sarcomeric contraction.

Carboxy-terminal charge differences between the neonatal and adult isoforms of TnI, slow skeletal TnI and cardiac TnI, respectively, are responsible for alterations in pH sensitivity of the myofilament[249, 252]. Recent studies indicate that a critical histidine residue underlies TnI regulation of myofilament pH sensitivity (Figure 3-1a)[246, 249, 250, 252]. When cardiac TnI is modified to contain a histidine at codon 164 it behaves as a titratable molecular switch regulating myofilament tension development in response to biochemical changes in the myocyte *in vitro* and in the whole heart *in vivo*[246]. Importantly, this engineered mutation increases myofilament sensitivity to activating calcium while retaining important PKA phosphorylation sites on the N-terminus of cTnI. PKA-mediated phosphorylation of TnI is a critical mediator of the β-adrenergic response in the adult heart[9]. Numerous studies have shown that increasing myofilament calcium sensitivity through mutations in the troponin complex results in varying forms of cardiomyopathy in the context of normal physiological growth and function (e.g.

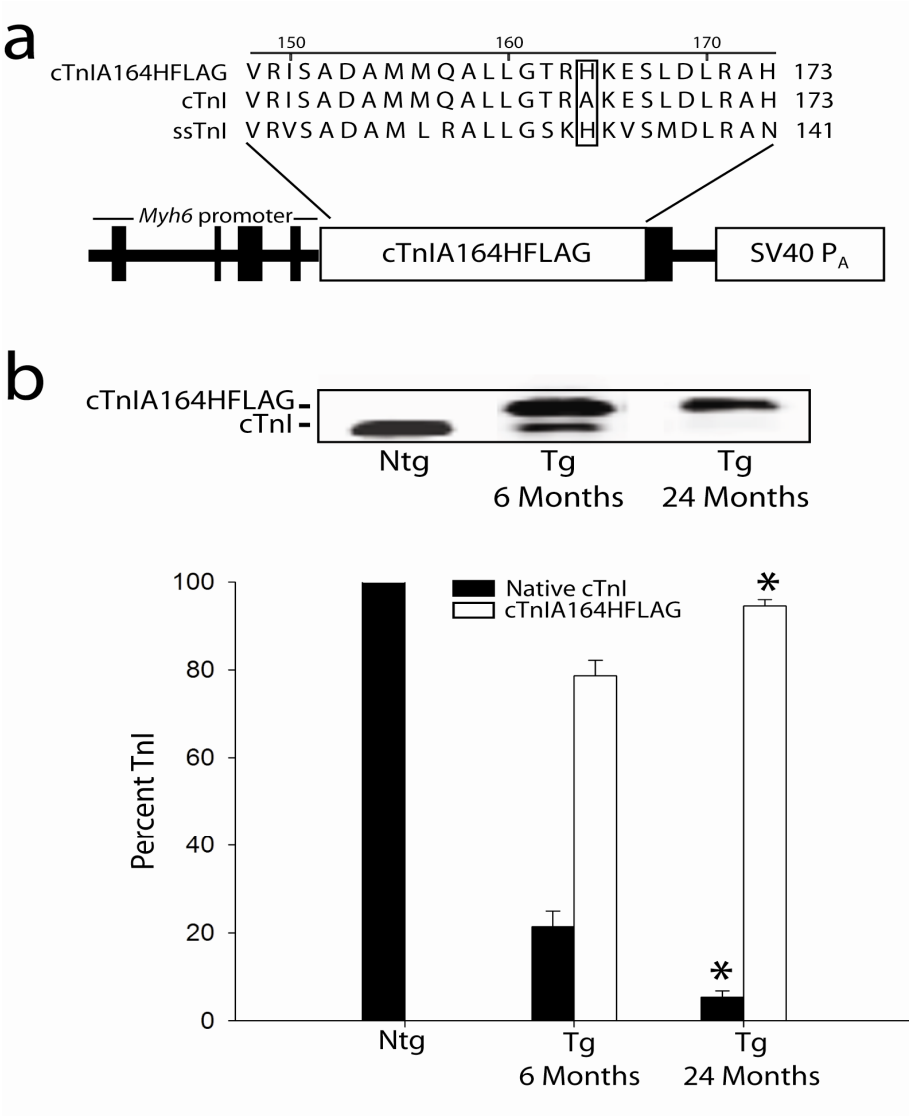

Figure 3-1. Age-dependent gene expression changes in cTnIA164H Tg mice. (a) Sequence alignment showing location of the single histidine substitution originally studied in ssTnI and subsequently introduced into cTnI (cTnI A164HFLAG). Expression of cDNA encoding cTnI A164H with an SV40 polyadenylation (pA) signal was driven by the 5.5-kb *Myh6* promoter. A C-terminal Flag epitope was used to aid detection of cTnI A164H. (b) Immunoblot and bar graph showing expression of native cTnI (■) in Ntg mice as well as stoichiometric incorporation of cTnI A164HFLAG (□) relative to endogenous cTnI (■) in Tg mice at six months (n=12) and two years (n=6). Values are expressed as mean ± SEM. * $P < 0.05$ for 2 year replacement vs. 6 month replacement.

cTnI R193H, cTnT R92Q)[333, 371]. In contrast, we have shown that cTnI A164H has cTnI R193H, cTnT R92Q)[333, 371]. In contrast, we have shown that cTnI A164H has no baseline pathology and significantly protects cardiac function in response to a variety of pathophysiologic challenges including acute and chronic ischemia[246]. Adding to the evidence supporting the therapeutic role of histidine modified troponin I, this paper is the first to show that improvement in inotropy through modification of a myofilament protein attenuates cardiovascular dysfunction in the aged heart *in vivo*.

Methods

Mouse model Generation and analysis of transgenic mice expressing a histidine-modified cardiac troponin I (cTnI A164H) with FLAG epitope was previously described (Figure 1a)[246]. The procedures used in this study are in agreement with the guidelines of the University of Michigan and approved by the University of Michigan Committee on the Use and Care of Animals. The University of Michigan is accredited by the American Association of Accreditation of Laboratory Animal Health Care, and the animal care use program conforms to the standards of the National Institutes of Health Guide for the Care and Use of Laboratory Animals (NIH Pub. No. 85-23). Aged mice were susceptible to complications during Millar catheterization resulting in significant loss of animals during the protocol. Three mice died (2 nontransgenic, 1 transgenic) during catheter placement and three had irreversible ventricular arrhythmias (1

nontransgenic, 2 transgenic) that prevented proper data acquisition either during baseline measurements or during the hypoxic challenge. Mice used in this study were exclusively from line 892, which was the highest expressing Tg mouse line for this model.

Conductance micromanometry Measurements of in vivo cardiovascular hemodynamics were obtained using conductance micromanometry as previously performed by this laboratory[246]. Mice were anesthetized and intubated via a tracheal cannulation and ventilated via a pressure controlled ventilator with 1% isoflurane. A 1.0 French Millar pressure-volume catheter (PVR-1045; Millar Instruments Inc., Houston, Texas, USA) was inserted into the right carotid artery and advanced into the left ventricle. Pressure-volume loops were collected on line at 1 kHz. Data were analyzed with PVAN 3.2 software (Millar Instruments Inc.). Inferior vena cava occlusions were also performed to obtain the end systolic and end diastolic pressure-volume relationships. After obtaining baseline hemodynamics (ventilated with 100% O_2), mice were exposed to an acute hypoxic challenge (12% O_2 balanced with nitrogen). Data were acquired until systolic failure which was defined as the point when LV pressure reached 65% of initial peak systolic pressure. At this point, mice were recovered using 100% O_2 in order to obtain calibration data.

Echocardiography Anesthesia was induced with 3% isoflurane and then maintained at 1% for the duration of the procedure. Transthoracic

echocardiography was performed in the supine or left lateral position. Two-dimensional, M-mode, Doppler and tissue Doppler echocardiographic images were recorded using a Visual Sonics' Vevo 770 high resolution *in vivo* micro-imaging system. We measured systolic and diastolic dimensions and wall thickness in M-mode in the parasternal short axis view at the level of the papillary muscles. Fractional shortening and ejection fraction were calculated from the M-mode parasternal short axis view. We assessed diastolic function by conventional pulsed-wave spectral Doppler analysis of mitral valve inflow patterns (early [E] and late [A] filling waves). Doppler tissue imaging (DTI) was used to measure the early (E_a) and late (A_a) diastolic tissue velocities of the lateral annulus.

Adult mouse myocyte isolation and analysis Adult mouse cardiac myocytes were isolated from 3-6 month old mice as described previously [425]. Between 5 x 105 and 1 x 106 rod-shaped cells were obtained from a single mouse heart and subjected to sarcomere shortening and Ca2+-transient analysis by loading with Fura 2AM (2 μM) as previously described[426]. An in vitro calibration was performed to convert the fluorescence ratio to [Ca2+] as described[24]. To determine the Ca2+ content of the sarcoplasmic reticulum, electrical pacing was discontinued and caffeine (20 mM) was rapidly applied using a capillary tube perfusion system (Warner Instruments, SF-77B Perfusion Fast-Step).

Immunoblot detection The stoichiometric ratio of cTnI A164HFLAG to native cTnI was accomplished by detection with the pan-TnI antibody MAB 1691 (Chemicon; 1:1000). Calcium handling proteins were detected using the following antibodies: phospholamban (Clone A1, Upstate), SERCA2a (MA3-919, ABR), NCX (11-13, Swant), and calsequestrin (PA1-913, ABR). Phosphorylation status was performed by Western blot using antibodies directed against the serine 16 phosphorylation site on phospholamban (07-052, Upstate) and the serine 23/24 tandem phosphorylation sites on cardiac troponin I (4004, Cell Signaling). Indirect immunodetection was carried out using a fluorescently labeled secondary antibody (Rockland, IRDye 680 conjugated affinity purified; 1:5000). Western blot analysis was accomplished using the infrared imaging system, Odyssey (Li-Cor, Inc.) and images analyzed using Odyssey software v. 1.2. For protein detection, samples from young and aged Ntg and Tg mice were run on the same gel. After protein transfer, the gel was stained with Coomassie for use in quantification to account for any loading differences.

Statistics All results are expressed as mean ± SEM. All two-group comparisons were assessed by two-tailed *t*-test. All multi-group comparisons were assessed using two way analysis of variance (ANOVA) with Tukey post-hoc test. Survival after the *in vivo* acute hypoxic challenge was assessed by the Fisher exact test.

Results

cTnIA164H transgene expression increases in aged murine hearts.

Consistent with recent findings[246], six month old mice (line 892) showed high levels of stoichiometric replacement of endogenous cTnI with cTnI A164H (78.6 ± 3.5 %) (Figure 3-1b). Aging of generation F2-F3 transgenic mice to 2 years revealed a significant increase in cTnI A164H replacement relative to native cTnI (94.6 ± 3.1%; $P < 0.05$, Tg 6 mo vs. 24 mo expression) as determined by Western blotting (Figure 3-1b).

cTnI A164H improves global cardiac function during aging

Analysis of systolic and diastolic cardiac function at four months, one year, and two years of age was assessed by serial echocardiography. Comparison of nontransgenic (Ntg) and transgenic (Tg) mice revealed significant differences in contractility and chamber geometry at all ages (Figure 3-2a,b). Compared to Ntg mice, Tg mice had significantly higher contractility as measured by the velocity of circumferential fiber shortening (Vcf_c) (Figure 3-2b). Ejection fraction correlated with the Vcf_c during this time course further validating the increased inotropy of Tg mice (Table 3-1b). Tg mice also had significantly smaller LV diastolic

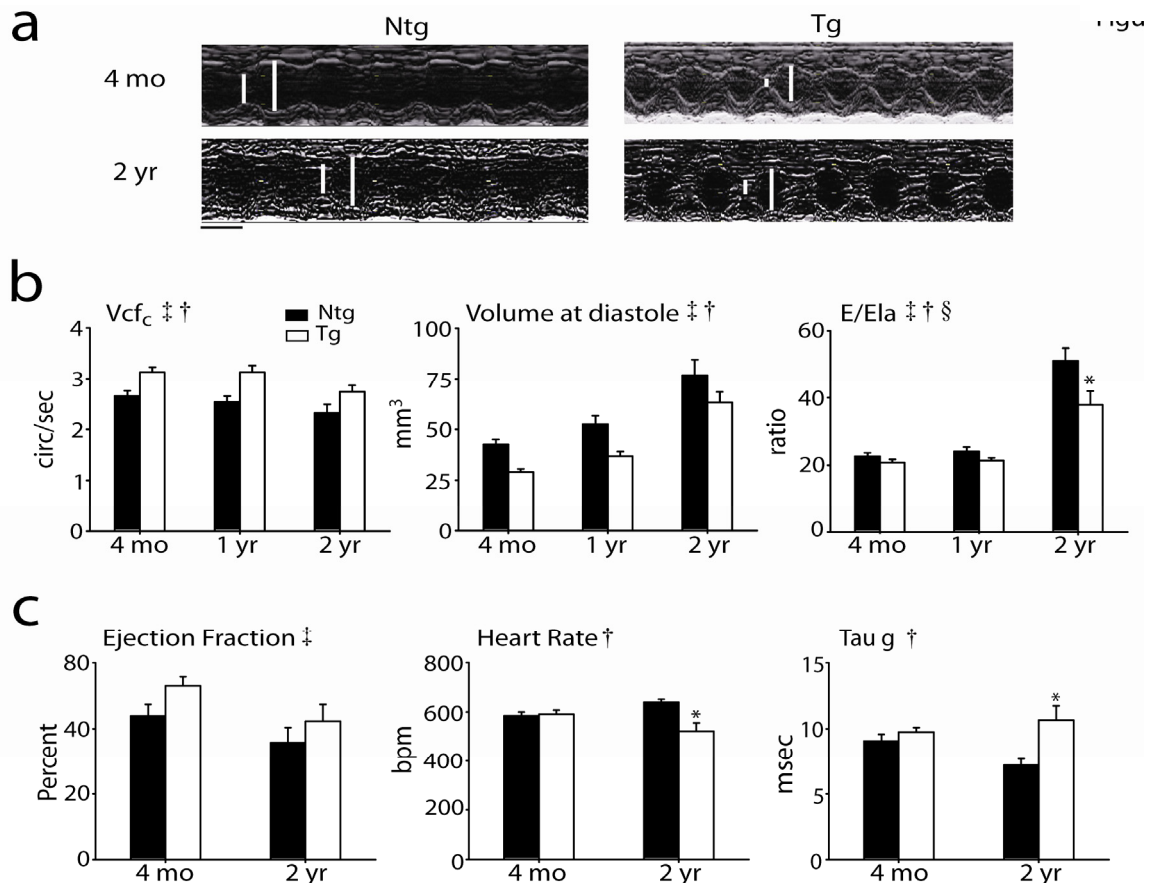

Figure 3-2. Age-dependent changes in baseline cardiac function by echocardiography and Millar catheterization. (a) Representative m-mode echocardiographic images along the parasternal short axis view showing changes in contractility of Ntg and Tg mice between four months and two years (scale bar = 0.1 sec). White bars delineate systole and diastole. (b) Summarized mean data showing age related differences in cardiac function as assessed by echocardiography including velocity of circumferential fiber shortening corrected for heart rate (Vcf_c), volume at diastole (Vol d), and the ratio of the Mitral E wave to lateral annular E wave (E/Ela) showing changes in cardiac function in Ntg (■) and Tg (□) mice at four months (Ntg, n=26; Tg, n=32), one year (Ntg, n=12; Tg, n=13), and two years (Ntg, n=13; Tg, n=15). Values are expressed as mean ± SEM. 2 way ANOVA main effects: age (‡) and genotype (†): Vcf_c, Vol d, E/Ela, $P < 0.05$. ANOVA interaction effects between genotype and age (§): E/Ela, * $P < 0.05$ for Ntg vs. Tg at 2 yrs of age. (c) Summarized mean data showing age related differences in hemodynamic function including the ejection fraction (EF), time constant for relaxation (tau g), and heart rate of Ntg (■) and Tg (□) mice at four months (n=12-14) and 2 years (n=3-4) of age. Values are expressed as mean ± SEM. * $P < 0.05$ for Ntg vs Tg at 24 mo. ANOVA main effects: genotype (†): tau g, HR, $P < 0.05$; age (‡): EF, $P < 0.05$. Ntg, nontransgenic; Tg, transgenic.

volume (Vol d) compared to Ntg mice at all ages (Figure 3-2b). Although the aging process had similar effects on both cohorts resulting in an age-dependent deterioration of cardiac function and geometry, cTnI A164H Tg mice had sustained improvements in contractility and reduced LV cavitary dilation compared to Ntg mice. These conclusions were supported by ANOVA main effects for genotype and age with measurements of contractility (Vcf_c), and cardiac geometry (Vol d) ($P < 0.05$).

Diastolic function was also assessed by conventional Doppler of the mitral valve early (Ea) and late (Aa) waves as well as Doppler tissue imaging (DTI) of the early (Ela) and late (Ala) tissue velocities of the lateral annulus. Although no differences in diastolic function were observed at four months, age related decrements in diastolic function were observed in Ntg mice that were significantly attenuated in Tg mice at two years. While the lateral annular E wave (Ela), as measured by DTI, tended to be greater for Tg versus Ntg mice, the difference did not reach statistical significance (Table 1b). However, the ratio of the mitral valve E wave to the lateral annular E wave (E/Ela) was significantly lower in Tg mice compared to Ntg mice at two years of age (Ntg vs. Tg: 51.0 ± 3.8 vs. 37.8 ± 4.1; $P < 0.05$) (Figure 3-2b). Taken together, the progression of diastolic dysfunction that accompanies the aging process, as observed in Ntg mice, was reduced by cTnI A164H resulting in an attenuation of diastolic dysfunction in aged transgenic mice. These conclusions were supported by ANOVA main effects for genotype and age ($P < 0.05$) as well as an interaction effect ($P < 0.05$) for E/Ela.

Parameter	Ntg	Tg
a. Conductance Micromanometry		
Cardiac Output (uL/min)	11,440.7 ±1,542.2	12,471.4 ± 2,984.3
Stroke Volume (uL)	17.8 ± 2.2	23.1 ± 4.5
Stroke Work (mmHg*uL)	1,228.7 ± 360.5	1,737.0 ± 478.3
End Systolic Pressure (mmHg)	97.4 ± 20.7	97.1 ± 15.8
dP/dt min (mmHg/sec)	-9,858.8 ± 2,756.6	-7,456.5 ± 1,789.6
Tau w (msec)	5.75 ± 0.2687	7.95 ± 0.6695
b. Echocardiography	Ntg	Tg
Ela (m/s)	23.2 ± 2.4	31.7 ± 3.4
Ala (m/s)	22.5 ± 1.6	25.3 ± 2.3
MV E (m/s)	1,050.4 ± 51.8	1,143.2 ± 72.9
MV A (cm/s)	771.4 ± 42.0	846.5 ± 40.5
EF (%)	64.0 ± 3.9	74.4 ±2.3 *

Table 3-1. Baseline Cardiac Function of Aged Mice For conductance micromanometry measurements n = 3-4/group. For echocardiography measurements n = 13-15/group. All values are from animals aged to two years. Echocardiography parameters: Doppler tissue imaging of the early (Ela) and late (Ala) tissue velocities of the lateral annulus; conventional Doppler imaging of the mitral valve early (MV E) and late (MV A) filling velocities; Ejection Fraction (EF). All values are expressed as mean ± s.e.m. * $P < 0.05$ for Ntg vs. Tg. Ntg: Nontransgenic, Tg: Transgenic.

Cardiac pressure-volume analysis was assessed by implantation of a Millar catheter into the left ventricle for acquisition of real-time conductance micromanometry measurements. Continuous monitoring of cardiac function revealed significant differences in age dependent baseline hemodynamics between Ntg and Tg mice. At four months of age, measurements of systolic function were consistent with echocardiographic findings in that Tg mice showed trends toward increases in the positive derivative of pressure development (data not shown) and a trend toward improved ejection fraction compared to Ntg mice (Figure 3-2c). In terms of diastolic function, conductance micromanometry measurements were inconclusive based on the rate constant for isovolumic relaxation (Tau) which showed either an increase (Tau Glanz (Figure 3-2c)) or no change (Tau Weiss (Table 3-1)) during the aging process. A significant decrease in heart rate was also observed in two year old Tg mice compared to their Ntg littermates (Figure 3-2c).

Analysis of heart weight to body weight ratio revealed significant age dependent changes (Table 3-2). At four months of age Tg mice had significantly lower body weights and heart weights compared to Ntg mice (4 month HW/BW ratio: 4.6 ± 0.1 vs. 4.0 ± 0.1; Ntg vs. Tg. $P < 0.05$). However, at two years HW/BW ratio was similar between Tg and Ntg mice (2 year HW/BW ratio: 5.6 ± 0.2 vs. 5.9 ± 0.4; Ntg vs. Tg. $P = 0.5$).

Four Months	Ntg	Tg
Heart Weight (mg)	126 ± 3.5	99.7 ± 3.7 *
Body Weight (g)	27.1 ± 0.8	25.1 ± 1.2
HW/BW ratio	4.6 ± 0.1	4.0 ± 0.1*
Two Years	Ntg	Tg
Heart Weight (mg)	168 ± 14.6	167 ± 13.2
Body Weight (g)	31.3 ± 2.2	31.0 ± 0.5
HW/BW ratio	5.6 ± 0.2	5.9 ± 0.4

Table 3-2. Heart and body weight analysis. All values are expressed as mean ± s.e.m. * $P < 0.05$

cTnI A164H aged mice retain cardiac hemodynamics during hypoxia

Previous studies have shown that young cTnI A164H Tg mice sustain cardiac function during an acute hypoxic challenge and consequently survive significantly longer than Ntg mice[246]. Similarly, to assess the physiologic and therapeutic role of cTnI A164H in the aged murine heart, mice were exposed to conditions of controlled hypoxia (12% O_2) during Millar catheterization and assessed for global cardiac function and survival (Figures 3-3 and 3-4). After four minutes of hypoxia, raw traces of LV pressure (LVP), the derivatives of LV pressure development (dP/dt), and volume, together with their corresponding pressure-volume loops revealed that aged Ntg mice have significantly compromised cardiac hemodynamics compared to aged Tg mice (Figure 3-3a,b). Mean hemodynamic data taken at four minutes into the acute hypoxic challenge and the delta change from baseline (Table 3-1a) to hypoxia showed improved systolic and diastolic performance of Tg mice compared to Ntg mice (Figure 3-3c). Specifically, compared to their Ntg littermates, LV performance was maintained during hypoxia in Tg mice as represented by higher stroke work (SW), end systolic pressure (ESP), and the positive derivative of pressure development (dP/dt max) (Figure 3-3c). Compared to baseline values, aged Tg mice showed improved contractility during hypoxia compared to a significant decrease in contractile function in aged Ntg mice based on measurements of stroke work (Δ SW), and the positive derivative of pressure development (Δ dP/dt max) (Figure 3-3c). The negative derivative of pressure development (dP/dt min)

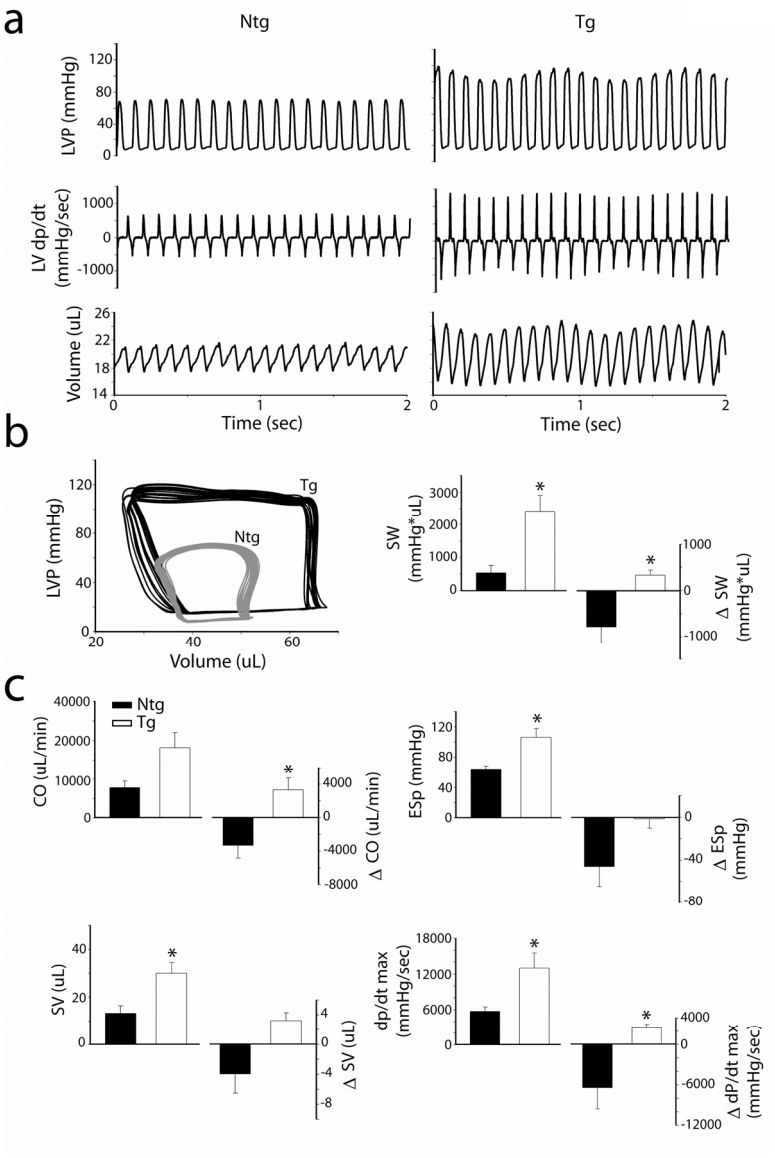

Figure 3-3. *In vivo* hemodynamic differences between aged Ntg and Tg mice during an acute hypoxic challenge. (a) Two second raw data sweeps derived by conductance micromanometry of left ventricular pressure (LVP), LV pressure derivatives (dP/dt), and LV volume of two year old Ntg and Tg mice during an acute hypoxic challenge (12% O_2). (b) Representative pressure-volume loops *in vivo* of Ntg (dark gray) and Tg (black) mice during hypoxia. (c) Mean data showing hemodynamic function as well as the delta change from baseline values for cardiac output (CO), stroke volume (SV), stroke work (SW), end systolic pressure (ESp), and positive pressure derivatives (dP/dt max) derived by Millar catheterization of two year old Ntg (■;n=3) and Tg (□;n=3) mice. * $P < 0.05$. Values are expressed as mean ± SEM. Ntg, nontransgenic; Tg, transgenic.

was also maintained during an acute hypoxic challenge in transgenic mice (data not shown). Finally, compared to Ntg littermates, Tg mice were able to sustain global cardiac function during hypoxia as shown by a higher stroke volume (SV) and cardiac output (Δ CO), (Figure 3-3c). These data show improved cardiac function in response to hypoxia in Tg mice compared to their Ntg littermates (Figure 3-4a). Consistent with improved hemodynamic function, aged Tg mice survived significantly longer during an acute hypoxic challenge than Ntg mice (11.6 ± 1.3 vs. 3.7 ± 1.9 min, $P < 0.05$) (Figure 3-4b).

Calcium cycling is different between Ntg and Tg mice

Functional analysis of calcium handling in acutely isolated cardiac myocytes showed that under conditions of 1 Hz pacing, young Tg mice had a reduced calcium transient amplitude compared to young Ntg myocytes (Figure 3-5a and c), consistent with previous reports[246]. Furthermore, experiments were performed to measure SR calcium load by means of acute addition of 20 mM caffeine (Figure 3-5b and c). Similar to baseline calcium transients, these data show that SR calcium load was lower in Tg versus Ntg mice (Figure 3-5a, b, and c). This supports the hypothesis that increased myofilament calcium sensitivity reduces calcium requirements in the cell and may contribute to the protection of Tg hearts during aging as well as cardiomyopathic challenges such as ischemia/reperfusion injury[246].

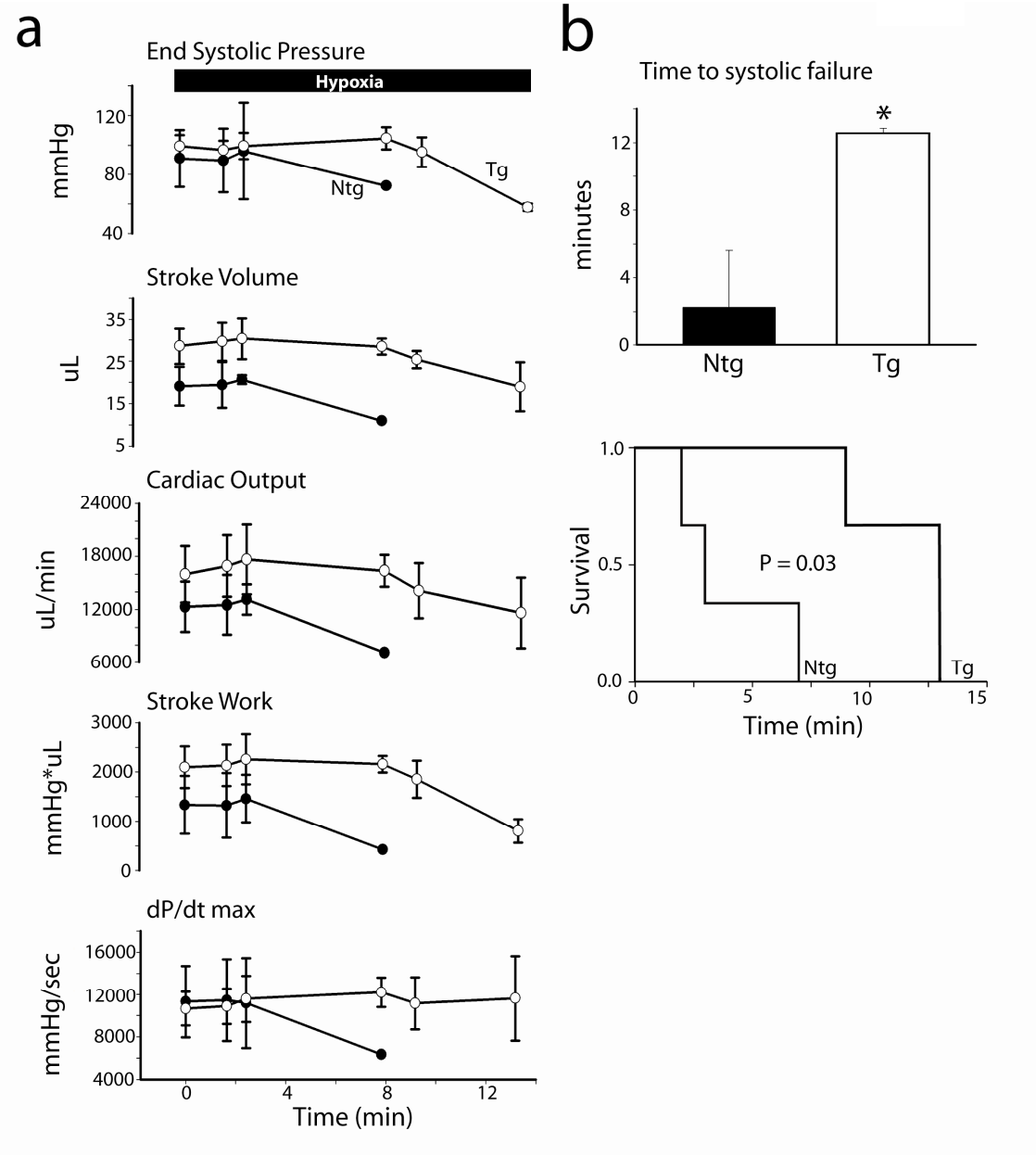

Figure 3-4. *In vivo* hemodynamic function and survival of aged mice during an acute hypoxic challenge. (a) Averaged LV hemodynamic function including end systolic pressure (ESp), stroke volume (SV), cardiac output (CO), stroke work (SW), and the positive derivative of pressure development (dP/dt max) during the time course of an acute hypoxic challenge for Ntg (●; n=3) and Tg (○; n=3) mice. (b) Summarized mean survival data and survival curve showing time to systolic heart failure for two year old Ntg (■ and — ; n=3) and Tg (□ and – –; n=3) mice. Values are expressed as mean ± SEM. * P<0.05.

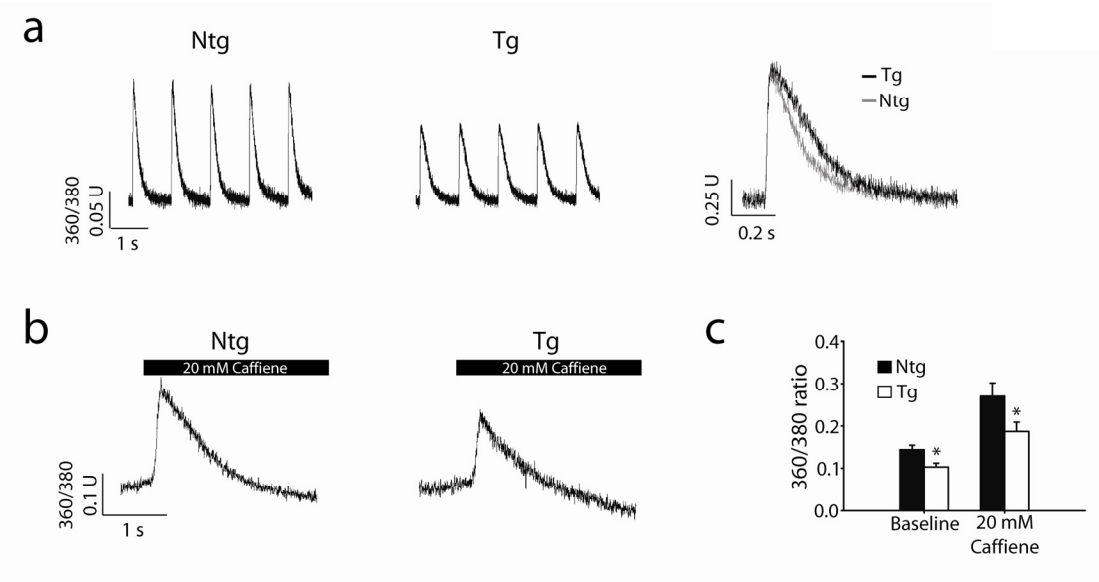

Figure 3-5. Analysis of calcium homeostasis in young mice. (a) Raw traces of calcium transients from FURA 2AM loaded isolated myocytes during pacing with 1Hz (left and middle) as well as raw calcium transient traces normalized to the peak amplitude (right). (b) Raw calcium transients after acute addition of 20 mM caffeine to release sarcoplasmic reticulum calcium. (c) Summarized data from calcium handling experiments (n= 20-24 myocytes per group). Values are expressed as mean ± SEM. * $P < 0.05$ for Ntg vs. Tg. Ntg, nontransgenic; Tg, transgenic.

Calcium handling protein expression and phosphorylation levels

Western blot analysis was performed to assess changes in calcium handling proteins between young (2-4 months) and aged (24 months) Ntg and Tg mice (Figure 3-6a and b). Alterations in the expression of proteins specifically involved in the regulation of calcium homeostasis have been established as one of the factors that contribute to the development of age-related cardiac dysfunction [137, 278, 279, 427-430]. These data show that calsequestrin (CSQ), the sodium calcium exchanger (NCX), and phospholamban (PLN) were not altered during aging by Two-way ANOVA. By contrast, SERCA2a was reduced in both Ntg and Tg aged mice based on a significant ANOVA main effect for age ($P < 0.05$), a finding that is consistent with previous reports in aging heart [200, 278]. Furthermore, these data show that the SERCA2a/PLN ratio was not different between Ntg and Tg mice during the aging process (Figure 3-6b). Although the SERCA2a levels are elevated in Tg hearts by Western blot (based on an ANOVA main effect for genotype), *in vitro* calcium handling measurements indicate a reduced level of SR calcium load in Tg hearts (Figure 3-5).

In addition, young and aged Ntg and Tg hearts were assessed for changes in protein phosphorylation (Figure 3-6a and b). These data showing serine 16 phosphorylation of phospholamban indicate that aged mice have a higher baseline level of phosphorylated PLN compared to young mice based on a significant ANOVA main effect for age. Cardiac troponin I serine 23/24 phosphorylation showed no statistical significance between groups.

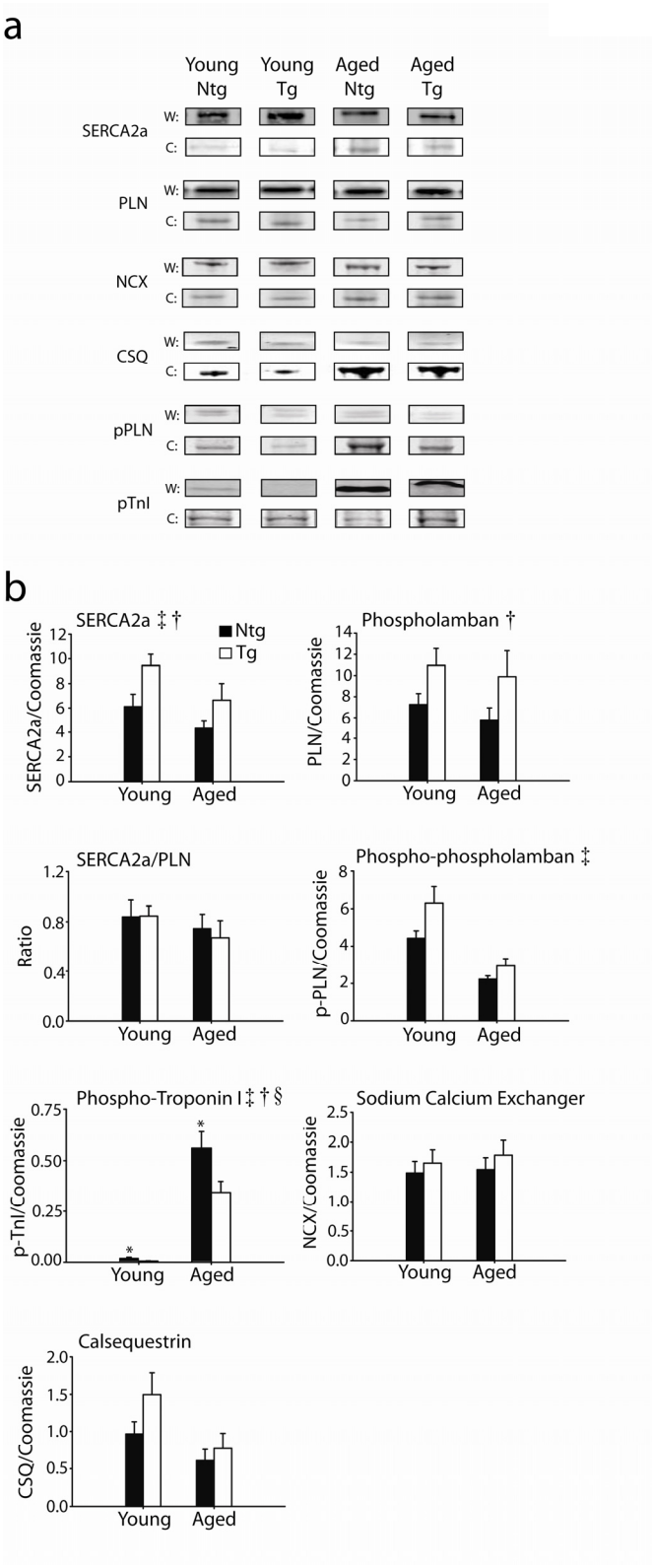

Figure 3-6. Changes in protein expression and phosphorylation in Ntg and Tg mice. (a) Western blots of calcium handling proteins including the sarco-endoplasmic reticulum ATPase (SERCA2a), phospholamban (PLN), the sodium calcium exchanger (NCX), serine 16 phosphorylation of phospholamban (pPLN), and tandem serine 23/24 phosphorylation of troponin I (pTnI) for young and aged Ntg and Tg mice. Coomassie was used to normalize for protein loading (W: Western, C: Coomassie). (b) Mean summary data for differences in the expression of calcium handling proteins including CSQ, NCX, PLN, SERCA2a, the SERCA2a/PLN ratio, pPLN, and pTnI. 2 way ANOVA main effects ($P < 0.05$): age (‡), SERCA2a, and p-PLN; and genotype (†), PLN, SERCA2a. Ntg, nontransgenic; Tg, transgenic.

Discussion

This study focused on the physiological impact of histidine-modified cardiac TnI (cTnI A164H) in aged mice. These data provide the first evidence that molecular manipulation of myofilament calcium sensitivity can preserve heart function during aging. Specifically, this study showed that age-related decrements in baseline cardiac systolic function were significantly attenuated in Tg mice compared Ntg littermates. Echocardiography studies also demonstrated that age-dependent diastolic dysfunction (elevated E/Ela) was attenuated in Tg animals. Importantly, when exposed to an acute hypoxic challenge *in vivo*, aged Tg mice maintained cardiac performance that significantly extended their survival compared to Ntg mice. These data support the hypothesis that myofilament-based enhanced function by single histidine-modified cTnI provides a mechanism for attenuating age-related decrements in cardiac function.

Increasing calcium sensitivity of the myofilament consequent to alterations in the biochemistry of cardiac troponin I (cTnI) has been well studied[9, 33, 246, 249, 252, 431]. A recent report of the crystal structure of cTnI places Ala164 at the critical switch domain that is key in regulating myofilament calcium activation[52]. Codon 164 is situated at the interface between the amphiphilic switch region, H3, and the C-terminal actin binding domain, H4. Together these regions are defined as the regulatory segment. In the calcium saturated state, the entire regulatory segment of cTnI (residues 137-210) undergoes a conformational change concomitant with binding of the H3 domain to the conserved N-terminal

hydrophobic patch of TnC. In the slow skeletal isoform of TnI (ssTnI), which is the fetal/neonatal isoform in mammals, a unique biochemical characteristic of the switch region was found to confer pH-dependent increases in calcium sensitivity to the myofilament[266, 319]. In initial studies, mutagenesis experiments identified a critical histidine at position 132 as responsible for this pH dependent functional outcome[246, 250]. The physiological effects of this mutation in the heart directly reflect the unique biochemical properties of histidine's imidazole moiety which, unique among all the amino acids, ionizes within the physiological range (pK_R = 6.0). Numerous studies have shown that under conditions of acidosis, ssTnI protects contractility of myocytes *in vitro* and the whole heart *in vivo*[133, 250, 318]. In light of these findings, we sought to introduce this pH sensitivity into the switch domain of cTnI. An engineered histidine modification in codon 164 of cTnI (A164H) takes advantage of this critical functional property of ssTnI transposed into the context of cTnI. This modification takes place without altering important physiological functions of cTnI in regulating global cardiac inotropic and lusitropic responses to β-adrenergic signaling[246]. Cardiac TnI A164H provides a titratable molecular switch mechanism regulating myofilament tension development in response to biochemical changes in the adult myocyte. One of the central hypotheses of this study was that increasing myofilament calcium sensitivity by means of cTnI A164H is a powerful molecular therapy for attenuating morbidity and mortality associated with ischemia/hypoxia-induced contractile failure in aged mice.

Declining cardiac function contributes to waning health in geriatric populations[423]. In many cases these age-related changes are secondary to coronary artery disease[424]. Of particular salience to this study is the propensity for chronic ischemia associated with vascular stenosis that prevent sufficient coronary blood flow, a condition typically associated with poor cardiovascular health of the elderly[422]. A portion of this study was based on an experimental protocol to impose a controlled state of hypoxia in aged mice through low inhaled oxygen. In the clinical setting, hypoxia is usually secondary to cardio-pulmonary pathologies frequently seen in geriatric populations. Physiologically these conditions are usually due to hypoventilation, vascular shunting, ventilation/perfusion mismatch and interstitial diffusion defects. Clinical diseases of the lungs, such as COPD, pneumonia, interstitial lung disease, or pulmonary embolic disease are common conditions associated with hypoxia which may lead to secondary ischemic cardiac injury. The aged heart is particularly at risk in these settings because of intrinsic muscle disease and underlying coronary artery disease with areas of marginally perfused myocardium. These clinically relevant etiologies, known risk factors for cardiovascular disease, provide contextual relevance for the key findings of this study. These important results include, first, that aged cTnI A164H Tg mice have enhanced cardiac function and extended survival capacity during an acute hypoxic challenge compared to Ntg mice.

Irrespective of etiology, systolic and diastolic dysfunction are strong predictors of heart failure in geriatric populations[432]. In this study we show that

cTnI A164H Tg mice have improved contractility during the aging process compared to Ntg mice. At four months of age, significantly larger hearts of Ntg mice could explain, at least in part, the corresponding decreases in contractility measurements compared to Tg mice. The equalization of the HW/BW ratio at two years of age, however, neutralizes any heart size-dependent variables that influence contractility measurements between groups at this time point. This lends credence to the conclusion that Tg mice, which retained the same relative increase in contractility over Ntg mice during the aging process, actually underwent an age-dependent and heart size-independent increase in absolute contractility. This could be explained in part by the increase in stoichiometric incorporation of cTnI A164H in old versus young Tg mice and could provide mechanistic basis for the observed increase in contractility at two years of age. Additionally, compared to Tg mice, increased LV cavitary dilation in aged Ntg mice may also, at least in part, contribute to the divergence of contractile efficiency at the two year time point. A shift toward higher sarcomere lengths, which occurs with dilated cardiomyopathies and may be a component of age-related dysfunction, could reduce the efficiency of contractility based on the Frank-Starling principle.

In addition to systolic dysfunction, decrements in diastolic function are also characteristic of the aging process. LV dilation together with stiffening of the aged myocardium prevents sufficient relaxation of the heart during the filling phase of the cardiac cycle. Unexpectedly, another key finding of this study is that cTnI A164H protects diastolic function during the aging process. These data indicate

that Ntg mice show evidence of diastolic dysfunction based on a decrease in the velocity of the lateral annulus during the early filling phase (Ela) of the LV as well as an increase in the mitral valve E wave flow velocity to lateral annular E wave ratio (E/Ela). This latter parameter (E/Ela) shows the ratio of the inflow velocity to the tissue velocity providing insight into the elastic properties of the ventricle. In essence, the E wave velocity controls for cardiac output, heart rate, and filling so that the ratio (E/Ela) correlates with left atrial pressure. Here, the E/Ela shows evidence of the transgene altering the typical progression of diastolic dysfunction based on a significant interaction effect ($P < 0.05$). These data indicate that cTnI A164H transgenic mice are able to retain improved diastolic function during the aging process compared to Ntg mice which experience predictable age-related diastolic dysfunction.

The relationship between cTnI A164H and diastolic performance, however, is complex as indicated by differences in echocardiographic and micromanometry data at baseline. Conflicting data based on measures of isovolumic relaxation (Tau) provide inconclusive evidence regarding baseline diastolic function in Tg mice, which is consistent with previous findings[246]. However, the mechanical component of relaxation during the late (filling) phase of diastole, as measured non-invasively by Doppler tissue imaging indicates that Ntg mice have compromised viscoelastic properties of the ventricle resulting in a decline in diastolic function during the aging process which is significantly attenuated in Tg mice.

Taking this whole organ functional analysis into consideration, it has been established that, at the sub-cellular level, changes in the expression of calcium handling proteins contribute to the progression of pump dysfunction during aging[188]. Our study supports these findings specifically in regard to the observation that SERCA2a levels are diminished at 2 years of age in Ntg and Tg mice. Reduced expression of SERCA2a has been implicated directly in the progression of age-induced cardiomyopathy[278] and provides a sub-cellular basis, at least in part, for the whole organ diastolic dysfunction observed in this study during aging. The lack of any *genotypic* differences in CSQ and NCX and the SERCA2a to PLN stoichiometry during aging suggests an alternative mechanism for improvement of cardiac function in the Tg mice during the aging process. We propose that this mechanism is predominantly the result of increasing inotropy by molecular manipulation of myofilament calcium sensitivity by means of cTnI A164H.

The results of this study show that Tg hearts have reduced SR calcium loading. Previous reports have found that aged hearts are more susceptible to calcium overload than young hearts[421, 433, 434]. This suggests that a reduced SR Ca2+ load may benefit cTnI A164H hearts in aging, similar to our recent report in the context of myocardial injury such as ischemia/reperfusion[15]. We hypothesize that the lower SR Ca2+ load and Ca2+ transient are made possible by myofilament activation enhancement by cTnIA164H. We propose that there is an interplay between the myofilament enhancement and SR functionality that could account for higher SERCA2a levels in Tg hearts.

The cardiac functional readout of these findings at the sub-cellular level are seen in the whole organ serial echocardiographic analysis of Ntg and Tg mice during the two year aging process. The decline in cardiac contractility (e.g. EF), increase in LV chamber geometry, and development of diastolic dysfunction (e.g. increased E/Ela) particularly evident at the two year time point are likely the consequence, at least in part, of the changes observed in calcium handling proteins.

In conclusion, ischemia-related cardiac dysfunction in aged populations remains a significant cause of morbidity and mortality. Therapies for ischemic heart disease and heart failure could be directed specifically toward improving the Ca^{2+} sensitivity of the myofilament. The consequent improvement in contractility that results from an increase in Ca^{2+} sensitivity may appear to counter the logic of commonly prescribed therapeutics, which calls for the use of beta blockers that decrease contractility acutely, allowing for reduced oxygen consumption and energy expenditure. Although there is proven value in the diverse effects of beta blockers, we have shown that targeted alteration of myofilament calcium sensitivity to increase contractile performance is an effective mechanism for treatment of ischemic heart disease and heart failure in small mammals[246]. This is in concurrence with Mann and Bristow's view that augmentation of myofilament responsiveness to calcium would improve the force generating capacity of the sarcomere and thus redress global cardiac dysfunction[4357]. In summary, this study together with previous work[246], strengthens the hypothesis that altering the functionality of troponin I is an

effective means of specifically augmenting myofilament calcium sensitivity and consequently enhancing cardiac contractility. Adding to the growing evidence for the therapeutic role of histidine-modified TnI in the heart, this study provides the first evidence that specific replacement of native cTnI with cTnI A164H in the adult heart protects cardiac function during aging. We propose that the progression of pathologic and age-related diminutions in cardiac function may be improved by myofilament-based molecular therapeutics for increasing cardiac performance.

Acknowledgements

We thank Jaime Predmore for technical expertise in mouse myocyte isolation with which SR calcium load experiments were performed. We appreciate Dr. Mark Russell, MD for his assistance with interpretation of echocardiography data and Dr. Margaret Westfall for helpful comments. We also thank Dr. Samuel Palpant, MD for his medical advice regarding cardio-pulmonary diseases in geriatric populations.

Chapter IV[2]

Single histidine button in cardiac troponin I sustains heart performance in response to severe hypercapnic respiratory acidosis in vivo

Abstract

Intracellular acidosis is a profound negative regulator of myocardial performance. We hypothesized that titrating myofilament calcium sensitivity by a single histidine substituted cardiac troponin I (A164H) would protect the whole animal physiological response to acidosis *in vivo*. **Methods/Results:** To experimentally induce severe hypercapnic acidosis, mice were exposed to a 40% CO_2 challenge. By echocardiography it was found that systolic function and ventricular geometry were maintained in cTnI A164H transgenic mice (Tg). By contrast, non-Tg littermates (Ntg) experienced rapid and marked cardiac decompensation during this same challenge. For detailed hemodymanic assessment, Millar pressure-conductance catheterization was performed while animals were treated with a β-blocker, esmolol, during a severe hypercapnic

[2] This chapter was adapted from: Palpant NJ, D'Alecy LG, Metzger JM. *Single histidine button in cardiac troponin I sustains heart performance in response to severe hypercapnic respiratory acidosis in vivo.* The FASEB Journal. 2009 May;23(5):1529-40. Epub 2009 Jan 13.

acidosis challenge. Survival and load independent measures of contractility were significantly greater in Tg vs. Ntg mice. This assay showed that Ntg mice had 100% mortality within five minutes of acidosis. By contrast, baseline systolic and diastolic function were protected in Tg mice during acidosis and they had 100% survival. **Conclusion:** This study shows that, independent of any beta adrenergic compensation, myofilament-based molecular manipulation of inotropy by histidine-modified troponin I maintains cardiac inotropic and lusitropic performance and markedly improves survival during severe acidosis *in vivo*.

Introduction

Acute heart failure can result from myocardial acidosis. Myocardial acidosis arises from reduced plasma oxygen tension (hypoxic acidosis) as in cases of myocardial ischemia[230, 236], or accumulated levels of plasma carbon dioxide (hypercapnic acidosis or hypercarbia) found with severe pulmonary diseases such as chronic obstructive pulmonary disease (COPD)[235], or emphysema[436]. Acidosis has numerous pathophysiological implications within the context of many organ systems, including significant deleterious effects on the contractile function of the heart[237-239, 241, 242]. Homeostasis is tightly regulated in the heart, which makes this organ particularly sensitive to whole animal metabolic changes and the downstream influence on pH status and energy availability [429, 437].

There are numerous changes that occur in the heart under conditions of acidosis, including altered calcium handling[240, 241, 427, 429, 431, 438]. The present study focused on altered sarcomeric protein function known to significantly reduce cardiac contractility during acute acidosis independent of altered Ca^{2+} handling[238, 439, 440]. A key regulator of myofibrillar contraction is the troponin complex, including the calcium binding subunit, troponin C (TnC), and the inhibitory subunit troponin I (TnI). Calcium increases the TnI-TnC interaction causing these subunits to act as a dynamic switch within the myofilament during systole and diastole. Acidosis diminishes myofilament Ca^{2+} sensitivity due in part to reduced Ca2+ binding to troponin C[238, 441], and impaired interactions between TnI and TnC during systole. Thus, this complex serves as a key regulator of beat-to-beat contractility in the heart[33]. In the whole heart this reduction in myofilament Ca^{2+} sensitivity is a key contributor to the reduction in acute myofilament force production and a consequent decrement in left ventricular developed pressure *in vivo*[9, 246].

Earlier biochemical studies established that neonatal myocardium is more resilient to low pH[239], a phenotype correlated with fetal expression of the slow skeletal isoform of TnI. The ssTnI isoform is able to retain proper myofibrillar contractility even in cases of severe acidosis[133, 251, 266, 314, 317-319, 324]. Specifically, the pCa (-log[Ca^{2+}]) required for 50% activation of myofilaments in adult cardiac myocytes, that express the adult isoform of TnI (cTnI), drops by more than 1 pCa units during acidification of pH (from pH 7.0 to 6.2). This is compared to adult myocytes transduced with an adenoviral construct expressing the slow skeletal

isoform of TnI (ssTnI), that show an attenuated pCa shift during acidification of pH (from pH 7.0 to 6.2)[133]. TnI isoform chimera structure-function studies[266, 314, 315, 319] have gone on to further demonstrate that the unique biochemistry of ssTnI could be reproduced by substituting a single histidine residue in ssTnI for alanine164 in cTnI, which is located at the interface between TnC and actin binding domains involved in the switch function of TnI[249, 250]. In recent work, this histidine button substitution has been engineered into the adult cardiac isoform of TnI (cTnI A164H) providing a biophysical basis for a functional molecular rheostat of intracellular pH in the adult heart[242, 246]. Cellular data has shown that myocytes expressing cTnI A164H have intact responses to isoproterinol and PKA by hastening relaxation kinetics and shifting the tension-pCa relationship[246]. Furthermore, calcium load is diminished in these myocytes which is manifest in a lower calcium transient amplitude[246, 290]. Studies of transgenic mice expressing this engineered mutant cTnI show improved cardiac inotropic function in response to a variety of pathophysiologic challenges, including acute and chronic ischemia[246] as well as in a mouse model of age-induced cardiomyopathy[290].

The current study focused exclusively on the *in vivo* whole animal response to acidosis in the context of this modified cTnI using an experimental model of severe respiratory hypercapnia. A major aim of this study was to block adrenergic support in the heart and subsequently analyze cardiac function *in vivo* under baseline conditions and during exposure to acidosis. Adrenergic stimulation is a major regulator of cardiac function at baseline in the rodent[246, 318]. Furthermore, high sympathetic stimulation of rodent hearts at baseline has been

shown to compensate and mask cardiomyopathic phenotypes that are revealed during suppression of catecholamine signaling[442]. In light of this, beta blockade in mouse models consisting of myofilament modifications[246, 333 213] is of particular importance for determining any functional aberrations caused by altered myofilament calcium responsiveness on systolic and diastolic performance. Furthermore, beta blockade allows for the functional readout of intrinsic inotropic performance of the heart *in vivo* which is important in determining the potential for cardiac contractile responsiveness to injury. These questions have not been addressed in the cTnI A164H Tg mouse to date. The new findings of this study show that cTnI A164H preserves baseline systolic *and* diastolic performance during acidosis *in vivo*. This study suggests that the biochemical function of cTnI A164H as a molecular rheostat in the sarcomere may protect cardiac performance in a range of pathologies associated with acidosis.

Materials and Methods

Mouse Model Generation and analysis of transgenic mice expressing a histidine-modified cardiac troponin I (cTnI A164H) with FLAG epitope was previously described[246]. The procedures used in this study are in agreement with the guidelines of the University of Michigan and approved by the University of Michigan Committee on the Use and Care of Animals. Veterinary care was provided by the University of Michigan Unit for Laboratory Animal Medicine. The University of Michigan is accredited by the American Association of Accreditation

of Laboratory Animal Health Care, and the animal care use program conforms to the standards of the National Institutes of Health Guide for the Care and Use of Laboratory Animals (NIH Pub. No. 85-23).

Conductance Micromanometry Measurements of in vivo cardiovascular hemodynamics were obtained using conductance micromanometry as previously performed by this laboratory[246]. Mice were anesthetized and ventilated via a tracheal cannulation and ventilated via a pressure controlled ventilator with 1% isoflurane at a peak inspiratory pressure of 15 cm H_2O and a respiratory rate of 60 breaths/min. With aid of a dissecting microscope, the heart was exposed via a thoracotomy. A 1.0 French Millar pressure-volume catheter (PVR-1045; Millar Instruments Inc., Houston, Texas, USA) was then placed into the left ventricular chamber via an apical stab. LV pressure and volume measurements were collected at a sampling rate of 1 kHz. Data were analyzed with Ponemah software, P3 Plus (DSI International, St. Paul, MN, USA). Transient inferior vena cava (IVC) occlusions were also performed to obtain the end systolic and end diastolic pressure-volume relationships. IVC occlusions were performed at baseline and at five minutes of esmolol infusion (Figure 4-3a). After obtaining baseline hemodynamics (ventilated with isoflurane and O_2), mice received a continuous infusion of esmolol (250 ug/kg/min) that continued until the completion of the assay. After five minutes of esmolol infusion mice were exposed to an acute hypercapnic acidosis challenge (40% CO_2 balanced with oxygen) (for schematic diagram of protocol see Figure 4-3a). Data were acquired

until systolic failure which was defined as the point when peak LV systolic pressure dropped to 50 mmHg. At this point, esmolol infusion was stopped and mice were recovered using 100% O_2 in order to obtain instrument calibration.

Echocardiography Anesthesia was induced with 3% isoflurane and then maintained at 1% for the duration of the procedure. The hair was removed from the upper abdominal and thoracic area with depilatory cream. ECG was monitored via non-invasive resting ECG electrodes. Transthoracic echocardiography was performed in the supine or left lateral position. Two-dimensional, M-mode, Doppler and tissue Doppler echocardiographic images were recorded using a VisualSonics' Vevo 770 high resolution *in vivo* micro-imaging system (VisualSonics Inc., Toronto, Ontario, Canada). The systolic and diastolic dimensions and wall thickness were measured in M-mode in the parasternal short axis view at the level of the papillary muscles[443, 444]. Fractional shortening and ejection fraction were calculated from the M-mode parasternal short axis view[444]. Diastolic function was assessed by conventional pulsed-wave spectral Doppler analysis of mitral valve inflow patterns (early [E] and late [A] filling waves). Doppler tissue imaging (DTI) was used to measure the early (E_a) and late (A_a) diastolic tissue velocities of the lateral annulus. As a combined measure of systolic and diastolic function, the TEI index was measured as (LVctetrt-LVet)/LVet where LVctetrt is the total time of LV contraction, ejection plus relaxation and LVet is LV ejection time. After acquiring baseline echocardiographic data mice were exposed to a hypercapnic acidosis challenge

(ventilation with 40% CO_2 balanced with oxygen) for ten minutes. During ventilation with CO_2 efforts were taken to confirm that the nose and mouth were within the nose cone to prevent any dilution of the inhaled gas due to gasping of room air. Data were acquired every 2.5 minutes for the duration of the challenge. All mice survived this challenge and were returned to their cage for recovery.

In vivo Arterial Pressure and ECG Telemetry Implantable radio-telemetry probes (C-10 implants, DSI International, St. Paul, MN, USA) for measurement of real time systemic blood pressure and ECG in freely moving unanesthetized animals was accomplished as described previously[445-447]. One week after implantation of telemetry probe, mice were placed in a flow-through chamber initially flushed with room air (20.93% O_2) allowing rodents time to equilibrate to the new environment. They were then exposed to a hypercapnic acidosis challenge (forty minutes exposure to 40% CO_2 balanced with oxygen). Upon completion of the challenge, mice were removed from the chamber and returned to their cage for recovery.

Blood Gas Analysis Mice were anesthetized with 1% isofluorane and exposed to a hypercapnic acidosis challenge (40% CO_2 balanced with oxygen) for ten minutes without external ventilator support. During ventilation with CO_2 efforts were taken to confirm that the nose and mouth were within the nose cone to prevent any dilution of the inhaled gas due to gasping of room air. At the end of the challenge the thoracic cavity was opened to expose the heart. Approximately

600 uL of oxygenated blood was drawn from the left ventricle and immediately analyzed using a Radiometer ABL505 blood gas analyzer (Radiometer, Westlake, Ohio, USA).

Statistics All results are expressed as mean ± SEM. All single variable assays were assessed by two-tailed t-test. All multivariable assays were assessed using either one way analysis of variance (ANOVA) or two way repeated measures ANOVA with Tukey post-hoc test. Survival after the *in vivo* acute hypercapnic acidosis challenge was assessed by the Fisher exact test.

Results

Echocardiography assessment during acute respiratory hypercapnic acidosis

Using echocardiography to track *in vivo* LV function, Tg mice retained global cardiac performance and proper LV dimensions during exposure to acidosis. By contrast, Ntg mice showed significant myocardial contractile dysfunction throughout the same challenge (e.g. EF(%) at ten minutes of acidosis [Tg] 68.1 ± 4.7 vs. [Ntg] 23.6 ± 4.9) (Figure 4-1). In addition to the summarized echo data (Figure 4-1b and c), Table 4-1 shows changes in cardiac

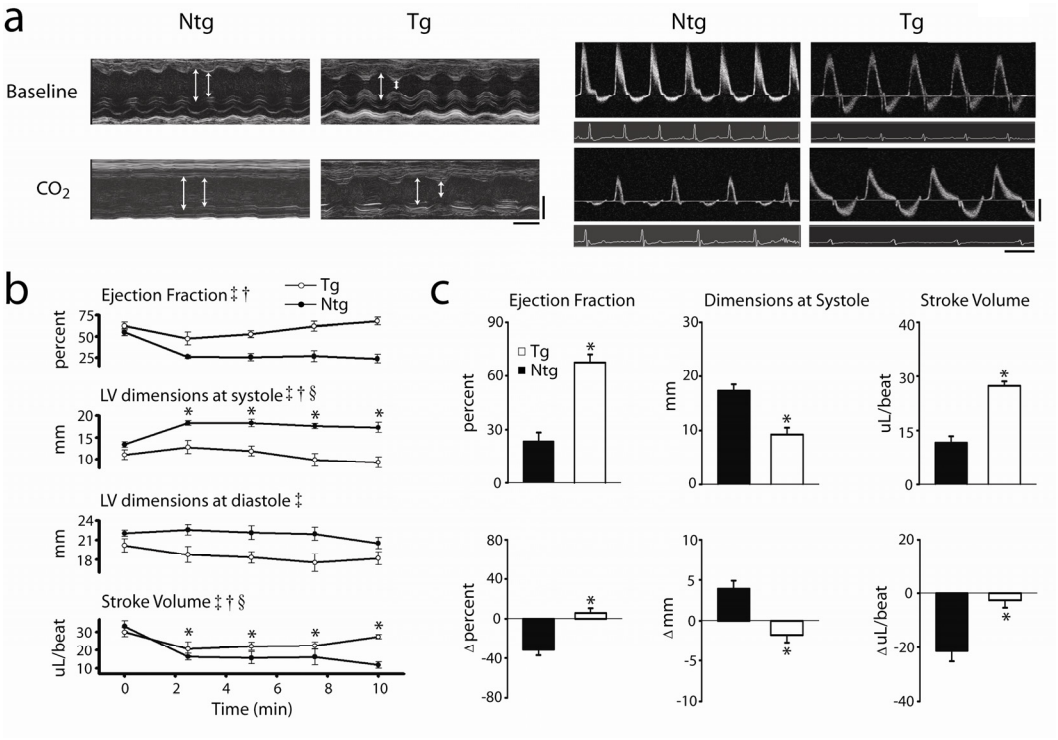

Figure 4-1. Cardiac function assessed by echocardiography at baseline and during acidosis. (a, left) Representative m-mode echocardiographic images along the parasternal short axis view showing changes in contractility of nontransgenic and transgenic mice at baseline and after ten minutes of exposure to 40% CO_2. White bars delineate systole and diastole. Time bar = 100 ms, distance bar = 2 mm. (a, right) Representative conventional pulsed-wave spectral Doppler analysis of mitral valve inflow and aortic valve outflow patterns at baseline and after ten minutes of exposure to 40% CO_2 in nontransgenic and transgenic mice. Time bar = 100 ms, flow rate bar = 40 cm/s. (b) Summarized mean data showing changes in cardiac functional parameters including ejection fraction, LV dimensions at systole and diastole, and stroke volume between Ntg (●) and Tg (○) mice during the time course of hypercapnic acidosis. (c) Mean data showing the difference in ejection fraction, LV dimensions at systole, and stroke volume after 10 minutes exposure to 40% CO_2 (top) as well as the change (Δ) in function from baseline (bottom) in Ntg (■) and Tg (□) mice. Values are expressed as mean ± SEM. 2 way repeated measures ANOVA main effects: time (‡) and genotype (†) $P < 0.05$. 2 way repeated measures ANOVA interaction effects between time and genotype (§) $P < 0.05$. * $P < 0.05$ for Ntg vs. Tg. Ntg, nontransgenic (n=5); Tg, transgenic (n=7).

Echocardiography	Baseline	Nadir	End	Nadir to End
Transgenic				
EF (%)	75.1 ± 4.7	28.5 ± 6.3 #	68.1 ± 5.7 †	20.4 ± 4.8 *
Vol s (uL)	12.9 ± 3.2	30.6 ± 5.3 #	11.4 ± 2.6 †	-10.1 ± 2.9 *
TEI Index	0.4 ± 0.03	0.6 ± 0.04 #	0.5 ± 0.03 † ‡	-0.1 ± 0.0 *
MV E (mm/s)	883.8 ± 24.4	541.1 ± 63.0 #	803.6 ± 36.6 †	262.5 ± 81.7 *
Nontransgenic				
EF (%)	55.0 ± 4.1	23.6 ± 4.9 #	23.6 ± 4.9 ‡	0.0 ± 0.0
Vol s (uL)	27.0 ± 2.6	45. 8 ± 2.4 #	40.6 ± 5.1‡	-5.1 ± 5.9
TEI Index	0.40 ± 0.02	0.65 ± 0.03 #	0.62 ± 0.05 ‡	-0.03 ± 0.07
MV E (mm/s)	1069.7 ± 57.1	646.6 ± 146.7 #	646.6 ± 146.7 ‡	0.0 ± 0.0
Hemodynamics	Baseline	Nadir	End	Nadir to End
Transgenic				
CI (+dPdt/mmHg)	196.9 ± 9.6	113.1 ± 2.4 #	126.4 ± 6.7‡	21.1 ± 6.5 *
Max Vol (uL)	27.3 ± 4.1	36.3 ± 5.0 #	32.5 ± 5.0 ‡	-3.8 ± 1.2 *
EDp (mmHg)	6.2 ± 1.1	12.3 ± 1.8 #	7.9 ± 1.8 †	-4.4 ± 0.8 *
Ea (ESp/SV)	5.4 ± 0.6	8.4 ± 0.4 #	6.2 ± 0.7 †	-2.2 ± 0.6 *
Nontransgenic				
CI (+dPdt/mmHg)	169.0 ± 26.6	95.7 ± 5.7 #	0.0 ± 0.0	0.0 ± 0.0
Max Vol (uL)	28.1 ± 5.4	55.1 ± 5.5 #	0.0 ± 0.0	0.0 ± 0.0
EDp (mmHg)	4.0 ± 1.0	10.8 ± 1.7 #	0.0 ± 0.0	0.0 ± 0.0
Ea (ESp/SV)	6.2 ± 0.4	11.2 ± 0.0 #	0.0 ± 0.0	0.0 ± 0.0

Table 4-1. Changes in Cardiac Function During Acidosis. Analysis of cardiac function during acidosis in Tg and Ntg mice showing changes between baseline, the nadir (worst value for a given parameter), and end of the challenge. Echocardiographic parameters: ejection fraction (EF), volume at systole (Vol s), TEI index, and inflow velocity of the Mitral valve E wave (MV E). Hemodynamic parameters: contractility index (CI), LV maximum volume (Max Vol), end diastolic pressure (EDp), and arterial elastance (Ea). Statistical analysis of points taken at baseline, the nadir, and end of the challenge were compared using a repeated measures 1 way analysis of variance: # $P < 0.05$ for baseline vs. nadir, † $P < 0.05$ for the nadir vs. end of the challenge, ‡ $P < 0.05$ for baseline vs. end of the challenge. Nadir to the end of the challenge (compared to a hypothetical zero), * $P < 0.05$ using a Dunnets one-sample t-test with Wilcoxon signed-rank post hoc. All values are expressed as mean ± s.e.m. Echocardiography, Tg n = 7 and Ntg n = 5; Hemodynamics, Tg n = 7 and Ntg n = 6.

function at the end of the challenge compared to measurements taken at the beginning and at the nadir for each parameter. We found that the function of Tg hearts at the end of the challenge was not significantly different from baseline based on a repeated measures one way ANOVA. In contrast, the lowest point of function for Ntg mice was at the end of the challenge in all cases or the nadir to the end of the challenge was not significant from zero based on a Dunnet's test.

In addition to being mildly hypercontractile at baseline, cumulative echo data show that measurements of contractility observed in Tg mice, such as ejection fraction (EF) and stroke volume (SV), all showed evidence of a modest decrease during the early stages of the acidosis challenge which reverted by the ten minute time point. At the end of the challenge aspects of Tg heart performance were not significantly different than baseline (e.g. Tg EF (%) at baseline 75.1 ± 4.7 vs. 68.1 ± 5.7 after 10 minutes of acidosis (NS)) (Figure 4-1b and c). By contrast Ntg mice showed a significant reduction in cardiac contractility throughout the challenge (e.g. EF at ten minutes of acidosis: [Ntg] 23.6 ± 4.9% vs. [Tg] 67.8 ± 4.5%) (Figure 4-1b and c, Appendix: Figure 4-7). Furthermore, Tg mice retained ventricular geometry during the hypercapnic acidosis challenge compared to Ntg mice that underwent significant left ventricular cavitary dilation (e.g. LV dimensions at systole at ten minutes of acidosis: [Ntg] 17.3 ± 1.2 mm vs. [Tg] 9.3 ± 1.3 mm) (Figure 4-1b and c). As a measure of diastolic function, the mitral valve inflow velocity (MV E), measured by Doppler, recovered to baseline function after the nadir in Tg mice compared to Ntg mice in which compromised diastolic function persisted throughout the

acidosis challenge (MV E change from nadir to end in Tg mice: 262.5 ± 81.7 mm/s) (Table 4-1). Lastly, as an assessment of overall diastolic and systolic function, the TEI index indicated that Tg mice underwent an initial phase of cardiac decompensation during the onset of acidosis but were able to recover function by the end of the challenge compared to Ntg mice that showed persistent cardiac dysfunction throughout the hypercapnic acidosis challenge (TEI index at ten minutes of acidosis: [Ntg] 0.61 ± 0.05 vs. [Tg] 0.5 ± 0.03) (Appendix: Figure 4-7). All mice recovered from this hypercapnic acidosis challenge.

Blood gas analysis during acidosis

To assess whether there were any differences in blood gas parameters during the acidosis challenge, arterial blood gases were analyzed during hypercapnic acidosis. These data indicate that, although significantly different from baseline values, blood gases taken at 10 minutes of exposure to 40% CO_2 were not different between Tg and Ntg mice (Table 4-2). In both Tg and Ntg mice, blood pH decreased from 7.2 at baseline to below 6.63 during the hypercapnic challenge demonstrating the development of significant acidemia. This is consistent with changes in pCO_2 which increased from baseline values at 55 to 60 mmHg to greater than 250 mmHg during acidosis in both Tg and Ntg animals. This increase in carbon dioxide was also confirmed in measures of total plasma CO_2 that were significantly increased during the hypercapnic challenge. Although

Parameter	Ntg Baseline	Ntg CO_2 (10 min)	Tg Baseline	Tg CO_2 (10 min)	Tg CO_2 (20 min)
pH	7.2 ± 0.02	6.61 ± 0.01*	7.2 ± 0.0	6.62 ± 0.02*	6.55 ± 0.0 ‡ †
pCO_2 (mmHg)	55.3 ± 1.8	258.6 ± 13.6*	59.1 ± 2.9	265.7 ± 8.5*	277.3 ± 14.5 ‡
pO_2 (mmHg)	383.6 ± 69.6	196.9 ± 43.9	296.8 ± 60.4	206.5 ± 38.7	301.0 ± 15.2
sO_2 (%)	102.9 ± 1.0	87.7 ± 5.1	102.4 ± 1.0	86.2 ± 6.4	94.9 ± 3.6
HCO_3^- (mmol/L)	23.5 ± 0.7	24.4 ± 0.9	23.1 ± 1.1	25.8 ± 0.6	23.2 ± 0.5
tCO_2 (Vol %)	56.5 ± 1.6	72.5 ± 2.7*	55.6 ± 2.6	76.0 ±1.4*	71.5 ± 1.9 ‡
SBE_c (mmol/L)	-2.8 ± 0.9	-13.4 ± 0.7*	-3.6 ± 0.9	-12.1 ± 0.8*	-15.7 ± 0.3 ‡ †

Table 4-2. Arterial blood gas analysis. Ntg measurements, *P < 0.05 based on t-test comparing baseline vs. CO_2 values. For Tg measurements statistics were performed using one way ANOVA where # P < 0.05 for baseline vs. CO_2 (10 min); † P < 0.05 for CO_2 (10 min) vs. CO_2 (20 min); and .‡ P < 0.05 for CO_2 (20 min) vs. baseline. All values are expressed as mean ± s.e.m. Abbreviations: partial pressure of carbon dioxide (pCO_2), partial pressure of oxygen (pO_2), fraction of oxyhemoglobin in deoxy-plus oxyhemoglobin of blood (plasma oxygen saturation: sO_2), bicarbonate (HCO_3^-), total plasma carbon dioxide of whole blood (tCO_2), and concentration of titratable base (standardized base excess: SBE_c). Ntg Baseline n= 5, Tg Baseline n= 5, Ntg CO_2 (10 min) n=5, Tg CO_2 (10 min) n=6, Tg CO_2 (20 min) n = 5

oxygen availability during acidosis was increased from room air values (60% compared to approximately 21%, respectively) oxygen saturation tended to decrease from baseline values of 102 % to below 88% during hypercapnia, although this trend did not reach statistical significance for either group. Lastly, plasma concentrations of titratable base (SBE_c) were significantly reduced ($P < 0.05$) during hypercapnia compared to baseline values, which is consistent with acidemia. There were no significant changes in plasma bicarbonate during ventilation with 40% CO_2 indicating that these mice were not experiencing metabolic acidosis.

Blood gas analysis was also performed on Tg mice after twenty minutes of exposure to 40% CO_2. Changes in pH indicate that the blood continued to acidify to a degree significantly lower than the pH reached after ten minutes of hypercapnic acidosis (serum pH [10 min] 6.62 ± 0.02 vs. [20 min] 6.55 ± 0.00**)**. Furthermore, SBE_c continued to decrease concomitant with the decrease in blood pH. These findings are consistent with the development of an increasingly severe respiratory hypercapnic acidemia. However, even at twenty minutes exposure to 40% CO_2, plasma bicarbonate remained steady indicating the absence of any metabolic acidosis.

Blood pressure and ECG telemetry in vivo during hypercapnic acidosis challenge

In vivo continuous arterial pressure telemetry of freely moving unanesthetized animals was carried out between Ntg and Tg mice. Furthermore, this study

analyzed the extent to which cTnI A164H mice were able to maintain systemic perfusion pressures during a prolonged hypercapnic acidosis challenge (40 minutes exposure to 40% CO_2) compared to Ntg littermates (Figure 4-2). At baseline, circadian rhythms showing changes in blood pressure over 24 hours indicate that Ntg mice have increased systolic blood pressure compared to Tg mice ($P < 0.05$). However, diastolic arterial pressure was not different between groups. Furthermore, these telemetered data show that Ntg mice also have a higher baseline heart rate than Tg mice (HR [Tg] 472.2 ± 15.6 vs. [Ntg] 555.4 ± 18.7, $P < 0.05$) (Figure 4-2a and b).

After one week of baseline blood pressure measurements, mice were exposed to a forty minute hypercapnic acidosis challenge. The change in arterial systolic pressure between baseline (avg. daytime systolic pressure) and the initial exposure to high flow 40% CO_2 indicated that both Ntg and Tg mice had a significant increase in blood pressure in response to this challenge (Figure 4-2c and d). This can be attributed as an indirect measure of whole animal adrenergic stimulation during this challenge in both groups. Furthermore, these data indicate that cTnI A164H mice had significantly higher systemic systolic and diastolic arterial pressures during the acidosis challenge compared to Ntg littermates (e.g. delta MAP [Ntg] -81.5 ± 18.4 vs. [Tg] -37.7 ± 6.3 mmHg) (Figure 4-2c, e, and f).

To determine if Tg mice were able to maintain proper sinus rhythm during acidosis we performed continuous telemetered electrocardiographic measurements during a 40 minute hypercapnic acidosis challenge. These data show that both Ntg and Tg mice experienced intermittent extended R-R intervals

Figure 4-2. Radio-telemetry based blood pressure recordings in vivo. (a) Representative raw arterial pressure and heart rate traces recording baseline circadian rhythms from Ntg and Tg mice over the course of five days. (b) Mean systolic arterial pressure (left), diastolic arterial pressure (middle) and heart rate (right) during a given 24 hours of baseline analysis for Ntg (■) and Tg (□) mice. (c) Representative raw pressure traces during forty minutes of exposure to 40% CO_2 for Ntg and Tg mice. (d) The average change in systolic arterial blood pressure at baseline (■) and at the onset of acidosis (□) illustrating the stress response in both Ntg and Tg mice. (e) Mean data for systolic and diastolic arterial pressure measurements between nontransgenic (●) and transgenic (○) mice during the time course of hypercapnic acidosis. (f) The change in mean arterial pressure (MAP) from baseline to the completion of the hypercapnic acidosis challenge for Ntg (■) and Tg (□) mice. Values are expressed as mean ± SEM. 2 way repeated measures ANOVA main effects: time (‡) and genotype (†) $P < 0.05$. 2 way repeated measures ANOVA interaction effects between time and genotype (§) $P < 0.05$. * $P < 0.05$ for Ntg vs. Tg. Ntg, nontransgenic (n=4); Tg, transgenic (n=7).

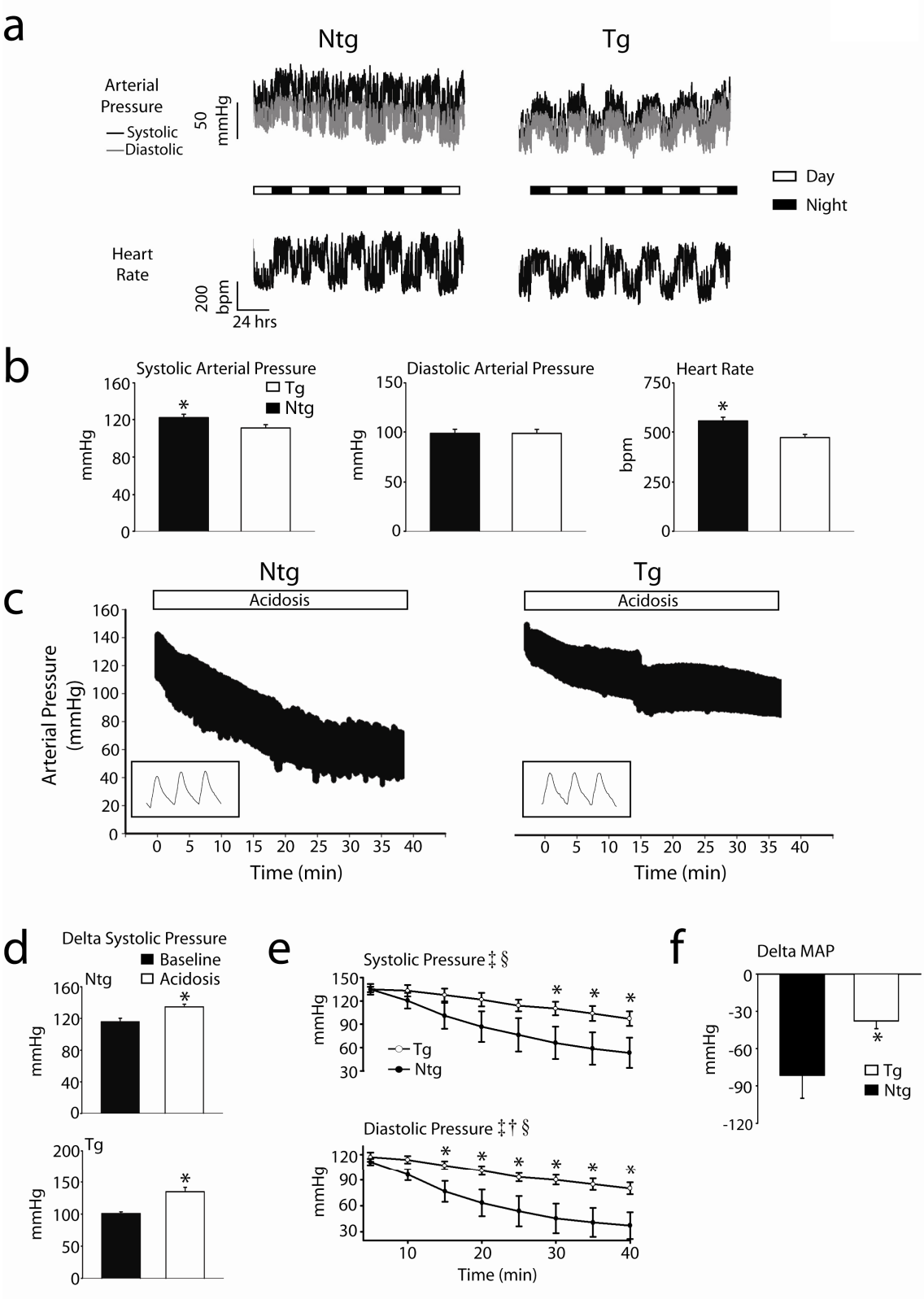
a
Ntg
Tg
Arterial Pressure
Systolic
Diastolic
50 mmHg
Day
Night
Heart Rate
200 bpm
24 hrs
b
Systolic Arterial Pressure
Tg
Ntg
mmHg
Diastolic Arterial Pressure
mmHg
Heart Rate
bpm
c
Ntg
Tg
Acidosis
Arterial Pressure (mmHg)
Time (min)
d
Delta Systolic Pressure
Baseline
Acidosis
Ntg
Tg
mmHg
e
Systolic Pressure ‡ §
Diastolic Pressure ‡ † §
Tg
Ntg
mmHg
Time (min)
f
Delta MAP
mmHg
Tg
Ntg

associated with sinus pause or sinus dysfunction throughout the time course of hypercapnic acidosis (Appendix: Figure 4-8). Overall, there was no difference in the frequency or duration of this episodic sinus dysfunction between Ntg and Tg mice during acidosis (Appendix Figure 4-8b and c). Furthermore, core body temperature and heart rate decreased similarly between Ntg and Ttg mice during prolonged acidosis (Appendix: Figure 4-8d, e). All mice recovered from this forty minute hypercapnic acidosis challenge.

Assessment of cardiac function during β-blockade

To directly assess cardiac hemodymanics, mice were surgically instrumented by implantation of a conductance micromanometry catheter into the LV. After stabilization of cardiac function, baseline measurements were acquired followed by an infusion of esmolol (250 ug/kg/min) to suppress adrenergic involvement in the cardiac response to acidosis. Inferior vena cava occlusions (IVCO) were performed just prior to the start and after five minutes of esmolol infusion to acquire load independent measures of contractility. These data show that during the initial five minutes of esmolol infusion Ntg and Tg mice experienced a slowing of the heart rate, left ventricular cavitary dilation (e.g. increased LV max volume), a slight diminution in measures of contractility (e.g. systolic pressure, + dP/dt, contractility index, ejection fraction, and stroke work) and evidence of marked slowing in diastolic function (increased LVEDP and Tau) (Figure 4-3a,b and Figure 4-4a). However, contractile performance was

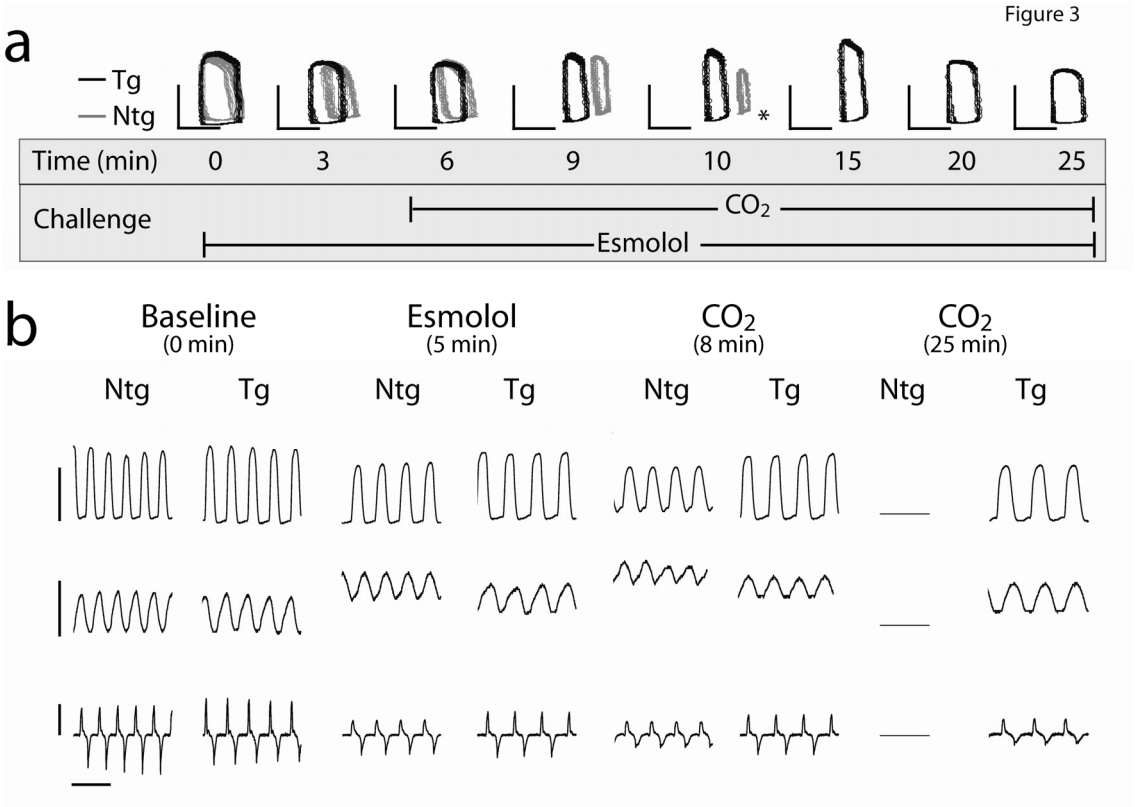

Figure 4-3. Raw data traces of real-time conductance micromanometry during hypercapnic acidosis. (a) Representative raw pressure-volume loops (pressure bar = 60 mmHg, volume bar = 20 uL) of a Ntg (gray) and Tg (black) mouse during the time course of an esmolol plus hypercapnic acidosis challenge (dotted line used as reference point for minimum volume at baseline, * indicates time of death for Ntg mouse). (b) Representative raw traces of pressure (bar = 60 mmHg), volume (bar = 30 uL), and pressure derivatives (bar = 10,000 mmHg/sec) for Ntg and Tg mice at baseline, during infusion of esmolol (5 minutes), at 8 minutes into the acidosis challenge, and at the end of the assay (25 minutes) illustrating changes in cardiac contractility and geometry during the time course of this challenge.

significantly better in cTnIA164H Tg than Ntg mice after five minutes of esmolol infusion based on higher ejection fraction, stroke work, and +dP/dt (e.g. +dP/dt, [Ntg] 4603.7 ± 612 vs. [Tg] 7094.1 ± 545 mmHg/sec, $P < 0.05$) (Figure 4-5a). Intrinsic inotropic function measured from the slope of the end systolic pressure-volume relationship (ESPVR; end systolic pressure: end systolic volume) and preload recruitable stroke work (PRSW; stroke work: end diastolic volume) assessed load independent measures of contractility (acquired by PV loop analysis during IVCO) (Figure 4-5b). This analysis showed a higher pre-load-independent inotropic capacity in Tg mice compared to Ntg mice at baseline and during esmolol infusion. The negative derivative of pressure development (-dP/dt, data not shown), end diastolic pressure (EDp), and tau were not different between Ntg and Tg mice during esmolol infusion, indicating comparable diastolic function between these groups (Figure 4-4a).

Cardiac function and survival during hypercapnic acidosis with β-blockade

We next tested the hypothesis that catecholaminergic stimulation played a significant role in the survival capacity of mice during the acute hypercapnic acidosis challenge. To address this, cardiac function was assessed during acute acidosis without β-adrenergic responsiveness. Mice were instrumented with a conductance micromanometry catheter and infused with esmolol for five minutes (as described above) and then exposed to 40% CO_2 for twenty minutes with the

Figure 4-4. Summary of real-time in vivo hemodynamic data. (a) Summarized mean data showing changes in cardiac functional and geometric parameters including systolic pressure, end diastolic pressure, the positive derivative of pressure development (+dP/dt), contractility index, ejection fraction, max volume, tau, heart rate, and stroke work between Ntg (●) and Tg (○) mice during the time course of esmolol infusion and acute hypercapnic acidosis. (b) Representative raw data (derived from 5 sec. averages) of ESp, EF, maximum volume, and tau during 20 minutes of esmolol plus acidosis showing transgene enhancement (light gray) of cTnI A164H. Values are expressed as mean ± SEM. Ntg, nontransgenic (n=6); Tg, transgenic (n=7).

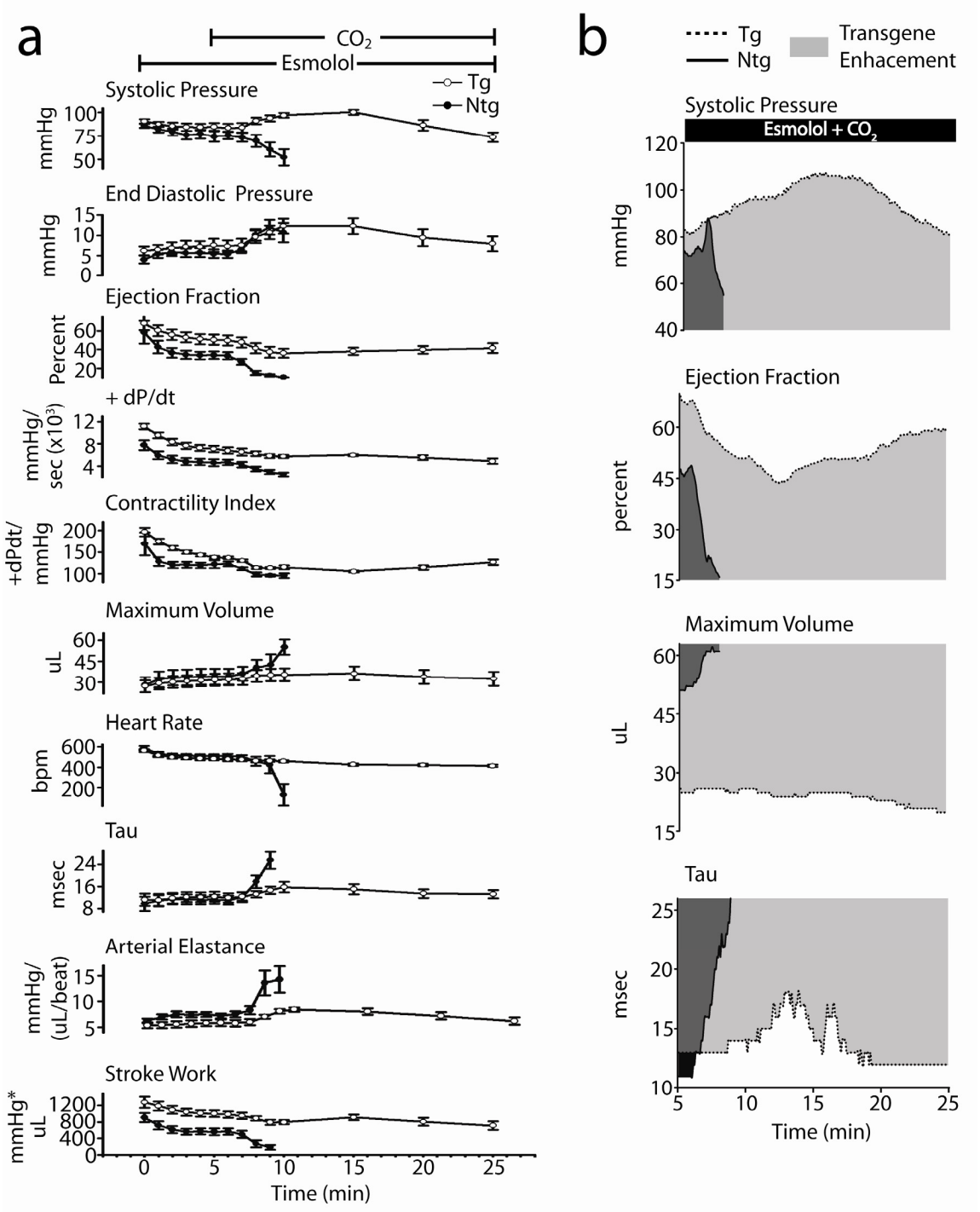
a
CO2
Esmolol
Tg
Ntg
Systolic Pressure
mmHg
End Diastolic Pressure
Ejection Fraction
Percent
+ dP/dt
mmHg/ sec (x10³)
Contractility Index
+dPdt/ mmHg
Maximum Volume
uL
Heart Rate
bpm
Tau
msec
Arterial Elastance
mmHg/ (uL/beat)
Stroke Work
mmHg* uL
Time (min)
b
Tg
Ntg
Transgene Enhacement
Systolic Pressure
Esmolol + CO2
mmHg
Ejection Fraction
percent
Maximum Volume
uL
Tau
msec
Time (min)

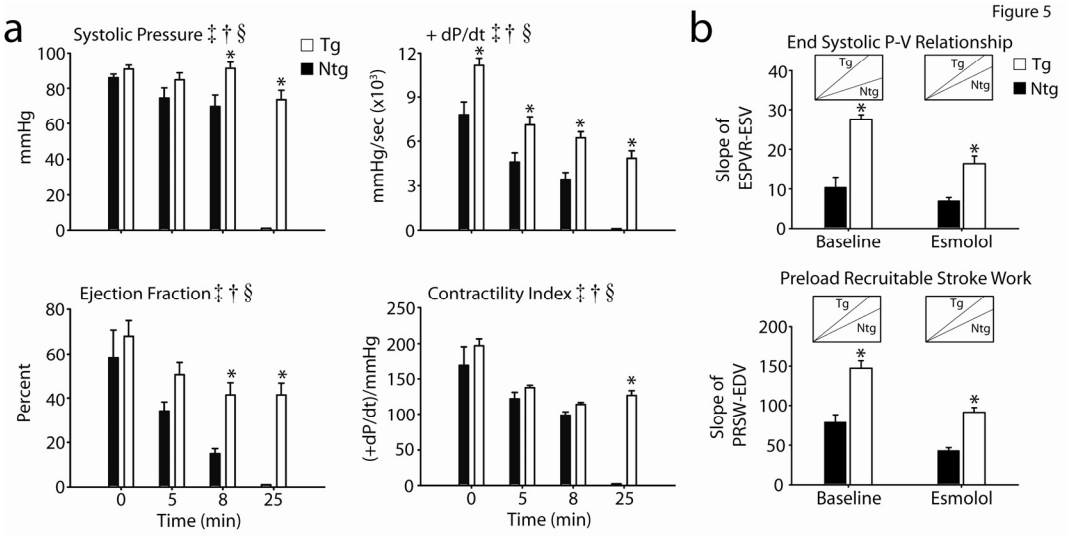

Figure 4-5. Hemodynamic analysis of inotropic function during esmolol and acidosis. (a) Mean data extracted at baseline, at five minutes after esmolol infusion, at 8 minutes into the acidosis challenge, and at the end of the protocol (25 minutes) showing a significant difference between Ntg (■) and Tg (□) mice based on contractile properties including systolic pressure, +dP/dt, ejection fraction, and contractile index. (b) Load independent measures of contractility acquired by inferior vena cava occlusions (ICVO) including end systolic pressure volume relationship (ESPVR) and preload recruitable stroke work (PRSW) showing the difference between Ntg (■) and Tg (□) mice at baseline and during infusion of esmolol. Inset boxes show representative slopes for Ntg and Tg mice. Values are expressed as mean ± SEM. 2 way repeated measures ANOVA main effects: time (‡) and genotype (†) $P < 0.05$. 2 way repeated measures ANOVA interaction effects between time and genotype (§) $P < 0.05$. * $P < 0.05$ for Ntg vs. Tg. Ntg, nontransgenic (n=6); Tg, transgenic (n=7).

esmolol infusion continuing to the completion of the challenge. By pressure-volume analysis, at the onset of respiratory hypercapnic acidosis Ntg mice underwent precipitous cardiac decompensation within the first five minutes of acidosis (Figures 4-3a and b). In terms of inotropic function, this decline in cardiac performance was characterized by a sudden decrease in systolic pressure, ejection fraction, contractility index, and stroke work (Figure 4-4 and Figure 4-5a). Furthermore, diastolic dysfunction emerged during the onset of acidosis (increased LVEDP and tau) together with further dilation of LV chamber geometry (Figure 4-4).

In marked contrast, Tg mice, showed sustained cardiac function during this respiratory hypercapnic acidosis challenge even in the absence of β-adrenergic support (Figure 4-3a and b). These data represent a transgene enhancement effect on the part cTnI A164H mice which contributes to their survival capacity compared to Ntg mice (Figure 4-4b). More specifically, Tg mice actually increased their developed pressure, made evident by an immediate increase in end systolic pressure and, more modestly, the positive derivative of pressure development (+dP/dt) and stroke work (Figure 4-4a,b and Figure 4-5a). This was sustained until the latter phases of acidosis when LV ESp decreased to slightly below baseline values together with a drop in the +dP/dt and stroke work (Figure 4-4a, b and Figure 4-5a).

Other hemodynamic parameters of cardiac function for Tg mice in this group showed an initial decrease during the onset of acidosis followed unexpectedly by a recovery toward baseline values during the latter stages of

acidosis (Figure 4-4, and Table 4-1). Similar to the echo data, Table 4-1 shows the restoration in function at the end of the challenge compared to measurements taken at the beginning and at the nadir for parameters derived by hemodynamic analysis. These measurements reveal that function at the end of the challenge was not significantly different than baseline in Tg mice. During the onset of acidosis, measures of contractility decreased initially but returned toward baseline during the latter phases of acidosis (e.g. from the nadir contractility index increased by 21.1 ± 26.5 U) (Figure 4-4a, Figure 4-5a, and Table 4-1). The contractility index (CI) is defined as the positive pressure derivative (+dP/dt) normalized to the ventricular pressure at that point. Taking this into consideration, this change in CI is understood as the maintenance of the positive pressure derivative despite decreases in the ESp during acidosis suggestive of an overall increase in contractility during this challenge. Diastolic function also increased initially but returned to baseline values by the end of the challenge (e.g. from the nadir LVEDp decreased in Tg mice 4.4 ± 0.8 mmHg) (Figure 4-4 and Table 4-1). Similarly, ventricular dilation occurred at the onset of acidosis followed by a restoration of the ventricular chamber geometry during the latter phases of hypercapnia (e.g. max volume decreased from the nadir in Tg mice 3.8 ± 1.2 uL) (Figure 4-4a and Table 4-1). In all cases, the absolute change between the nadir and the end of the challenge for parameters given in Table 1 were different from zero based on a Dunnet's analysis showing a recovery of hemodynamic function *during* acidosis in Tg mice. However, in stark contrast to the functionality of Tg mice throughout this challenge, the lowest point for Ntg

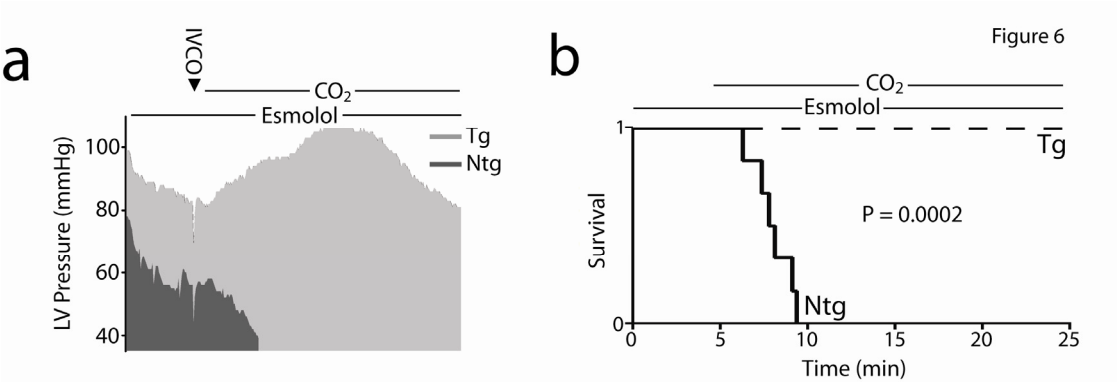

Figure 4-6. Survival data during respiratory hypercapnic acidosis. (a) Representative raw data (derived from 5 sec. averages) for ESp over the full time course of the experimental protocol including esmolol infusion followed by CO_2 ventilation for Ntg and Tg mice. (b) Survival curve showing the time of death for Ntg mice which occurred after the onset of ventilation with 40% CO_2 compared to the 100% survival of Tg mice after 25 minutes of exposure to this challenge. Ntg, nontransgenic (n=6); Tg, transgenic (n=7).

mice was at the time of death (Table 4-1). When assessed for survival, cTnI A164H mice show a significant transgene-mediated enhancement of cardiac function while Ntg mice develop severe cardiac dysfunction and death in response to hypercapnic acidosis induced with β-adrenergic blockade. The 100% survival of Tg mice compared to 100% mortality in Ntg mice within 5 min of the onset of CO_2 is a striking indicator of the improved inotropy caused by this amino acid substitution (Figure 4-6a and b).

Discussion

Cardiomyopathies associated with myocardial acidosis can result in profound systolic and diastolic dysfunction. Understanding mechanisms associated with protecting cardiac pump performance during acidosis are important in developing therapies. This study reveals whole animal responses in transgenic mice expressing a single histidine modified cardiac TnI during acute respiratory hypercapnic acidosis. During hypercapnia cTnI A164H mice had a significantly greater capacity for maintaining cardiac geometry and function during acidosis compared to Ntg. Furthermore, in the absence of catecholaminergic support, Tg mice showed markedly improved survival versus Ntg mice. This outcome resulted from the ability of Tg mice to maintain significantly higher intrinsic cardiac function without compromising diastolic performance compared to Ntg mice. Among studies seeking to preserve pump function in disease [246, 301, 318], results from the present study show a unique

response of improved systolic *and* diastolic performance during acidosis *in vivo*. Overall, the results of this study illustrate that molecular manipulation of myofilament performance by means of a histidine button engineered into the switch region of cTnI results in significant protection of cardiac geometry and function, and improved survival in the context of severe respiratory hypercapnic acidosis *in vivo*.

Myofilament calcium sensitivity and acidosis

Elevated plasma CO_2 occurs in numerous pathophysiological contexts such as severe COPD[448], conditions of hypercarbic respiratory failure[449], respiratory infections[450], or congenital central hypoventilation syndrome[451]. A fundamental consequence of even modest decreases in pH results in the *uncoupling* of excitation-contraction (E-C) events which are necessary for the tight regulation of beat to beat pump activity in the heart[134, 237]. At the sub-cellular level E-C uncoupling is made evident by an acidosis-induced reduction in force generating capacity by the sarcomere for any given $[Ca^{2+}]_i$. Acidosis decreases both maximal Ca^{2+}-activated tension and the Ca^{2+} sensitivity of tension [236, 246, 249-252]. Acidosis also decreases myocyte maximal sarcomere length shortening amplitude and shortening velocity[246, 253, 254]. These experiments illustrate that myofilament Ca2+ desensitization at low pH is a fundamental molecular deficiency responsible for cardiac organ pathologies associated with myocardial acidosis[242]. Importantly, results from this study demonstrate that cTnI A164H

works effectively to prevent this Ca^{2+} desensitization and provides a survival benefit to respiratory acidosis in an intact animal model.

Adrenergic blockade and cTnI A164H performance

Sympathetic stimulation increases cardiac inotropy and lusitropy. It has been shown that rodent hearts are under high β-adrenergic tone under baseline conditions[246, 318]. This may mask cardiomyopathies associated with alterations in myofilament calcium handling[442]. Consequently, we addressed the role played by β-adrenergic signaling using a beta blocker, esmolol, during hemodynamic analysis to determine the intrinsic systolic and diastolic properties of the cTnI A164H heart. Importantly, we found load-independent measures of contractility were significantly higher in Tg versus Ntg mice under β-blockade, suggesting a higher intrinsic capacity for contractile function at baseline on the part of cTnI A164H Tg mice. Importantly, hemodynamic measurements obtained in this study demonstrate the first evidence that cTnI A164H mice can maintain cardiac function during acidosis *in vivo*.

Although enhanced systolic function is expected with this model, diastolic function (e.g Tau, EDp) can be problematic for Tg mouse models expressing altered myofilament proteins. For example, calcium sensitizing models show diastolic dysfunction such as cTnI R193H[333], cTnT R92Q[371], and ssTnI mice in vivo [213]. Importantly, this study shows that, in the absence of sympathetic activity,

baseline diastolic function of cTnI A164H Tg mice is not different from the Ntg cohort.

cTnI A164H: a titratable myofilament inotrope

Multiple investigators have proposed that targeting myofilament calcium responsiveness via manipulation of TnC and TnI interactions is desirable for protecting cardiac function during acidosis[246, 249, 297, 301, 318, 435, 452]. However, previous approaches have found that enhancement of systolic function often concomitantly results in diastolic dysfunction, as discussed above. For example, Tg mice expressing ssTnI show improved cardiac function during acidosis[318]. However, they also show significant diastolic dysfunction during this challenge[213, 318], and more generally, these hearts lack the ability to modulate TnI function via PKA activation by β-adrenergic signaling. Pharmacologic alterations of the myofilament using TnC Ca2+ sensitizers such as levosimendan also improve inotropy[289, 299-301] but have significant non-TnC actions. In contrast, the present study now shows that cTnIA164H is capable of improving myofilament function in response to acidosis, without concomitant diastolic dysfunction, alterations in β-adrenergic signaling, or non-specific effects on myocyte function.

The underlying biochemistry of a histidine button engineered into TnI provides insights into potential mechanisms supporting this concept. Specifically, histidine ionizes near physiological pH with a pK_R around 6.0. Consequently, under mildly acidic conditions the increasing propensity for the ionization of

histidine changes the biochemical function of surrounding residues and any interactions mediated by this region of the protein. In cardiac troponin I, this histidine substitution (A164H) is positioned in the regulatory domain between the amphiphilic switch region (helix 3) and the C-terminal actin binding domain (helix 4). Previous studies have shown that this region is critically involved in the interaction between TnI and TnC during systole through the electrostatic binding of the switch region of TnI with the calcium saturated N-terminal hydrophobic patch of TnC[52, 96-98, 327]. Although further studies are required to address the specific biophysical consequences of these potential interactions, the physiological implications of this histidine modification have been studied by this and other studies[246] showing that cTnI A164H acts as a molecular rheostat maintaining systolic and diastolic pump function in models of severe acidosis and ischemic cardiomyopathy *in vitro* and *in vivo*.

This study contributes new evidence showing a potential therapeutic role of cTnI A164H in the heart. Specifically, evidence from these experiments demonstrate a marked transgene enhancement effect that confers protection from acidosis-induced pump failure and death in living animals. We hypothesize that this response is mediated foremost by the underlying biochemistry of the histidine modified cTnI acting as a molecular rheostat of the intracellular milieu. This study contributes to the growing evidence that histidine-modified troponin I is an effective target protein for the protection of cardiac performance during severe acidosis *in vivo*.

Acknowledgements

We thank Dr. Robert Bartlett for generous use of his blood gas analysis machine and Dr. Terry Major for assistance with analysis of blood gas parameters. Drs. Margaret Westfall and Sharlene Day provided invaluable insight into the development of this manuscript. We also thank Steven Whitesall for his assistance with telemetered mice and Kimber Converso for her expert murine echocardiography measurements. This work was supported by grants from the NIH (JM) and the American Heart Association (NP).

Appendix

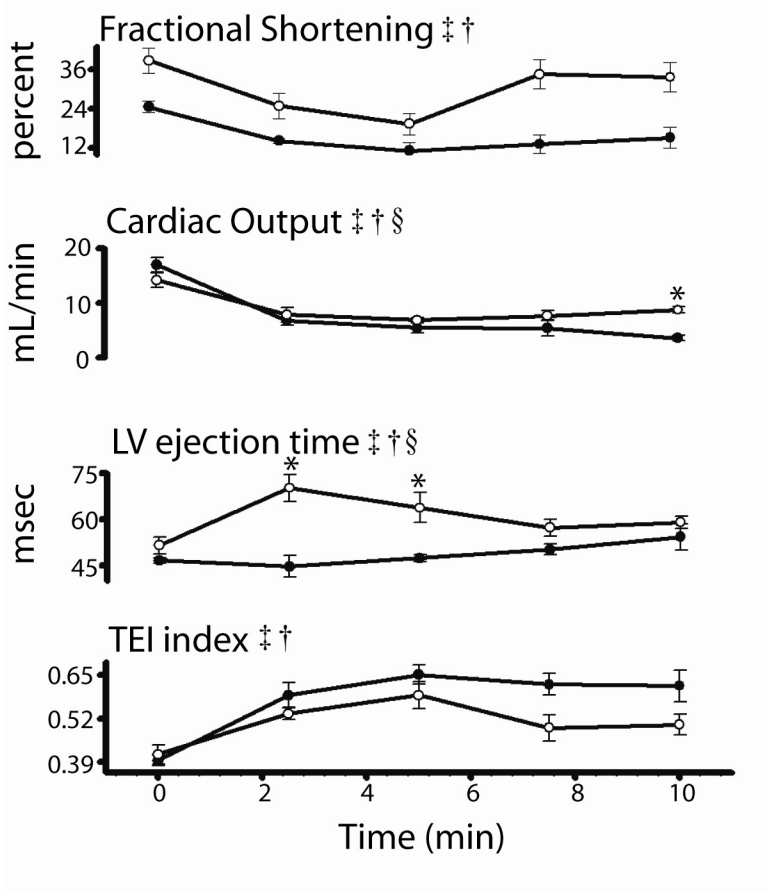

Figure 4-7. Mean data showing cardiac function by echocardiography at baseline and during hypercapnia. Summarized mean data showing changes in cardiac functional parameters including fractional shortening, cardiac output, LV ejection time, and TEI Index between Ntg (●) and Tg (○) mice during the time course of hypercapnic acidosis. Values are expressed as mean ± SEM. 2 way repeated measures ANOVA main effects: time (‡) and genotype (†) $P < 0.05$. 2 way repeated measures ANOVA interaction effects between time and genotype (§) $P < 0.05$. * $P < 0.05$ for Ntg vs. Tg. Ntg, nontransgenic (n=5); Tg, transgenic (n=7).

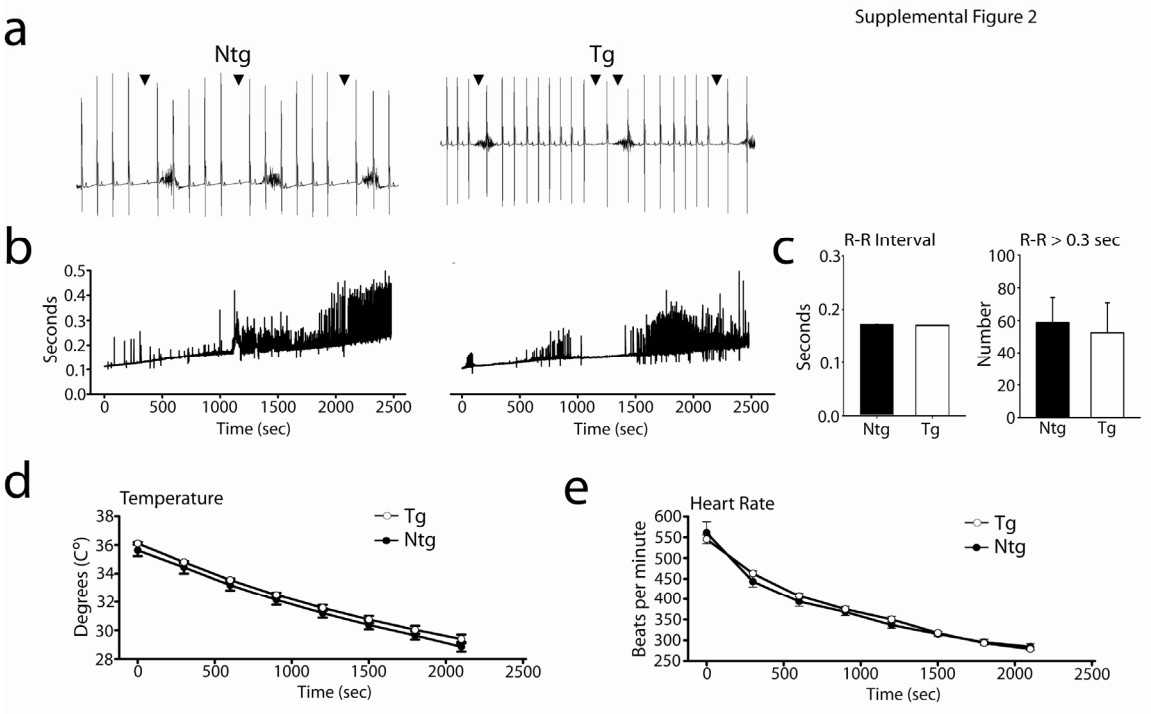

Figure 4-8. Continuous *in vivo* radio-telemetry ECG measurements during a prolonged hypercapnic acidosis challenge. (a) Representative raw ECG tracings extracted during the final five minutes of the acidosis challenge showing arrhythmias in both Ntg and Tg mice. (b) Representative graphs showing the R-R interval as a measure of time during the forty minute acidosis challenge for Ntg and Tg mice. (c) Distribution and average R-R interval (left) and number of R-R intervals greater than 0.3 sec (right) during the acidosis challenge for Ntg (■) and Tg (□) mice. (d and e) The change in body temperature (d) and heart rate (e) during the time course of hypercapnic acidosis. Values are expressed as mean ± SEM. Ntg, nontransgenic (n=5); Tg, transgenic (n=5).

Chapter V

pH responsive titratable inotropic performance of histidine-modified cardiac troponin I attributed to imidazole ionization

Abstract

Cardiac troponin I (cTnI) functions as the molecular switch of the thin filament. At the level of the sarcomere, cTnI regulates inotropic capacity during systole by engaging with the calcium saturated N-terminal lobe of cTnC and thus permitting actomyosin cross bridge formation. Acidosis significantly attenuates contractility causing severe cardiomyopathy at the whole organ level. However, studies have shown that a histidine button engineered into cTnI therapeutically protects ionotropic function in the context of numerous pathophysiological challenges. This study provides a molecular mechanism for this observation. **Methods** The role of ionization was analyzed by studying myofilament calcium sensitivity and sarcomere shortening kinetics of arginine substituted cTnI (A164R), a biochemical correlate to the protonated histidine. Atomic resolution molecular dynamics (MD) simulations of WT cTnI as well as cTnI A164H in different ionization states were also performed. **Results** Under physiological conditions, cTnI H164 is deprotonated (pK_a = 6.14) and behaves functionally and structurally similar to WT cTnI. Newly observed intermolecular electrostatic

interactions (cTnI R163: cTnCE19/D25) as well as hydrophobic side chain contacts are involved in regulating cTnI function at baseline. Under acidic conditions, cTnI A164H has similar function compared to the constitutively protonated cTnI A164R variant. Consistent with this, MD simulations indicate that a single proton added to the imidazole side chain of cTnI H164 results in a translocation of cTnI H4 toward cTnC resulting in added intermolecular electrostatic (cTnI R163: cTnC D25 and cTnI H164: cTnC E19) and hydrophobic side chain interactions (cTnI L170: cTnC A22). **Conclusion** These data indicate that differential histidine ionization is required for cTnI A164H to act as a molecular rheostat capable of therapeutically modulating sarcomere performance in response to changes in the cytosolic milieu.

Introduction

Cardiac contraction and relaxation occur through the rhythmic interactions of the thin and thick filaments of the sarcomere. The key allosteric regulatory complex that mediates the transition between the systolic and diastolic phases of the cardiac cycle is troponin. Troponin is a heterotrimeric protein complex comprised of three subunits. These include the tropomyosin binding subunit, troponin T (TnT), the calcium binding subunit, troponin C (TnC), and the actomyosin ATPase inhibitory subunit, troponin I (TnI)[49, 50]. As originally proposed by Herzberg and colleagues[63, 153], calcium binding fundamentally changes the structure of TnC from the apo “closed” conformation, its

thermodynamic nadir, to the calcium saturated “open” conformation. With the change in the structure and biochemistry of the calcium-bound N-terminal region of TnC, the switch arm of TnI develops an affinity for TnC measured as an increase of two orders of magnitude[158]. This increased affinity causes a translocation of the entire regulatory arm of TnI and binds with TnC by multiple van der Waals contacts[52, 161]. During diastole, calcium is re-sequestered into the sarcoplasmic reticulum causing its dissociation from the TnC EF hand. TnI subsequently releases TnC and binds actin both at the inhibitory region (IR) and the C-terminal region. This initiates diastole by inhibition of actin-myosin cross bridge formation. With this important role in differentially toggling between actin and TnC and thus regulating cross-bridge cycling events, TnI has come to be known as the molecular switch of the myofilament[9].

Studies using acutely isolated adult rat myocytes have shown that myofilament sensitivity to activating calcium is markedly diminished during acidosis[133]. These reports show that the pCa (-log[Ca^{2+}]) required for 50% activation of myofilaments in acutely isolated adult cardiac myocytes drops during acidification of pH (from pH 7.0 to 6.2)[133]. Decreases in myocyte maximal sarcomere length shortening amplitude and shortening velocity are also found to occur during acidosis[246, 253, 254]. These experiments illustrate that myofilament Ca^{2+} desensitization at low pH is a fundamental molecular maladaptation responsible for myocyte and cardiac organ pathologies associated with myocardial acidosis[242].

Importantly, numerous studies have shown that a unique histidine moiety in the regulatory arm of TnI (ssTnI H132 and cTnI A164H) acts as a pH-dependent titratable inotrope capable of ameliorating contractile deficiencies caused by acidosis *in vitro*[133, 246] and *in vivo*[203, 246, 290]. These reports show that a histidine button in cardiac TnI functions as a molecular rheostat with no significant contractile effects at baseline but marked enhancement of inotropic performance under various pathophysiological stresses including acute and chronic myocardial ischemia and acidosis[203, 246, 290].

The switch mechanism of histidine buttons play a critical role in mediating key functions in numerous molecules by altering intramolecular and intermolecular structures and interactions. This property has been well studied in hemoglobin, for example, where H146β appears to mediate the Bohr affect by altering its pH dependent intramolecular interaction with D94β[303, 326]. Numerous other histidine buttons have been identified in molecules including HLA-DR molecules[306], GABA ρ1 receptors[364], the pacemaker channel HCN2 (H321)[309], the acid sensitive potassium channel TASK-3 (H98)[310], the inward rectifying potassium channel HIR (H117)[308], and the G-protein-coupled inward rectifying potassium channel (GIRK1/GIRK4)(H64, H228, and H352)[307].

The chemical nature of histidine and its pH responsive binary ionization states make it unique among all of the amino acids as capable of mediating the so-called “switch function” of these pH responsive buttons. The differential ionization of histidine within the physiologic range is principally due to its unique imidazole side chain which has a pK_a around 6.0. The non-protonated histidine is

hydrophobic and aromatic in character whereas the protonated histidine is hydrophilic and positively charged.

The implications of histidine ionization on cardiac troponin I structure and function have not been investigated. Numerous strategies involving site directed protein mutagenesis have been employed in previous studies analyzing the molecular mechanism of histidine buttons in other molecules[303, 306, 308, 310, 326]. Here, we studied the functional implications of arginine (cTnI A164R) as a biochemical mimic of the protonated histidine compared to contractile dynamics of WT cTnI (A164) and cTnI A164H. Atomic resolution *in silico* molecular dynamics (MD) simulations were also used to analyze the implications of the ionization state of histidine's imidazole side chain on structural engagement with cTnC in the calcium saturated state. This study provides evidence that structural changes caused by differential imidizole side chain ionization are a necessary and sufficient molecular basis for titratable inotropic performance of histidine-modified cardiac troponin I.

Methods

TnI mutagenesis and viral vector construction. We used a pDC315 vector containing cTnI and the QuikChange mutagenesis kit (Stratagene) to generate site directed mutagenesis. As previously described[246], the primers used for mutagenesis of cTnI to cTnIA164H FLAG removed an Xma1 site and were 5'-ggcactactggggacccggcacaaggaatccttggacctg-3' (sense) and 5'-

caggtccaaggattccttgtgccgggtccccagtagtgcc-3' (antisense). Mutagenesis of cTnI A164R FLAG and cTnI A164Y FLAG were generated from the cTnI A164H FLAG cDNA. Primers used for mutagenesis from cTnI A164H FLAG to cTnI A164R FLAG were 5'- GCACTACTGGGGACCCGGCGCAAGGAATCCTTGG-3' (sense) and 5'- CCAAGGATTCCTTGCGCCGGGTCCCCAGTAGTGC -3' (antisense). Primers used to mutagenesis from cTnI A164H FLAG to cTnI A164Y FLAG were 5'-GCACTACTGGGGACCCGGTACAAGGAATCCTTGG-3' (sense) and 5-CCAAGGATTCCTTGTACCGGGTCCCCAGTAGTGC-3' (antisense). In all cases, primers were extended using Pfu DNA polymerase and methylated parental DNA was subsequently digested with Dpn I. DNA was transformed into competent bacterial cells. Mutated DNA with appropriate restriction enzyme sites was sequenced prior to ligation of mutant cTnI cDNA into Ad5 viral shuttle vectors. All DNA sequences were verified by overlapping sequence runs. The cTnI FLAG vector was produced and used as previously described[453] and used here as control for viral transduction and the FLAG epitope. Recombinant vectors were produced and purified as described previously[454]. The cTnI A164Y mutant did not provide any additive insight into the current data set and so results are not shown.

Ventricular myocyte isolation, gene transfer, and primary culture Rat ventricular myocytes isolation was performed as previously described[24, 290, 333]. Briefly, rats were anaesthetized by inhalation of isoflurane followed by i.p. injection of heparin (1500 U/kg) and Nembutal (162.5 U/kg). Following enzymatic

digestion by retro-grade perfusion with collagenase and hyaluronidase and gentle mincing of the cardiac ventricles, cardiac myocytes were plated on laminin-coated glass coverslips ($2x10^4$ myocytes/coverslip) and cultured in M199 media (Sigma, supplemented with 10 mmol/L glutathione, 26.2 mmol/L sodium bicarbonate, 0.02% bovine serum albumin, and 50 U/ml penicillin-streptomycin, with pH adjusted to 7.4, as described previously[426]). Recombinant adenovirus was applied to the cells immediately after plating as previously described[24]. Cells were subsequently cultured for four days to provide sufficient time for stoichiometric replacement of troponin I proteins delivered by adenoviral gene transfer (Figure 2).

Immunoblot detection Myocytes were removed from cover slips using Laemmli sample buffer. Proteins were separated by SDS-PAGE and transferred to a nitrocellulose membrane for immunodetection. After blocking in 5% milk (in Tris-buffered saline), membranes were probed with a pan troponin I antibody (MAB1691, Chemicon). Indirect immunodetection was carried out using a fluorescently labeled secondary antibody (Rockland, IRDye 680 conjugated affinity purified; 1:5000). Western blot analysis was accomplished using the infrared imaging system, Odyssey (Li-Cor, Inc.) and images analyzed using Odyssey software v. 1.2.

Indirect expression and incorporation by immunofluorescence and confocal microscopy Dual labeling immunofluorescence was performed as

previously described[9]. Briefly, cultured cardiac myocytes were fixed in 3% paraformaldehyde/PBS and blocked in 20% normal goat serum (NGS). Myocytes were incubated in the first primary antibody directed against the Flag epitope (M2, 1:500, Sigma) and detected with an Alexa 488-conjugated secondary antibody directed against mouse IgG (1:100, Molecular Probes). Myocytes were incubated in the second primary antibody directed against α-actinin (EA53, 1:500, Sigma) and detected with Texas Red-conjugated secondary antibody directed against mouse IgG. All antibodies were diluted in 2% NGS + 0.5%Triton X-100/PBS. Immunofluorescence was visualized on a Zeiss Axioskop LSM 510 laser scanning confocal microscope.

Contractility measurements in single myocytes Sarcomere length shortening and relaxation kinetics were performed as previously described[24, 290]. Briefly, cover slips containing single isolated myocytes were placed on an inverted microscope (Nikon, Eclipse TE2000) and stimulated at 0.2 Hz. The chamber's temperature was maintained at 37°C. Myocyte images were collected (240Hz) using a CCD camera (MyoCam, IonOptix). Myocytes that did not follow the pacing protocol (0.2Hz) were excluded, as were myocytes with a resting sarcomere length less than 1.70 μm. Sarcomere length shortening and relaxation kineitics were calculated using IonOptix software. Myocytes were initially analyzed under baseline conditions in M199 (pH 7.4). To understand the changes in myocyte performance during exposure to acidosis, myocytes were subsequently incubated with acidic M199 (pH 6.2). Since control (non-

transduced) and cTnIFLAG transduced myocytes had no functional difference in sarcomere contractile kinetics the data were combined into the control dataset. The summary data for myocyte kinetics are outlined in Supplemental Table 1.

Skinned myocyte tension pCa measurements Single rod-shaped cardiac myocytes were attached to micropipettes coated in silicone adhesive and permeabilized in 0.2% Triton X-100 for one minute. All measurements were made at 15°C in relaxation (RS) or activating solutions (AS). Both RS and AS contained 1mM/L free Mg^{2+}, 4 mM/L MgATP, 14.5 mM/L creatine phosphate, 20 mM/L imidazole, and KCL to yield an ionic strength of 180 mM/L. Solution pH was adjusted to 7.00 (or 6.20 for acidic pH experiments) with KOH/HCl. The pCa (-log[Ca^{2+}]) of the RS was 9.0 and the pCa of maximal AS was 4.0. Sarcomere length was set to 2.1 um and the isometric tension-pCa relation was constructed by measuring the calcium activated isometric tension at basal (pCa=9.0), maximal (pCa=4.0), and various submaximal calcium levels as previously described[246]. Every third contraction was taken at maximal activating calcium concentrations in order to normalize tension values. A non-linear least squares fitting algorithm was used to determine Hill coefficient (n) and pCa_{50}, the calcium concentration at which 50% of maximal tension was produced. Since control (non-transduced) and cTnIFLAG genetically engineered myocytes had no functional difference in steady state isometric tension-Ca^{2+} relationship the data were combined into the control dataset. The summary data for myocyte tension pCa analysis and hill coefficients are outlined in Supplemental Table 2.

Molecular Dynamics Simulation Molecular Dynamics (MD) simulations were performed for the solved X-ray structures of the cardiac troponin complex (PDB:1J1E) using NAMD [353] version 2.6 with CHARMM27 forcefield [354]. The cTn regulatory complex between cTnC and cTnI was isolated by exclusion of all other residues in the crystal structure except cTnI R148 – L173 and cTnC M1 – K90. Residue mutagenesis was performed to substitute cTnI alanine 164 for histidine (cTnI A164H). This histidine was analyzed in the deprotonated state with the hydrogen atom present (cTnI A164H protonated) or removed (cTnI A164H deprotonated) at position NE2 of the imidazole side chain. All the X-ray structures were prepared by CHARMM version c35b1. Each of the complex was solvated with explicit TIP3P water model [355] using a simulation solvent box with a 15 Å buffer region around the protein. Sodium counter ions were placed at 5 Å from the box boundary to neutralize the system. The solvated system was initialized with 5000 steps of conjugate gradient energy minimization with protein heavy atoms restrained at 50kcal/(mol•$Å^2$). The system was then gradually heated with the same restraint from 25K to 300K at 25 K increment at 10 ps interval for 100 ps followed by a 100 ps equilibration with gradual removal of the heavy atoms restraint at 10 ps interval under NVT condition. The final unrestrained equilibration was carried out for 100 ps followed by 20 ns of production simulation at 1 atm and 300K NPT condition. All simulations were carried with periodic boundary condition using Particle Mesh Ewald (PME) [356] with SHAKE [357] method employed to constrain bond lengths involving hydrogen

atoms. The time step in the simulations was 2 fs with coordinates saved at 1-ps time intervals, resulting in a total of 20,000 configurations for analysis.

Interatomic distance calculations All distances were measured in angstroms over the 40 ns simulations for each of the simulated trajectories. For the simulations of the cTnI-cTnC complex involving wild type as well as protonated and deprotonated cTnI A164H, the following distances were evaluated: (1) cTnI R163 HH22:cTnC D25 OD1, (2) cTnI R163 HH22:cTnC E19 OE1, (3) cTnI H164 HD1:cTnC E19 OE2, and (4) cTnI L170 CD2:cTnC A22 CB.

Theoretical pK_a calculations of cTn molecular dynamics structures The starting structures (frame 1) of the simulated cTnI A164H (protonated and deprotonated):cTnC complex were analyzed for determination of the theoretical residue ionization titration curve. Analysis was accomplished as previously described and implemented on the Virginia tech H++ server[347-352]. Calculation was derived using the following inputs: salinity = 0.15; internal dielectric = 10; external dielectric = 80; structure protonation assuming pH = 7.2. Calculated by the Poisson Boltzmann method.

Statistics All results are expressed as mean ± SEM. Multi-group comparisons were assessed using two way analysis of variance (ANOVA) with Newman Keuls post-hoc test with $P < 0.05$ considered statistically different.

Results

Stoichiometric incorporation of TnI into myocytes after adenoviral gene transfer

Acute genetic manipulation of adult cardiac myocytes can be accomplished by adenoviral gene transfer. Recombinant adenoviruses were generated containing various troponin I genes to achieve synchronous and efficient genetic modification of adult cardiac myocytes. Over-expression of exogenously delivered myofilament proteins causes dose dependent competitive replacement of endogenous proteins as shown previously[24, 133, 246, 290]. In this study, adenoviral gene transfer of specific TnI genes (WT cTnI, cTnI A164H, and cTnI A164R) was performed in order to assess the functional implications of specific TnI proteins in the context of the adult rat cardiac myocyte. Beginning at day one, stoichiometric replacement of endogenous cTnI by AdTnI could be detected by western blot (Figure 5-1a). AdTnI expression increased progressively until day four after gene transfer at which point genetically modified myocytes showed, in all cases, approximately 80-90% replacement of endogenous cTnI (Figure 5-1a). Laser scanning confocal microscopy using indirect immunoflourescence against the FLAG epitope showed ubiquitous and precise localization of exogenous TnI proteins in the thin filament of the sarcomere (Figure 5-1b).

Figure 5-1. Adenoviral gene transfer of TnI into adult rat cardiac myocytes. (a) Protein expression by western blot showing precise stoichiometric replacement of endogenous TnI by cTnI FLAG, cTnI A164H, or cTnI A164R over the time course of four days of *in vitro* cell culture. (b) Immunofluorescence images showing proper incorporation of cTnI FLAG, cTnI A164H, or cTnI A164R in the thin filament of adult cardiac myocytes after adenoviral gene transfer.

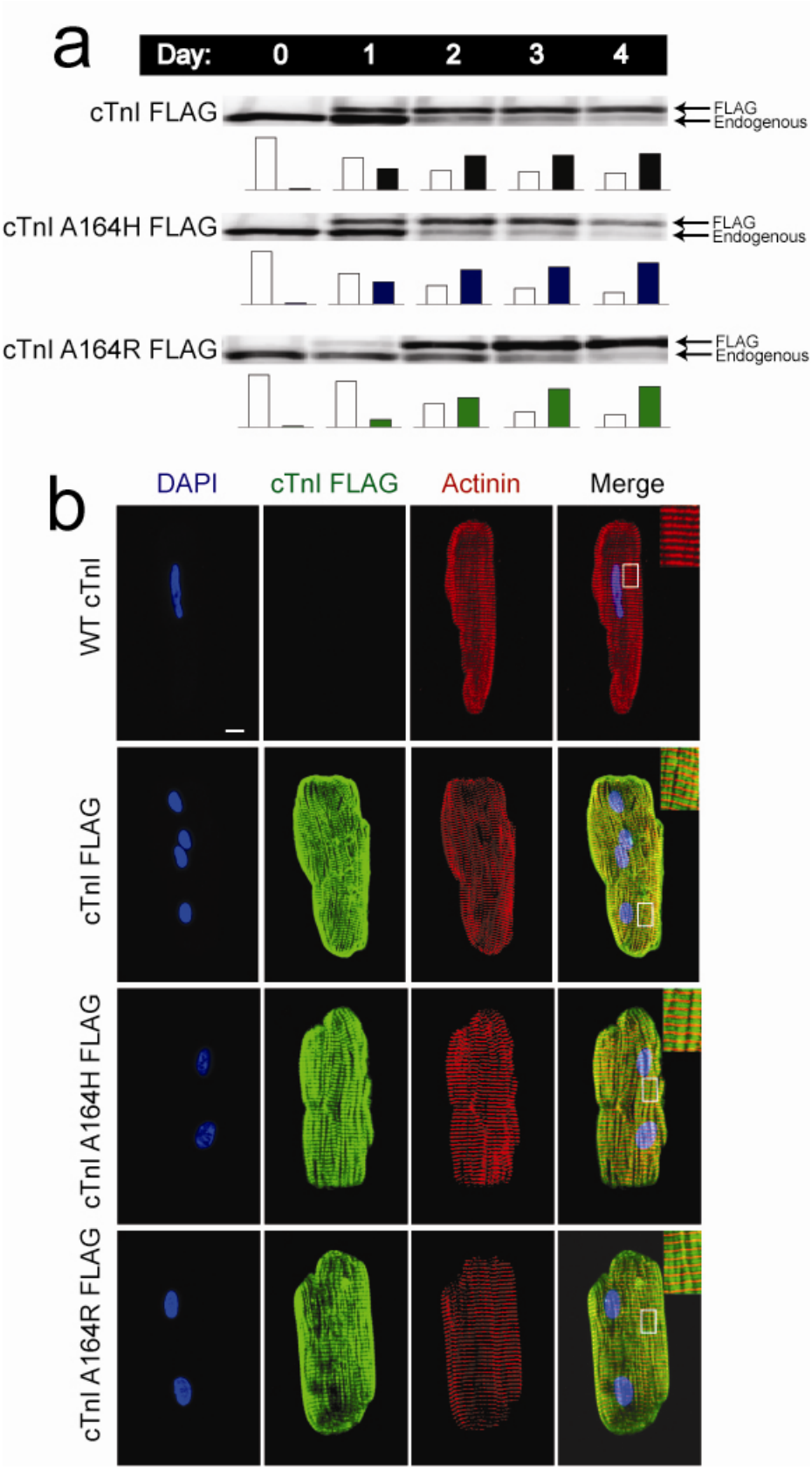
a
Day: 0 1 2 3 4
cTnI FLAG
FLAG
Endogenous
cTnI A164H FLAG
FLAG
Endogenous
cTnI A164R FLAG
FLAG
Endogenous
b
DAPI
cTnI FLAG
Actinin
Merge
WT cTnI
cTnI FLAG
cTnI A164H FLAG
cTnI A164R FLAG

Myocyte sarcomere function at baseline and acidosis

Dynamic sarcomere length shortening and relaxation kinetics as well as the steady state isometric tension-pCa relationship were analyzed four days after acute adenoviral-mediated gene transfer into isolated single adult rat cardiac myocytes (Figure 5-2a). Measurements were taken under baseline and acidic conditions. As a measure of contractility, calcium activated isometric tension (pCa_{50}) and normalized sarcomere length shortening were used as markers of inotropic performance in the context of WT and TnI modified thin filaments. Baseline analysis of SL shortening and pCa_{50} showed that WT and cTnI A164H modified myofilaments were not different compared to heightened inotropy observed in myocytes expressing cTnI A164R ($P < 0.05$ vs. WT and cTnI A164H) (Figure 5-2b). When myocytes were exposed to acidosis, contractile function of cTnI A164H and cTnI A164R was not statistically different compared to a significantly compromised inotropic capacity observed in WT myocytes ($P < 0.05$ vs. cTnI A164H and cTnI A164R) (Figure 5-2c). The delta change from baseline to acidosis was calculated to determine the net change in inotropy attributable to reduced pH (Figure 5-2d). This data showed that only cTnI A164H had pH-dependent titratable inotropy indicated by the maintenance of contractile function during the pH shift. In contrast, WT cTnI and cTnI A164R were equally affected by the acidosis as seen by a similar decrease in normalized sarcomere length shortening and rightward shift of the pCa_{50} during the pH change.

Figure 5-2. Sarcomere length shortening and tension pCa measurements under physiologic and acidic conditions. (a) Raw traces illustrating the change in sarcomere shortening kinetics between 7.4 and 6.2 for each group (horizontal bar (time) = 0.1 seconds; vertical bar (SL) = 0.1 umeter) (top). Normalized tension-pCa_{50} curves illustrating the change in myofilament calcium sensitivity between 7.0 and 6.2 for each group (horizontal bar (pCa50) = 1 unit) (bottom). (b) Mean values of percent sarcomere length peak height and myofilament calcium sensitivity (pCa_{50}) at baseline. (c) Mean values of percent sarcomere length peak height and myofilament calcium sensitivity (pCa_{50}) during exposure to acidosis. (d) Mean values showing the delta change from baseline to acidosis in terms of sarcomere length shortening as a percent of peak height and (left) myofilament calcium sensitivity (pCa_{50}) (right). For all groups $n > 50$ myocytes from greater than 3 independent myocyte preparations. * $P < 0.05$ compared to all other groups by 1 way ANOVA.

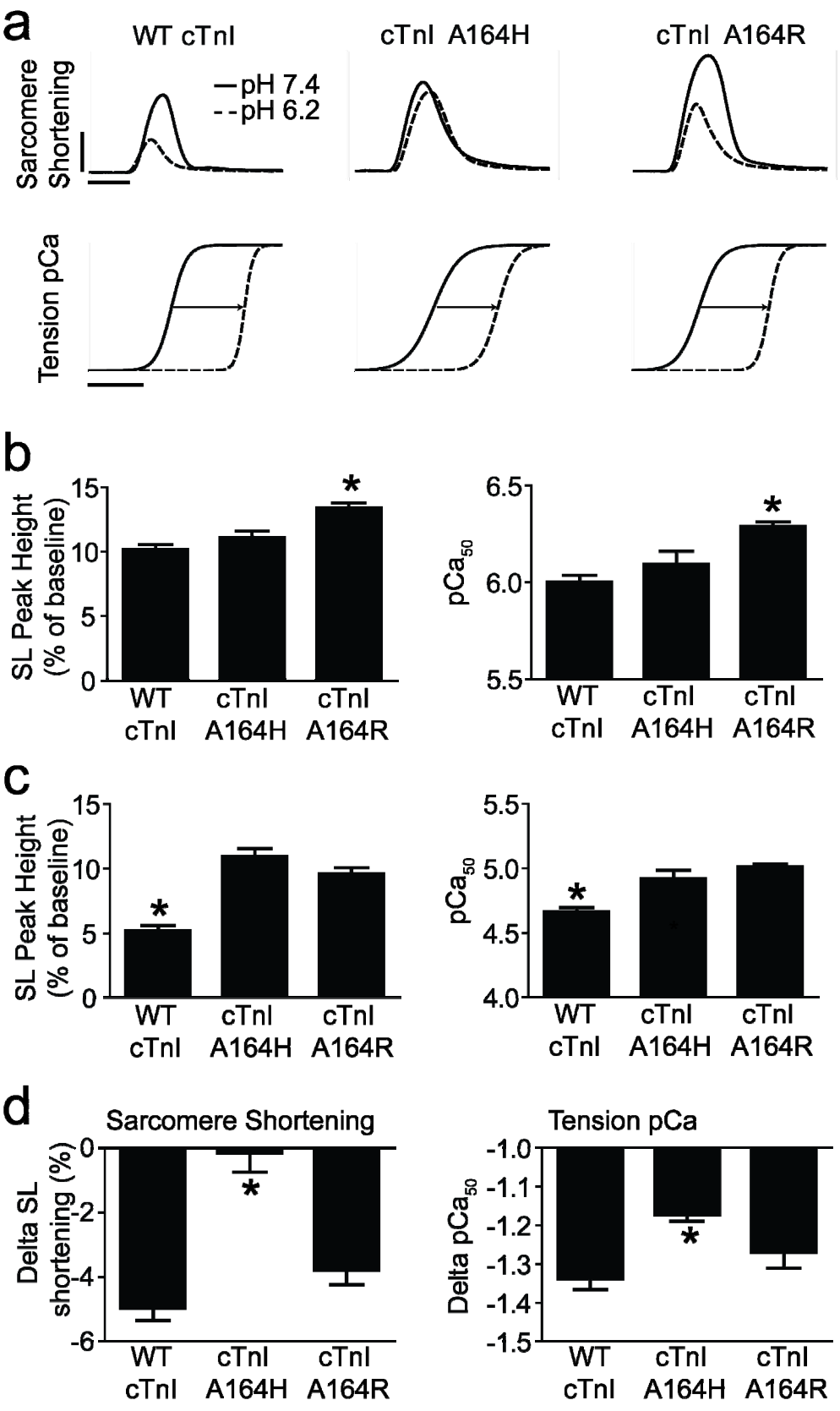
a
WT cTnI
cTnI A164H
cTnI A164R
Sarcomere Shortening
—pH 7.4
--pH 6.2
Tension pCa
b
SL Peak Height (% of baseline)
15
10
5
0
*
WT cTnI
cTnI A164H
cTnI A164R
pCa50
6.5
6.0
5.5
*
c
SL Peak Height (% of baseline)
15
10
5
0
*
pCa50
5.5
5.0
4.5
4.0
*
d
Sarcomere Shortening
Delta SL shortening (%)
0
-2
-4
-6
*
Tension pCa
Delta pCa50
-1.0
-1.1
-1.2
-1.3
-1.4
-1.5
*

Atomic resolution molecular dynamics simulations

To correlate with the *in vitro* inotropic functional analysis the calcium saturated state of the cTn complex[52] was used to provide atomistic insight into the implications of differential ionization of histidine's imidazole side chain on the structural engagement of cTnI:cTnC during systole. This was accomplished by *in silico* protein mutagenesis followed by forty nanosecond molecular dynamics simulations (Figure 5-3a,b and Supplemental movie 4 (WTcTnI:cTnC), movie 5 (cTnI A164H deprotonated: cTnC), and movie 6 (cTnI A164H protonated:cTnC). In addition to the well defined hydrophobic contacts[52, 420], this analysis revealed novel electrostatic interactions at the intramolecular interface of the calcium saturated WT cTn complex (Figure 5-3c, 5- 4a, Supplemental movie 4). Specifically, interatomic distance measurements showed cTnI R163 transiently engaging highly conserved acidic residues decorating the hydrophobic patch in the N-terminal cTnC helix A including E19 and D25 (Figure 5-3c, 5-4a).

Histidine substitution at cTnI residue 164 (cTnI A164H) was subsequently simulated in different protonation states at position NE2 of the imidazole side chain. Theoretical side chain ionization pH titration analysis showed that H164 (protonated or deprotonated) was not affected by close structural electrostatic interactions (cTnI H164: pK_{int} = 6.32, pK_a = 6.14). This indicates that only solvent

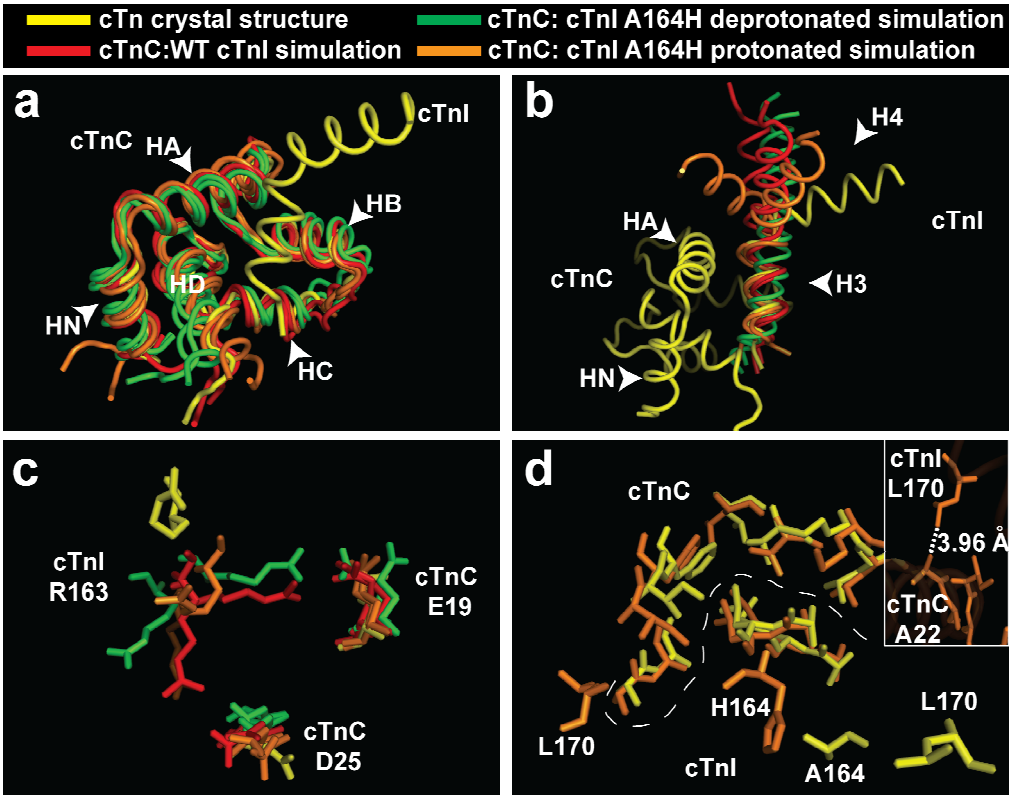

Figure 5-3. Structural analysis of cTn molecular simulations. Simulated structures shown here were extracted at 20 and 40 nanoseconds with reference to the starting cTn structure 1 (yellow). Structural alignments of cTnC (a) and cTnI (b). Helix N-D of cTnC denoted as HN-HD; Helix 3 and 4 of cTnI denoted as H3 and H4. (c) Residue focus on electrostatic interactions during cTn simulations, specifically cTnI R163 interacting with cTnC E19:D25. (d) Residue focus on hydrophobic contacts with emphasis on the interaction between cTnC A22 and L170 in the final structure of the cTnI A164H protonated simulation (inset). Hydrophobic residues shown for cTnC include A22, A23, I26, F27, L41, V44, M47, and L48; for cTnI include A154, M155, A158, L159, and L170. For reference, A164 and H164 are also shown. Interface between cTnC and cTnI is demarked by dotted white line.

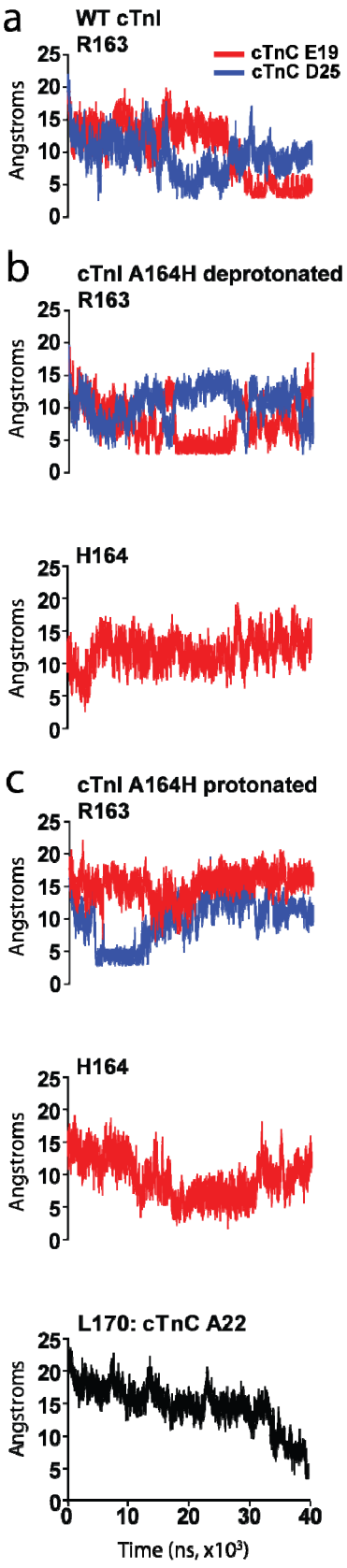

Figure 5-4. Interatomic distance measurements during cTn simulations. Interatomic distances were calculated during the 40 nanosecond simulations including: (a) WT cTnI R163: cTnC E19 and cTnC D25; (b) cTnI A164H deprotonated R163: cTnC E19 and cTnC D25 (top) as well as H164: cTnC E19 (bottom); (c) cTnI A164H protonated R163: cTnC E19 and cTnC D25 (top), H164: cTnC E19 (middle), and L170: cTnC A22 (bottom).

effects contribute to the H164 imidazole ionization state in the calcium saturated cTn complex and that histidine protonation is increasingly likely under acidic conditions. MD simulations of the deprotonated cTnI A164H showed interatomic distance measurements and structural dynamics similar to WT cTn including transient engagements between cTnI R163 and cTnC E19:D25 (Figure 5-3c, 5-4a, Supplemental movie 5). The deprotonated H164 primarily remained disengaged from residue contacts at the intramolecular interface (Figure 5-4b). In marked contrast, a single proton added to the imidazole side chain of cTnI A164H markedly affected the intermolecular structural characteristics of the calcium saturated cTn regulatory complex (Figure 5-3b, Supplemental movie 6). Histidine ionization resulted in a complete translocation of cTnI helix 4 toward the N-terminal hydrophobic patch of cTnC. Structural analysis indicated that helix 4 engagement with cTnC was associated with numerous intermolecular electrostatic contacts (cTnI R163: cTnC D25 and cTnI H164: cTnC E19) (Figure 5-3c, 5-4c) and increased hydrophobic interactions (cTnI L170:cTnC A22) (Figure 5-3d, 5-4d) across the cTnI:cTnC interface.

Discussion

This study assessed the molecular mechanism for pH responsive titratable inotropy observed with cTnI A164H. Prior reports have revealed that a histidine button engineered into the regulatory domain of cTnI provides a substrate for therapeutically modulating cardiac performance in response to various

pathophysiological stresses[203, 246, 290]. However, the molecular mechanism for this phenotype has not been analyzed. This study used *in vitro* functional analysis and *in silico* molecular dynamics simulations to elucidate the basis for differential imidizole ionization in regulating the unique function of histidine modified cardiac TnI. These data support the hypothesis that differential protonation of histidine enables cTnI A164H to act as a molecular rheostat capable of regulating sarcomere function in response to acute and chronic changes to the intracellular biochemical milieu.

Early studies by Rarick et al assessed calcium sensitivity of myofibrillar ATPase activity after extraction and exchange with cTnI peptide fragments to show the requirement for the C-terminal region of cTnI (residues 152-199) in regulating cardiac contractility[120, 266, 319]. Furthermore, Förster resonance energy transfer (FRET) experiments have shown that the movements of the regulatory arm of TnI during systole and diastole are essential for the transmission of the calcium signal to the rest of the myofilament proteins[159, 160]. As a basis for this observation, Li et al used multinuclear, multidimensional NMR spectroscopy to show that side chain contacts between the switch peptide of cTnI (residues 147-163) engaged the calcium saturated N-terminal region of cTnC through multiple hydrophobic interactions[327]. This observation was supported more recently by crystal structure analysis of the calcium saturated cTn core complex[52]. These hydrophobic side chain contacts are similarly observed in the regulatory interaction between slow skeletal TnI (ssTnI) and cTnC[51]. In the current study, *in silico* modeling during unrestrained molecular dynamics simulations revealed

novel electrostatic side chain contacts involving cTnI R163 toggling between cTnC E19 and D25 contribute to the binding interaction at the engaged interface between cTnI and cTnC.

Gene transfer and transgenic studies have shown that alterations in the peptide composition of the TnI switch arm can markedly alter myofilament performance[246, 249, 252, 325]. Importantly, a histidine residue in the switch arm has emerged as a key moiety responsible for modulating performance in ssTnI[133] and, more recently, cTnI[246, 249]. Site directed mutagenesis studies have shown that a single histidine to alanine substitution in the switch arm of slow skeletal TnI (ssTnI H132A) causes increased pH sensitivity, reduced inotropy, and a significant enhancement of relaxation analogous to WT cTnI[252]. Crystal structure analysis of a closely related TnI, fast skeletal TnI (fsTnI), would suggest that H132 engages closely with cTnC E19 in the calcium saturated state[51]. As such, alanine substitution would break this close intermolecular electrostatic interaction required for heightened inotropy as well as eliminate the substrate for pH responsive histidine ionization necessary for titratable contractile performance observed with ssTnI. The reciprocal substitution in cTnI (cTnI A164H) has been shown to provide a means for pH responsive contractile performance without markedly enhanced inotropy at baseline[203, 246]. Taken together, these functional studies indicate that sarcomere function of cTnI A164H does not completely recapitulate ssTnI. Fundamental differences in the structural position of histidine in the switch arm of ssTnI H132 (engaged with cTnC E19) compared to cTnI A164H (solvent exposed) in the calcium saturated Tn complex would suggest

different mechanisms of influence. The molecular basis for histidine ionization in ssTnI function has not been elucidated.

This study provides evidence that histidine imidazole ionization as the primary mechanism for pH responsive titratable inotropy observed with cTnI A164H. Under baseline conditions (pH 7.2), WT cTnI and cTnI A164H have similar inotropic function based on myofilament sensitivity to activating calcium (pCa) and SL shortening kinetics. Given that pK analysis showed increased propensity for H164 imidazole protonation only by acidic solvent, we hypothesize that under physiologic conditions the H164 side chain remains deprotonated. Compared to A164H, hypercontractility observed with constitutive protonation at residue 164 (cTnI A164R) at baseline supports this conclusion. Consistent with this, MD simulations showed similar helical behavior of WT cTnI and the deprotonated cTnI A164H. Thus, at physiological pH, WT cTnI and cTnI A164H have similar inotropic function mediated by structural dynamics involving electrostatic interactions between cTnI R163: cTnC E19/D25 and hydrophobic side chain contacts[52, 327].

In contrast, under acidic conditions measures of myofilament sensitivity to activating calcium and sarcomere length shortening dynamics indicate that WT cTnI had significantly compromised inotropic function compared to cTnI A164H and the cTnI A164R variant. Titration analysis of side chain ionization indicates that solvent effects on H164 would support imidazole protonation under acidic conditions. As such, the functional implications of histidine ionization are corroborated by structural modeling of the protonated cTnI A164H. A single

proton added to the imidizole side chain of histidine modified cTnI resulted in a marked structural change that enabled cTnI to engage more extensively with cTnC. Interestingly, this simulation analysis suggests that protonation of histidine is not solely responsible for mediating the enhanced interface engagement. Rather, these data show that H164 ionization supports more intricate structural alterations that involve both electrostatic (cTnI R163:cTnC D25 and cTnI H164:cTnC E19) and hydrophobic (cTnI L170:cTnC A22) intermolecular side chain contacts that alter engagement of the cTnI switch arm to the calcium saturated N-terminal hydrophobic patch of cTnC during acidosis. Taken together, these data indicate that solvent-mediated differential ionization of histidine enables cTnI A164H to remain deprotonated at baseline resulting in inotropy similar to WT cTnI. As pH becomes increasingly acidic, protonation of histidine's imidazole group enables the maintenance of baseline myofilament contractile performance.

This analysis does not exclude the possibility that pH dependent effects of histidine modified cTnI might occur in structural positions other than the calcium saturated state. For example, differential histidine ionization may also decrease TnI:actin interactions during diastole or alter TnI structural dynamics during translocation of the TnI regulatory arm thoughout systole. As such, MD simulations in this study focused on the implications of histidine ionization in the calcium saturated state with a particular emphasis on the regulatory interaction between the switch arm of cTnI and the N-terminal domain of cTnC.

Understanding the basis for the therapeutic implications of a histidine button in cTnI provides important insights into mechanisms of modulating cardiac performance in response to ischemia or acidosis. Use of cTnI A164H as a gene therapy vector or identification of small molecules that mimic the pH responsive features of histidine-modified cTnI may be a valuable approach for treatment of numerous cardiomyopathies. Specifically, this molecule has mild to no side effects on contractile function at baseline but protects inotropic performance in response to acute or chronic stresses such as myocardial ischemia. This study provides evidence to show that imidazole ionization is required for pH responsive titratable inotropy observed with myofilaments containing histidine modified cardiac TnI.

Acknowledgements

This study was supported by the National Institutes of Health (JM) and the American Heart Assocation (NP).

Appendix A

Supplemental movies 4-6. Forty nanosecond molecular dynamics simulations of WT cTnI (movie 4), cTnI A164H deprotonated (movie 5), and cTnI A164H protonated (movie 6). In all cases cTnC is shown in red and cTnI is shown in blue.

Appendix B

Table 5-1. Sarcomere dynamics at baseline and acidosis

Parameter	pH	WT cTnI	cTnI A164H	cTnI A164R
Baseline SL (um)	7.4	1.820 ± 0.006*	1.773 ± 0.005	1.776 ± 0.005
Baseline SL (um)	6.2	1.808 ± 0.004*	1.755 ± 0.005	1.746 ± 0.005
Time to peak (s)	7.4	0.108 ± 0.002	0.110 ± 0.002	0.117 ± 0.002*
Time to peak (s)	6.2	0.094 ± 0.002*	0.110 ± 0.003	0.104 ± 0.002
Normalized peak height (%)	7.4	10.18 ± 0.379	11.11 ± 0.498	13.40 ± 0.383*
Normalized peak height (%)	6.2	5.219 ± 0.382*	10.96 ± 0.596	9.619 ± 0.451
Time to baseline 50% (s)	7.4	0.0405 ± 0.001*	0.0466 ± 0.001	0.0504 ± 0.001
Time to baseline 50% (s)	6.2	0.0364 ± 0.001*	0.0464 ± 0.002	0.0470 ± 0.002
Time to baseline 75% (s)	7.4	0.0627 ± 0.002*	0.0750 ± 0.002	0.0781 ± 0.002
Time to baseline 75% (s)	6.2	0.0634 ± 0.003*	0.0741 ± 0.003	0.0768 ± 0.003

All values are expressed as mean ± SEM. n > 50 myocytes from > 3 myocyte isolations. P < 0.05 vs. all other groups.

Table 5-2. Myofilament calcium sensitivity and coorperativity analysis at baseline and acidosis

Parameter	pH	WT cTnI	cTnI A164H	cTnI A164R
Hill Coefficient	7.0	3.14 ± 0.46	1.83 ± 0.25	2.30 ± 0.28
Hill Coefficient	6.2	5.62 ± 1.94	2.74 ± 0.50	4.35 ± 1.11
pCa_{50}	7.0	6.00 ± 0.03	6.09 ±0.07	6.29 ± 0.02 *
pCa_{50}	6.2	4.66 ± 0.03*	4.92 ± 0.07	5.02 ± 0.02

All values are expressed as mean ± SEM. n > 50 myocytes from > 3 myocyte isolations. P < 0.05 vs. all other groups.

Chapter VI

Conclusion

Troponin I is a critical mediator of myofilament function. As a consequence, significant effort has been vested in understanding the structure and function of this protein in physiology and pathophysiology. The studies outlined here provide a significant step forward in elucidating our knowledge of this protein within the context of its related troponin proteins (TnC and TnT) and its functional regulation of other members of the myofilament. These studies provide a new level of knowledge encompassing *in silico* molecular modeling, *in vitro* analysis using genetically engineered isolated cardiac myocytes, and whole organ hemodynamic analysis *in vivo*. Brought into the context of other important studies of troponin I, these studies collectively provide an emerging knowledge of how troponin I (its various isoforms and targeted modifications) influences both the inotropic and lusitropic aspects of heart muscle function. This conclusion will outline the current state of knowledge of how TnI histidine buttons affect systolic function (part I) and diastolic function (part II). The second part will also draw on current knowledge about and potential implications of adaptations attributed to cTnI A164H

Part I: Systolic function

Classic studies in the field of troponin function have rigorously assessed the role of a histidine button in the regulatory domain as a pH responsive moiety[133, 246, 252]. Evolutionary studies show that this histidine is found in all isoforms of TnI in all species across chordate evolution with the exception of a proline in the platypus cTnI sequence followed by an alanine in all other mammalian cTnI sequences. Histidine has been shown to act as an effective pH-dependent titratable moiety within the ssTnI complex[133, 317, 318].

The working model to explain the functional implications of a histidine in the switch arm of TnI focuses on the differential ionization of the histidine residue (Figure 6-1). The model relies on the presumed biophysical effects of histidine ionization on the performance of the regulatory arm of cTnI interacting with the N-terminal hydrophobic patch of cTnC. Under baseline physiological conditions, we hypothesize that histidine is deprotonated resulting in a switch arm somewhat analogous to function to the WT cTnI. Under these conditions, myofilament activation at the myocyte level and hemodynamic function at the whole organ level are not markedly different. However, during acidosis, pH falls precipitously resulting in ionization of histidine. A positively charged moiety is hypothesized to enhance the binding affinity of the cTnI switch arm to cTnC such that contractility is maintained during acidosis. As such, a histidine residue in the TnI switch arm is thought to act as a molecular rheostat that modulates myofilament performance in response to changes in the intracellular mileu.

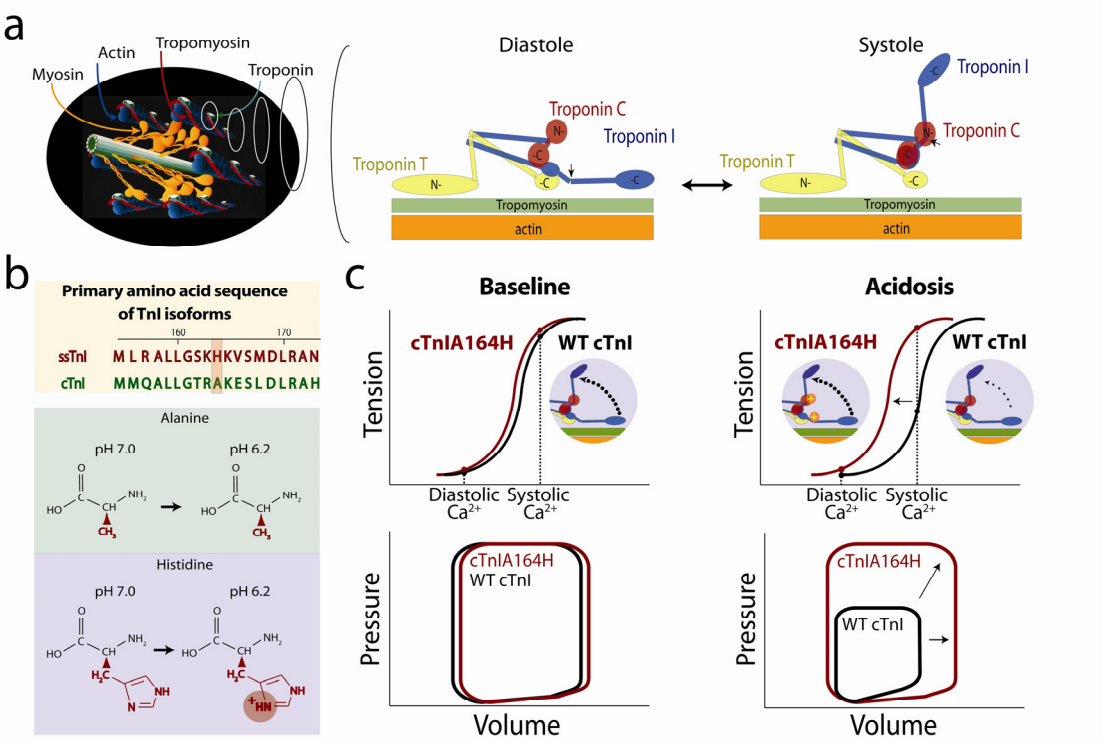

Figure 6-1. Funcutional implications of different switch arm motifs in TnI. Histidine-modified cardiac troponin I acts as a molecular rheostat of intracellular pH. a) The heterotrimeric troponin complex is part of the thin filament and functions as the molecular switch of the sarcomere. b) Differences in the primary amino acid sequence of troponin I led to the discovery of a critical histidine residue in ssTnI (and ancestral cTnI) which conferrs pH dependent activation of the myofilament. This histidine was substituted for an alanine to confer this biochemical advantage to the adult mammalian cTnI isoform (cTnI A164H). c) Under baseline conditions cTnI A164H has similar functional characteristics as WT cTnI *in vitro* and *in vivo.* However, under conditions of ischemia, protonation of the histidine in cTnI A164H protects myofilament calcium responsiveness thus protecting cardiac function compared to WT cTnI.

Numerous studies at the whole organ, single cell, and atomic level have provided evidence to assert this model[133, 203, 246, 249, 252, 290, 318, 405-408]. To begin, evolutionary studies have shown that ancestral species such as fish and amphibians require heightened calcium sensitivity of the myofilaments and pH responsive regulation of inotropy due to normal physiological conditions of cold temperatures and periods of chronic hypoxia experienced by these ectothermic species[4, 5, 331, 334, 405-408]. *In vitro* analysis of genetically modified cardiac myocytes showed that changes in the N-terminal domain of cTnC were at least partly responsible for increasing myofilament sensitivity to calcium in pre-mammalian species[4, 331, 334, 395]. Studies of perfused frog hearts have also shown that amphibians can maintain normal cardiac function during severe hypoxia or ischemia[408].

New phylogenetic analysis of TnI has shown that ancestral cardiac troponin I homologues have high sequence similarity to the ssTnI isoform found in all chordate species. There are a plethora of studies showing heightened calcium sensitivity attributable to ssTnI in large part because of the key histidine residue in the switch domain[246, 249, 252]. These studies provide strong evidence that the heightened calcium sensitivity as well as resistance to pH alterations of ancenstral myofilaments is the result of key residues in cTnC as well as a histidine moiety in the cTnI switch arm.

Interestingly, these and other studies have also shown that heightened calcium sensitivity of the myofilaments and pH insensitivity are critical for development of every species across chordate evolution. Studies have shown

that a single TnI isoform (cardiac) is expressed in all phases of amphibian development from the larva to the adult. However, in avian and mammalian species the developmental isoform changes to ssTnI which is stoichiometrically replaced with cTnI in the adult heart. The evolutionary pressure for this phenotype is likely the preserved nature of heart development in all species. Specifically, studies have shown that the fetal heart has high lactate levels and relies on glucose metabolism[384]. Second, there is evidence that the critical cardiac developmental transcription factor Nkx2.5 is regulated by hypoxia-inducible factor (HIF-1α)[385]. Together these would require contractile function that is not affected by changes in pH. Third, immature sarcoplasmic reticulum and calcium cycling in the developing heart require heightened sensitization of the myofilaments to establish sufficient inotropy[387]. These data would suggest that mutations that eliminate this key feature of pH responsiveness and heightened calcium sensitivity (e.g. ssTnI H132A) would be embryonic lethal if expressed during the developmental stages of any species. This hypothesis is yet to be tested.

Atomic level molecular dynamics simulations and modeling have provided an immense amount of knowledge regarding the mechanism by which this histidine button affects intramolecular and intermolecular structural characteristics of TnI within the calcium saturated troponin complex. To begin, 20 nanosecond simulations of ssTnI:cTnC structure showed a tight and nearly inflexible interaction at the interface between these proteins. Structural analysis was performed to calculate theoretical residue ionization titration (pK) and

electrostatic atomic energy binding interaction between all ionizable groups. This showed that sTnI histidine132 and cTnC glutamate19 develop a salt bridge and generate an electrostatic interaction strength of 5.24 kcal/mol. This level of interatomic bonding far exceeds the interaction strength between any other two ionizable groups within the entire regulatory complex of either sTnI:cTnC or cTnI:cTnC structures. The reciprocal effect of these residues on each others' pK shift further confirms the importance of this interaction in mediating the intermolecular stability of the sTnI:cTnC regulatory complex. Functionally, these atomic resolution structural modeling data are consistent with heightened myofilament calcium sensitivity and pH responsive inotropy as observed with hearts containing ssTnI or ancestral cTnI molecules[4, 133, 252, 331].

Given this abundance of data supporting the important role of histidine in TnI, the hypothesis was tested that a histidine button in cTnI (cTnI A164H) could act as a molecular rheostat capable of augmenting contractility in response to injury. Day and colleagues elegantly showed that cTnI A164H had a mild effect on contractility at baseline but therapeutically enhanced cardiac performance in the context of a variety of pathological models *in vitro, ex vivo, and in vivo*[246]*.* Similarly, recent studies have shown that cTnI A164H is able to protect cardiac function during aging[290] and in the context of a severe hypercapnic acidosis challenge[203]. In the latter study, cardiac conductance micromanometry analysis during severe acidosis (pH 6.5) showed that cTnI A164H mice were able to sustain heart function without mortality in the absence of adrenergic support. Statistical analysis showed that systolic, diastolic, and geometric parameters

were not significantly different after 20 minutes of acidosis compared to baseline values. This was in marked contrast to Ntg mice that, in the absence of adrenergic support, experienced acute pump failure and 100% mortality within the first 5 minutes of acidosis. Taken together with the study by Day et al[246], these observations provide strong evidence that cTnI A164H can act as a therapeutic molecule to augment cardiac performance in the context of various pathophysiological challenges.

These *in vivo* studies are supported by *in vitro* analysis of myocytes genetically modified to express cTnI A164H and assessed for inotropic capacity. Under baseline conditions, measures of sarcomere length shortening kinetics and myofilament calcium sensitivity of cTnI A164H myocytes was not significantly different from myocytes expressing WT cTnI. Atomic resolution molecular dynamics simulations and pH titration analysis indicates that histidine (H164) remains deprotonated under baseline conditions causing structural dynamics similar to WT cTnI. However, when exposed to acidic media myocytes expressing WT cTnI have markedly diminished contractility compared to myofilaments expressing either cTnI A164H or arginine modified cTnI (A164R) which is a constitutively protonated correlate to the ionized histidine. Consistent with this, pK analysis indicates increased propensity for imidazole protonation under acidic conditions. Furthermore, molecular simulations where a single proton is added to histidine's imidazole group show markedly different structural dynamics involving added intermolecular electrostatic and hydrophobic side chain contacts across the cTnI:cTnC interface in the calcium saturated state.

Taken together, these data provide evidence to show that imidazole ionization is required for pH responsive titratable inotropy observed with myofilaments containing histidine modified cardiac TnI.

Part II: Diastolic function and physiological adaptations

Functional studies of chordate species indicate that myofilament calcium sensitivity has significantly decreased during evolution[4, 332]. As discussed above, studies of ancestral species indicate the requirement for heightened sensitivity to activating calcium and pH responsive inotropy in these organisms[405-408]. The earliest known sequence within the mammalian taxa is derived from the platypus. Alignment data show that a proline residue in the switch domain likely acted as a key molecular intermediate that broke the high energy histidine-glutamate interaction of ancestral cTnI isoforms. All other mammals have an alanine at this position.

To understand the structural implications of breaking this His-Glu interaction, molecular dynamics simulation and *in silico* alanine scanning was performed. In this analysis the change in the binding free energy (ΔΔG) was calculated for alanine substitutions of all residues involved in the interface bonding of the sTnI:cTnC calcium saturated crystal structure. Of the cTnC residues, these data show that E19A had the greatest impact on ΔΔG (ΔΔG E19A = 0.91kcal/mol). However, the greatest impact on the binding free energy among all residues engaged at the cTnC:sTnI interface was observed with the

sTnI H132A substitution (ΔΔG H132 = 2.46 kcal/mol). Structural comparison of sTnI:cTnC and cTnI:cTnC indicate that breaking this His-Glu interaction resulted in a molecularly untethered TnI helix 4. Importantly, this decreased the binding free energy of the TnI:TnC interface resulting in enhanced relaxation of the troponin complex. Twenty nanosecond molecular dynamics simulations of the alanine substituted sTnI H132A:cTnC structure support this hypothesis.

Furthermore, functional studies of genetically engineered adult cardiac myocytes have shown that a single amino acid substitution in the TnI switch domain (ssTnI H132A) is able to fully recapitulate the phenotype of the mammalian cTnI isoform[252]. Compared to ssTnI, the functionality of cTnI/ssTnI H132A includes reduced myofilament calcium sensitivity, reduced inotropic function, enhanced relaxation, and increased pH sensitivity[252]. These data support the conclusion that evolutionary pressures were aimed at enhancing the relaxation efficiency of the troponin complex in order to meet changing lusitropic requirements during evolution of the mammalian cardiovascular system.

In support of this hypothesis, studies of human disease causing mutations within the cTn complex can result in an evolutionary revertant phenotype; that is, heightened calcium sensitivity of the myofilaments[333, 335, 337, 358]. Patients with these SNPs have shown symptoms of heart failure including diastolic dysfunction, increased propensity for arrhythmias, and susceptibility to sudden cardiac death[329, 333, 335, 337, 358]. Animal models of these diseases together with the well studied ssTnI transgenic mouse all recapitulate aspects of these heart failure phenotypes[213, 333, 374, 455]. The observation of significant cardiomyopathy and

heart failure when mammalian cardiac myofilaments have heightened calcium sensitivity supports the hypothesis that evolutionary pressures required a troponin complex with enhanced relaxation in order to meet the lusitropic requirements of mammalian heart. Phylogenetic analysis, molecular modeling, and functional data suggest that this occurred by means of a critical histidine to alanine substitution in the switch arm of cTnI.

These observations are in marked contrast to the finding that a histidine engineered back into cTnI (cTnI A164H) does not cause diastolic dysfunction *in vivo*. In fact, numerous assays using cTnI A164H Tg mice have shown that diastolic performance is markedly protected by the cTnI A164H molecule[203, 246, 290]. The study by Day et al was the first to reveal the protective nature of cTnI A164H on diastolic function[246]. During ischemia/reperfusion injury *ex vivo,* Tg hearts on the Langendorff apparatus recovered baseline diastolic performance immediately upon reperfusion compared to Ntg mice which never recovered baseline diastolic function (EDp). Furthermore, diastolic function during aging, as measured by the ratio of the mitral valve E wave to the lateral annular E wave (E/Ela), was significantly lower in Tg than Ntg mice at the 2 year time point[290]. Lastly, during an extended acidosis challenge with beta blockade, cTnI A164H Tg mice were able to protect diastolic function during the entire time course of the challenge[203]. Surprisingly, diastolic performance in Tg mice was not statistically different at the end of the challenge (20 min of acidosis) compared to the beginning (e.g. EDp). In contrast, severe diastolic dysfunction occurred in Ntg mice resulting on whole organ cardiac decompensation within 5 minutes after the

onset of acidosis. Taken together, data from cTnI A164H Tg mice provide strong evidence for the advantage conferred by a histidine-modified cTnI on diastolic performance.

The proposed model for the biophysical implications of cTnI A164H (Figure 6-1) are not sufficient to explain the observed advantage on diastolic performance. Adaptive modifications to the cTnI A164H heart have been described in detail elsewhere[246, 290] and must be considered. Specifically, studies have shown that myocytes isolated from Tg hearts have reduced calcium transients and SR calcium load[246, 290]. In terms of regulating calcium cycling, Tg hearts have increased levels of SERCA2a and phospholamban[290]. Energetically, Tg mice have been shown to be more economical compared to Ntg littermates[246]. Morphometric measurements showed that Tg mice have small hearts and myocytes than Ntg hearts[246]. For various reasons, it has been hypothesized that all of these adaptations contribute to the protective nature of cTnI A164H during various cardiac challenges[242, 246, 290].

On the basis of diastolic function, it could be argued that adaptations associated with calcium regulation are required to protect baseline diastolic parameters in the presence of a molecule that, *in vitro,* is shown to cause diastolic dysfunction. Reduced calcium load and enhanced reuptake by higher levels of SERCA2a would enhance relaxation through calcium cycling mechanisms. These changes also contribute to the advantage conferred to cTnI A164H mice during injury such as I/R where reduced calcium may attenuate the post-ischemic calcium overload[246]. Differing observations in terms of cTnI

phosphorylation[246, 290] make potential differences in PKA signaling unclear. If PKA signaling is increased in cTnI A164H hearts[246] this may also enhance diastolic performance to compensate for a heightened myofilament responsiveness.

Elasticity of the myocardium may also be enhanced in cTnI A164H mice which would augment LV relaxation capacity. Reduced E/Ela during 2 years of aging[290] showed improvement in the ratio of the inflow velocity to the tissue velocity providing insight into the elastic properties of the ventricle[290]. In essence, the E wave velocity controls for cardiac output, heart rate, and filling so that the ratio (E/Ela) correlates with left atrial pressure. The link between cTnI A164H and increased ventricular elasticity is currently unclear. Based on our current knowledge, there is no direct evidence that cTnI A164H itself confers any advantage to diastolic performance outside of significant contributions associated with myocardial remodeling. In the absence of these adaptive changes as seen with genetically engineered rat myocytes, diastolic dysfunction is observed when cTnIA164H is incorporated into the myofilament at high stoichiometric levels.

Experiments are underway to determine the molecular mechanism for calcium modulation in the cTnI A164H Tg hearts. I outline novel methodologies to determining the mechanism for this observation in the future directions. Whether the purpose for modulation of calcium handling in this model is aimed at regulating systolic and/or diastolic function (or neither) is not known. Taking these data together, the physiological phenotype of hearts containing cTnI A164H is inextricably tied to the adaptive effects it elicits. As discussed in future

directions, defining the physiological phenotype of cTnI A164H without developmental adaptations will be critical for further understanding the therapeutic value of this molecule in the adult heart.

Conclusions

Given the expanded knowledge provided by these studies, an interesting model has emerged regarding the role of the cardiac troponin complex in mammalian cardiovascular function (Figure 6-2). To begin, ancestral cTnI molecules together with TnI isoforms expressed during development in all chordates indicate that the physiological demands of these hearts require heightened calcium sensitivity of the myofilaments and resilience to changes in pH. This characteristic is, at least in part, attributed to a key histidine residue in TnI and its interatomic bonding with a highly conserved glutamate moiety in helix A of cTnC. During evolution of the mammalian cardiovascular system, the histidine residue of the cTnI switch domain was modified to a proline initially (platypus) and subsequently changed to an alanine in all other mammals. This alteration was required to achieve appropriate relaxation of the cTn complex to meet lusitropic demands of the mammalian heart. This modified cTnI molecule has increased mobility of helix 4 involving interactions with cTnC that are largely hydrophobic mediated by cTnI L159 but also include electrostatic contacts

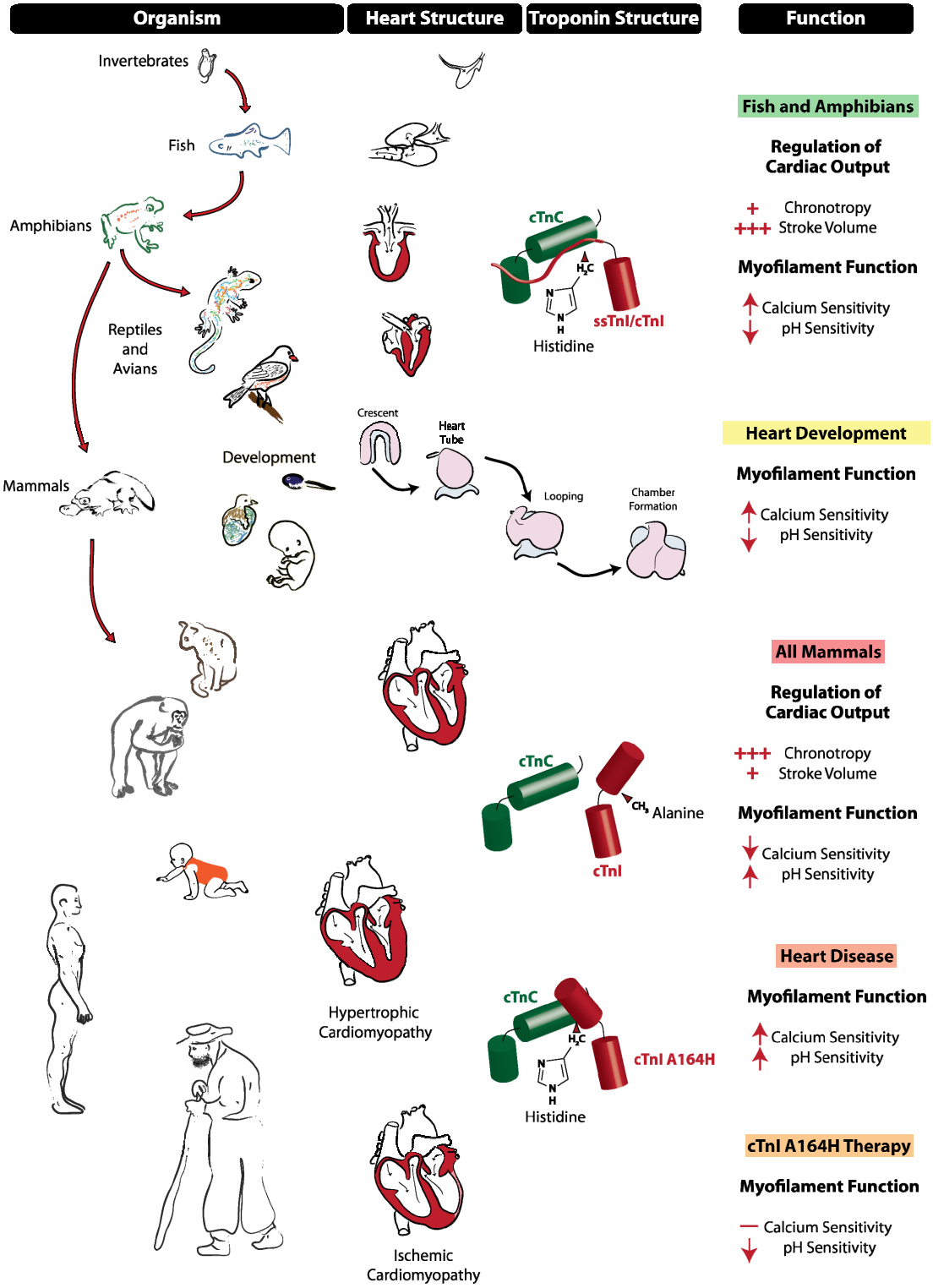

Figure 6-2. Model for structural, functional, and evolutionary implications of a histidine moiety in cardiac troponin I.

primarily observed between cTnI R163 and cTnC E19/D25. Cardiomyopathies that cause evolutionary revertant phenotypes (e.g. cTn SNPs that cause heightened myofilament calcium sensitivity) result in symptoms of heart failure including arrhythmias, diastolic dysfunction, and increase susceptibility to sudden cardiac death. The emergence of heart disease phenotypes in patients with revertant phenotypes supports the conclusion that enhanced relaxation by cTn was required to meet lusitropic demands of the mammalian heart.

Other heart diseases such as ischemic cardiomyopathy, primarily observed in the modern aging population suggest potential therapeutic value of pH-dependent titration of inotropy in response to cardiac challenges. A histidine placed back into its original position in the switch domain of cTnI provides this sort of cardiovascular advantage in response to numerous pathophysiological insults[203, 246, 290]. At the molecular level, the capacity for cTnI A164H to act as a molecular rheostat is based on the differential ionization of histidine's imidizole side chain.

Chapter VII

Future Directions

The studies outlined in this dissertation provide a strong basis for a number of additional studies to help elucidate the role of troponin in regulating myofilament function. The first part will outline an extensive array of proposed experiments related to the translational research potential of the cTnI A164H protein as a therapeutic tool. The second section will outline some basic science questions designed to understand the fundamental nature of the critical interaction between TnI and TnC in the intact myofilament. The third section will outline experiments designed to understand the correlation between myofilament calcium sensitivity and calcium handling using Tg mouse models of Tn mutants.

Part I: Structural and Functional Protection of the Acute and Chronically Ischemic Heart Using Gene Transfer of Cardiac TnIA164H

We have found in our initial studies that cTnIA164H enables differential changes in myofilament calcium sensitivity based on alterations in the biochemical milieu of the cell during myocardial ischemia/acidosis[203, 246, 290].

Under these conditions, histidine-modified cTnI provides a substrate for increased myofilament responsiveness to intracellular calcium transients which translate functionally to improve sarcomere-based force production and, subsequently, ventricular contractility**.** These conclusions from studies using the cTnIA164H transgenic mouse are encouraging and informative. This proposal is significant because it invokes the use of rAAV technology for temporal regulation of gene delivery to the heart together with an array of powerful methodologies which will enable observation of effects specifically attributable to cTnIA164H within the context of clinically relevant models of ischemic heart disease. This is opposed to potential limitations of the transgenesis study wherein expression of the cTnIA164H transgene early during developmental growth may have been causal to compensatory changes in structure and function of the heart. These compensatory changes raise some questions as to what is and what is not a true effect of histidine-engineered cTnI. As a consequence, several major questions remain which this proposal is uniquely designed to address. First, does rAAV mediated transduction of cTnIA164H into the adult heart protect contractility during acute ischemia? Second, does cardiac transduction of cTnIA164H prevent myocardial remodeling in a model of chronic ischemic cardiomyopathy? Third, is the therapeutic effect of cTnIA164H restricted to protecting contractility during the initial ischemic injury or can it also therapeutically improve cardiac structure and function when delivered after an ischemic insult? The nature of these questions emphasizes the need to temporally regulate gene transfer and subsequent expression of cTnIA164H. The methodologies outlined here will improve the

specificity of truly defining the consequent impact of cTnIA164H on the normal and pathologic heart in vivo.

To begin, it will be necessary to determine the transduction efficiency of *in vivo* viral-mediated systemic gene transfer of rAAV-cTnIA164H to the hearts of adult mice and assess whether subsequent incorporation into the sarcomere protects global cardiac contractility in the acutely ischemic heart. As a part of this, it will be important to determine the transduction efficiency of rAAV-cTnIA164H and the extent of replacement of endogenous cTnI to cTnIA164H in transduced hearts.

Based on preliminary results using control vectors *transduction efficiency* of rAAV is expected to be nearly 90% of the heart (Figure 7-1). Consequently, initial assays showing the rate and extent of cTnIA164H incorporation into the myofilament will provide supportive evidence for functional effects observed. Correspondingly, the control virus, cTnIFLAG, will similarly be assayed for rate and duration of incorporation to show efficacy of this as a control virus in acute and chronic models employed in this proposal. This will be the first study to use AAV-mediated delivery of a modified myofilament protein to the heart *in vivo* to show competitive stoichiometric replacement of the endogenous protein.

To accomplish this it will be necessary to assess the rate and extent of competitive stoichiometric replacement of endogenous cTnI by cTnIFLAG and cTnIA164HFLAG. To accomplish this rAAV-cTnIFLAG or rAAV-cTnIA164HFLAG will be delivered systemically by a single tail vein injection with subsequent

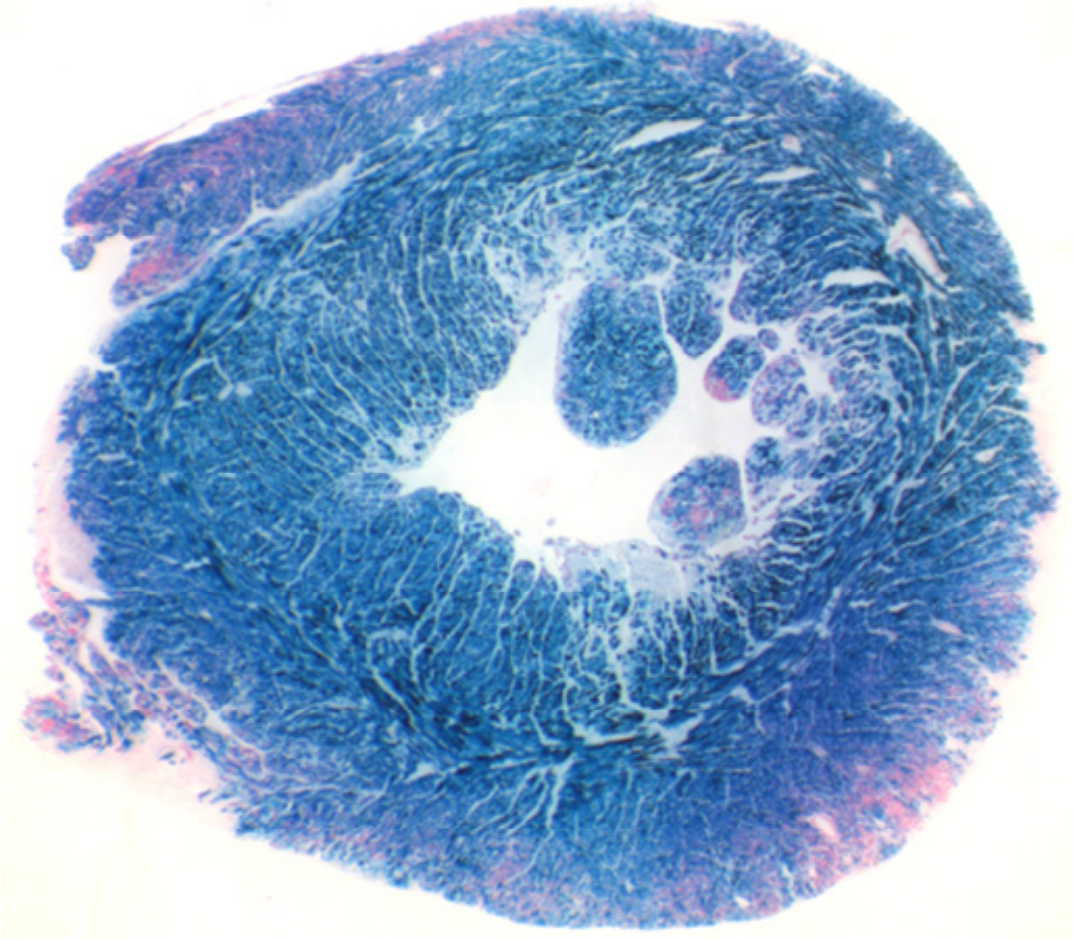

Figure 7-1. Evidence of global *in vivo* transduction of cardiac tissue after intravenous injection with rAAV-LacZ. Image courtesy of DT.

analysis of whole heart lysate every four days until day twenty post-injection. Consistent with previous reports[456, 457], we will confirm long term transcriptional activity by isolating lysate from transduced hearts once every month for six months. Expression of endogenous cTnI and cTnIFLAG or TnIA164HFLAG will be immunodetected by Western blot analysis using a cTnI specific antibody (Chemicon, AB1627) and a fluorescence tagged secondary (Alexa Fluor 680, Molecular Probes). Incorporation into the intact myofilament will be determined by indirect dual immunofluorescence detection for flag-tagged cTnIA164H and actin in isolated myocytes from transduced hearts. Mouse myocyte isolation will be as previously described by our lab[24]. For dual immunofluorescence, antibodies used will include anti-flag antibody (mouse monoclonal, M2 Flag, Sigma) conjugated to Alexa Flour 488 (Molecular Probes) and anti-actin N-terminal antibody (rabbit polyclonal, A2103, Sigma) conjugated to Texas Red (Molecular Probes). Analysis will be performed with a laser scanning confocal microscope.

Based on preliminary data using rAAV, global myocardial expression of control protein is noted at ten to twelve days post gene transfer (Figure 7-1). However, in the case of gene transfer using a sarcomeric protein, the rate of incorporation into the myofilament is dependent on the half life of the endogenous protein. Adenoviral mediated gene transfer of cTnIA164H into isolated adult rat myocytes *in vitro* has shown greater than fifty percent replacement of native cTnI occuring at day four post gene transfer (Figure 5B). Furthermore, this data indicates that native cTnI can be separated from

cTnIFLAG or cTnIA164HFLAG by SDS-PAGE in order to determine the stoichiometric ratio of each protein in the myofilament. In this study, incorporation of cTnIA164HFLAG or cTnIFLAG into the myofilament is expected to begin ten to twelve days post AAV-mediated gene transfer with complete replacement between fourteen and sixteen days. Proper incorporation into the sarcomere is expected as shown by dual immunofluorescence.

Studies using mice injected with a reporter construct (rAAV CMV Luciferase) have provided strong evidence for global gene transfer to striated muscle after a single tail vein injection **(**Figure 7-2**).** Vector production has been accomplished in a similar fashion with rAAV cTnI A164H. After a single tail vein injection of extremely high vector genomes results show that the maximum extent of stoichiometric replacement occurring in cardiac tissues is perhaps 5-10% of endogenous cTnI levels (Figure 7-2a). This is in marked contrast to the transgenic mouse and isolated rat myocytes trandsuced with Ad cTnI A164H which show 80-90% replacement. This is a surprising result given that lower doses of vector containing micro dystrophin have been sufficient to transducer the entire heart and replace dystrophin deficient heart muscle to a therapeutic level[458].

We hypothesize that differences in regulation of protein expression between cTnI and dystrophin are responsible for this observation. Specifically,

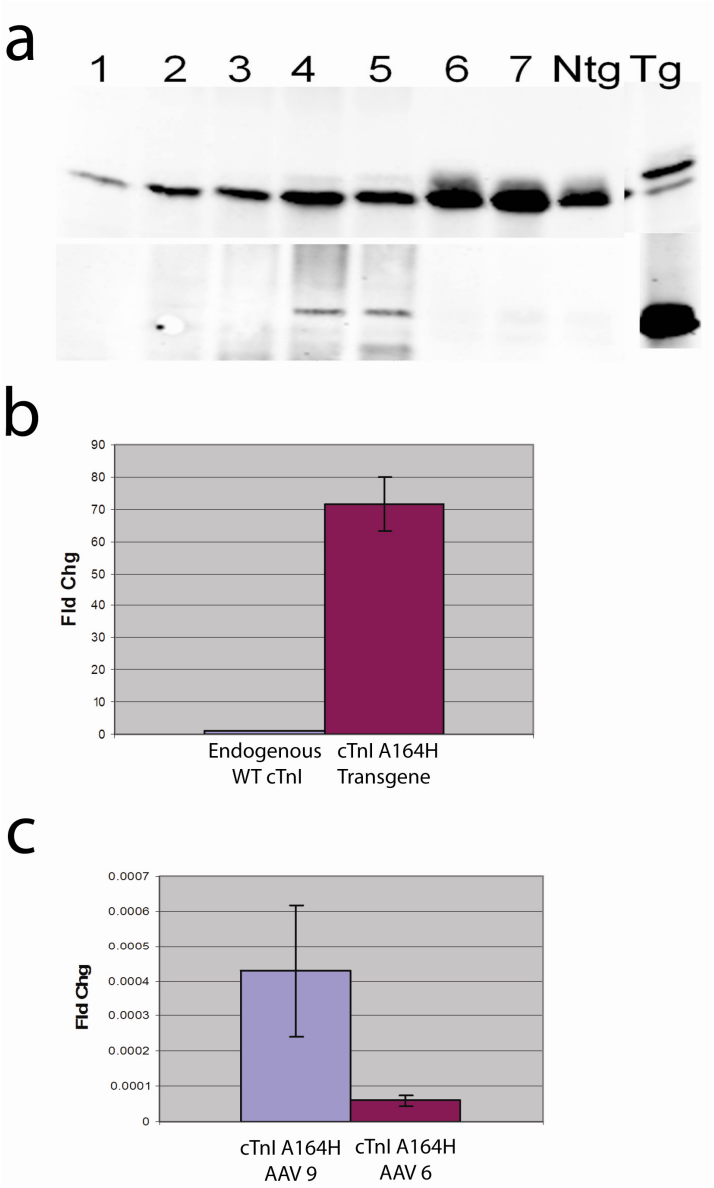

Figure 7-2. Analysis of mRNA and protein expression of hearts transduced with AAV cTnI A164H. (a) Western blot analysis showing protein expression level after AAV injection of cTnI A164H. Tail vein injection of 250-300 uL virus containing 3-4x10^{13} vector genomes. Western blot was performed 3 months after injection (antibodies: MAB 1691 (top) and M2 FLAG (bottom)). Lanes 4 and 5 show approximately 5% replacement of endogenous cTnI. (b, c) mRNA analysis of hearts expressing cTnI A164H by transgenesis (b) or AAV injection (3 months post injection) (c). Transgenic expression of cTnI A164H achieved 70 fold higher expression level compared to endogenous and resulted in ~ 80% stoichiometric replacement. AAV gene transfer of cTnI A164H (serotype 6 and 9) resulted in mRNA levels markedly below endogenous levels.

dystrophin is not a stoichiometrically regulated protein. As such, over-expression of this protein is possible in both dystrophin deficient and normal skeletal muscle. However, cTnI is a component of the myofilament where stringent stoichiometric replacement is absolutely necessary in order to protect the integrity and thus proper functionality of the sarcomere. As such “over-expression” of myofilament proteins is only manifest in the way of stoichiometric replacement of endogenous proteins via a competitive mechanism. Recent studies have shown that although the cTnI knockout is lethal, haploid under-expression of cTnI is sufficient to attain proper stoichiometric incorporation into the myofilaments, an indication that endogenous levels of TnI are naturally higher than is required for minimal incorporation and function of the myofilaments[459].

Studies of transgene mRNA levels of the cTnI A164H transgenic mouse show a remarkable degree of overexpression of exogenous cTnI A164H compared to endogenous levels (Figure 7-2b)**.** This indicates that a significant level of overexpression is required to achieve stoichiometric replacement to levels sufficient for a therapeutic effect (80-90% replacement). We hypothesize that rAAV cTnI A164H is not achieving the level of vector genome copy number per cell relative to what is achieved either by transgenesis *in vivo* or adenoviral mediated gene transfer into isolated myocytes *in vitro*. Preliminary data support this conclusion (Figure 7-2c). However, further experiments are required to substantiate this assertion. If sufficient levels of replacement can be achieved progression to Sub-aim 1B and Specific aim 2 would be important.

Standard neonatal cardiac-specific overexpression studies are useful for defining candidate genes that have a pathophysiologic or, conversely, therapeutic impact on the heart. Transgene mediated manipulation of the physiologic norm during early cardiac developmental stages will, however, induce compensatory alterations in various components of the underlying structure and function of the heart. In other words, during development the immature heart is able to undergo a global phenotypic adjustment in response to specific genotypic alterations. The fully differentiated adult heart, however, responds exclusively to transgene-mediated effects[460]. In light of this, subsequent conditional and temporally defined gene manipulation studies provide clarity for the relevance of that gene within the context of various physiologic or pathologic states[461].

Our previous studies have shown that cTnIA164H is a candidate gene useful for therapeutic treatment of ischemic heart disease[246, 290]. However, it is likely that compensation occurred in the cTnIA164H transgenic mouse where transgene expression was driven by the alpha myosin heavy chain promoter which is active during the early post-natal stages of cardiac growth and differentiation. This may have influenced the development of structural and functional differences (e.g. calcium homeostasis, global cardiac morphology, and energetics) observed at baseline and under various cardiomyopathic stresses. This raises a significant question: what aspects of myocardial protection during acute and chronic ischemia can really be directly attributed to cTnIA164H?

Taking this rationale into consideration provides background for the importance of the experimental model employed in this aim. It is important to note that compensatory changes will also likely occur in the adult heart in response to cTnIA164H. The crux of this aim, however, is based on the fact that AAV gene transfer into the mature adult heart will provide a means of understanding the extent to which cTnIA164H protects contractility during an acute ischemic challenge devoid of developmentally induced cardiac compensatory changes. Preliminary data show that critical functional aspects of myofilament calcium sensitivity are similar between the cTnIA164H transgenic heart and acutely isolated adult rat myocytes transduced with cTnIA164H. Comparable to transgenic hearts, adenoviral transduction of cTnIA164H into adult rat cardiac myocytes replaces greater than 80% of native cTnI. Based on this level of replacement, preliminary data indicate that the calcium sensitivity of isometric force (pCa_{50}) at baseline (pH 7.0) and under acidic conditions (pH 6.2) is higher in acutely isolated adult rat myocytes transduced with cTnIA164H compared to controls. Furthermore, the pCa_{50} observed in cTnIA164H adenovirally transduced myocytes at neutral and acidic pH is analogous to that observed in myocytes isolated from cTnIA164H transgenic hearts. These data indicate that under acidic conditions contractile performance can be significantly improved in adult myocytes transduced with cTnIA164H. This conclusion supports my hypothesis that cTnIA164H transduced hearts *in vivo* will correspondingly show protection of myocardial contractility during an acute ischemic challenge.

Similar methodological approaches will be employed first to assess changes in baseline cardiac function and second to assess whether cTnIA164H acutely protects inotropic function in the ischemic adult heart. To begin, rAAV cTnIA164H will be delivered systemically by a single tail vein injection. All experiments will be performed four weeks after injection to allow sufficient time for viral transduction of the heart, transgene expression and protein incorporation into the myofilament. Assays will involve echocardiography, Millar catheterization, and the Langendorff isolated heart preparation as described previously in detail by our lab[246] with some modifications. Echo will be used to assess cardiac structure as measured in M-mode in the parasternal short axis view at the level of the papillary muscle. Furthermore, systolic function will be analyzed in M-mode and diastolic function by pulsed-wave spectral Doppler analysis and Doppler tissue imaging of the mitral valve annulus. For millar catheterization, mice will be anesthetized and ventilated via a tracheal cannulation. A Millar pressure-volume catheter (Millar Instruments Inc.) will be inserted into the right carotid artery and advanced into the left ventricle. Inferior vena cava occlusions will also be performed to obtain the end systolic and end diastolic pressure-volume relationships. In each assay (Millar, Langendorff, Echo) baseline data will be acquired with hearts exposed to normal physiologic conditions. In assays involving millar catheterization and Langendorff isolated hearts, physiologic conditions will subsequently be altered to determine if transduced hearts retain improved inotropic function in the context of an acute ischemic stress. The Langendorff perfused hearts will be exposed to one of the

following two different ischemic challenges. Isolated hearts in Cohort 1 will be exposed to twenty minutes of acidic perfusate (pH 6.8) followed by thirty minutes of exposure to neutral perfusate (pH 7.4). Cohort 2 will be exposed to twenty minutes of no-flow ischemia followed by thirty minutes of reperfusion. Hearts that have undergone conductance catheterization will also be exposed to one of two different ischemic challenges. In cohort 1, baseline data will be acquired during ventilation with 100% oxygen. A hypoxic challenge will then be introduced by altering the composition of ventilated air to include 7% oxygen and 93% nitrogenIn cohort 2 during cardiac catheterization the left coronary artery (LCA) will be permanently ligated to induce a 30-40% infarction of the LV free wall.

At baseline, hearts transduced with cTnIA164H are expected to have an improvement in systolic performance while diastolic function will remain unaltered. Concerning the ischemic challenges, previous reports have made strong arguments for the fact that myocardium in the peri-infarct zone is inadequately perfused, and consequently hypoxic, which supports the hypothesis that cTnIA164H will increase contractility in this critical region of the injured myocardium[462]. Furthermore, the cTnIA164H transgenic study showed whole heart improvements in contractility at baseline compared to non-transgenics. Based on these data, it is expected, in general, that cTnIA164H transduced hearts stressed by an acute ischemic challenge will have improved contractility compared to controls. In the Langendorff isolated heart method these observations will be mild in hearts that are exposed to acidosis with reperfusion (cohort 1) and accentuated in hearts that undergo no-flow ischemia with

reperfusion (cohort 2). In assays involving conductance micromanometry global cardiac hypoxia as well as an induced myocardial infarction of 40-50% of the LV will significantly challenge contractile function. Specifically, hearts transduced with cTnIA164H are expected to have improved contractility during an acute ischemic challenge as characterized in part by increased left ventricular developed pressure (LVDP) compared to controls. Furthermore, consistent with data derived from the transgenic mouse, cTnIA164H transduced hearts are expected to show an attenuation of diastolic dysfunction based on maintenance of LV end diastolic pressure (LVEDP) in contrast to severe diastolic dysfunction expected in control hearts. In summary, the experimental model used in this aim is significant because it eliminates the variable of developmental compensation which likely influenced these assays in the transgenic mouse study. Together, these data would support the hypothesis that rAAV-mediated cardiac transduction of histidine-modified cTnI into an adult heart improves inotropy and decreases diastolic chamber stiffness during an acute ischemic stress.

Data at baseline and during ischemic challenges will be compared to control hearts transduced with cTnIFLAG to account for any effects attributable to the flag epitope. We have previously shown no effect of the FLAG epitope on cTnI function[246, 251].

Despite evidence showing improved inotropy in isolated adult rat myocytes transduced with cTnIA164H (Figure 4D), *in vivo* differences in contractile function may not be observed between rAAV-cTnIA164H transduced hearts and controls. Assuming that sufficient gene transfer can be accomplished,

the most probable alternative explanation includes the observed changes in calcium handling in transgenic hearts. To account for this possibility, experiments are already underway to understand how compensatory changes in calcium homeostasis could account for the phenotype observed in the cTnIA164H transgenic mouse. If differences are not significant between groups, a beta adrenergic receptor agonist (e.g. dobutamine) infusion protocol during acute ischemic challenges could be used to exacerbate these differences. Despite these considerations, previous reports support the alternative argument that developmental compensatory changes in the transgenic mouse may *blunt* the potent effects of cTnIA164H[461].

It is established that compensatory LV dilation and eccentric myocardial hypertrophy are signs of cardiac remodeling which significantly contribute to the pathology of chronic ischemic cardiomyopathy[463-465]. Over time this leads to severe systolic and diastolic dysfunction antecedent to cardiac decompensation and death[466, 467]. LV volume in particular is a powerful prognostic indicator of survival in patients with coronary heart disease[468]. Cavitary dilation of the LV is in part the result of asymmetric aneurismal expansion of necrotic tissue. However, compensatory stretch of the non-infarcted myocardium also increases contractility and subsequently cardiac output[468, 469]. Furthermore, contractile dysfunction after an MI is associated with regional hypertrophy of the non-infarcted myocardium. This response enables the heart to compensate for the loss of myocytes in the infarct zone in order to improve contractility and retain

cardiac output. These mechanisms of increasing wall tension must be generated by the ventricle due to the law of LaPlace. However, this need for increased tension development ultimately results in the negative spiral of events leading to decompensation and heart failure. Based on this, reports have suggested that therapeutically increasing myofilament-based inotropy may provide a mechanism for maintaining cardiac output and consequently attenuate LV dilation and myocardial hypertrophy associated with cardiac remodeling after an MI[435]. To address this, our lab has engineered cTnIA164H which is specifically designed to increase calcium sensitivity of the myofilament. The physiologic result of this biochemical alteration in cTnI leads to a shift wherein the same cardiac output can be generated with reduced end diastolic volume. To support this, our data indicate that cTnIA164H attenuates LV remodeling while maintaining inotropy in a model of chronic ischemic cardiomyopathy[246]. Additionally, adenoviral-mediated delivery of cTnIA164H to failing human myocytes was found to partially restore contractility[246]. Recognizing the merits of this data, however, several important questions remain. First, to what extent can cTnIA164H therapeutically improve contractility and alter the progression of remodeling in the mature adult heart *in vivo* using temporally different treatment modalities for chronic ischemic cardiomyopathy? Furthermore, emergency intervention for ischemic heart disease often does not occur until significant myocardial damage has already taken place post MI. Taking this intervention model into consideration, the question remains whether the therapeutic effect of cTnIA164H is related to its presence only during the initial acute ischemic injury or whether cTnIA164H has

a more global affect on the heart which is capable of preventing or even reversing myocardial remodeling when delivered after the initial ischemic injury? These questions take engineered cTnIA164H out of the context of initial transgenic studies and into the applicable realm of clinical medicine and the diverse mechanisms of delivering therapeutics relative to disease onset.

Clinical approaches for therapeutic treatment of ischemic cardiomyopathy are variable based on the temporal separation of injury from intervention. Specifically, for high risk patients therapies are often prescribed preemptively. In other cases interventions occur at the time of ischemic injury or, as in chronic ischemic cardiomyopathy, may occur long after the injury. To determine if cTnIA164H is effective for treatment of ischemic heart disease, these time points will be incorporated into the experimental design as separate clinical models. Permanent ligation of the LCA as previously described[246, 470] will be used to model chronic ischemic cardiomyopathy with an expected infarct size of thirty to forty percent of the left ventricle. The general experimental approach for Specific Aim 2 will be as follows: relative to the time of LCA ligation, rAAV cTnIA164H will be delivered systemically by a single tail vein injection four weeks prior to injury (cohort 1), at the time of injury (cohort 2), two weeks after the injury (cohort 3), and two months after the injury (cohort 4).

To assess the efficacy of this treatment in these models, several methodological assays will be used to measure changes in cardiac structure and function. To begin, after acquiring baseline echo data on mice from all groups, serial echo measurements will continue to be performed at specific time points to

observe changes in disease progression. As a terminal experiment at six months post LCA ligation all mice will undergo conductance micromanometry for acquisition of hemodynamic function. Heart weight to body weight ratios will be measured in addition to analysis of infarct size and area at risk. Lastly, histology of frozen whole heart sections will be performed using H&E as well as trichrome staining to show any post-MI morphological changes as well as the extent of necrosis.

Results from all assays performed in Specific Aim 2 are expected to show that *preemptive* gene therapy of cTnIA164H (cohort 1) will be the most efficacious at improving inotropy and attenuating myocardial remodeling during the disease progression of chronic ischemic cardiomyopathy. In this model, improved calcium sensitivity and the subsequent shift in the Frank-Starling curve at baseline and increasingly during post-infarction ischemia will enable the heart to retain contractility, and consequently cardiac output, while protecting global left ventricular geometry. Over six months of serial echo, this will be characterized by improved systolic function, decreased LV diastolic dimensions and volumes, and reduced heart-weight to body weight ratio in cTnIA164H transduced mice compared to controls. At the six month endpoint, analysis by conductance micromanometry is expected to corroborate echo data showing that improved myocardial structure and function correlate with cTnIA164H treatment. Consistent with previous data, an abrogated hypertrophic response in cTnIA164H transduced hearts is expected to yield an increase in *relative* infarct size and area at risk compared to controls. However, histological analysis of

heart sections is expected to show that cTnIA164H treated hearts have reduced necrosis and less myofibrillar disarray in the peri-infarct zone and non infarcted myocardium relative to controls. In cohorts two, three, and four gradations of improved inotropy and attenuated remodeling are expected to show a correlation between time of injury and delivery of cTnIA164H. Despite the delay in treatment, these clinically relevant treatment modalities are expected to show that in all cases therapeutic intervention using cTnIA164H will improve contractility and alter the course of myocardial remodeling. Furthermore, experimental designs for cohorts three and four will provide models to determine whether AAV-mediated delivery of cTnIA164H results in *reverse myocardial remodeling.* Improved inotropy as well as changes in myocyte morphology and calcium homeostasis associated with long term cTnIA164H expression may provide a basis for reverse remodeling[246]. It is arguable that these structural and functional improvements would result in a reduction of both eccentric hypertrophy and LV dilation. Previous studies have shown reverse remodeling after mechanical interventions using left ventricular assist devices (LVAD)[471]. LVADs are specifically designed to attenuate LV wall stress by reducing end diastolic volume while still retaining sufficient cardiac output. Based on the Frank-Starling law, reverse remodeling is an achievable outcome of this therapy. Similarly, it follows that the biochemistry of cTnIA164H provides a mechanism for improving contractility such that, again, the same cardiac output can be achieved with reduced LV end diastolic volume. This would be the first study to show reverse myocardial remodeling by means of a simple biochemical alteration of a myofilament protein.

Mice transduced with cTnIA164H will be compared to controls including sham operated mice transduced with cTnIA164H as well as mice with LCA ligation transduced with wild type cTnIFLAG.

Evidence to support the null hypothesis would suggest that certain developmentally acquired compensatory traits in the cTnIA164H transgenic mouse likely account for maintenance of contractility and attenuation of myocardial remodeling observed in a model of chronic myocardial ischemia. In addition to changes in calcium homeostasis that may contribute to abrogating the pathophysiology of chronic ischemia, acquired morphologic changes including a reduced myocyte size in transgenic hearts could also account for attenuated remodeling in the case of chronic myocardial infarction. In this way, the null hypothesis is informative, providing the basis for further analysis of morphologic changes and alterations in calcium homeostasis in protecting the heart from chronic ischemic injury. However, the argument remains that developmentally acquired compensatory changes in the transgenic mouse may *blunt* the potent effects of cTnIA164H[461]. AAV mediated gene transfer into the adult heart would consequently enhance the functional and structural effects of cTnIA164H. Other potentially informative non-hemodynamic assays to study the efficacy of cTnIA164H to protect cardiovascular function include analysis of metabolic oxygen consumption or expression of heart failure markers such as β-MyHC, BNP/ANF, and changes in the SERCA/Plb ratio.

Part II: Site directed mutagenesis to determine the mechanism of the regulatory interaction between TnI and TnC

The studies outlined in this dissertation provide some progress in the way of understanding troponin function in the context of the myofilaments. However, our basic understanding of troponin performance as a critical regulatory complex requires further investigation. A powerful methodology to further delineate the role of single amino acids in this regulatory interaction of troponin can be accomplished by site-directed mutagenesis followed by adenoviral-mediated gene transfer into adult cardiac myocytes (as described previously[104, 202, 246, 314, 319, 333, 392]). Genetically modified cardiac myocytes can then be used to understand the effect of specific protein modifications on contractile performance of intact myocytes and calcium sensitivity of the myofilaments in permeabilized myocytes.

Overall, the goal of these assays would be to determine the role of amino acids at the interface of the calcium saturated cTnI:cTnC structure in regulating contractility.

To begin, it would be interesting to determine whether cTnC E19, as opposed to any other acidic residue in the N-terminal hydrophobic patch, has a dominant effect in regulating contact with cTnI in the calcium saturated state. The studies outlined in this dissertation provide a basis with which to generate additional troponin mutants to further understand this regulatory interaction

between TnI and TnC. Specifically, I have generated cTnC mutants containing alanine mutants of some of the key acidic residues known to decorate the rim of the hydrophobic patch (E19A and D25A). The molecular modeling studies (chapters 2 and 5) provide strong evidence for the role of E19A as a key residue involved in the electrostatic binding between cTnC and TnI (slow skeletal and cardiac) in the calcium saturated state. If this is true, I would hypothesize that the E19A mutant will markedly diminish the contractile performance of myocytes compared to D25A. Furthermore, given the very close and stabile interaction between H132 and E19 in the slow skeletal complex compared to the transient interaction between R163 and E19 in the cardiac complex I would hypothesize that the E19A mutant would have a greater effect on the contractile performance of the skeletal complex. Using permeabilized myocytes and assessing calcium activated isometric tension, I would hypothesize that the E19A mutant would decrease the calcium sensitivity of the myofilaments, again, with the greater effect being seen in the skeletal complex compared to the cardiac complex. Furthermore, I would hypothesize that the D25A mutant would have very minimal effects on calcium sensitivity of the myofilaments, at least based on structural modeling of the TnI interaction with this residue. Together, these studies would provide key insights into the role of acidic residues of the hydrophobic patch of cTnC on troponin regulatory function.

In additional experiments, it would be interesting to determine whether a proline in the cTnI switch arm functions as a biochemical correlate to alanine.

Phylogenetic data provide evidence that a proline residue may have acted as an intermediate moiety between the cTnI histidine of ancestral species and the alanine observed in mammals. To test the hypothesis that proline acts to break the key high energy intermolecular contact with cTnC E19, mutagenesis experiments could be performed by generating an ssTnI H132P molecule. I would hypothesize that very similar results would be obtained compared to the ssTnI H132A mutant. Alternatively, one could generate a cTnI A164P molecule. I would hypothesize that this protein would not have marked differences in contractility compared to WT cTnI.

In other mutagenesis experiments, it would be informative to determine whether a single amino acid modification, ssTnI L122 to cTnI M156 markedly alters contractility and provides insight into the functional difference between the cTnI and ssTnI isoforms. Molecular dynamic simulations using alanine scanning to calculate the binding free energy at the interface of sTnI and cTnC showed that ssTnI leucine 122 contributes significantly to the free energy of binding between TnC and TnI (0.84 kcal/mol). This is compared to the >0.99 kcal/mol contribution generated by histidine. Structural analysis of sTnI-cTnC show that Leu122 interacts with cTnC Phe20 (2.3 angstroms) providing a substrate for intermolecular hydrophobic contacts. In all species ssTnI L122 is converted to methionine (M156) in cardiac TnI. This would indicate that there is a unique function for these hydrophobic residues in mediating the functional difference between ssTnI and cTnI. In the simulated cTnI structure, M156 has an

intermolecular distance from Phe20 of 2.4 angstroms which likely is a significant contributor to the hydrophobic strength of the cTnI-cTnC interaction (Figure 7-3a). If mutagenesis was performed on cTnC Phe20 (F20A) I would hypothesize a similar reduction in contractile performance when cTnC F20A is complexed with ssTnI and cTnI.

Furthermore, it would be interesting to determine the role of basic residues in mediating the electrostatic contacts between cTnI and cTnC in the calcium saturated state. The molecular simulations show that cTnI R163 is critical for generating electrostatic interactions with cTnC E19 (distance = 2.0 angstroms) (Figure 7-3b). In contrast, K 165 which flanks the opposite side of the alanine, does not appear to have any role in electrostatically mediating the interaction between cTnI and cTnC. One could test this hypothesis by mutating both residues (R163A and K165A) to determine which of these is most important for electrastic binding to TnC. Molecular modeling supports R163 in this role suggesting that K165 would not have any (or mild) effect on contractility of cTnI. Alignment data show that R163 and K165 are basic residues in all TnI isoforms of all species across chordate evolution (with the exception of a threonine in place of R163 in xenopus). Assuming that K165 does not effect cTnI binding to cTnC in the calcium saturated state, it is possible (given the high conservation of this residue) that it is a key mediator for the binding of this domain to actin during diastole. However, there is no structural evidence to support this.

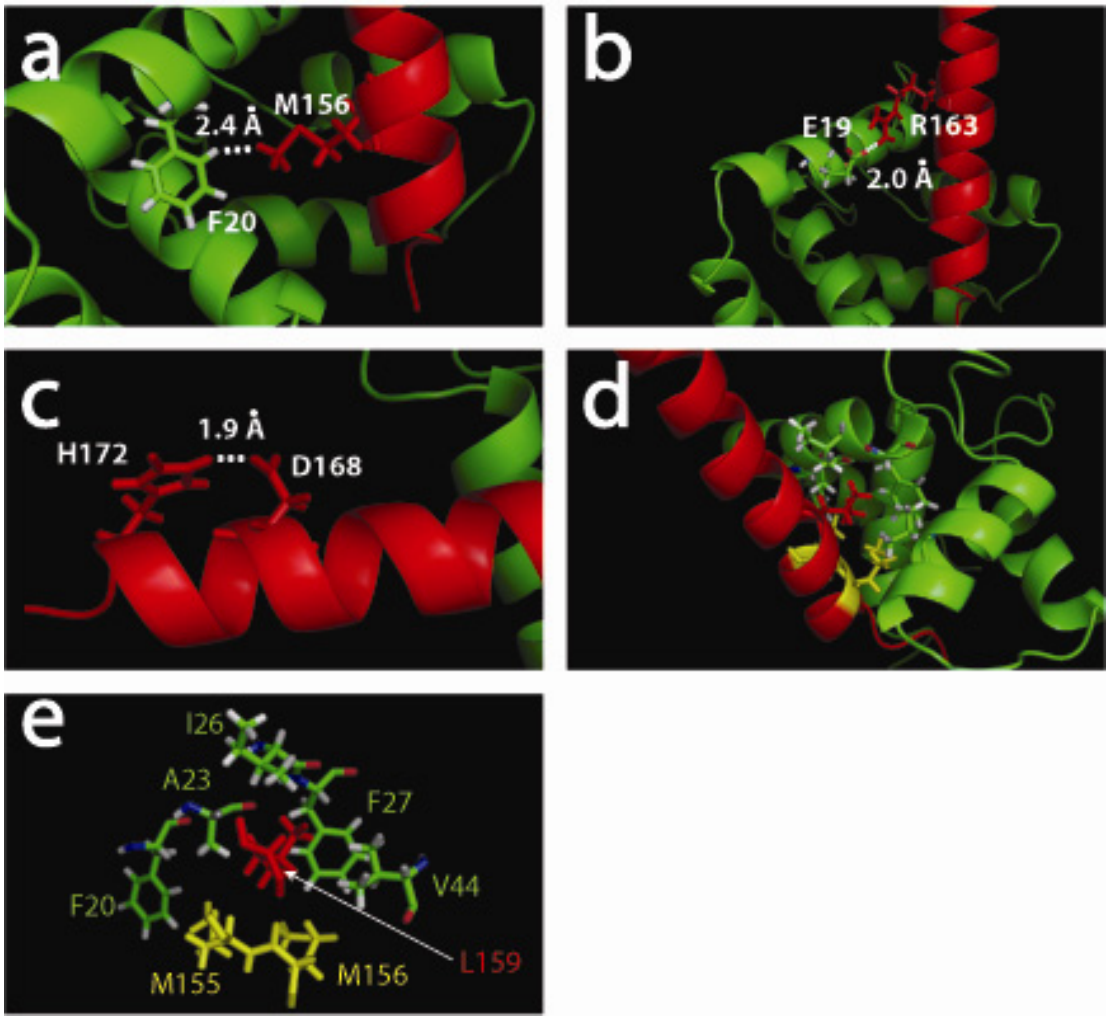

Figure 7-3. Testable hypotheses for residues important in cTn function. (a) cTnI M156 interaction with cTnC F20. (b) cTnI R163 interaction with cTnC E19 is the key electrostatic interaction of cTn. (c) cTnI H172 – D168 interaction potentially important in helix stabilization. (d, e) Residues important for the hydrophobic contacts between cTnC and cTnI with an emphasis on L159. (d) Residues within the ribbon structure and (e) clearer representation of the position of hydrophobic residues between cTnC (green) and cTnI (Methionine residues: yellow; Leucine 159: red).

To study the importance of structural features, it would be interesting to determine if cTnI switch domain helix stability is important for mediating contractility. In contrast to ssTnI which has an extended, unstructured domain interacting with cTnC, the cTnI switch domain is helical. Based on molecular simulation structures, the substitutions that would theoretically disrupt the helical stability of cTnI H4 include: H172A and D168A (these residues form a salt bridge in the simulated structure; distance = 1.9 angstroms) (Figure 7-3c). Mutagenesis experiments that disrupt this salt bridge would like extend the helix. Given that this helical stabilization is beyond the key cTnC E19- cTnI R163 interaction, it is difficult to determine exactly what effect this might have on contractile performance.

Lastly, it would be interesting to determine whether cTnI L159 is the most important residue involved in the hydrophobic contact with cTnC in the calcium saturated state. It has long been established that hydrophobic interactions mediate a large part of the contact of the cTnI switch domain to the N-terminus of cTnC. Molecular simulations of the calcium saturated cTn structure indicate that L159 is likely the most important hydrophobic moiety in cTnI that interacts with a number of hydrophobic residues on numerous helices of cTnC (Figure 7-3d,e). In the original 1j1e crystal structure, L160 is shown to make hydrophobic contacts with cTnC. However, molecular simulation structures indicate that L160 is solvent exposed and thus has no interactions with cTnC. Furthermore, cTnI M155 and M156 interact with Phe moieties on cTnC but have markedly reduced

hydrophobic contacts compared to L159. These data would suggest that, more than any other hydrophobic residue on cTnI, mutation of L156 would significantly decrease the binding affinity of the switch domain and thus diminish contractility because of the loss of a key hydrophobic interaction between these molecules. Molecular dynamics simulations with alanine scanning (as performed in chapter 2) could be used to *in silico* prove this point followed by functional assessments *in vitro.*

Part III: Calcium cycling and myofilament calcium sensitivity

I would like to propose a hypothesis that ties together regulation of calcium sensitivity of the myofilaments and dynamic modulation of calcium activation. The current data indicate that cTnI A164H alone is able to modulate calcium cycling in single and double (cross with PLN KO) Tg mice. Several studies of Tg mice containing amino acid mutations in the Tn complex indicate a correlation between heightened myofilament calcium sensitivity and differential remodeling of calcium handling. First, in a study by Du et al. a knock-in model of dilated cardiomyopathy caused by a deletion in TnT (TnT Δ210-219) showed decreased calcium sensitivity with a correlative increase in calcium transient amplitude compaired to control[472]. A report by Baudenbacher et al showed that the TnT F110I mutant has a mild increase in calcium sensitivity compared to controls. However, calcium cycling and SR storage have not been reported on this model. In terms of the cTnI A164H Tg mouse, there is a marked increase in

calcium sensitivity of the myofilaments compared to controls with a correlative decrease in SR calcium storage compared to controls[246, 290]. Studies by Knollmann and colleagues have shown that the TnT I79N mutation has increased myofilament calcium sensitivity with reduced calcium transients[473]. As mentioned previously, the ssTnI Tg mouse has heightend calcium sensitivity of the myofilaments with no changes in calcium transient amplitude[213]. Lastly, unpublished data of the cTnI R193H transgenic mouse also indicate that myofilaments containing this mutant protein have heightened calcium sensitivity without changes in calcium transients compared to WT mice. Reported measures of myofilament calcium sensitivity place these mice in the following order: TnTΔ210-219 < WT < TnT F110I < cTnI A164H = TnT I79N = ssTnI = cTnI R193H. With the exception of unreported data on the TnT F110I mutant, calcium appears to increase with decreased myofilament calcium sensitivity (TnT Δ210-219) and subsequently decrease with progressive increases in calcium sensitivity (WT through TnT I79N). In the last 2 cases (ssTnI and cTnI R193H) calcium is not different from WT levels. Functionally, reports have shown that compared to WT mice, cTnI A164H and TnT I79N do not have reproducible diastolic dysfunction in every assay[246, 474]. In contrast, ssTnI and cTnI R193H show profound diastolic dysfunction compared to WT mice in every measure of lusitropy[213](R193H data not reported).

These data indicate that there may be a correlation between calcium cycling and myofilament calcium sensitivity within a certain working range. In other words, remodeling of calcium cycling may be allowable within a range

where decreases in activating calcium are advantageous to maintain diastolic performance as much as possible. To test this hypothesis, we could cross the PLN KO mouse with all or some of these lines with a specific focus on models that provide a range of calcium sensitization. If the hypothesis is true then the TnT Δ210-219 would perhaps increase calcium cycling compared to WT mice. In contrast, TnT F110I and TnT I79N would decrease activating calcium similar to observations with cTnI A164H. Lastly, similar with the ssTnI PLN KO double Tg mouse, cTnI R193H crossed with PLN KO would not decrease calcium cycling because it is outside of the domain in which modulation of calcium cycling would benefit cardiac performance. At the very least, these observed differences at the level of single Tg mice are consistant with the hypothesis and as such lead to the potential of testing whether similar modulation occurs in a model of heightened calcium cycling such as the PLN KO mouse.

These assays simply address whether calcium sensitivity actually influences calcium cycling. However it provides no insight into the mechanism by which this occurs. Additionally, important questions to assess include whether this modulation of calcium cycling occurs exclusively during heart development *in vivo.* It would also be important to determine if calcium cycling is modulated *in vitro* after genetic modification of myocytes and if there is a dose dependent response of protein incorporation with calcium activation.

BIBLIOGRAPHY

1. Bishopric NH. Evolution of the heart from bacteria to man. *Ann N Y Acad Sci.* 2005;1047:13-29.
2. Schiaffino S, Reggiani C. Molecular diversity of myofibrillar proteins: Gene regulation and functional significance. *Physiological Reviews.* 1996;76(2):371-423.
3. Willis MS, Schisler JC, Portbury AL, Patterson C. Build it up-Tear it down: protein quality control in the cardiac sarcomere. *Cardiovasc Res.* 2009;81(3):439-448.
4. Shiels HA, White E. The Frank-Starling mechanism in vertebrate cardiac myocytes. *J Exp Biol.* 2008;211(Pt 13):2005-2013.
5. Lillywhite HB, Zippel KC, Farrell AP. Resting and maximal heart rates in ectothermic vertebrates. *Comp Biochem Physiol A Mol Integr Physiol.* 1999;124(4):369-382.
6. Mendonca PC, Genge AG, Deitch EJ, Gamperl AK. Mechanisms responsible for the enhanced pumping capacity of the in situ winter flounder heart (Pseudopleuronectes americanus). *Am J Physiol Regul Integr Comp Physiol.* 2007;293(5):R2112-2119.
7. Jurgens KD, Fons R, Peters T, Sender S. Heart and respiratory rates and their significance for convective oxygen transport rates in the smallest mammal, the Etruscan shrew Suncus etruscus. *J Exp Biol.* 1996;199(Pt 12):2579-2584.
8. Stanley WC, Recchia FA, Lopaschuk GD. Myocardial Substrate Metabolism in the Normal and Failing Heart. *Physiol. Rev.* 2005;85(3):1093-1129.
9. Metzger JM, Westfall MV. Covalent and Noncovalent Modification of Thin Filament Action: The Essential Role of Troponin in Cardiac Muscle Regulation. *Circulation Research.* 2004;94(2):146-158.
10. Brodde OE. Beta-adrenoceptor blocker treatment and the cardiac beta-adrenoceptor-G-protein(s)-adenylyl cyclase system in chronic heart failure. *Naunyn Schmiedebergs Arch Pharmacol.* 2007;374(5-6):361-372.
11. Brutsaert DL, Sys SU. Relaxation and diastole of the heart. *Physiol Rev.* 1989;69(4):1228-1315.
12. Swynghedauw B. Molecular mechanisms of myocardial remodeling. *Physiol Rev.* 1999;79(1):215-262.
13. Taylor EW, Jordan D, Coote JH. Central control of the cardiovascular and respiratory systems and their interactions in vertebrates. *Physiol Rev.* 1999;79(3):855-916.
14. Thom T, Haase N, Rosamond W, Howard VJ, Rumsfeld J, Manolio T, Zheng ZJ, Flegal K, O'Donnell C, Kittner S, Lloyd-Jones D, Goff DC, Jr., Hong Y, Adams R, Friday G, Furie K, Gorelick P, Kissela B, Marler J, Meigs J, Roger V, Sidney S, Sorlie P, Steinberger J, Wasserthiel-Smoller

S, Wilson M, Wolf P. Heart disease and stroke statistics--2006 update: a report from the American Heart Association Statistics Committee and Stroke Statistics Subcommittee. *Circulation.* 2006;113(6):e85-151.
15. Huxley HE. Fifty years of muscle and the sliding filament hypothesis. *Eur J Biochem.* 2004;271(8):1403-1415.
16. Maughan DW. Kinetics and energetics of the crossbridge cycle. *Heart Fail Rev.* 2005;10(3):175-185.
17. Gordon AM, ter Keurs HE. Molecular and cellular aspects of muscle contraction. General discussion part II. *Adv Exp Med Biol.* 2003;538:661-669, 687-668.
18. Gordon AM, Homsher E, Regnier M. Regulation of Contraction in Striated Muscle. *Physiol. Rev.* 2000;80(2):853-924.
19. Moss RL, Razumova M, Fitzsimons DP. Myosin Crossbridge Activation of Cardiac Thin Filaments: Implications for Myocardial Function in Health and Disease. *Circ Res.* 2004;94(10):1290-1300.
20. Moss RL, Fitzsimons DP. Myosin Light Chain 2 Into the Mainstream of Cardiac Development and Contractility. *Circulation Research.* 2006;99(3):225-227.
21. Herron TJ, Devaney EJ, Metzger JM. Modulation of cardiac performance by motor protein gene transfer. *Ann N Y Acad Sci.* 2008;1123:96-104.
22. Hinken AC, Solaro RJ. A Dominant Role of Cardiac Molecular Motors in the Intrinsic Regulation of Ventricular Ejection and Relaxation. *Physiology.* 2007;22(2):73-80.
23. Haselgrove JC, Huxley HE. X-ray evidence for radial cross-bridge movement and for the sliding filament model in actively contracting skeletal muscle. *J Mol Biol.* 1973;77(4):549-568.
24. Herron TJ, Vandenboom R, Fomicheva E, Mundada L, Edwards T, Metzger JM. Calcium-independent negative inotropy by beta-myosin heavy chain gene transfer in cardiac myocytes. *Circ Res.* 2007;100(8):1182-1190.
25. Harris DE, Work SS, Wright RK, Alpert NR, Warshaw DM. Smooth, cardiac and skeletal muscle myosin force and motion generation assessed by cross-bridge mechanical interactions in vitro. *J Muscle Res Cell Motil.* 1994;15(1):11-19.
26. Malmqvist UP, Aronshtam A, Lowey S. Cardiac myosin isoforms from different species have unique enzymatic and mechanical properties. *Biochemistry.* 2004;43(47):15058-15065.
27. Palmiter KA, Tyska MJ, Dupuis DE, Alpert NR, Warshaw DM. Kinetic differences at the single molecule level account for the functional diversity of rabbit cardiac myosin isoforms. *J Physiol.* 1999;519 Pt 3:669-678.
28. Cooke R. Actomyosin interaction in striated muscle. *Physiol. Rev.* 1997;77(3):671-697.
29. Kobayashi T, Solaro RJ. CALCIUM, THIN FILAMENTS, AND THE INTEGRATIVE BIOLOGY OF CARDIAC CONTRACTILITY. *Annual Review of Physiology.* 2005;67(1):39-67.

30. Guan JQ, Takamoto K, Almo SC, Reisler E, Chance MR. Structure and dynamics of the actin filament. *Biochemistry.* 2005;44(9):3166-3175.
31. Holmes KC, Popp D, Gebhard W, Kabsch W. Atomic model of the actin filament. *Nature.* 1990;347(6288):44-49.
32. Lorenz M, Poole KJ, Popp D, Rosenbaum G, Holmes KC. An atomic model of the unregulated thin filament obtained by X-ray fiber diffraction on oriented actin-tropomyosin gels. *J Mol Biol.* 1995;246(1):108-119.
33. Farah CS, Reinach FC. The troponin complex and regulation of muscle contraction. *The FASEB Journal.* 1995;9(9):755-767.
34. Phillips GN, Jr., Cohen C, Stewart M. A new crystal form of tropomyosin. Preliminary X-ray diffraction analysis. *J Mol Biol.* 1987;195(1):219-223.
35. Whitby FG, Phillips GN, Jr. Crystal structure of tropomyosin at 7 Angstroms resolution. *Proteins.* 2000;38(1):49-59.
36. Phillips GN, Jr., Fillers JP, Cohen C. Tropomyosin crystal structure and muscle regulation. *J Mol Biol.* 1986;192(1):111-131.
37. Brown JH, Kim KH, Jun G, Greenfield NJ, Dominguez R, Volkmann N, Hitchcock-DeGregori SE, Cohen C. Deciphering the design of the tropomyosin molecule. *Proc Natl Acad Sci U S A.* 2001;98(15):8496-8501.
38. Murakami K, Stewart M, Nozawa K, Tomii K, Kudou N, Igarashi N, Shirakihara Y, Wakatsuki S, Yasunaga T, Wakabayashi T. Structural basis for tropomyosin overlap in thin (actin) filaments and the generation of a molecular swivel by troponin-T. *Proceedings of the National Academy of Sciences.* 2008;105(20):7200-7205.
39. Potter JD. The content of troponin, tropomyosin, actin, and myosin in rabbit skeletal muscle myofibrils. *Arch Biochem Biophys.* 1974;162(2):436-441.
40. Yates LD, Greaser ML. Troponin subunit stoichiometry and content in rabbit skeletal muscle and myofibrils. *J Biol Chem.* 1983;258(9):5770-5774.
41. Shiner JS, Solaro RJ. Activation of thin-filament-regulated muscle by calcium ion: considerations based on nearest-neighbor lattice statistics. *Proc Natl Acad Sci U S A.* 1982;79(15):4637-4641.
42. Solaro RJ, Van Eyk J. Altered interactions among thin filament proteins modulate cardiac function. *J Mol Cell Cardiol.* 1996;28(2):217-230.
43. Parry DA, Squire JM. Structural role of tropomyosin in muscle regulation: analysis of the x-ray diffraction patterns from relaxed and contracting muscles. *J Mol Biol.* 1973;75(1):33-55.
44. Chalovich JM, Eisenberg E. Inhibition of actomyosin ATPase activity by troponin-tropomyosin without blocking the binding of myosin to actin. *J. Biol. Chem.* 1982;257(5):2432-2437.
45. Lehrer SS, Morris EP. Comparison of the effects of smooth and skeletal tropomyosin on skeletal actomyosin subfragment 1 ATPase. *J. Biol. Chem.* 1984;259(4):2070-2072.

46. Valerie B. Patchell CEGMAHAFSVPBAL. The inhibitory region of troponin-I alters the ability of F-actin to interact with different segments of myosin. *European Journal of Biochemistry.* 2002;269(20):5088-5100.
47. Patchell VB, Gallon CE, Evans JS, Gao Y, Perry SV, Levine BA. The Regulatory Effects of Tropomyosin and Troponin-I on the Interaction of Myosin Loop Regions with F-actin. *J. Biol. Chem.* 2005;280(15):14469-14475.
48. Ebashi S, Kodama A. A new protein factor promoting aggregation of tropomyosin. *J Biochem.* 1965;58(1):107-108.
49. Greaser ML, Gergely J. Reconstitution of troponin activity from three protein components. *J Biol Chem.* 1971;246(13):4226-4233.
50. Filatov VL, Katrukha AG, Bulargina TV, Gusev NB. Troponin: structure, properties, and mechanism of functioning. *Biochemistry (Mosc).* 1999;64(9):969-985.
51. Vinogradova MV, Stone DB, Malanina GG, Karatzaferi C, Cooke R, Mendelson RA, Fletterick RJ. Ca(2+)-regulated structural changes in troponin. *Proc Natl Acad Sci U S A.* 2005;102(14):5038-5043.
52. Takeda S, Yamashita A, Maeda K, Maeda Y. Structure of the core domain of human cardiac troponin in the Ca2+-saturated form. *Nature.* 2003;424(6944):35-41.
53. Nassar R, Malouf NN, Kelly MB, Oakeley AE, Anderson PA. Force-pCa relation and troponin T isoforms of rabbit myocardium. *Circ Res.* 1991;69(6):1470-1475.
54. Schachat FH, Diamond MS, Brandt PW. Effect of different troponin T-tropomyosin combinations on thin filament activation. *J Mol Biol.* 1987;198(3):551-554.
55. Farah CS, Miyamoto CA, Ramos CH, da Silva AC, Quaggio RB, Fujimori K, Smillie LB, Reinach FC. Structural and regulatory functions of the NH2- and COOH-terminal regions of skeletal muscle troponin I. *Journal of Biological Chemistry.* 1994;269(7):5230-5240.
56. Potter JD, Sheng Z, Pan BS, Zhao J. A direct regulatory role for troponin T and a dual role for troponin C in the Ca2+ regulation of muscle contraction. *J Biol Chem.* 1995;270(6):2557-2562.
57. Mak AS, Smillie LB. Non-polymerizable tropomyosin: preparation, some properties and F-actin binding. *Biochem Biophys Res Commun.* 1981;101(1):208-214.
58. Blumenschein TM, Tripet BP, Hodges RS, Sykes BD. Mapping the interacting regions between troponins T and C. Binding of TnT and TnI peptides to TnC and NMR mapping of the TnT-binding site on TnC. *J Biol Chem.* 2001;276(39):36606-36612.
59. Maytum R, Geeves MA, Lehrer SS. A modulatory role for the troponin T tail domain in thin filament regulation. *J Biol Chem.* 2002;277(33):29774-29780.
60. Tobacman LS, Nihli M, Butters C, Heller M, Hatch V, Craig R, Lehman W, Homsher E. The troponin tail domain promotes a conformational state of

the thin filament that suppresses myosin activity. *J Biol Chem.* 2002;277(31):27636-27642.
61. van Eerd JP, Takahashi K. The amino acid sequence of bovine cardiac tamponin-C. Comparison with rabbit skeletal troponin-C. *Biochem Biophys Res Commun.* 1975;64(1):122-127.
62. Zot HG, Potter JD. A structural role for the Ca2+-Mg2+ sites on troponin C in the regulation of muscle contraction. Preparation and properties of troponin C depleted myofibrils. *J Biol Chem.* 1982;257(13):7678-7683.
63. Herzberg O, James MN. Structure of the calcium regulatory muscle protein troponin-C at 2.8 A resolution. *Nature.* 1985;313(6004):653-659.
64. Sia SK, Li MX, Spyracopoulos L, Gagne SM, Liu W, Putkey JA, Sykes BD. Structure of cardiac muscle troponin C unexpectedly reveals a closed regulatory domain. *J Biol Chem.* 1997;272(29):18216-18221.
65. Slupsky CM, Sykes BD. NMR solution structure of calcium-saturated skeletal muscle troponin C. *Biochemistry.* 1995;34(49):15953-15964.
66. Sun YB, Brandmeier B, Irving M. Structural changes in troponin in response to Ca2+ and myosin binding to thin filaments during activation of skeletal muscle. *Proc Natl Acad Sci U S A.* 2006;103(47):17771-17776.
67. Babu A, Rao VG, Su H, Gulati J. Critical minimum length of the central helix in troponin C for the Ca2+ switch in muscular contraction. *J Biol Chem.* 1993;268(26):19232-19238.
68. Sheng ZL, Francois JM, Hitchcock-DeGregori SE, Potter JD. Effects of mutations in the central helix of troponin C on its biological activity. *J Biol Chem.* 1991;266(9):5711-5715.
69. Babu A, Scordilis SP, Sonnenblick EH, Gulati J. The control of myocardial contraction with skeletal fast muscle troponin C. *J Biol Chem.* 1987;262(12):5815-5822.
70. Gulati J, Scordilis S, Babu A. Effect of troponin C on the cooperativity in Ca2+ activation of cardiac muscle. *FEBS Lett.* 1988;236(2):441-444.
71. Holroyde MJ, Robertson SP, Johnson JD, Solaro RJ, Potter JD. The calcium and magnesium binding sites on cardiac troponin and their role in the regulation of myofibrillar adenosine triphosphatase. *J Biol Chem.* 1980;255(24):11688-11693.
72. Kretsinger RH, Nockolds CE. Carp muscle calcium-binding protein. II. Structure determination and general description. *J Biol Chem.* 1973;248(9):3313-3326.
73. Sweeney HL, Brito RM, Rosevear PR, Putkey JA. The low-affinity Ca2(+)-binding sites in cardiac/slow skeletal muscle troponin C perform distinct functions: site I alone cannot trigger contraction. *Proc Natl Acad Sci U S A.* 1990;87(24):9538-9542.
74. Putkey JA, Sweeney HL, Campbell ST. Site-directed mutation of the trigger calcium-binding sites in cardiac troponin C. *J Biol Chem.* 1989;264(21):12370-12378.

75. Robertson SP, Johnson JD, Potter JD. The time-course of Ca2+ exchange with calmodulin, troponin, parvalbumin, and myosin in response to transient increases in Ca2+. *Biophys J.* 1981;34(3):559-569.
76. Johnson JD, Charlton SC, Potter JD. A fluorescence stopped flow analysis of Ca2+ exchange with troponin C. *J Biol Chem.* 1979;254(9):3497-3502.
77. Gagne SM, Tsuda S, Li MX, Smillie LB, Sykes BD. Structures of the troponin C regulatory domains in the apo and calcium-saturated states. *Nat Struct Biol.* 1995;2(9):784-789.
78. Li MX, Gagne SM, Spyracopoulos L, Kloks CP, Audette G, Chandra M, Solaro RJ, Smillie LB, Sykes BD. NMR studies of Ca2+ binding to the regulatory domains of cardiac and E41A skeletal muscle troponin C reveal the importance of site I to energetics of the induced structural changes. *Biochemistry.* 1997;36(41):12519-12525.
79. McKay RT, Saltibus LF, Li MX, Sykes BD. Energetics of the induced structural change in a Ca2+ regulatory protein: Ca2+ and troponin I peptide binding to the E41A mutant of the N-domain of skeletal troponin C. *Biochemistry.* 2000;39(41):12731-12738.
80. Brito RM, Putkey JA, Strynadka NC, James MN, Rosevear PR. Comparative NMR studies on cardiac troponin C and a mutant incapable of binding calcium at site II. *Biochemistry.* 1991;30(42):10236-10245.
81. Kobayashi T, Zhao X, Wade R, Collins JH. Involvement of conserved, acidic residues in the N-terminal domain of troponin C in calcium-dependent regulation. *Biochemistry.* 1999;38(17):5386-5391.
82. Brito RM, Krudy GA, Negele JC, Putkey JA, Rosevear PR. Calcium plays distinctive structural roles in the N- and C-terminal domains of cardiac troponin C. *J Biol Chem.* 1993;268(28):20966-20973.
83. Pan BS, Solaro RJ. Calcium-binding properties of troponin C in detergent-skinned heart muscle fibers. *J Biol Chem.* 1987;262(16):7839-7849.
84. Hazard AL, Kohout SC, Stricker NL, Putkey JA, Falke JJ. The kinetic cycle of cardiac troponin C: calcium binding and dissociation at site II trigger slow conformational rearrangements. *Protein Sci.* 1998;7(11):2451-2459.
85. Johnson JD, Collins JH, Robertson SP, Potter JD. A fluorescent probe study of Ca2+ binding to the Ca2+-specific sites of cardiac troponin and troponin C. *J Biol Chem.* 1980;255(20):9635-9640.
86. Dong WJ, Cheung HC. Calcium-induced conformational change in cardiac troponin C studied by fluorescence probes attached to Cys-84. *Biochim Biophys Acta.* 1996;1295(2):139-146.
87. Putkey JA, Liu W, Lin X, Ahmed S, Zhang M, Potter JD, Kerrick WG. Fluorescent probes attached to Cys 35 or Cys 84 in cardiac troponin C are differentially sensitive to Ca(2+)-dependent events in vitro and in situ. *Biochemistry.* 1997;36(4):970-978.
88. Perry SV. Troponin I: inhibitor or facilitator. *Mol Cell Biochem.* 1999;190(1-2):9-32.
89. Siedner S, Kruger M, Schroeter M, Metzler D, Roell W, Fleischmann BK, Hescheler J, Pfitzer G, Stehle R. Developmental changes in contractility

and sarcomeric proteins from the early embryonic to the adult stage in the mouse heart. *Journal of Physiology-London.* 2003;548(2):493-505.
90. Hunkeler NM, Kullman J, Murphy AM. Troponin I isoform expression in human heart. *Circ Res.* 1991;69(5):1409-1414.
91. Van Eyk JE, Thomas LT, Tripet B, Wiesner RJ, Pearlstone JR, Farah CS, Reinach FC, Hodges RS. Distinct regions of troponin I regulate Ca2+-dependent activation and Ca2+ sensitivity of the acto-S1-TM ATPase activity of the thin filament. *J Biol Chem.* 1997;272(16):10529-10537.
92. Robinson JM, Dong W-J, Xing J, Cheung HC. Switching of Troponin I: Ca2+ and Myosin-induced Activation of Heart Muscle. *Journal of Molecular Biology.* 2004;340(2):295-305.
93. Westfall MV, Albayya FP, Metzger JM. Functional Analysis of Troponin I Regulatory Domains in the Intact Myofilament of Adult Single Cardiac Myocytes. *Journal of Biological Chemistry.* 1999;274(32):22508-22516.
94. Brown LJ, Sale KL, Hills R, Rouviere C, Song L, Zhang X, Fajer PG. Structure of the inhibitory region of troponin by site directed spin labeling electron paramagnetic resonance. *Proceedings of the National Academy of Sciences.* 2002;99(20):12765-12770.
95. Vassylyev DG, Takeda S, Wakatsuki S, Maeda K, Maeda Y. Crystal structure of troponin C in complex with troponin I fragment at 2.3-A resolution. *Proceedings of the National Academy of Sciences.* 1998;95(9):4847-4852.
96. Blumenschein TMA, Tripet BP, Hodges RS, Sykes BD. Mapping the Interacting Regions between Troponins T and C. BINDING OF TnT AND TnI PEPTIDES TO TnC AND NMR MAPPING OF THE TnT-BINDING SITE ON TnC. *J. Biol. Chem.* 2001;276(39):36606-36612.
97. Campbell AP, Sykes BD. Interaction of troponin I and troponin C : Use of the two-dimensional nuclear magnetic resonance transferred nuclear overhauser effect to determine the structure of the inhibitory troponin I peptide when bound to skeletal troponin C. *Journal of Molecular Biology.* 1991;222(2):405-421.
98. Lindhout DA, Sykes BD. Structure and Dynamics of the C-domain of Human Cardiac Troponin C in Complex with the Inhibitory Region of Human Cardiac Troponin I. *J. Biol. Chem.* 2003;278(29):27024-27034.
99. Syska H, Wilkinson JM, Grand RJ, Perry SV. The relationship between biological activity and primary structure of troponin I from white skeletal muscle of the rabbit. *Biochem J.* 1976;153(2):375-387.
100. Sheng Z, Pan BS, Miller TE, Potter JD. Isolation, expression, and mutation of a rabbit skeletal muscle cDNA clone for troponin I. The role of the NH2 terminus of fast skeletal muscle troponin I in its biological activity. *J Biol Chem.* 1992;267(35):25407-25413.
101. Abbott MB, Dong WJ, Dvoretsky A, DaGue B, Caprioli RM, Cheung HC, Rosevear PR. Modulation of Cardiac Troponin C-Cardiac Troponin I Regulatory Interactions by the Amino-terminus of Cardiac Troponin I. *Biochemistry.* 2001;40(20):5992-6001.

102. Baryshnikova OK, Li MX, Sykes BD. Modulation of Cardiac Troponin C Function by the Cardiac-Specific N-Terminus of Troponin I: Influence of PKA Phosphorylation and Involvement in Cardiomyopathies. *Journal of Molecular Biology.* 2008;375(3):735-751.
103. Rarick HM, Tang H-p, Guo X-d, Martin AF, Solaro RJ. Interactions at the NH2-Terminal Interface of Cardiac Troponin I Modulate Myofilament Activation. *Journal of Molecular and Cellular Cardiology.* 1999;31(2):363-375.
104. Westfall MV, Turner I, Albayya FP, Metzger JM. Troponin I chimera analysis of the cardiac myofilament tension response to protein kinase A. *Am J Physiol Cell Physiol.* 2001;280(2):C324-332.
105. Ward DG, Brewer SM, Calvert MJ, Gallon CE, Gao Y, Trayer IP. Characterization of the interaction between the N-terminal extension of human cardiac troponin I and troponin C. *Biochemistry.* 2004;43(13):4020-4027.
106. Ward DG, Brewer SM, Cornes MP, Trayer IP. A cross-linking study of the N-terminal extension of human cardiac troponin I. *Biochemistry.* 2003;42(34):10324-10332.
107. Sadayappan S, Finley N, Howarth JW, Osinska H, Klevitsky R, Lorenz JN, Rosevear PR, Robbins J. Role of the acidic N' region of cardiac troponin I in regulating myocardial function. *FASEB J.* 2008;22(4):1246-1257.
108. Howarth JW, Meller J, Solaro RJ, Trewhella J, Rosevear PR. Phosphorylation-dependent Conformational Transition of the Cardiac Specific N-Extension of Troponin I in Cardiac Troponin. *Journal of Molecular Biology.* 2007;373(3):706-722.
109. Jaquet K, Lohmann K, Czisch M, Holak T, Gulati J, Jaquet R. A model for the function of the bisphosphorylated heart-specific troponin-I N-terminus. *J Muscle Res Cell Motil.* 1998;19(6):647-659.
110. Cachia PJ, Sykes BD, Hodges RS. Calcium-dependent inhibitory region of troponin: a proton nuclear magnetic resonance study on the interaction between troponin C and the synthetic peptide N alpha-acetyl[FPhe106]TnI-(104-115) amide. *Biochemistry.* 1983;22(17):4145-4152.
111. Talbot JA, Hodges RS. Synthetic studies on the inhibitory region of rabbit skeletal troponin I. Relationship of amino acid sequence to biological activity. *J Biol Chem.* 1981;256(6):2798-2802.
112. Talbot JA, Hodges RS. Comparative studies on the inhibitory region of selected species of troponin-I. The use of synthetic peptide analogs to probe structure-function relationships. *J Biol Chem.* 1981;256(23):12374-12378.
113. Van Eyk JE, Hodges RS. The biological importance of each amino acid residue of the troponin I inhibitory sequence 104-115 in the interaction with troponin C and tropomyosin-actin. *J Biol Chem.* 1988;263(4):1726-1732.

114. Tung CS, Wall ME, Gallagher SC, Trewhella J. A model of troponin-I in complex with troponin-C using hybrid experimental data: the inhibitory region is a beta-hairpin. *Protein Sci.* 2000;9(7):1312-1326.
115. Barry A. Levine AJGMSVP. The interaction of troponin-I with the N-terminal region of actin. *European Journal of Biochemistry.* 1988;172(2):389-397.
116. Lehman W, Rosol M, Tobacman LS, Craig R. Troponin organization on relaxed and activated thin filaments revealed by electron microscopy and three-dimensional reconstruction. *J Mol Biol.* 2001;307(3):739-744.
117. Kobayashi T, Patrick SE, Kobayashi M. Ala-scanning of the inhibitory region of cardiac troponin I. *J. Biol. Chem.* 2009:M109.001396.
118. Aihara T, Ueki S, Nakamura M, Arata T. Calcium-dependent movement of troponin I between troponin C and actin as revealed by spin-labeling EPR. *Biochem Biophys Res Commun.* 2006;340(2):462-468.
119. Tripet B, Van Eyk JE, Hodges RS. Mapping of a second actin-tropomyosin and a second troponin C binding site within the C terminus of troponin I, and their importance in the Ca2+-dependent regulation of muscle contraction. *Journal of Molecular Biology.* 1997;271(5):728-750.
120. Rarick HM, Tu XH, Solaro RJ, Martin AF. The C terminus of cardiac troponin I is essential for full inhibitory activity and Ca2+ sensitivity of rat myofibrils. *J Biol Chem.* 1997;272(43):26887-26892.
121. Foster DB, Huang R, Hatch V, Craig R, Graceffa P, Lehman W, Wang CL. Modes of caldesmon binding to actin: sites of caldesmon contact and modulation of interactions by phosphorylation. *J Biol Chem.* 2004;279(51):53387-53394.
122. Galinska-Rakoczy A, Engel P, Xu C, Jung H, Craig R, Tobacman LS, Lehman W. Structural Basis for the Regulation of Muscle Contraction by Troponin and Tropomyosin. *Journal of Molecular Biology.* 2008;379(5):929-935.
123. Tachampa K, Kobayashi T, Wang H, Martin AF, Biesiadecki BJ, Solaro RJ, de Tombe PP. Increased cross-bridge cycling kinetics after exchange of C-terminal truncated troponin I in skinned rat cardiac muscle. *J Biol Chem.* 2008;283(22):15114-15121.
124. Murakami K, Yumoto F, Ohki S-y, Yasunaga T, Tanokura M, Wakabayashi T. Structural Basis for Ca2+-regulated Muscle Relaxation at Interaction Sites of Troponin with Actin and Tropomyosin. *Journal of Molecular Biology.* 2005;352(1):178-201.
125. Hatch V, Zhi G, Smith L, Stull JT, Craig R, Lehman W. Myosin light chain kinase binding to a unique site on F-actin revealed by three-dimensional image reconstruction. *J Cell Biol.* 2001;154(3):611-617.
126. Kobayashi T, Solaro RJ. Increased Ca2+ affinity of cardiac thin filaments reconstituted with cardiomyopathy-related mutant cardiac troponin I. *J Biol Chem.* 2006;281(19):13471-13477.

127. Solaro RJ, Rosevear P, Kobayashi T. The unique functions of cardiac troponin I in the control of cardiac muscle contraction and relaxation. *Biochem Biophys Res Commun.* 2008;369(1):82-87.
128. Greenberg MJ, Wang CL, Lehman W, Moore JR. Modulation of actin mechanics by caldesmon and tropomyosin. *Cell Motil Cytoskeleton.* 2008;65(2):156-164.
129. Isambert H, Venier P, Maggs AC, Fattoum A, Kassab R, Pantaloni D, Carlier MF. Flexibility of actin filaments derived from thermal fluctuations. Effect of bound nucleotide, phalloidin, and muscle regulatory proteins. *J Biol Chem.* 1995;270(19):11437-11444.
130. Gordon AM, Huxley AF, Julian FJ. The variation in isometric tension with sarcomere length in vertebrate muscle fibres. *J Physiol.* 1966;184(1):170-192.
131. Davis J, Westfall MV, Townsend D, Blankinship M, Herron TJ, Guerrero-Serna G, Wang W, Devaney E, Metzger JM. Designing heart performance by gene transfer. *Physiol Rev.* 2008;88(4):1567-1651.
132. Yasuda S, Townsend D, Michele DE, Favre EG, Day SM, Metzger JM. Dystrophic heart failure blocked by membrane sealant poloxamer. *Nature.* 2005;436(7053):1025-1029.
133. Westfall MV, Rust EM, Metzger JM. Slow skeletal troponin I gene transfer, expression, and myofilament incorporation enhances adult cardiac myocyte contractile function. *Proceedings of the National Academy of Sciences.* 1997;94(10):5444-5449.
134. Bers DM. Cardiac excitation-contraction coupling. *Nature.* 2002;415(6868):198-205.
135. Bers DM, Despa S. Cardiac myocytes Ca2+ and Na+ regulation in normal and failing hearts. *J Pharmacol Sci.* 2006;100(5):315-322.
136. Bers DM. Calcium Cycling and Signaling in Cardiac Myocytes. *Annual Review of Physiology.* 2008;70(1):23-49.
137. Kranias EG, Bers DM. Calcium and cardiomyopathies. *Subcell Biochem.* 2007;45:523-537.
138. Wolff MR, McDonald KS, Moss RL. Rate of tension development in cardiac muscle varies with level of activator calcium. *Circ Res.* 1995;76(1):154-160.
139. Fitzsimons DP, Patel JR, Moss RL. Role of myosin heavy chain composition in kinetics of force development and relaxation in rat myocardium. *J Physiol.* 1998;513 (Pt 1):171-183.
140. Kentish JC, McCloskey DT, Layland J, Palmer S, Leiden JM, Martin AF, Solaro RJ. Phosphorylation of troponin I by protein kinase A accelerates relaxation and crossbridge cycle kinetics in mouse ventricular muscle. *Circ Res.* 2001;88(10):1059-1065.
141. Palmer S, Kentish JC. Roles of Ca2+ and crossbridge kinetics in determining the maximum rates of Ca2+ activation and relaxation in rat and guinea pig skinned trabeculae. *Circ Res.* 1998;83(2):179-186.

142. Swartz DR, Yang Z, Sen A, Tikunova SB, Davis JP. Myofibrillar troponin exists in three states and there is signal transduction along skeletal myofibrillar thin filaments. *J Mol Biol.* 2006;361(3):420-435.
143. Hill TL, Eisenberg E, Greene L. Theoretical model for the cooperative equilibrium binding of myosin subfragment 1 to the actin-troponin-tropomyosin complex. *Proc Natl Acad Sci U S A.* 1980;77(6):3186-3190.
144. McKillop DF, Geeves MA. Regulation of the interaction between actin and myosin subfragment 1: evidence for three states of the thin filament. *Biophys J.* 1993;65(2):693-701.
145. Tobacman LS, Butters CA. A new model of cooperative myosin-thin filament binding. *J Biol Chem.* 2000;275(36):27587-27593.
146. Galinska-Rakoczy A, Engel P, Xu C, Jung H, Craig R, Tobacman LS, Lehman W. Structural basis for the regulation of muscle contraction by troponin and tropomyosin. *J Mol Biol.* 2008;379(5):929-935.
147. Lehman W, Galinska-Rakoczy A, Hatch V, Tobacman LS, Craig R. Structural basis for the activation of muscle contraction by troponin and tropomyosin. *J Mol Biol.* 2009;388(4):673-681.
148. Maytum R, Westerdorf B, Jaquet K, Geeves MA. Differential regulation of the actomyosin interaction by skeletal and cardiac troponin isoforms. *J Biol Chem.* 2003;278(9):6696-6701.
149. Homsher E, Lacktis J, Regnier M. Strain-dependent modulation of phosphate transients in rabbit skeletal muscle fibers. *Biophys J.* 1997;72(4):1780-1791.
150. Fitzsimons DP, Moss RL. Strong binding of myosin modulates length-dependent Ca2+ activation of rat ventricular myocytes. *Circ Res.* 1998;83(6):602-607.
151. Fitzsimons DP, Patel JR, Moss RL. Cross-bridge interaction kinetics in rat myocardium are accelerated by strong binding of myosin to the thin filament. *J Physiol.* 2001;530(Pt 2):263-272.
152. Stelzer JE, Moss RL. Contributions of stretch activation to length-dependent contraction in murine myocardium. *J Gen Physiol.* 2006;128(4):461-471.
153. Herzberg O, Moult J, James MN. A model for the Ca2+-induced conformational transition of troponin C. A trigger for muscle contraction. *J Biol Chem.* 1986;261(6):2638-2644.
154. Dong WJ, Robinson JM, Xing J, Cheung HC. Kinetics of conformational transitions in cardiac troponin induced by Ca2+ dissociation determined by Forster resonance energy transfer. *J Biol Chem.* 2003;278(43):42394-42402.
155. Gomes AV, Venkatraman G, Davis JP, Tikunova SB, Engel P, Solaro RJ, Potter JD. Cardiac troponin T isoforms affect the Ca(2+) sensitivity of force development in the presence of slow skeletal troponin I: insights into the role of troponin T isoforms in the fetal heart. *J Biol Chem.* 2004;279(48):49579-49587.

156. Davis JP, Norman C, Kobayashi T, Solaro RJ, Swartz DR, Tikunova SB. Effects of thin and thick filament proteins on calcium binding and exchange with cardiac troponin C. *Biophys J.* 2007;92(9):3195-3206.
157. Spyracopoulos L, Gagne SM, Li MX, Sykes BD. Dynamics and thermodynamics of the regulatory domain of human cardiac troponin C in the apo- and calcium-saturated states. *Biochemistry.* 1998;37(51):18032-18044.
158. Liao R, Wang CK, Cheung HC. Coupling of calcium to the interaction of troponin I with troponin C from cardiac muscle. *Biochemistry.* 1994;33(42):12729-12734.
159. Miki M, Kobayashi T, Kimura H, Hagiwara A, Hai H, Maeda Y. Ca2+-induced distance change between points on actin and troponin in skeletal muscle thin filaments estimated by fluorescence energy transfer spectroscopy. *J Biochem.* 1998;123(2):324-331.
160. Li Z, Gergely J, Tao T. Proximity relationships between residue 117 of rabbit skeletal troponin-I and residues in troponin-C and actin. *Biophys J.* 2001;81(1):321-333.
161. Dong WJ, Robinson JM, Stagg S, Xing J, Cheung HC. Ca2+-induced conformational transition in the inhibitory and regulatory regions of cardiac troponin I. *J Biol Chem.* 2003;278(10):8686-8692.
162. Xing J, Chinnaraj M, Zhang Z, Cheung HC, Dong WJ. Structural studies of interactions between cardiac troponin I and actin in regulated thin filament using Forster resonance energy transfer. *Biochemistry.* 2008;47(50):13383-13393.
163. Li MX, Spyracopoulos L, Sykes BD. Binding of cardiac troponin-I147-163 induces a structural opening in human cardiac troponin-C. *Biochemistry.* 1999;38(26):8289-8298.
164. Dong W-J, Xing J, Villain M, Hellinger M, Robinson JM, Chandra M, Solaro RJ, Umeda PK, Cheung HC. Conformation of the Regulatory Domain of Cardiac Muscle Troponin C in Its Complex with Cardiac Troponin I. *J. Biol. Chem.* 1999;274(44):31382-31390.
165. Bell MG, Lankford EB, Gonye GE, Ellis-Davies GC, Martyn DA, Regnier M, Barsotti RJ. Kinetics of cardiac thin-filament activation probed by fluorescence polarization of rhodamine-labeled troponin C in skinned guinea pig trabeculae. *Biophys J.* 2006;90(2):531-543.
166. de Tombe PP, Belus A, Piroddi N, Scellini B, Walker JS, Martin AF, Tesi C, Poggesi C. Myofilament calcium sensitivity does not affect cross-bridge activation-relaxation kinetics. *Am J Physiol Regul Integr Comp Physiol.* 2007;292(3):R1129-1136.
167. Solzin J, Iorga B, Sierakowski E, Gomez Alcazar DP, Ruess DF, Kubacki T, Zittrich S, Blaudeck N, Pfitzer G, Stehle R. Kinetic mechanism of the Ca2+-dependent switch-on and switch-off of cardiac troponin in myofibrils. *Biophys J.* 2007;93(11):3917-3931.

168. Regnier M, Martin H, Barsotti RJ, Rivera AJ, Martyn DA, Clemmens E. Cross-bridge versus thin filament contributions to the level and rate of force development in cardiac muscle. *Biophys J.* 2004;87(3):1815-1824.
169. Hoffman RM, Sykes BD. Isoform-specific variation in the intrinsic disorder of troponin I. *Proteins.* 2008;73(2):338-350.
170. Dong WJ, Xing J, Robinson JM, Cheung HC. Ca(2+) induces an extended conformation of the inhibitory region of troponin I in cardiac muscle troponin. *J Mol Biol.* 2001;314(1):51-61.
171. McKay RT, Pearlstone JR, Corson DC, Gagne SM, Smillie LB, Sykes BD. Structure and interaction site of the regulatory domain of troponin-C when complexed with the 96-148 region of troponin-I. *Biochemistry.* 1998;37(36):12419-12430.
172. McKay RT, Tripet BP, Hodges RS, Sykes BD. Interaction of the second binding region of troponin I with the regulatory domain of skeletal muscle troponin C as determined by NMR spectroscopy. *J Biol Chem.* 1997;272(45):28494-28500.
173. McKay RT, Tripet BP, Pearlstone JR, Smillie LB, Sykes BD. Defining the region of troponin-I that binds to troponin-C. *Biochemistry.* 1999;38(17):5478-5489.
174. Ramakrishnan S, Hitchcock-DeGregori SE. Investigation of the structural requirements of the troponin C central helix for function. *Biochemistry.* 1995;34(51):16789-16796.
175. Ramakrishnan S, Hitchcock-DeGregori SE. Structural and functional significance of aspartic acid 89 of the troponin C central helix in Ca2+ signaling. *Biochemistry.* 1996;35(48):15515-15521.
176. Lehman W, Craig R, Vibert P. Ca(2+)-induced tropomyosin movement in Limulus thin filaments revealed by three-dimensional reconstruction. *Nature.* 1994;368(6466):65-67.
177. Zhao Y, Kawai M. The effect of the lattice spacing change on cross-bridge kinetics in chemically skinned rabbit psoas muscle fibers. II. Elementary steps affected by the spacing change. *Biophys J.* 1993;64(1):197-210.
178. Lidke DS, Thomas DD. Coordination of the two heads of myosin during muscle contraction. *Proc Natl Acad Sci U S A.* 2002;99(23):14801-14806.
179. Thomas DD, Prochniewicz E, Roopnarine O. Changes in actin and myosin structural dynamics due to their weak and strong interactions. *Results Probl Cell Differ.* 2002;36:7-19.
180. Stehle R, Iorga B, Pfitzer G. Calcium regulation of troponin and its role in the dynamics of contraction and relaxation. *Am J Physiol Regul Integr Comp Physiol.* 2007;292(3):R1125-1128.
181. Hinken AC, McDonald KS. Inorganic phosphate speeds loaded shortening in rat skinned cardiac myocytes. *Am J Physiol Cell Physiol.* 2004;287(2):C500-507.
182. Solaro RJ, Rarick HM. Troponin and tropomyosin: proteins that switch on and tune in the activity of cardiac myofilaments. *Circ Res.* 1998;83(5):471-480.

183. Heeley DH, Belknap B, White HD. Maximal activation of skeletal muscle thin filaments requires both rigor myosin S1 and calcium. *J Biol Chem.* 2006;281(1):668-676.
184. Pirani A, Vinogradova MV, Curmi PM, King WA, Fletterick RJ, Craig R, Tobacman LS, Xu C, Hatch V, Lehman W. An atomic model of the thin filament in the relaxed and Ca2+-activated states. *J Mol Biol.* 2006;357(3):707-717.
185. Tregear RT, Reedy MC, Goldman YE, Taylor KA, Winkler H, Franzini-Armstrong C, Sasaki H, Lucaveche C, Reedy MK. Cross-bridge number, position, and angle in target zones of cryofixed isometrically active insect flight muscle. *Biophys J.* 2004;86(5):3009-3019.
186. Poggesi C, Tesi C, Stehle R. Sarcomeric determinants of striated muscle relaxation kinetics. *Pflugers Arch.* 2005;449(6):505-517.
187. Tesi C, Piroddi N, Colomo F, Poggesi C. Relaxation kinetics following sudden Ca(2+) reduction in single myofibrils from skeletal muscle. *Biophys J.* 2002;83(4):2142-2151.
188. Hunter WC. Role of myofilaments and calcium handling in left ventricular relaxation. *Cardiol Clin.* 2000;18(3):443-457.
189. Peterson JN, Hunter WC, Berman MR. Estimated time course of Ca2+ bound to troponin C during relaxation in isolated cardiac muscle. *Am J Physiol.* 1991;260(3 Pt 2):H1013-1024.
190. Ishikawa T, J OU, Mochizuki S, Kurihara S. Evaluation of the cross-bridge-dependent change in the Ca2+ affinity of troponin C in aequorin-injected ferret ventricular muscles. *Cell Calcium.* 2005;37(2):153-162.
191. Tikunova SB, Davis JP. Designing calcium-sensitizing mutations in the regulatory domain of cardiac troponin C. *J Biol Chem.* 2004;279(34):35341-35352.
192. Davis JP, Tikunova SB. Ca(2+) exchange with troponin C and cardiac muscle dynamics. *Cardiovasc Res.* 2008;77(4):619-626.
193. Dong W, Rosenfeld SS, Wang CK, Gordon AM, Cheung HC. Kinetic studies of calcium binding to the regulatory site of troponin C from cardiac muscle. *J Biol Chem.* 1996;271(2):688-694.
194. Xing J, Jayasundar JJ, Ouyang Y, Dong WJ. Forster resonance energy transfer structural kinetic studies of cardiac thin filament deactivation. *J Biol Chem.* 2009;284(24):16432-16441.
195. Janssen PM, Stull LB, Marban E. Myofilament properties comprise the rate-limiting step for cardiac relaxation at body temperature in the rat. *Am J Physiol Heart Circ Physiol.* 2002;282(2):H499-507.
196. Bodem R, Sonnenblick EH. Deactivation of contraction by quick releases in the isolated papillary muscle of the cat. Effects of lever damping, caffeine, and tetanization. *Circ Res.* 1974;34(2):214-225.
197. Brady AJ. Time and displacement dependence of cardiac contractility: problems in defining the active state and force-velocity relations. *Fed Proc.* 1965;24(6):1410-1420.

198. Brutsaert DL, Housmans PR, Goethals MA. Dual control of relaxation. Its role in the ventricular function in the mammalian heart. *Circ Res.* 1980;47(5):637-652.
199. O'Rourke B, Kass DA, Tomaselli GF, Kaab S, Tunin R, Marban E. Mechanisms of altered excitation-contraction coupling in canine tachycardia-induced heart failure, I: experimental studies. *Circ Res.* 1999;84(5):562-570.
200. del Monte F, Hajjar RJ, Harding SE. Overwhelming evidence of the beneficial effects of SERCA gene transfer in heart failure. *Circ Res.* 2001;88(11):E66-67.
201. Xiang Y, Kobilka BK. Myocyte adrenoceptor signaling pathways. *Science.* 2003;300(5625):1530-1532.
202. Yasuda S, Coutu P, Sadayappan S, Robbins J, Metzger JM. Cardiac transgenic and gene transfer strategies converge to support an important role for troponin I in regulating relaxation in cardiac myocytes. *Circ Res.* 2007;101(4):377-386.
203. Palpant NJ, D'Alecy LG, Metzger JM. Single histidine button in cardiac troponin I sustains heart performance in response to severe hypercapnic respiratory acidosis in vivo. *FASEB J.* 2009.
204. Xiao RP, Zhu W, Zheng M, Cao C, Zhang Y, Lakatta EG, Han Q. Subtype-specific alpha1- and beta-adrenoceptor signaling in the heart. *Trends Pharmacol Sci.* 2006;27(6):330-337.
205. Layland J, Solaro RJ, Shah AM. Regulation of cardiac contractile function by troponin I phosphorylation. *Cardiovascular Research.* 2005;66(1):12-21.
206. Solaro RJ, Moir AJG, Perry SV. Phosphorylation of Troponin-I and Inotropic Effect of Adrenaline in Perfused Rabbit Heart. *Nature.* 1976;262(5569):615-617.
207. Jweied EE, McKinney RD, Walker LA, Brodsky I, Geha AS, Massad MG, Buttrick PM, de Tombe PP. Depressed cardiac myofilament function in human diabetes mellitus. *Am J Physiol Heart Circ Physiol.* 2005;289(6):H2478-2483.
208. McConnell BK, Moravec CS, Bond M. Troponin I phosphorylation and myofilament calcium sensitivity during decompensated cardiac hypertrophy. *Am J Physiol.* 1998;274(2 Pt 2):H385-396.
209. van der Velden J, Papp Z, Zaremba R, Boontje NM, de Jong JW, Owen VJ, Burton PB, Goldmann P, Jaquet K, Stienen GJ. Increased Ca2+-sensitivity of the contractile apparatus in end-stage human heart failure results from altered phosphorylation of contractile proteins. *Cardiovasc Res.* 2003;57(1):37-47.
210. Hamdani N, Kooij V, van Dijk S, Merkus D, Paulus WJ, Remedios Cd, Duncker DJ, Stienen GJM, van der Velden J. Sarcomeric dysfunction in heart failure. *Cardiovasc Res.* 2008;77(4):649-658.
211. Heller WT, Finley NL, Dong WJ, Timmins P, Cheung HC, Rosevear PR, Trewhella J. Small-angle neutron scattering with contrast variation reveals

spatial relationships between the three subunits in the ternary cardiac troponin complex and the effects of troponin I phosphorylation. *Biochemistry.* 2003;42(25):7790-7800.
212. Layland J, Grieve DJ, Cave AC, Sparks E, Solaro RJ, Shah AM. Essential role of troponin I in the positive inotropic response to isoprenaline in mouse hearts contracting auxotonically. *J Physiol.* 2004;556(Pt 3):835-847.
213. Fentzke RC, Buck SH, Patel JR, Lin H, Wolska BM, Stojanovic MO, Martin AF, Solaro RJ, Moss RL, Leiden JM. Impaired cardiomyocyte relaxation and diastolic function in transgenic mice expressing slow skeletal troponin I in the heart. *J Physiol.* 1999;517 (Pt 1):143-157.
214. Herron TJ, Korte FS, McDonald KS. Power output is increased after phosphorylation of myofibrillar proteins in rat skinned cardiac myocytes. *Circ Res.* 2001;89(12):1184-1190.
215. Takimoto E, Soergel DG, Janssen PM, Stull LB, Kass DA, Murphy AM. Frequency- and afterload-dependent cardiac modulation in vivo by troponin I with constitutively active protein kinase A phosphorylation sites. *Circ Res.* 2004;94(4):496-504.
216. Hanft LM, McDonald KS. Sarcomere length dependence of power output is increased after PKA treatment in rat cardiac myocytes. *Am J Physiol Heart Circ Physiol.* 2009;296(5):H1524-1531.
217. Gwathmey JK, Hajjar RJ. Effect of protein kinase C activation on sarcoplasmic reticulum function and apparent myofibrillar Ca2+ sensitivity in intact and skinned muscles from normal and diseased human myocardium. *Circ Res.* 1990;67(3):744-752.
218. Puceat M, Clement O, Lechene P, Pelosin JM, Ventura-Clapier R, Vassort G. Neurohormonal control of calcium sensitivity of myofilaments in rat single heart cells. *Circ Res.* 1990;67(2):517-524.
219. Westfall MV, Borton AR. Role of troponin I phosphorylation in protein kinase C-mediated enhanced contractile performance of rat myocytes. *J Biol Chem.* 2003;278(36):33694-33700.
220. Alden KJ, Goldspink PH, Ruch SW, Buttrick PM, Garcia J. Enhancement of L-type Ca(2+) current from neonatal mouse ventricular myocytes by constitutively active PKC-betaII. *Am J Physiol Cell Physiol.* 2002;282(4):C768-774.
221. Westfall MV, Lee AM, Robinson DA. Differential contribution of troponin I phosphorylation sites to the endothelin-modulated contractile response. *J Biol Chem.* 2005;280(50):41324-41331.
222. Noland TA, Jr., Raynor RL, Kuo JF. Identification of sites phosphorylated in bovine cardiac troponin I and troponin T by protein kinase C and comparative substrate activity of synthetic peptides containing the phosphorylation sites. *J Biol Chem.* 1989;264(34):20778-20785.
223. Damron DS, Darvish A, Murphy L, Sweet W, Moravec CS, Bond M. Arachidonic acid-dependent phosphorylation of troponin I and myosin light chain 2 in cardiac myocytes. *Circ Res.* 1995;76(6):1011-1019.

224. Bowling N, Walsh RA, Song G, Estridge T, Sandusky GE, Fouts RL, Mintze K, Pickard T, Roden R, Bristow MR, Sabbah HN, Mizrahi JL, Gromo G, King GL, Vlahos CJ. Increased protein kinase C activity and expression of Ca2+-sensitive isoforms in the failing human heart. *Circulation.* 1999;99(3):384-391.
225. Molnar A, Borbely A, Czuriga D, Ivetta SM, Szilagyi S, Hertelendi Z, Pasztor ET, Balogh A, Galajda Z, Szerafin T, Jaquet K, Papp Z, Edes I, Toth A. Protein kinase C contributes to the maintenance of contractile force in human ventricular cardiomyocytes. *J Biol Chem.* 2009;284(2):1031-1039.
226. Burkart EM, Sumandea MP, Kobayashi T, Nili M, Martin AF, Homsher E, Solaro RJ. Phosphorylation or glutamic acid substitution at protein kinase C sites on cardiac troponin I differentially depress myofilament tension and shortening velocity. *J Biol Chem.* 2003;278(13):11265-11272.
227. Pyle WG, Sumandea MP, Solaro RJ, De Tombe PP. Troponin I serines 43/45 and regulation of cardiac myofilament function. *Am J Physiol Heart Circ Physiol.* 2002;283(3):H1215-1224.
228. Noland TA, Jr., Guo X, Raynor RL, Jideama NM, Averyhart-Fullard V, Solaro RJ, Kuo JF. Cardiac troponin I mutants. Phosphorylation by protein kinases C and A and regulation of Ca(2+)-stimulated MgATPase of reconstituted actomyosin S-1. *J Biol Chem.* 1995;270(43):25445-25454.
229. MacKay J, Mensah G. The Atlas of Heart Disease and Stroke. *World Health Organization.* 2006.
230. Steg PG, Dabbous OH, Feldman LJ, Cohen-Solal A, Aumont MC, Lopez-Sendon J, Budaj A, Goldberg RJ, Klein W, Anderson FA, Jr., for the Global Registry of Acute Coronary Events I. Determinants and Prognostic Impact of Heart Failure Complicating Acute Coronary Syndromes: Observations From the Global Registry of Acute Coronary Events (GRACE). *Circulation.* 2004;109(4):494-499.
231. Atar D, Gao WD, Marban E. Alterations of excitation--contraction coupling in stunned myocardium and in failing myocardium. *Journal of Molecular and Cellular Cardiology.* 1995;27(2):783-791.
232. Michaud CM, Murray CJL, Bloom BR. Burden of Disease--Implications for Future Research. *JAMA: The Journal of the American Medical Association.* 2001;285(5):535-539.
233. Deedwania PC. The key to unraveling the mystery of mortality in heart failure - An integrated approach. *Circulation.* 2003;107(13):1719-1721.
234. Dubin A, Estenssoro E. Mechanisms of tissue hypercarbia in sepsis. *Front Biosci.* 2008;13:1340-1351.
235. Windisch W, Kostic S, Dreher M, Virchow JC, Jr., Sorichter S. Outcome of patients with stable COPD receiving controlled noninvasive positive pressure ventilation aimed at a maximal reduction of Pa(CO2). *Chest.* 2005;128(2):657-662.

236. Godt RE, Nosek TM. Changes of intracellular milieu with fatigue or hypoxia depress contraction of skinned rabbit skeletal and cardiac muscle. *J Physiol.* 1989;412:155-180.
237. Orchard CH, Kentish JC. Effects of changes of pH on the contractile function of cardiac muscle. *Am J Physiol.* 1990;258(6 Pt 1):C967-981.
238. Parsons B, Szczesna D, Zhao J, Van Slooten G, Kerrick WG, Putkey JA, Potter JD. The effect of pH on the Ca2+ affinity of the Ca2+ regulatory sites of skeletal and cardiac troponin C in skinned muscle fibres. *J Muscle Res Cell Motil.* 1997;18(5):599-609.
239. Solaro RJ, Lee JA, Kentish JC, Allen DG. Effects of acidosis on ventricular muscle from adult and neonatal rats. *Circulation Research.* 1988;63(4):779-787.
240. Allen DG, Orchard CH. The effects of changes of pH on intracellular calcium transients in mammalian cardiac muscle. *J Physiol.* 1983;335:555-567.
241. Crampin EJ, Smith NP. A dynamic model of excitation-contraction coupling during acidosis in cardiac ventricular myocytes. *Biophys J.* 2006;90(9):3074-3090.
242. Day SM, Westfall MV, Metzger JM. Tuning cardiac performance in ischemic heart disease and failure by modulating myofilament function. *J Mol Med.* 2007;85(9):911-921.
243. Murphy AM. Heart failure, myocardial stunning, and troponin: a key regulator of the cardiac myofilament. *Congest Heart Fail.* 2006;12(1):32-38; quiz 39-40.
244. Day S, Davis J, Westfall M, Metzger J. Genetic engineering and therapy for inherited and acquired cardiomyopathies. *Ann N Y Acad Sci.* 2006;1080:437-450.
245. Ball KL, Johnson MD, Solaro RJ. Isoform specific interactions of troponin I and troponin C determine pH sensitivity of myofibrillar Ca2+ activation. *Biochemistry.* 1994;33(28):8464-8471.
246. Day SM, Westfall MV, Fomicheva EV, Hoyer K, Yasuda S, La Cross NC, D'Alecy LG, Ingwall JS, Metzger JM. Histidine button engineered into cardiac troponin I protects the ischemic and failing heart. *Nat.Med.* 2006;12(2):181-189.
247. Bolli R, Marban E. Molecular and cellular mechanisms of myocardial stunning. *Physiol Rev.* 1999;79(2):609-634.
248. Van Eyk JE, Powers F, Law W, Larue C, Hodges RS, Solaro RJ. Breakdown and release of myofilament proteins during ischemia and ischemia/reperfusion in rat hearts: identification of degradation products and effects on the pCa-force relation. *Circ Res.* 1998;82(2):261-271.
249. Dargis R, Pearlstone JR, Barrette-Ng I, Edwards H, Smillie LB. Single mutation (A162H) in human cardiac troponin I corrects acid pH sensitivity of Ca2+-regulated actomyosin S1 ATPase. *Journal of Biological Chemistry.* 2002;277(38):34662-34665.

250. Westfall MV, Borton AR, Albayya FP, Metzger JM. Specific charge differences in troponin I isoforms influence myofilament Ca2+ sensitivity of tension in adult cardiac myocytes. *Biophysical Journal.* 2001;80(1):356A-356A.
251. Westfall MV, Borton AR, Albayya FP, Metzger JM. Myofilament Calcium Sensitivity and Cardiac Disease: Insights From Troponin I Isoforms and Mutants. *Circulation Research.* 2002;91(6):525-531.
252. Westfall MV, Metzger JM. Single amino acid substitutions define isoform-specific effects of troponin I on myofilament Ca2+ and pH sensitivity. *J Mol Cell Cardiol.* 2007;43(2):107-118.
253. Ricciardi L, Bottinelli R, Canepari M, Reggiani C. Effects of acidosis on maximum shortening velocity and force-velocity relation of skinned rat cardiac muscle. *J Mol Cell Cardiol.* 1994;26(5):601-607.
254. Ricciardi L, Bucx JJ, ter Keurs HE. Effects of acidosis on force-sarcomere length and force-velocity relations of rat cardiac muscle. *Cardiovasc Res.* 1986;20(2):117-123.
255. Robertson SP, Kerrick WG. The effects of pH on Ca2+-activated force in frog skeletal muscle fibers. *Pflugers Arch.* 1979;380(1):41-45.
256. el-Saleh SC, Solaro RJ. Troponin I enhances acidic pH-induced depression of Ca2+ binding to the regulatory sites in skeletal troponin C. *J Biol Chem.* 1988;263(7):3274-3278.
257. Linse S, Forsen S. Determinants that govern high-affinity calcium binding. *Adv Second Messenger Phosphoprotein Res.* 1995;30:89-151.
258. Metzger JM. Effects of troponin C isoforms on pH sensitivity of contraction in mammalian fast and slow skeletal muscle fibres. *J Physiol.* 1996;492 (Pt 1):163-172.
259. Metzger JM, Parmacek MS, Barr E, Pasyk K, Lin WI, Cochrane KL, Field LJ, Leiden JM. Skeletal troponin C reduces contractile sensitivity to acidosis in cardiac myocytes from transgenic mice. *Proc Natl Acad Sci U S A.* 1993;90(19):9036-9040.
260. Metzger JM, Moss RL. Kinetics of a Ca(2+)-sensitive cross-bridge state transition in skeletal muscle fibers. Effects due to variations in thin filament activation by extraction of troponin C. *J Gen Physiol.* 1991;98(2):233-248.
261. Ebus JP, Stienen GJ, Elzinga G. Influence of phosphate and pH on myofibrillar ATPase activity and force in skinned cardiac trabeculae from rat. *J Physiol.* 1994;476(3):501-516.
262. Higuchi H, Takemori S, Umazume Y. Suppressing effect of 2,3-butanedione monoxime on contraction and ATPase activity of rabbit skeletal muscle. *Prog Clin Biol Res.* 1989;315:225-226.
263. Wattanapermpool J, Reiser PJ, Solaro RJ. Troponin I isoforms and differential effects of acidic pH on soleus and cardiac myofilaments. *Am J Physiol.* 1995;268(2 Pt 1):C323-330.
264. Liou YM, Chang JC. Differential pH effect on calcium-induced conformational changes of cardiac troponin C complexed with cardiac and

fast skeletal isoforms of troponin I and troponin T. *J Biochem.* 2004;136(5):683-692.
265. Guo X, Wattanapermpool J, Palmiter KA, Murphy AM, Solaro RJ. Mutagenesis of cardiac troponin I. Role of the unique NH2-terminal peptide in myofilament activation. *J Biol Chem.* 1994;269(21):15210-15216.
266. Westfall MV, Albayya FP, Turner II, Metzger JM. Chimera Analysis of Troponin I Domains That Influence Ca2+-Activated Myofilament Tension in Adult Cardiac Myocytes. *Circulation Research.* 2000;86(4):470-477.
267. Li G, Martin AF, Solaro JR. Localization of regions of troponin I important in deactivation of cardiac myofilaments by acidic pH. *J Mol Cell Cardiol.* 2001;33(7):1309-1320.
268. Lyn D, Liu X, Bennett NA, Emmett NL. Gene expression profile in mouse myocardium after ischemia. *Physiol Genomics.* 2000;2(3):93-100.
269. Rajabi M, Kassiotis C, Razeghi P, Taegtmeyer H. Return to the fetal gene program protects the stressed heart: a strong hypothesis. *Heart Fail Rev.* 2007;12(3-4):331-343.
270. Lompre AM, Schwartz K, d'Albis A, Lacombe G, Van Thiem N, Swynghedauw B. Myosin isoenzyme redistribution in chronic heart overload. *Nature.* 1979;282(5734):105-107.
271. Mercadier JJ, Samuel JL, Michel JB, Zongazo MA, de la Bastie D, Lompre AM, Wisnewsky C, Rappaport L, Levy B, Schwartz K. Atrial natriuretic factor gene expression in rat ventricle during experimental hypertension. *Am J Physiol.* 1989;257(3 Pt 2):H979-987.
272. Mercadier JJ, Zongazo MA, Wisnewsky C, Butler-Brown G, Gros D, Carayon A, Schwartz K. Atrial natriuretic factor messenger ribonucleic acid and peptide in the human heart during ontogenic development. *Biochem Biophys Res Commun.* 1989;159(2):777-782.
273. Nagai R, Zarain-Herzberg A, Brandl CJ, Fujii J, Tada M, MacLennan DH, Alpert NR, Periasamy M. Regulation of myocardial Ca2+-ATPase and phospholamban mRNA expression in response to pressure overload and thyroid hormone. *Proc Natl Acad Sci U S A.* 1989;86(8):2966-2970.
274. Arai M, Alpert NR, MacLennan DH, Barton P, Periasamy M. Alterations in sarcoplasmic reticulum gene expression in human heart failure. A possible mechanism for alterations in systolic and diastolic properties of the failing myocardium. *Circ Res.* 1993;72(2):463-469.
275. Arai M, Matsui H, Periasamy M. Sarcoplasmic reticulum gene expression in cardiac hypertrophy and heart failure. *Circ Res.* 1994;74(4):555-564.
276. Otsu K, Fujii J, Periasamy M, Difilippantonio M, Uppender M, Ward DC, MacLennan DH. Chromosome mapping of five human cardiac and skeletal muscle sarcoplasmic reticulum protein genes. *Genomics.* 1993;17(2):507-509.
277. Mondry A, Bourgeois F, Carre F, Swynghedauw B, Moalic JM. Decrease in beta 1-adrenergic and M2-muscarinic receptor mRNA levels and unchanged accumulation of mRNAs coding for G alpha i-2 and G alpha s

proteins in rat cardiac hypertrophy. *J Mol Cell Cardiol.* 1995;27(10):2287-2294.
278. Hasenfuss G, Meyer M, Schillinger W, Preuss M, Pieske B, Just H. Calcium handling proteins in the failing human heart. *Basic Res Cardiol.* 1997;92 Suppl 1:87-93.
279. Hasenfuss G, Pieske B. Calcium Cycling in Congestive Heart Failure. *Journal of Molecular and Cellular Cardiology.* 2002;34(8):951-969.
280. Baartscheer A, Schumacher CA, Belterman CN, Coronel R, Fiolet JW. SR calcium handling and calcium after-transients in a rabbit model of heart failure. *Cardiovasc Res.* 2003;58(1):99-108.
281. Hobai IA, O'Rourke B. Decreased sarcoplasmic reticulum calcium content is responsible for defective excitation-contraction coupling in canine heart failure. *Circulation.* 2001;103(11):1577-1584.
282. Allard MF, Henning SL, Wambolt RB, Granleese SR, English DR, Lopaschuk GD. Glycogen metabolism in the aerobic hypertrophied rat heart. *Circulation.* 1997;96(2):676-682.
283. Apstein CS, Opie LH. A challenge to the metabolic approach to myocardial ischaemia. *Eur Heart J.* 2005;26(10):956-959.
284. Bye A, Langaas M, Hoydal MA, Kemi OJ, Heinrich G, Koch LG, Britton SL, Najjar SM, Ellingsen O, Wisloff U. Aerobic capacity-dependent differences in cardiac gene expression. *Physiol Genomics.* 2008;33(1):100-109.
285. Gerdes AM, Capasso JM. Structural remodeling and mechanical dysfunction of cardiac myocytes in heart failure. *J Mol Cell Cardiol.* 1995;27(3):849-856.
286. Brodde OE, Bruck H, Leineweber K. Cardiac adrenoceptors: physiological and pathophysiological relevance. *J Pharmacol Sci.* 2006;100(5):323-337.
287. Zhu WZ, Wang SQ, Chakir K, Yang D, Zhang T, Brown JH, Devic E, Kobilka BK, Cheng H, Xiao RP. Linkage of beta1-adrenergic stimulation to apoptotic heart cell death through protein kinase A-independent activation of Ca2+/calmodulin kinase II. *J Clin Invest.* 2003;111(5):617-625.
288. Bristow MR, Ginsburg R, Minobe W, Cubicciotti RS, Sageman WS, Lurie K, Billingham ME, Harrison DC, Stinson EB. Decreased catecholamine sensitivity and beta-adrenergic-receptor density in failing human hearts. *N Engl J Med.* 1982;307(4):205-211.
289. Sorsa T, Pollesello P, Solaro RJ. The contractile apparatus as a target for drugs against heart failure: interaction of levosimendan, a calcium sensitiser, with cardiac troponin c. *Mol Cell Biochem.* 2004;266(1-2):87-107.
290. Palpant NJ, Day SM, Herron TJ, Converso KL, Metzger JM. Single histidine-substituted cardiac troponin I confers protection from age-related systolic and diastolic dysfunction. *Cardiovasc Res.* 2008:cvn198.
291. Kass DA, Solaro RJ. Mechanisms and Use of Calcium-Sensitizing Agents in the Failing Heart. *Circulation.* 2006;113(2):305-315.
292. Bers DM. *Excitation Contraction Coupling and Cardiac Contractile Force*. Dordecht, Netherlands: Kluwer Academic Publishers; 2001.

293. Endoh M, Hori M. Acute heart failure: inotropic agents and their clinical uses. *Expert Opin Pharmacother.* 2006;7(16):2179-2202.
294. Teerlink JR. Overview of randomized clinical trials in acute heart failure syndromes. *Am J Cardiol.* 2005;96(6A):59G-67G.
295. Bayram M, De Luca L, Massie MB, Gheorghiade M. Reassessment of dobutamine, dopamine, and milrinone in the management of acute heart failure syndromes. *Am J Cardiol.* 2005;96(6A):47G-58G.
296. Li Y, Love ML, Putkey JA, Cohen C. Bepridil opens the regulatory N-terminal lobe of cardiac troponin C. *Proc Natl Acad Sci U S A.* 2000;97(10):5140-5145.
297. Arteaga GM, Warren CM, Milutinovic S, Martin AF, Solaro RJ. Specific enhancement of sarcomeric response to Ca2+ protects murine myocardium against ischemia-reperfusion dysfunction. *American Journal of Physiology-Heart and Circulatory Physiology.* 2005;289(5):H2183-H2192.
298. Cunha-Goncalves D, Perez-de-Sa V, Dahm P, Grins E, Thorne J, Blomquist S. Cardiovascular effects of levosimendan in the early stages of endotoxemia. *Shock.* 2007;28(1):71-77.
299. Givertz MM, Andreou C, Conrad CH, Colucci WS. Direct myocardial effects of levosimendan in humans with left ventricular dysfunction: alteration of force-frequency and relaxation-frequency relationships. *Circulation.* 2007;115(10):1218-1224.
300. Jorgensen K, Bech-Hanssen O, Houltz E, Ricksten SE. Effects of levosimendan on left ventricular relaxation and early filling at maintained preload and afterload conditions after aortic valve replacement for aortic stenosis. *Circulation.* 2008;117(8):1075-1081.
301. Oldner A, Konrad D, Weitzberg E, Rudehill A, Rossi P, Wanecek M. Effects of levosimendan, a novel inotropic calcium-sensitizing drug, in experimental septic shock. *Crit Care Med.* 2001;29(11):2185-2193.
302. Segreti JA, Marsh KC, Polakowski JS, Fryer RM. Evoked Changes in Cardiovascular Function in Rats by Infusion of Levosimendan, OR-1896 [(R)-N-(4-(4-Methyl-6-oxo-1,4,5,6-tetrahydropyridazin-3-yl)phenyl)acetamide], OR-1855 [(R)-6-(4-Aminophenyl)-5-methyl-4,5-dihydropyridazin-3(2H)-one], Dobutamine, and Milrinone: Comparative Effects on Peripheral Resistance, Cardiac Output, dP/dt, Pulse Rate, and Blood Pressure. *J Pharmacol Exp Ther.* 2008;325(1):331-340.
303. Perutz MF, Gronenborn AM, Clore GM, Fogg JH, Shih DTb. The pKa values of two histidine residues in human haemoglobin, the Bohr effect, and the dipole moments of [alpha]-helices. *Journal of Molecular Biology.* 1985;183(3):491-498.
304. T.b.-Shih D, Luisi BF, Miyazaki G, Perutz MF, Nagai K. A Mutagenic Study of the Allosteric Linkage of His(HC3)146[beta] in Haemoglobin. *Journal of Molecular Biology.* 1993;230(4):1291-1296.

305. Perutz MF, Kilmartin JV, Nishikura K, Fogg JH, Butler PJG, Rollema HS. Identification of residues contributing to the Bohr effect of human haemoglobin. *Journal of Molecular Biology.* 1980;138(3):649-668.
306. RÃ¶tzschke O, Lau JM, HofstÃ¤tter M, Falk K, Strominger JL. A pH-sensitive histidine residue as control element for ligand release from HLA-DR molecules. *Proceedings of the National Academy of Sciences of the United States of America.* 2002;99(26):16946-16950.
307. Mao J, Wu J, Chen F, Wang X, Jiang C. Inhibition of G-protein-coupled Inward Rectifying K+ Channels by Intracellular Acidosis. *J. Biol. Chem.* 2003;278(9):7091-7098.
308. Coulter KL, Pe´rier F, Redeke CM, Vanderberg CA. Identification and molecular localization of a pH-sensing domain for the inward rectifier potassium channel HIR. *Neuron.* 1995;15(5):1157-1168.
309. Zong X, Stieber J, Ludwig A, Hofmann F, Biel M. A Single Histidine Residue Determines the pH Sensitivity of the Pacemaker Channel HCN2. *J. Biol. Chem.* 2001;276(9):6313-6319.
310. Rajan S, Wischmeyer E, Xin Liu G, Preisig-Muller R, Daut J, Karschin A, Derst C. TASK-3, a Novel Tandem Pore Domain Acid-sensitive K+ Channel. AN EXTRACELLULAR HISTIDINE AS pH SENSOR. *J. Biol. Chem.* 2000;275(22):16650-16657.
311. Sabry MA, Dhoot GK. Identification and pattern of expression of a developmental isoform of troponin I in chicken and rat cardiac muscle. *J Muscle Res Cell Motil.* 1989;10(1):85-91.
312. Saggin L, Gorza L, Ausoni S, Schiaffino S. Troponin I switching in the developing heart. *J Biol Chem.* 1989;264(27):16299-16302.
313. Kruger M, Kohl T, Linke WA. Developmental changes in passive stiffness and myofilament Ca2+ sensitivity due to titin and troponin-I isoform switching are not critically triggered by birth. *Am J Physiol Heart Circ Physiol.* 2006;291(2):H496-506.
314. Westfall MV, Metzger JM. Gene transfer of troponin I isoforms, mutants, and chimeras. *Adv Exp Med Biol.* 2003;538:169-174; discussion 174.
315. Westfall MV, Albayya FP, Turner, II, Metzger JM. Chimera analysis of troponin I domains that influence Ca(2+)-activated myofilament tension in adult cardiac myocytes. *Circ Res.* 2000;86(4):470-477.
316. Wolska BM, Arteaga GM, Pena JR, Nowak G, Phillips RM, Sahai S, de Tombe PP, Martin AF, Kranias EG, Solaro RJ. Expression of slow skeletal troponin I in hearts of phospholamban knockout mice alters the relaxant effect of beta-adrenergic stimulation. *Circ Res.* 2002;90(8):882-888.
317. Wolska BM, Vijayan K, Arteaga GM, Konhilas JP, Phillips RM, Kim R, Naya T, Leiden JM, Martin AF, de Tombe PP, Solaro RJ. Expression of slow skeletal troponin I in adult transgenic mouse heart muscle reduces the force decline observed during acidic conditions. *J Physiol.* 2001;536(Pt 3):863-870.
318. Urboniene D, Dias FAL, Pena JR, Walker LA, Solaro RJ, Wolska BM. Expression of slow skeletal troponin I in adult mouse heart helps to

maintain the left ventricular systolic function during respiratory hypercapnia. *Circulation Research.* 2005;97(1):70-77.
319. Westfall MV, Metzger JM. Troponin I Isoforms and Chimeras: Tuning the Molecular Switch of Cardiac Contraction. *News in Physiological Sciences.* 2001;16(6):278-281.
320. Frank K, Kranias EG. Phospholamban and cardiac contractility. *Ann Med.* 2000;32(8):572-578.
321. MacLennan DH, Kranias EG. Phospholamban: A crucial regulator of cardiac contractility. *Nature Reviews Molecular Cell Biology.* 2003;4(7):566-577.
322. Li L, Desantiago J, Chu G, Kranias EG, Bers DM. Phosphorylation of phospholamban and troponin I in beta-adrenergic-induced acceleration of cardiac relaxation. *Am J Physiol Heart Circ Physiol.* 2000;278(3):H769-779.
323. Chu G, Lester JW, Young KB, Luo W, Zhai J, Kranias EG. A single site (Ser16) phosphorylation in phospholamban is sufficient in mediating its maximal cardiac responses to beta -agonists. *J Biol Chem.* 2000;275(49):38938-38943.
324. Metzger JM, Michele DE, Rust EM, Borton AR, Westfall MV. Sarcomere Thin Filament Regulatory Isoforms. EVIDENCE OF A DOMINANT EFFECT OF SLOW SKELETAL TROPONIN I ON CARDIAC CONTRACTION. *Journal of Biological Chemistry.* 2003;278(15):13118-13123.
325. Pearlstone JR, Sykes BD, Smillie LB. Interactions of structural C and regulatory N domains of troponin C with repeated sequence motifs in troponin I. *Biochemistry.* 1997;36(24):7601-7606.
326. Berenbrink M. Evolution of vertebrate haemoglobins: Histidine side chains, specific buffer value and Bohr effect. *Respiratory Physiology & Neurobiology.* 2006;154(1-2):165-184.
327. Li MX, Spyracopoulos L, Sykes BD. Binding of Cardiac Troponin-I147-163 Induces a Structural Opening in Human Cardiac Troponin-C. *Biochemistry.* 1999;38(26):8289-8298.
328. Ebashi S, Kodama A. A New Protein Factor Promoting Aggregation of Tropomyosin. *Biochemical and Biophysical Research Communications.* 2008;369(1):13-14.
329. Carballo S, Robinson P, Otway R, Fatkin D, Jongbloed JD, de Jonge N, Blair E, van Tintelen JP, Redwood C, Watkins H. Identification and Functional Characterization of Cardiac Troponin I As a Novel Disease Gene in Autosomal Dominant Dilated Cardiomyopathy. *Circ Res.* 2009.
330. Dong WJ, An J, Xing J, Cheung HC. Structural transition of the inhibitory region of troponin I within the regulated cardiac thin filament. *Arch Biochem Biophys.* 2006;456(2):135-142.
331. Stecyk JA, Galli GL, Shiels HA, Farrell AP. Cardiac survival in anoxia-tolerant vertebrates: An electrophysiological perspective. *Comp Biochem Physiol C Toxicol Pharmacol.* 2008;148(4):339-354.

332. Gillis TE, Marshall CR, Tibbits GF. Functional and evolutionary relationships of troponin C. *Physiol Genomics.* 2007;32(1):16-27.
333. Davis J, Wen H, Edwards T, Metzger JM. Thin filament disinhibition by restrictive cardiomyopathy mutant R193H troponin I induces Ca2+-independent mechanical tone and acute myocyte remodeling. *Circ Res.* 2007;100(10):1494-1502.
334. Shiels HA, Calaghan SC, White E. The cellular basis for enhanced volume-modulated cardiac output in fish hearts. *J Gen Physiol.* 2006;128(1):37-44.
335. Baudenbacher F. Myofilament Ca2+ sensitization causes susceptibility to cardiac arrhythmia in mice. *The Journal of Clinical Investigation.* 2008;118(12):3893-3903.
336. Moolman JC, Corfield VA, Posen B, Ngumbela K, Seidman C, Brink PA, Watkins H. Sudden death due to troponin T mutations. *J Am Coll Cardiol.* 1997;29(3):549-555.
337. Tsoutsman T, Kelly M, Ng DC, Tan JE, Tu E, Lam L, Bogoyevitch MA, Seidman CE, Seidman JG, Semsarian C. Severe heart failure and early mortality in a double-mutation mouse model of familial hypertrophic cardiomyopathy. *Circulation.* 2008;117(14):1820-1831.
338. Thompson JD, Higgins DG, Gibson TJ. CLUSTAL W: improving the sensitivity of progressive multiple sequence alignment through sequence weighting, position-specific gap penalties and weight matrix choice. *Nucleic Acids Res.* 1994;22(22):4673-4680.
339. Anisimova M, Kosiol C. Investigating protein-coding sequence evolution with probabilistic codon substitution models. *Mol Biol Evol.* 2009;26(2):255-271.
340. Delport W, Scheffler K, Seoighe C. Models of coding sequence evolution. *Brief Bioinform.* 2009;10(1):97-109.
341. Guindon S, Gascuel O. A simple, fast, and accurate algorithm to estimate large phylogenies by maximum likelihood. *Syst Biol.* 2003;52(5):696-704.
342. Kosakovsky Pond SL, Posada D, Gravenor MB, Woelk CH, Frost SD. GARD: a genetic algorithm for recombination detection. *Bioinformatics.* 2006;22(24):3096-3098.
343. Kosakovsky Pond SL, Posada D, Gravenor MB, Woelk CH, Frost SD. Automated phylogenetic detection of recombination using a genetic algorithm. *Mol Biol Evol.* 2006;23(10):1891-1901.
344. Sugiura N. Further analysis of the data by {Akaike's} information criterion and the finite corrections. *Communications in Statistics - Theory and Methods.* 1978;A7.
345. Pond SL, Frost SD. Datamonkey: rapid detection of selective pressure on individual sites of codon alignments. *Bioinformatics.* 2005;21(10):2531-2533.
346. Bjellqvist B, Hughes GJ, Pasquali C, Paquet N, Ravier F, Sanchez JC, Frutiger S, Hochstrasser D. The focusing positions of polypeptides in

immobilized pH gradients can be predicted from their amino acid sequences. *Electrophoresis.* 1993;14(10):1023-1031.
347. Case DA, Cheatham TE, 3rd, Darden T, Gohlke H, Luo R, Merz KM, Jr., Onufriev A, Simmerling C, Wang B, Woods RJ. The Amber biomolecular simulation programs. *J Comput Chem.* 2005;26(16):1668-1688.
348. Anandakrishnan R, Onufriev A. Analysis of basic clustering algorithms for numerical estimation of statistical averages in biomolecules. *J Comput Biol.* 2008;15(2):165-184.
349. Fenley AT, Gordon JC, Onufriev A. An analytical approach to computing biomolecular electrostatic potential. I. Derivation and analysis. *J Chem Phys.* 2008;129(7):075101.
350. Gordon JC, Fenley AT, Onufriev A. An analytical approach to computing biomolecular electrostatic potential. II. Validation and applications. *J Chem Phys.* 2008;129(7):075102.
351. Sigalov G, Fenley A, Onufriev A. Analytical electrostatics for biomolecules: beyond the generalized Born approximation. *J Chem Phys.* 2006;124(12):124902.
352. Gordon JC, Myers JB, Folta T, Shoja V, Heath LS, Onufriev A. H++: a server for estimating pKas and adding missing hydrogens to macromolecules. *Nucleic Acids Res.* 2005;33(Web Server issue):W368-371.
353. Phillips JC, Braun R, Wang W, Gumbart J, Tajkhorshid E, Villa E, Chipot C, Skeel RD, Kale L, Schulten K. Scalable molecular dynamics with NAMD. *J Comput Chem.* 2005;26(16):1781-1802.
354. MacKerell AD, Jr., Bashford, D., Bellott, M., Dunbrack, R. L., Evanseck, J. D., Field, M. J., Fischer, S., Gao, J., Guo, H., Ha, S., Joseph-McCarthy, D., Kuchnir, L., Kuczera, K., Lau, F. T. K., Mattos, C., Michnick, S., Ngo, T., Nguyen, D. T., Prodhom, B., Reiher, W. E., III, Roux, B., Schlenkrich, M., Smith, J. C., Stote, R., Straub, J., Watanabe, M., Wiorkiewicz-Kuczera, J., Yin, D., and Karplus, M. *J. Phys. Chem.* 1998;102(18):3586-3616.
355. Jorgensen W, Chandrasekar, J., Madura, J., Impey, R., and Klein, M. . *J. Chem. Phys.* 1983;79:926-935.
356. Essmann U, Perera, L., Berkowitz, M., Darden, T., Lee, H., and Pedersen, L. G. . *J. Chem. Phys.* 1995;103:8577-8593.
357. Ryckaert JP, Ciccotti, G., and Berendsen, H. J. C. . *J. Comput. Phys.* 1977;23:327-341.
358. Richard P, Charron P, Carrier L, Ledeuil C, Cheav T, Pichereau C, Benaiche A, Isnard R, Dubourg O, Burban M, Gueffet J-P, Millaire A, Desnos M, Schwartz K, Hainque B, Komajda M, for the EUROGENE Heart Failure Project. Hypertrophic Cardiomyopathy: Distribution of Disease Genes, Spectrum of Mutations, and Implications for a Molecular Diagnosis Strategy. *Circulation.* 2003;107(17):2227-2232.

359. Warkman AS, Atkinson BG. Amphibian cardiac troponin I gene's organization, developmental expression, and regulatory properties are different from its mammalian homologue. *Dev Dyn.* 2004;229(2):275-288.
360. Warkman AS, Atkinson BG. The slow isoform of Xenopus troponin I is expressed in developing skeletal muscle but not in the heart. *Mech Dev.* 2002;115(1-2):143-146.
361. Drysdale TA, Tonissen KF, Patterson KD, Crawford MJ, Krieg PA. Cardiac troponin I is a heart-specific marker in the Xenopus embryo: expression during abnormal heart morphogenesis. *Dev Biol.* 1994;165(2):432-441.
362. Palpant NJ, Yasuda S-i, MacDougald O, Metzger JM. Non-canonical Wnt signaling enhances differentiation of Sca1+/c-kit+ adipose-derived murine stromal vascular cells into spontaneously beating cardiac myocytes. *Journal of Molecular and Cellular Cardiology.* 2007;43(3):362-370.
363. Metzger JM, Michele DE, Rust EM, Borton AR, Westfall MV. Sarcomere Thin Filament Regulatory Isoforms. EVIDENCE OF A DOMINANT EFFECT OF SLOW SKELETAL TROPONIN I ON CARDIAC CONTRACTION. *J. Biol. Chem.* 2003;278(15):13118-13123.
364. Wang T, Hackam A, Guggino W, Cutting G. A single histidine residue is essential for zinc inhibition of GABA rho 1 receptors. *J. Neurosci.* 1995;15(11):7684-7691.
365. Liang B, Chung F, Qu Y, Pavlov D, Gillis TE, Tikunova SB, Davis JP, Tibbits GF. Familial hypertrophic cardiomyopathy-related cardiac troponin C mutation L29Q affects Ca2+ binding and myofilament contractility. *Physiol Genomics.* 2008;33(2):257-266.
366. Hoffmann B, Schmidt-Traub H, Perrot A, Osterziel KJ, Gessner R. First mutation in cardiac troponin C, L29Q, in a patient with hypertrophic cardiomyopathy. *Hum Mutat.* 2001;17(6):524.
367. Landstrom AP, Parvatiyar MS, Pinto JR, Marquardt ML, Bos JM, Tester DJ, Ommen SR, Potter JD, Ackerman MJ. Molecular and functional characterization of novel hypertrophic cardiomyopathy susceptibility mutations in TNNC1-encoded troponin C. *J Mol Cell Cardiol.* 2008;45(2):281-288.
368. Pinto JR, Parvatiyar MS, Jones MA, Liang J, Ackerman MJ, Potter JD. A functional and structural study of troponin C mutations related to hypertrophic cardiomyopathy. *J Biol Chem.* 2009;284(28):19090-19100.
369. Baudenbacher F, Schober T, Pinto JR, Sidorov VY, Hilliard F, Solaro RJ, Potter JD, Knollmann BC. Myofilament Ca2+ sensitization causes susceptibility to cardiac arrhythmia in mice. *J Clin Invest.* 2008;118(12):3893-3903.
370. Xu C, Wei M, Su B, Hua XW, Zhang GW, Xue XP, Pan CM, Liu R, Sheng Y, Lu ZG, Jin LR, Song HD. Ile90Met, a novel mutation in the cardiac troponin T gene for familial hypertrophic cardiomyopathy in a Chinese pedigree. *Genet Res.* 2008;90(5):445-450.
371. Tardiff JC, Hewett TE, Palmer BM, Olsson C, Factor SM, Moore RL, Robbins J, Leinwand LA. Cardiac troponin T mutations result in allele-

specific phenotypes in a mouse model for hypertrophic cardiomyopathy. *J Clin Invest.* 1999;104(4):469-481.
372. Mukherjea P, Tong L, Seidman JG, Seidman CE, Hitchcock-DeGregori SE. Altered regulatory function of two familial hypertrophic cardiomyopathy troponin T mutants. *Biochemistry.* 1999;38(40):13296-13301.
373. Thierfelder L, Watkins H, MacRae C, Lamas R, McKenna W, Vosberg HP, Seidman JG, Seidman CE. Alpha-tropomyosin and cardiac troponin T mutations cause familial hypertrophic cardiomyopathy: a disease of the sarcomere. *Cell.* 1994;77(5):701-712.
374. Fiset C, Giles WR. Cardiac troponin T mutations promote life-threatening arrhythmias. *J Clin Invest.* 2008;118(12):3845-3847.
375. Victor S, Nayak VM. Evolutionary anticipation of the human heart. *Ann R Coll Surg Engl.* 2000;82(5):297-302.
376. Victor S, Nayak VM, Rajasingh R. Evolution of the ventricles. *Tex Heart Inst J.* 1999;26(3):168-175; discussion 175-166.
377. Taylor EW. The evolution of efferent vagal control of the heart in vertebrates. *Cardioscience.* 1994;5(3):173-182.
378. Kubler W. The sympathetic system in evolution and in ischaemic heart disease--a controversy? *Eur Heart J.* 1992;13(10):1301-1303.
379. MacLean DW, Meedel TH, Hastings KE. Tissue-specific alternative splicing of ascidian troponin I isoforms. Redesign of a protein isoform-generating mechanism during chordate evolution. *J Biol Chem.* 1997;272(51):32115-32120.
380. Hastings KE. Strong evolutionary conservation of broadly expressed protein isoforms in the troponin I gene family and other vertebrate gene families. *J Mol Evol.* 1996;42(6):631-640.
381. Hastings KE. Molecular evolution of the vertebrate troponin I gene family. *Cell Struct Funct.* 1997;22(1):205-211.
382. Maisonpierre PC, Hastings KE, Emerson CP, Jr. The cloning and the codon and amino acid sequence of the quail slow/cardiac troponin C cDNA. *Methods Enzymol.* 1987;139:326-337.
383. Cleto CL, Vandenberghe AE, MacLean DW, Pannunzio P, Tortorelli C, Meedel TH, Satou Y, Satoh N, Hastings KE. Ascidian larva reveals ancient origin of vertebrate-skeletal-muscle troponin I characteristics in chordate locomotory muscle. *Mol Biol Evol.* 2003;20(12):2113-2122.
384. Makinde AO, Kantor PF, Lopaschuk GD. Maturation of fatty acid and carbohydrate metabolism in the newborn heart. *Mol Cell Biochem.* 1998;188(1-2):49-56.
385. Nagao K, Taniyama Y, Kietzmann T, Doi T, Komuro I, Morishita R. HIF-1{alpha} Signaling Upstream of NKX2.5 Is Required for Cardiac Development in Xenopus. *J. Biol. Chem.* 2008;283(17):11841-11849.
386. Seki S, Nagashima M, Yamada Y, Tsutsuura M, Kobayashi T, Namiki A, Tohse N. Fetal and postnatal development of Ca2+ transients and Ca2+ sparks in rat cardiomyocytes. *Cardiovasc Res.* 2003;58(3):535-548.

387. Fu JD, Yang HT. Developmental regulation of intracellular calcium homeostasis in early cardiac myocytes. *Sheng Li Xue.Bao.* 2006;58(2):95-103.
388. Redfield MM. Understanding "diastolic" heart failure. *N Engl J Med.* 2004;350(19):1930-1931.
389. James J, Zhang Y, Osinska H, Sanbe A, Klevitsky R, Hewett TE, Robbins J. Transgenic modeling of a cardiac troponin I mutation linked to familial hypertrophic cardiomyopathy. *Circulation Research.* 2000;87(9):805-811.
390. Sheng HZ, Shan QJ, Wu X, Cao KJ. [Cardiac troponin I gene mutation (Asp127Tyr) in a Chinese patient with hypertrophic cardiomyopathy]. *Zhonghua Xin Xue Guan Bing Za Zhi.* 2008;36(12):1063-1065.
391. Wen Y, Pinto JR, Gomes AV, Xu Y, Wang Y, Potter JD, Kerrick WG. Functional consequences of the human cardiac troponin I hypertrophic cardiomyopathy mutation R145G in transgenic mice. *J Biol Chem.* 2008;283(29):20484-20494.
392. Davis J, Wen H, Edwards T, Metzger JM. Allele and species dependent contractile defects by restrictive and hypertrophic cardiomyopathy-linked troponin I mutants. *J Mol Cell Cardiol.* 2008;44(5):891-904.
393. Du J, Liu J, Feng H-Z, Hossain MM, Gobara N, Zhang C, Li Y, Jean-Charles P-Y, Jin J-P, Huang X-P. Impaired relaxation is the main manifestation in transgenic mice expressing a restrictive cardiomyopathy mutation, R193H, in cardiac TnI. *Am J Physiol Heart Circ Physiol.* 2008;294(6):H2604-2613.
394. Iorga B, Blaudeck N, Solzin J, Neulen A, Stehle I, Davila AJL, Pfitzer G, Stehle R. Lys184 deletion in troponin I impairs relaxation kinetics and induces hypercontractility in murine cardiac myofibrils. *Cardiovasc Res.* 2008;77(4):676-686.
395. Shiels HA, White E. Temporal and spatial properties of cellular Ca2+ flux in trout ventricular myocytes. *Am J Physiol Regul Integr Comp Physiol.* 2005;288(6):R1756-1766.
396. Bonaventura C, Crumbliss AL, Weber RE. New insights into the proton-dependent oxygen affinity of Root effect haemoglobins. *Acta Physiol Scand.* 2004;182(3):245-258.
397. Root RW. The respiratory function of the blood of marine fishes. *Biol Bull.* 1931.;61:427–456.
398. Franklin CE, Davie PS. Dimensional analysis of the ventricle of an in situ perfused trout heart using echocardiography. *J Exp Biol.* 1992;166:47-60.
399. Hedrick MS, Palioca WB, Hillman SS. Effects of temperature and physical activity on blood flow shunts and intracardiac mixing in the toad Bufo marinus. *Physiol Biochem Zool.* 1999;72(5):509-519.
400. Farrell TG, Bashir Y, Cripps T, Malik M, Poloniecki J, Bennett ED, Ward DE, Camm AJ. Risk stratification for arrhythmic events in postinfarction patients based on heart rate variability, ambulatory electrocardiographic variables and the signal-averaged electrocardiogram. *J Am Coll Cardiol.* 1991;18(3):687-697.

401. Syme DA, Josephson RK. Influence of muscle length on work from trabecular muscle of frog atrium and ventricle. *J Exp Biol.* 1995;198(Pt 10):2221-2227.
402. Fabiato A, Fabiato F. Myofilament-generated tension oscillations during partial calcium activation and activation dependence of the sarcomere length-tension relation of skinned cardiac cells. *J Gen Physiol.* 1978;72(5):667-699.
403. Axelsson M, Davison W, Forster ME, Farrell AP. Cardiovascular responses of the red-blooded antarctic fishes Pagothenia bernacchii and P. borchgrevinki. *J Exp Biol.* 1992;167:179-201.
404. Franklin C, Axelsson M. The Intrinsic Properties of an in Situ Perfused Crocodile Heart. *J Exp Biol.* 1994;186(1):269-288.
405. Pelster B. Environmental influences on the development of the cardiac system in fish and amphibians. *Comp Biochem Physiol A Mol Integr Physiol.* 1999;124(4):407-412.
406. Currie S, Boutilier RG. Strategies of hypoxia and anoxia tolerance in cardiomyocytes from the overwintering common frog, Rana temporaria. *Physiol Biochem Zool.* 2001;74(3):420-428.
407. Joseph T, Coirault C, Lecarpentier Y. Species-dependent changes in mechano-energetics of isolated cardiac muscle during hypoxia. *Basic Res Cardiol.* 2000;95(5):378-384.
408. McKean T, Scherzer A, Park H. Hypoxia and ischaemia in buffer-perfused toad hearts. *J Exp Biol.* 1997;200(Pt 19):2575-2581.
409. Park IS, Michael LH, Driscoll DJ. Comparative response of the developing canine myocardium to inotropic agents. *Am J Physiol.* 1982;242(1):H13-18.
410. Swiderek K, Jaquet K, Meyer HE, Heilmeyer LM, Jr. Cardiac troponin I, isolated from bovine heart, contains two adjacent phosphoserines. A first example of phosphoserine determination by derivatization to S-ethylcysteine. *Eur J Biochem.* 1988;176(2):335-342.
411. Robertson SP, Johnson JD, Holroyde MJ, Kranias EG, Potter JD, Solaro RJ. The effect of troponin I phosphorylation on the Ca2+-binding properties of the Ca2+-regulatory site of bovine cardiac troponin. *J Biol Chem.* 1982;257(1):260-263.
412. Solaro RJ, Moir AJ, Perry SV. Phosphorylation of troponin I and the inotropic effect of adrenaline in the perfused rabbit heart. *Nature.* 1976;262(5569):615-617.
413. Tong CW, Gaffin RD, Zawieja DC, Muthuchamy M. Roles of phosphorylation of myosin binding protein-C and troponin I in mouse cardiac muscle twitch dynamics. *J Physiol.* 2004;558(Pt 3):927-941.
414. McClellan G, Kulikovskaya I, Winegrad S. Changes in cardiac contractility related to calcium-mediated changes in phosphorylation of myosin-binding protein C. *Biophys J.* 2001;81(2):1083-1092.

415. Flashman E, Redwood C, Moolman-Smook J, Watkins H. Cardiac Myosin Binding Protein C: Its Role in Physiology and Disease. *Circ Res.* 2004;94(10):1279-1289.
416. Gautel M, Zuffardi O, Freiburg A, Labeit S. Phosphorylation switches specific for the cardiac isoform of myosin binding protein-C: a modulator of cardiac contraction? *EMBO J.* 1995;14(9):1952-1960.
417. Mattiazzi A, Mundina-Weilenmann C, Guoxiang C, Vittone L, Kranias E. Role of phospholamban phosphorylation on Thr17 in cardiac physiological and pathological conditions. *Cardiovasc Res.* 2005;68(3):366-375.
418. Luo W, Chu G, Sato Y, Zhou Z, Kadambi VJ, Kranias EG. Transgenic approaches to define the functional role of dual site phospholamban phosphorylation. *J Biol Chem.* 1998;273(8):4734-4739.
419. Pond SLK, Frost SDW. A Genetic Algorithm Approach to Detecting Lineage-Specific Variation in Selection Pressure. *Mol Biol Evol.* 2005;22(3):478-485.
420. Mercier P, Ferguson RE, Irving M, Corrie JE, Trentham DR, Sykes BD. NMR structure of a bifunctional rhodamine labeled N-domain of troponin C complexed with the regulatory "switch" peptide from troponin I: implications for in situ fluorescence studies in muscle fibers. *Biochemistry.* 2003;42(15):4333-4348.
421. Jahangir A, Sagar S, Terzic A. Aging and cardioprotection. *J Appl Physiol.* 2007;103(6):2120-2128.
422. Lakatta EG. Arterial and cardiac aging: major shareholders in cardiovascular disease enterprises: Part III: cellular and molecular clues to heart and arterial aging. *Circulation.* 2003;107(3):490-497.
423. Lakatta EG, Levy D. Arterial and cardiac aging: major shareholders in cardiovascular disease enterprises: Part II: the aging heart in health: links to heart disease. *Circulation.* 2003;107(2):346-354.
424. Lakatta EG, Levy D. Arterial and cardiac aging: major shareholders in cardiovascular disease enterprises: Part I: aging arteries: a "set up" for vascular disease. *Circulation.* 2003;107(1):139-146.
425. Coutu P, Bennett CN, Favre EG, Day SM, Metzger JM. Parvalbumin corrects slowed relaxation in adult cardiac myocytes expressing hypertrophic cardiomyopathy-linked alpha-tropomyosin mutations. *Circ Res.* 2004;94(9):1235-1241.
426. Coutu P, Metzger JM. Optimal range for parvalbumin as relaxing agent in adult cardiac myocytes: gene transfer and mathematical modeling. *Biophys J.* 2002;82(5):2565-2579.
427. Koretsune Y, Marban E. Cell Calcium in the Patho-Physiology of Ventricular-Fibrillation and in the Pathogenesis of Postarrhythmic Contractile Dysfunction. *Circulation.* 1989;80(2):369-379.
428. Lakatta EG, Sollott SJ. Perspectives on mammalian cardiovascular aging: humans to molecules. *Comparative Biochemistry and Physiology - Part A: Molecular & Integrative Physiology.* 2002;132(4):699-721.

429. Lee JA, Allen DG. Mechanisms of acute ischemic contractile failure of the heart. Role of intracellular calcium. *J Clin.Invest.* 1991;88(2):361-367.
430. Wehrens XHT, Lehnart SE, Marks AR. INTRACELLULAR CALCIUM RELEASE AND CARDIAC DISEASE. *Annual Review of Physiology.* 2005;67(1):69-98.
431. Solaro RJ, el Saleh SC, Kentish JC. Ca2+, pH and the regulation of cardiac myofilament force and ATPase activity. *Mol.Cell Biochem.* 1989;89(2):163-167.
432. Redfield MM, Jacobsen SJ, Burnett JC, Jr., Mahoney DW, Bailey KR, Rodeheffer RJ. Burden of Systolic and Diastolic Ventricular Dysfunction in the Community: Appreciating the Scope of the Heart Failure Epidemic. *JAMA.* 2003;289(2):194-202.
433. Ataka K, Chen D, Levitsky S, Jimenez E, Feinberg H. Effect of aging on intracellular Ca2+, pHi, and contractility during ischemia and reperfusion. *Circulation.* 1992;86(5 Suppl):II371-376.
434. Frolkis VV, Frolkis RA, Mkhitarian LS, Shevchuk VG, Fraifeld VE, Vakulenko LG, Syrovy I. Contractile function and Ca2+ transport system of myocardium in ageing. *Gerontology.* 1988;34(1-2):64-74.
435. Mann DL, Bristow MR. Mechanisms and Models in Heart Failure: The Biomechanical Model and Beyond. *Circulation.* 2005;111(21):2837-2849.
436. Tsunezuka Y, Sato H, Tsubota M, Seki M. Significance of percutaneous cardiopulmonary bypass support for volume reduction surgery with severe hypercapnia. *Artif Organs.* 2000;24(1):70-73.
437. Lutgens E, Daemen MJAP, de Muinck ED, Debets J, Leenders P, Smits JFM. Chronic myocardial infarction in the mouse: cardiac structural and functional change. *Cardiovascular Research.* 1999;41(3):586-593.
438. del Monte F, Lebeche D, Guerrero JL, Tsuji T, Doye AA, Gwathmey JK, Hajjar RJ. From the Cover: Abrogation of ventricular arrhythmias in a model of ischemia and reperfusion by targeting myocardial calcium cycling. *Proceedings of the National Academy of Sciences.* 2004;101(15):5622-5627.
439. Fukuda N, J OU, Sasaki D, Kajiwara H, Ishiwata S, Kurihara S. Acidosis or inorganic phosphate enhances the length dependence of tension in rat skinned cardiac muscle. *J Physiol.* 2001;536(Pt 1):153-160.
440. Ding XL, Akella AB, Gulati J. Contributions of troponin I and troponin C to the acidic pH-induced depression of contractile Ca2+ sensitivity in cardiotrabeculae. *Biochemistry.* 1995;34(7):2309-2316.
441. Ding XL, Akella AB, Sonnenblick EH, Rao VG, Gulati J. Molecular basis of depression of Ca2+ sensitivity of tension by acid pH in cardiac muscles of the mouse and the rat. *J Card Fail.* 1996;2(4):319-326.
442. Cho MC, Rapacciuolo A, Koch WJ, Kobayashi Y, Jones LR, Rockman HA. Defective beta-adrenergic receptor signaling precedes the development of dilated cardiomyopathy in transgenic mice with calsequestrin overexpression. *J Biol Chem.* 1999;274(32):22251-22256.

443. Szatkowski ML, Westfall MV, Gomez CA, Wahr PA, Michele DE, DelloRusso C, Turner II, Hong KE, Albayya FP, Metzger JM. In vivo acceleration of heart relaxation performance by parvalbumin gene delivery. *Journal of Clinical Investigation.* 2001;107(2):191-197.
444. Michele DE, Gomez CA, Hong KE, Westfall MV, Metzger JM. Cardiac dysfunction in hypertrophic cardiomyopathy mutant tropomyosin mice is transgene-dependent, hypertrophy-independent, and improved by beta-blockade. *Circulation Research.* 2002;91(3):255-262.
445. Whitesall SE, Hoff JB, Vollmer AP, D'Alecy LG. Comparison of simultaneous measurement of mouse systolic arterial blood pressure by radiotelemetry and tail-cuff methods. *Am J Physiol Heart Circ Physiol.* 2004;286(6):H2408-2415.
446. Fu Y, Huang X, Zhong H, Mortensen RM, D'Alecy LG, Neubig RR. Endogenous RGS proteins and Galpha subtypes differentially control muscarinic and adenosine-mediated chronotropic effects. *Circ Res.* 2006;98(5):659-666.
447. Linder AE, Weber DS, Whitesall SE, D'Alecy LG, Webb RC. Altered vascular reactivity in mice made hypertensive by nitric oxide synthase inhibition. *J Cardiovasc Pharmacol.* 2005;46(4):438-444.
448. Ucgun I, Oztuna F, Dagli CE, Yildirim H, Bal C. Relationship of Metabolic Alkalosis, Azotemia and Morbidity in Patients with Chronic Obstructive Pulmonary Disease and Hypercapnia. *Respiration.* 2008.
449. Rocker GM, Mackenzie M-G, Williams B, Logan PM. Noninvasive Positive Pressure Ventilation: Successful Outcome in Patients With Acute Lung Injury/ARDS. *Chest.* 1999;115(1):173-177.
450. O'Croinin DF, Nichol AD, Hopkins N, Boylan J, O'Brien S, O'Connor C, Laffey JG, McLoughlin P. Sustained hypercapnic acidosis during pulmonary infection increases bacterial load and worsens lung injury. *Crit Care Med.* 2008;36(7):2128-2135.
451. Harper RM, Macey PM, Woo MA, Macey KE, Keens TG, Gozal D, Alger JR. Hypercapnic Exposure in Congenital Central Hypoventilation Syndrome Reveals CNS Respiratory Control Mechanisms. *J Neurophysiol.* 2005;93(3):1647-1658.
452. Liou YM, Kuo SC, Hsieh SR. Differential effects of a green tea-derived polyphenol (-)-epigallocatechin-3-gallate on the acidosis-induced decrease in the Ca(2+) sensitivity of cardiac and skeletal muscle. *Pflugers Arch.* 2008.
453. Michele DE, Albayya FP, Metzger JM. Thin Filament Protein Dynamics in Fully Differentiated Adult Cardiac Myocytes: Toward A Model of Sarcomere Maintenance. *J. Cell Biol.* 1999;145(7):1483-1495.
454. Westfall MV, Rust EM, Albayya F, Metzger JM. Adenovirus-mediated myofilament gene transfer into adult cardiac myocytes. *Methods Cell Biol.* 1997;52:307-322.

455. Baudenbacher F, Schober T, Pinto JR, Sidorov VY, Hilliard F, Solaro RJ, Potter JD, Knollmann BC. Myofilament Ca sensitization causes susceptibility to cardiac arrhythmia in mice. *J Clin Invest.* 2008.
456. Bessis N, GarciaCozar FJ, Boissier MC. Immune responses to gene therapy vectors: influence on vector function and effector mechanisms. *Gene Therapy.* 2004;11:S10-S17.
457. Manno CS, Chew AJ, Hutchison S, Larson PJ, Herzog RW, Arruda VP, Tai SJ, Ragni MV, Thompson A, Ozelo M, Couto LB, Leonard DGB, Johnson FA, McClelland A, Scallan C, Skarsgard E, Flake AW, Kay MA, High KA, Glader B. AAV-mediated factor IX gene transfer to skeletal muscle in patients with severe hemophilia B. *Blood.* 2003;101(8):2963-2972.
458. Townsend D, Blankinship MJ, Allen JM, Gregorevic P, Chamberlain JS, Metzger JM. Systemic administration of micro-dystrophin restores cardiac geometry and prevents dobutamine-induced cardiac pump failure. *Mol Ther.* 2007;15(6):1086-1092.
459. Feng HZ, Hossain MM, Huang XP, Jin JP. Myofilament incorporation determines the stoichiometry of troponin I in transgenic expression and the rescue of a null mutation. *Arch Biochem Biophys.* 2009;487(1):36-41.
460. Syed F, Odley A, Hahn HS, Brunskill EW, Lynch RA, Marreez Y, Sanbe A, Robbins J, Dorn GW, II. Physiological Growth Synergizes With Pathological Genes in Experimental Cardiomyopathy. *Circulation Research.* 2004;95(12):1200-1206.
461. Dorn Ii GW. Physiologic Growth and Pathologic Genes in Cardiac Development and Cardiomyopathy. *Trends in Cardiovascular Medicine.* 2005;15(5):185-189.
462. Kido M, Du LL, Sullivan CC, Li XD, Deutsch R, Jamieson SW, Thistlethwaite PA. Hypoxia-inducible factor 1-alpha reduces infarction and attenuates progression of cardiac dysfunction after myocardial infarction in the mouse. *Journal of the American College of Cardiology.* 2005;46(11):2116-2124.
463. Kumar D, Hacker TA, Buck J, Whitesell LF, Kaji EH, Douglas PS, Kamp TJ. Distinct mouse coronary anatomy and myocardial infarction consequent to ligation. *Coron.Artery Dis.* 2005;16(1):41-44.
464. Yang F, Liu YH, Yang XP, Xu J, Kapke A, Carretero OA. Myocardial infarction and cardiac remodelling in mice. *Experimental Physiology.* 2002;87(5):547-555.
465. Hunter JJ, Chien KR. Signaling Pathways for Cardiac Hypertrophy and Failure. *The New England Journal of Medicine.* 1999;341(17):1276-1283.
466. Kenchaiah S, Pfeffer MA, John Sutton M, Plappert T, Rouleau JL, Lamas GA, Sasson Z, Parker JO, Geltman EM, Solomon SD. Effect of antecedent systemic hypertension on subsequent left ventricular dilation after acute myocardial infarction (from the Survival and Ventricular Enlargement trial). *The American Journal of Cardiology.* 2004;94(1):1-8.

467. Poulsen SH. Clinical aspects of left ventricular diastolic function assessed by Doppler echocardiography following acute myocardial infarction. *Dan.Med Bull.* 2001;48(4):199-210.
468. Gaudron P, Eilles C, Kugler I, Ertl G. Progressive Left-Ventricular Dysfunction and Remodeling After Myocardial-Infarction - Potential Mechanisms and Early Predictors. *Circulation.* 1993;87(3):755-763.
469. Hubka M, McDonald JA, Wong S, Bolson EL, Sheehan FH. Monitoring change in the three-dimensional shape of the human left ventricle. *Journal of the American Society of Echocardiography.* 2004;17(5):404-410.
470. Tarnavski O, McMullen JR, Schinke M, Nie Q, Kong S, Izumo S. Mouse cardiac surgery: comprehensive techniques for the generation of mouse models of human diseases and their application for genomic studies. *Physiological Genomics.* 2004;16(3):349-360.
471. Birks EJ, Tansley PD, Hardy J, George RS, Bowles CT, Burke M, Banner NR, Khaghani A, Yacoub MH. Left Ventricular Assist Device and Drug Therapy for the Reversal of Heart Failure. *The New England Journal of Medicine.* 2006;355(18):1873-1884.
472. Du CK, Morimoto S, Nishii K, Minakami R, Ohta M, Tadano N, Lu QW, Wang YY, Zhan DY, Mochizuki M, Kita S, Miwa Y, Takahashi-Yanaga F, Iwamoto T, Ohtsuki I, Sasaguri T. Knock-in mouse model of dilated cardiomyopathy caused by troponin mutation. *Circ Res.* 2007;101(2):185-194.
473. Knollmann BC, Kirchhof P, Sirenko SG, Degen H, Greene AE, Schober T, Mackow JC, Fabritz L, Potter JD, Morad M. Familial Hypertrophic Cardiomyopathy-Linked Mutant Troponin T Causes Stress-Induced Ventricular Tachycardia and Ca2+-Dependent Action Potential Remodeling. *Circ Res.* 2003;92(4):428-436.
474. Knollmann BC, Blatt SA, Horton K, de Freitas F, Miller T, Bell M, Housmans PR, Weissman NJ, Morad M, Potter JD. Inotropic stimulation induces cardiac dysfunction in transgenic mice expressing a troponin T (I79N) mutation linked to familial hypertrophic cardiomyopathy. *J Biol Chem.* 2001;276(13):10039-10048.